

MICROWAVE ANTENNAS

DEVELOPMENT AND ANALYSIS OF COMPACT MICROSTRIP ANTENNAS

A thesis submitted by

SONA O. KUNDUKULAM

in partial fulfillment of the
requirements for the degree of

DOCTOR OF PHILOSOPHY
UNDER THE FACULTY OF TECHNOLOGY

DEPARTMENT OF ELECTRONICS
FACULTY OF TECHNOLOGY
COCHIN UNIVERSITY OF SCIENCE AND TECHNOLOGY
COCHIN 682 022, INDIA

JUNE 2002





**Dedicated
to my teachers and family**

CERTIFICATE

This is to certify that this thesis entitled “DEVELOPMENT AND ANALYSIS OF COMPACT MICROSTRIP ANTENNAS” is a bona fide record of the research work carried out by Mrs. Sona O. Kundukulam, under my supervision in the Department of Electronics, Cochin University of Science and Technology. The result presented in this thesis or parts of it have not been presented for any other degree.



Dr. C. K. Aanandan
(Supervising Teacher)
Reader

Cochin 682 022
15th June 2002

Department of Electronics
Cochin University of Science and Technology

DECLARATION

I hereby declare that the work presented in this thesis entitled "DEVELOPMENT AND ANALYSIS OF COMPACT MICROSTRIP ANTENNAS" is based on the original work done by me under the supervision of **Dr. C. K. Aanandan** in the Department of Electronics, Cochin University of science and Technology, and that no part thereof has been presented for any other degree.

COCHIN 682 022
15th June 2002



SONA O. KUNDUKULAM

ACKNOWLEDGEMENTS

I would like to express my sincere gratitude and thankfulness to Dr. C.K. Aanandan, Reader, Department of Electronics, Cochin University of Science and Technology whose valuable guidance and encouragement were indispensable for the progress and completion of the thesis. It has been really a great privilege to work under him.

Let me thank Dr. K. G. Balakrishnan, Professor & Head, Department of Electronics, Cochin University of Science and Technology for his wholehearted support during my research work.

I am expressing my sincere thanks to former Heads of The Department, Prof. P.R.S. Pillai and Prof. C. S. Sridhar (presently, Principal, SBMS Institute of Technology, Bangalore) for their support and interest shown in my work.

I am indebted to Prof. K. G. Nair, Director, STIC, CUSAT, for his valuable support and suggestions for the successful completion of my research work.

I am much obliged to Dr. P. Mohanan, Professor, Department of Electronics, for his timely suggestions and discussions, which helped me to complete significant part of my work.

It is with great pleasure I thank my colleague and friend Ms. Manju Paulson, Research Scholar, Dept. of Electronics, for her valuable help and cooperation .

In the course of my work I have been enjoying a Junior Research fellowship of Cochin University of Science and Technology and Senior Research Fellowship of Council of Scientific and Industrial Research, Govt. of India. The financial supports provided are thankfully acknowledged.

I would like to acknowledge the financial support received from International Centre for Theoretical Physics(ICTP) , Italy for attending the Young Collaborator Programme.

I also take this opportunity to record my sincere thanks to Prof. K. Vasudevan and Prof. K.T. Mathew for their support and cooperation extended. I would also like to express my sincere thanks to all the teaching staff in Department of Electronics, CUSAT for their support and encouragements.

I thankfully acknowledge the generous support and co operation given by Dr. Jacob George, Corning Inc., USA, Dr. Joe Jacob, Research Associate, Dept. of Electronics, CUSAT, Dr. Sebastian Mathew. Lecturer, K.E. College, Mannanam, Dr. V. P. Joseph, Sr. Lecturer, Christ College, Irinjalakuda, Prof. V. P. Devassia, Model Engg. College, Thrikkakara, Dr. Thomaskutty Mathew, M. G. University Regional Centre, Edapilly, Mr. Cyriac M. Odackal, Lecturer, Dept. of Electronics, Dr. K. K. Narayanan, Lecturer, SD College Alappuzha and Mr. Paul V John, Scientist, STIC for the successful completion of my Ph.D programme.

My colleagues in the department, Mr. Biju Kumar, Mr. Binoy G.S., Mr. Mani T.K., Ms. Mini M.G., Ms. Mridula. M, Ms. Binu Paul, Ms. Sree Devi, Ms. Latha Kumari, Mr. Shabeer Ali, Dr. C. P. Anil Kumar, Mr. Sajith N Pai, Mr. Prakash Kumar, Mr. Binu George, Mr. Anil Lonappan, Mr. Jayaram, Dr. Jaimon Yohannan; Librarians Dr. Beena C., Dept. of Physics, Mr. Suresh, Department of Electronics, all other office/technical staff of Department of Electronics and all my well wishers have given their co-operation and help during my works and I expresses my thanks to them.

SONA O. KUNDUKULAM

Contents

Chapter 1

INTRODUCTION	1
1.1 MICROSTRIP PATCH ANTENNAS	2
1.1.1 Basic characteristics	2
1.1.2 Advantages and disadvantages	3
1.1.3 Applications	4
1.1.4 Radiation mechanism	6
1.2 VARIOUS FEEDS FOR MICROSTRIP ANTENNAS	6
1.2.1 Microstrip feed	6
1.2.2 Coaxial feed	7
1.2.3 Aperture coupling	7
1.2.4 Electromagnetic coupling	7
1.3 MICROSTRIP SUBSTRATES	11
1.4 VARIOUS MICROSTRIP ANTENNA CONFIGURATIONS	11
1.4.1 Microstrip patch antennas	11
1.4.2 Microstrip travelling-wave antennas	11
1.4.3 Microstrip slot antennas	13
1.5 METHODS OF ANALYSIS OF MICROSTRIP PATCH ANTENNAS	13
1.6 BASIC CHARACTERISTICS OF RECTANGULAR AND CIRCULAR DISK PATCHES	14
1.6.1 Rectangular microstrip patch antenna	14
1.6.1.1 Magnetic current distribution	16
1.6.1.2 Radiation Patterns	16
1.6.2 Circular microstrip antenna	18
1.6.2.1 Magnetic current distribution	18
1.7 OUTLINE OF THE PRESENT WORK	22
1.8 ORGANISATION OF THE CHAPTERS	22

Chapter 2

REVIEW OF THE PAST WORK	24
2.1 DEVELOPMENT OF MICROSTRIP ANTENNAS	25
2.2 COMPACT MICROSTRIP ANTENNAS	32

Chapter 3

METHODOLOGY - EXPERIMENTAL SETUP AND MEASUREMENT TECHNIQUES

3.1	ANTENNA FABRICATION	44
3.2	EXCITATION TECHNIQUE	45
3.3	ANTENNA MEASUREMENTS	47
3.3.1	Network Analyser	47
3.3.2	Measurement Of Return Loss, Resonant Frequency And Bandwidth	49
3.3.3	Measurement Of Radiation Pattern	50
3.3.4	Measurement Of Gain	52
3.3.5	Measurement Of Axial Ratio For Circularly Polarised Microstrip Antenna	52
3.3.6	1e3d Simulation Technique	53

Chapter 4

EXPERIMENTAL OBSERVATIONS

4.1	INTRODUCTION	61
4.2	CHARACTERISTIC PROPERTIES OF RECTANGULAR AND CIRCULAR DISK MICROSTRIP ANTENNAS	61
4.3.	CIRCULAR-SIDED COMPACT MICROSTRIP ANTENNA (with two concave sides)	63
4.3.1	Geometry	63
4.3.2	Excitation technique	64
4.3.3	Characteristics of a typical example	64
	4.3.3.1 Resonant modes	65
	4.3.3.2 Gain	66
	4.3.3.4 Radiation patterns	66
4.3.4	Characteristic features	68
	4.3.4.1 Compactness	68
	4.3.4.2 Dual band operation and circular polarization	68
4.3.5	Characteristics of TM_{10} and TM_{01} mode frequencies (f_{10} and f_{01})	69
	4.3.5.1 Resonant frequency variation with respect to the length	69
	4.3.5.2 Resonant frequency variation with respect to the width.	71
	4.3.5.3 Variation of frequencies for patches of different radii	73
	4.3.5.4 Variation of frequencies for patches of different h and ϵ_r .	78
4.3.6	Impedance bandwidth and VSWR	80
4.3.7	Radiation characteristics	80
4.3.8	Antenna Fabrication and Measurement	83

4.3.8.1	Geometry and design	83
4.3.8.2	Experimental results	83
4.3.9	Circularly polarized compact microstrip antenna	86
4.3.9.1	Geometry and design	86
4.3.9.2	Experimental results	87
4.4	CIRCULAR-SIDED PATCH (with one convex and other concave side)	90
4.4.1	Geometry and excitation technique	90
4.4.2	Characteristics of a typical example	91
4.4.2.1	Resonant modes	91
4.4.2.2	Gain	92
4.4.2.3	Radiation patterns	92
4.4.3	Characteristic features	94
4.4.3.1	Compactness	94
4.4.3.2	Dual band operation and circular polarization	94
4.4.4	Characteristics of TM_{10} and TM_{01} mode frequencies (f_{10} and f_{01})	95
4.4.4.1	Resonant frequency variation with respect to the length	95
4.4.4.2	Resonant frequency variation with respect to the width	98
4.4.4.3	Variation of frequencies for the patches of different radii	99
4.4.4.4	Variation of TM_{10} mode frequency for patches of different h and ϵ_r	101
4.4.5	Impedance bandwidth and VSWR	102
4.4.6	Radiation characteristics	104
4.4.7	Antenna Fabrication and Measurement	105
4.4.7.1	Geometry and design	105
4.4.7.2	Experimental results	105
4.5	CRESCENT SHAPED MICROSTRIP ANTENNA	107
4.5.1	Antenna Geometry and excitation technique	107
4.5.2	Characteristics of a typical example	107
4.5.2.1	Resonant modes	108
4.5.2.2	Radiation patterns and gain	108
4.5.3	Characteristic features	110
4.5.3.1	Compactness	110
4.5.3.2	Dual port operation	110
4.5.4	Variation of TM_{11} and TM_{21} mode frequencies	110
4.5.5	Radiation characteristics	117
4.5.6	Compact dual frequency microstrip antenna with dual port	118
4.5.6.1	Geometry and design	118
4.5.6.2	Experimental and Simulated Results	119

4.6	COMPARISON OF CHARACTERISTICS OF THE RECTANGULAR, CIRCULAR, OTHER CIRCULAR SIDED PATCHES	123
4.7	CONCLUDING REMARKS	126

Chapter 5

	THEORETICAL INVESTIGATIONS	127
5.1	IDENTIFICATION AND VERIFICATION OF DOMINANT MODES OF COMPACT MICROSTRIP PATCHES	128
5.1.1	Discussion on different modes of a rectangular microstrip antenna	128
5.1.2	Resonating modes of the circular sided patch (with two concave sides)	129
5.1.3	Resonant modes of the circular sided patch (with one concave and other convex side)	129
5.1.4	Discussion on different modes of a circular disk microstrip antenna	133
5.1.5	Modes of the crescent-shaped microstrip antenna	133
5.2	DESIGN OF THE MICROSTRIP FEEDLINE	135
5.2.1	Characteristic impedance of microstrip line	137
5.2.2	Microstrip line synthesis	138
5.3	RESONANT FREQUENCY CALCULATION OF RECTANGULAR MICROSTRIP ANTENNA	139
5.4	RESONANT FREQUENCY CALCULATION OF CIRCULAR SIDED MICROSTRIP ANTENNA (with one concave and other convex side)	143
5.4.1	Comparison between the measured and calculated results	145
5.5	PATCH AREA CALCULATION OF CIRCULAR SIDED PATCH (with one concave and other convex side)	154
5.6	RESONANT FREQUENCY CALCULATION OF CIRCULAR DISK MICROSTRIP ANTENNA	155
5.7	RESONANT FREQUENCY CALCULATION OF CRESCENT-SHAPED MICROSTRIP ANTENNA	156
5.7.1	Comparison of theory and experiment	159
5.8	PATCH AREA CALCULATION OF CRESCENT-SHAPED MICROSTRIP ANTENNA	164
5.9	PATCH AREA CALCULATION OF CIRCULAR SIDED PATCH (with two concave sides)	166
5.10	CONCLUDING REMARKS	167

Chapter 6

CONCLUSIONS	168
6.1 INTRODUCTION	169
6.2 INFERENCES FROM EXPERIMENTAL INVESTIGATIONS	169
6.3 INFERENCES FROM THEORETICAL INTERPRETATIONS	172
6.4 SOME POSSIBLE APPLICATIONS OF THE PRESENT WORK	173
6.5 SUGGESTIONS FOR FURTHER WORK IN THE FIELD	174

Appendix A

DRUM SHAPED COMPACT MICROSTRIP ANTENNA FOR DUAL FREQUENCY OPERATION AND CIRCULAR POLARIZATION	175
--	------------

Appendix B

SLOT-LOADED COMPACT MICROSTRIP ANTENNAS FOR DUAL FREQUENCY OPERATION AND BAND WIDTH ENHANCEMENT	183
--	------------

Appendix C

COMPACT DUAL BAND MICROSTRIP ANTENNA WITH LINEAR AND CIRCULAR POLARISED OPERATION	192
--	------------

REFERENCES	197
-------------------	------------

INDEX	214
--------------	------------

LIST OF PUBLICATIONS OF THE AUTHOR	215
---	------------

RESUME OF THE AUTHOR	217
-----------------------------	------------

INTRODUCTION

The term 'antenna' is defined as "a usually metallic device (as a rod or wire) for radiating or receiving radio waves". As per the terminology of The Institute of Electrical and Electronics Engineers (IEEE) Antenna is "A means for radiating or receiving radio waves". Antennas launch energy into space as electromagnetic waves or, in the reverse process, extract energy from an existing electromagnetic field.

Prior to World War II, most antenna elements were of the wire type (long wires, dipoles, helices, rhombuses, fans, etc.), and they were used either as single elements or in arrays. During and after World War II, many other radiators, which were relatively new, were put into service. Many of these antennas were of the aperture type (such as open-ended waveguides, slots, horns, reflectors, lenses) and they were used for communication, radar, remote sensing etc.

The concept of microstrip radiators was first proposed by Deschamps in the year 1953. However, twenty years passed before practical microstrip antennas were fabricated, as better theoretical models and photo-etching techniques for dielectric substrates were developed. The first practical microstrip antennas were developed in 1970's by Howell and Munson. Since then development of numerous types of microstrip antennas were reported for different applications.

1.1 MICROSTRIP PATCH ANTENNAS

Basically the microstrip element consists of an area of metallization supported above a ground plane, named as microstrip patch. A microstrip patch antenna uses the "Microstrip" structure to make an antenna. Microwave engineers first used "stripline" to fabricate circuits from circuit board. Stripline uses two ground planes, and a flat strip (circuit board trace) in between, to guide RF. In the course of time, many circuits were found to be easily made with the so called "Microstrip" structure, which is similar to the stripline, but with one ground plane removed. The key to its utility has been that it can be fabricated with low cost lithographic techniques. It can also be produced by monolithic integrated circuit techniques that fabricate phase shifters, amplifiers, and other necessary devices, all on the same substrate and all by automated processes. The basic geometries were the rectangular patch described by Munson [15] and the circular disk radiator of Howell [16].

1.1.1 Basic characteristics

Microstrip antennas consists of a very thin (thickness $t \ll \lambda_0$ where λ_0 is the free-space wavelength) metallic strip (patch) placed a small fraction of a wavelength ($h \ll \lambda_0$) above a ground plane, as shown in Fig 1.1. The patch antenna is designed so that its maximum radiation is in a direction normal to its surface (broadside radiator). This is accomplished by properly choosing the mode of excitation.

The upper surface of the dielectric substrate supports the printed conducting strip which is suitably contoured while the entire lower surface of the substrate is backed by a conducting ground plate. Such an antenna is sometimes called a printed antenna because the fabrication procedure is similar to that of a printed circuit board. Many types of microstrip antennas have been evolved which are variations of the basic structure. Microstrip antennas can be designed as very

thin planar printed antennas and they are very useful elements for different types of arrays, especially conformal arrays which can be designed on a surface of any type and shape.

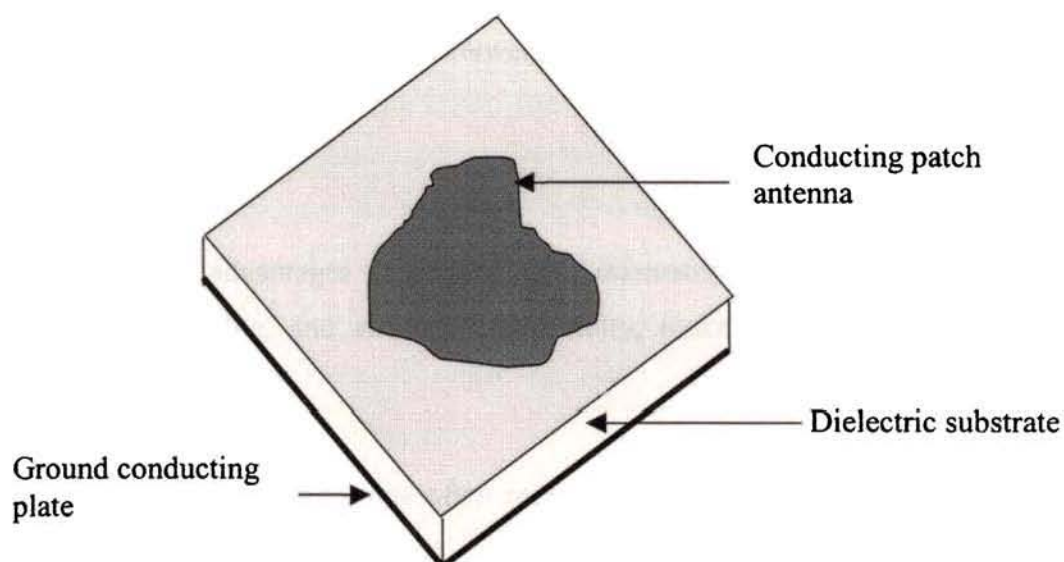


Fig 1.1 Geometry of the basic microstrip antenna structure

1.1.2 Advantages and disadvantages

Microstrip antennas are low profile, conformable to planar and nonplanar surfaces, simple and inexpensive to manufacture using modern printed-circuit technology, mechanically robust and compatible with MMIC designs. When the particular patch shape and mode are selected they are very versatile in terms of resonant frequency, polarization, pattern and impedance. In addition, by adding loads between the patch and the ground plane, such as pins and varactor diodes, adaptive elements with variable resonant frequency, impedance, polarization and pattern can be designed. Since it is of planar structure, it has all the advantages of printed circuit technology.

The major operational disadvantages of microstrip antennas are their low efficiency, low power, poor polarization purity, poor scan performance, spurious feed radiation, half plane radiation, limitation on the maximum gain (about 20dB) and very narrow frequency bandwidth, which is typically only a fraction of a percent or at most a few percent. However for many practical designs, the advantages of microstrip antennas outweigh their disadvantages.

1.1.3 Applications

Several advantages associated with microstrip antennas, namely light weight, low profile, and structural conformity, make them ideally suited to aerospace applications.

Mobile communications often require antennas having small size, light weight, low profile and low cost. Microstrip antennas (MSA) form a class of antennas which meet these requirements, and various MSAs have so far been developed and used for mobile communication systems. The practical applications for mobile systems are in portable or pocket-size equipment and in vehicles. UHF pagers, manpack radars, and car telephones are typical of those. Base stations for mobile communications favour simple antennas since the antenna tower built for the base station can then be smaller and need less support for the weight. Ships and aircraft also demand small, lightweight antennas, and sometimes conformal structures are desirable to allow antennas to be mounted flush on the body of the moving vehicle. MSAs are considered to be suitable for such conditions and many antennas have been developed and installed on ships and aircraft.

In satellite communications, circularly polarized radiation patterns are required and MSAs of either square or circular patches with one or two feeding points can be used for generating the circular polarization. A flat structure can be a feature of an MSA array used for receiving satellite broadcasting. Parabolic antennas are very popular for receiving broadcasts from satellites, but replacing

them by small flat antennas is preferable, especially for the home use. A large parabolic antenna, with the primary feed placed in front of the reflector, needs a wide area for installation, while a small, flat antenna can be possibly be mounted flush on the wall of the house or even placed inside the window at home, depending on the field strength at the receiving environment.

While specifications for defence and space application antennas typically emphasize maximum performance with little constraint on cost, commercial applications demand low cost components, often at the expense of reduced electrical performance. Thus, microstrip antennas for commercial systems require low-cost materials, and simple and inexpensive fabrication techniques. Some of the commercial systems that presently use microstrip antennas are listed in the table below:

Application	Frequency
Global Positioning Satellite	1575 MHz and 1227 MHz
Paging	931-932 MHz
Cellular Phone	824-849 MHz and 869-895 MHz
Personal Communication System	1.85-1.99GHz and 2.18-2.20GHz
GSM	890-915 MHz and 935-960 MHz
Wireless Local Area Networks	2.40-2.48 GHz and 5.4 GHz
Cellular Video	28GHz
Direct Broadcast Satellite	11.7-12.5 GHz
Automatic Toll Collection	905 MHz and 5-6 GHz
Collision Avoidance Radar	60 GHz, 77 GHz, and 94 GHz
Wide Area Computer Networks	60 GHz

1.1.4 Radiation mechanism

Radiation from microstrip antennas can be understood by considering the simple case of a rectangular microstrip patch spaced a small fraction of a wavelength above a ground plane, as shown in Fig.1.2 (a). Assuming no variations of the electric field along the width and the thickness of the microstrip structure, the electric field configuration of the radiator can be represented as shown in Fig.1.2 (b). The fields vary along the patch length which is about half a wavelength ($\lambda/2$). The fringing fields at the end can be resolved into normal and tangential components with respect to the ground plane. The normal components are out of phase because the patch line is $\lambda/2$ long; therefore the far field produced by them cancel in the broadside direction. The tangential components are in phase, and the resulting fields combine to maximum radiated field normal to the surface of the structure. Therefore, the patch may be represented by two slots $\lambda/2$ apart (Fig.1.2(c)) excited in phase and radiating in the half space above the ground plane.

1.2 Various feeds for Microstrip antennas

There are many configurations that can be used to feed microstrip antennas. The four most popular are the microstrip line, coaxial probe, aperture coupling and proximity coupling.

1.2.1 Microstrip feed

The microstrip feedline (Fig 1.3) is also a conducting strip, usually of much smaller width compared to the patch. The microstrip feedline is easy to fabricate, simple to match by controlling the inset position and rather simple to model. However as the substrate thickness increases, surface waves and spurious feed radiation increase, which for practical designs limit the bandwidth.

1.2.2 Coaxial feed

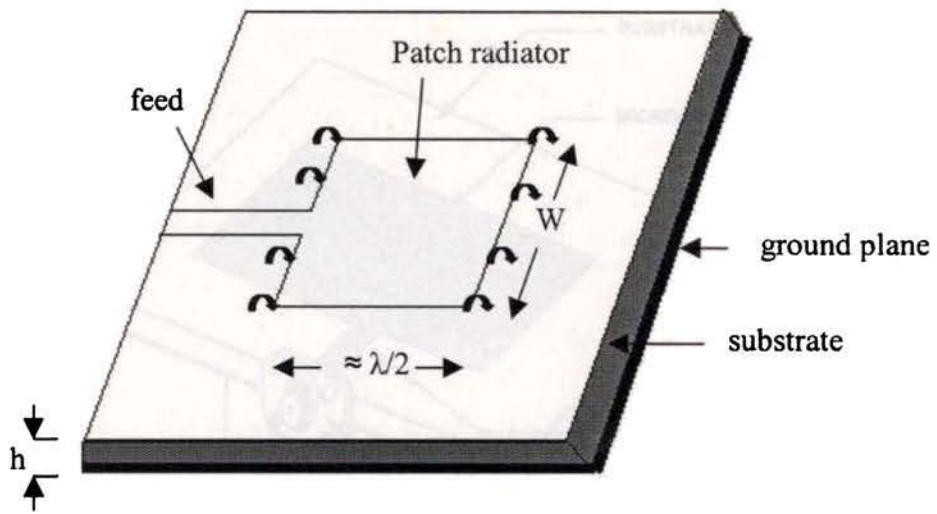
In this type, the inner conductor of the coaxial cable is attached to the patch while the outer conductor is connected to the ground plane as shown in Fig. 1.4. This is the widely used type of feeding. The coaxial probe feed is also easy to fabricate and match, and it has low spurious radiation. However, it also has narrow bandwidth and it is more difficult to model, especially for thick substrates ($h > 0.02 \lambda_0$).

1.2.3 Aperture coupling

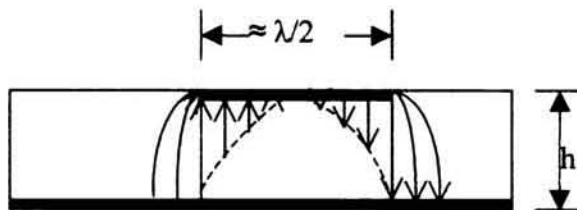
The aperture coupling of Fig. 1.5 is the most difficult of all four to fabricate and it also has narrow bandwidth. However, it is somewhat easier to model and has moderate spurious radiation. The aperture coupling consists of two substrates separated by a ground plane. On the bottom side of the lower substrate there is a microstrip feedline whose energy is coupled to the patch through a slot on the ground plane separating the two substrates. Typically a high dielectric material is used for the bottom substrate, and thick low dielectric constant material for the top substrate. The ground plane between the substrates also isolates the feed from the radiating element and minimizes interference of spurious radiation.

1.2.4 Electromagnetic coupling

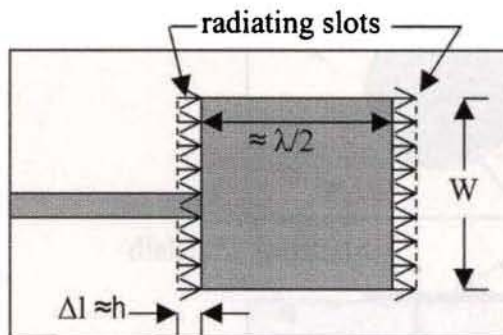
Electromagnetic coupling (also termed as proximity coupling) (Fig 1.6) has the largest bandwidth, low spurious radiation and is easy to model. However its fabrication is somewhat more difficult. The feed system is a covered microstrip network, and the radiating elements are etched on to the covering substrate immediately above the open-ended feedlines. The elements are thus parasitically coupled to the feed network. They may be regarded as microstrip patches on a double-thickness substrate sharing a common ground plane with the feed network.



a



b



c

Fig 1.2 (a) Rectangular microstrip patch antenna

(b) Side view

(c) Top view

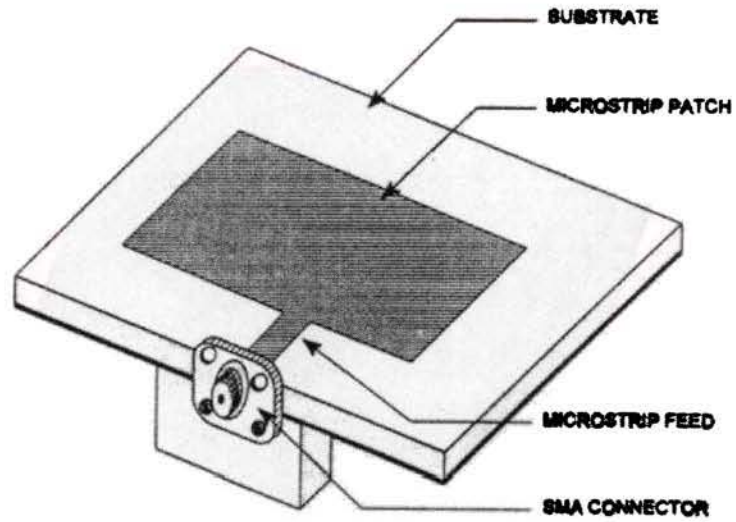


Fig. 1.3 Microstrip line feed

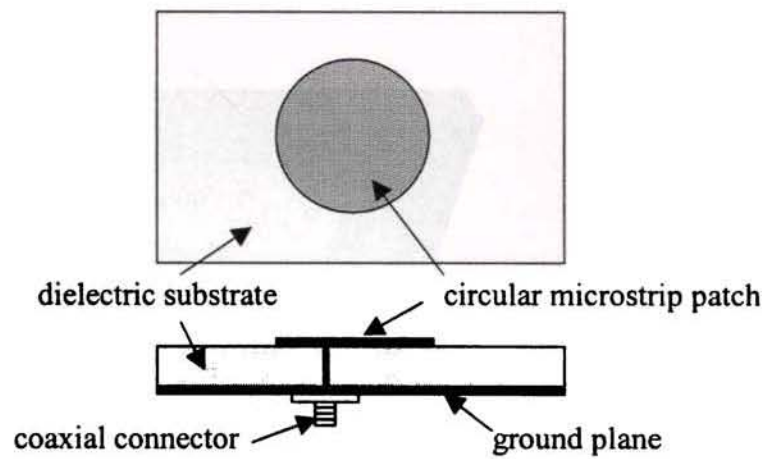


Fig. 1.4 Coaxial probe feed

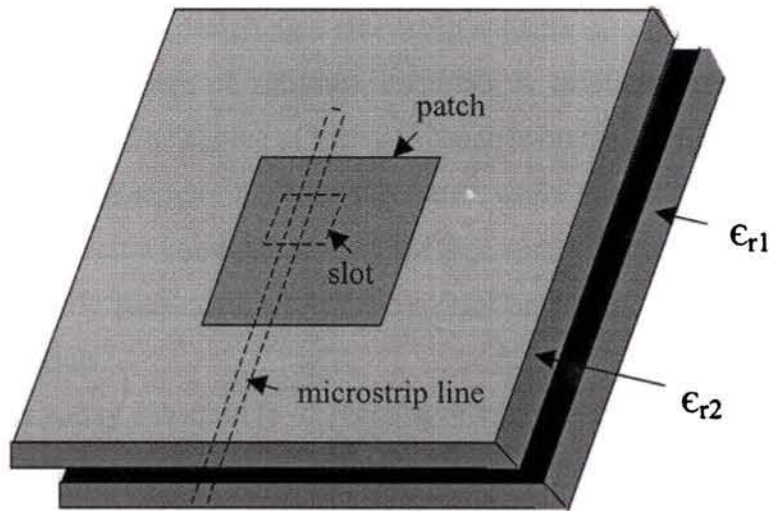


Fig. 1.5 Aperture-coupled feed

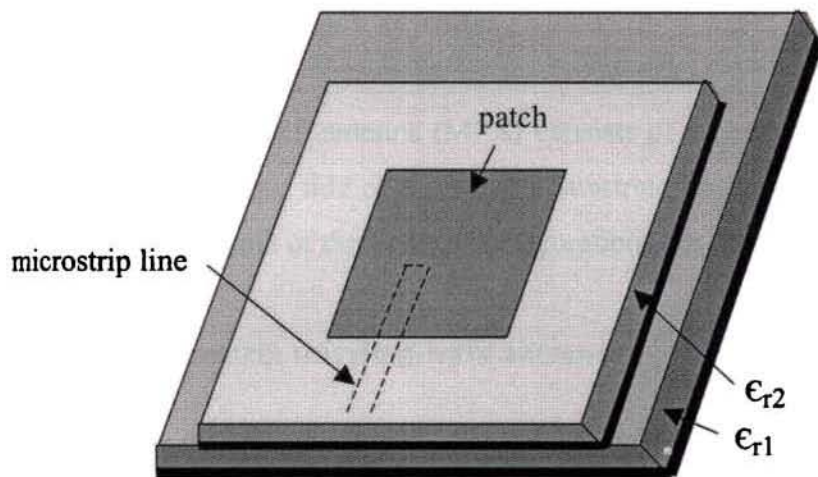


Fig. 1.6 Proximity-coupled feed

1.3 Microstrip substrates

The first step in designing a microstrip antenna is to choose an appropriate substrate. A wide range of substrate materials is available, clad with copper, aluminium or gold. The choice of material depends on the application. Conformal microstrip antennas require flexible substrates, while low frequency applications require high dielectric constants to keep the size small. Microstrip patch antennas use low dielectric substrates, while tapered slot antennas require high dielectric constant materials.

Glass epoxy substrate ($h=0.16\text{cm}$, $\epsilon_r = 4.28$), is used for the development of microstrip antennas described in this thesis work.

1.4 Various microstrip antenna configurations

All microstrip antennas can be divided into three basic categories: microstrip patch antennas, microstrip traveling-wave antennas, and microstrip slot antennas. Their characteristics are as follows:

1.4.1 Microstrip patch antennas

A microstrip patch antenna (MPA) consists of a conducting patch of any planar geometry on one side of a dielectric substrate backed by a ground plane on the other side. Some of the various configurations are shown in the Fig. 1.7.

1.4.2 Microstrip traveling-wave antennas

Microstrip traveling-wave antennas (MTA) consists of chain-shaped periodic conductors or an ordinary long TEM line which also supports a TE mode, on a substrate backed by a ground plane. The open end of the TEM line is terminated in a matched resistive load. Different configurations for MTA are shown in Fig. 1.8.

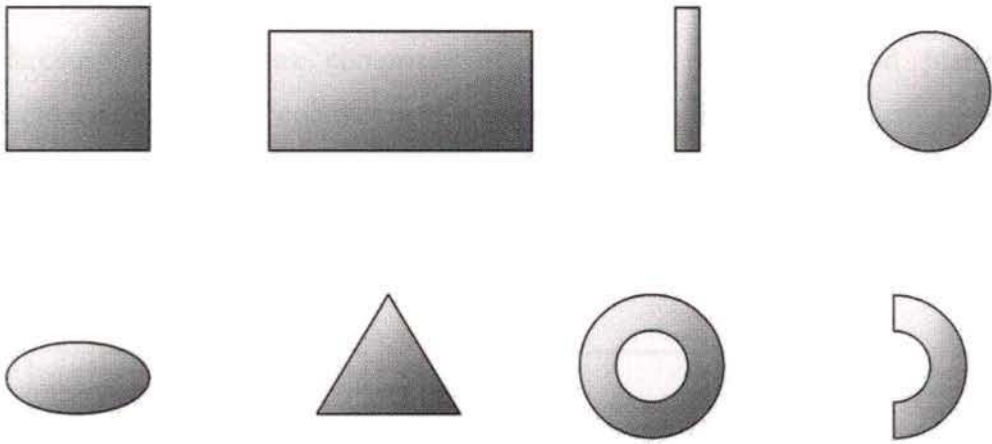


Fig. 1.7 Various microstrip antenna configurations used in practice

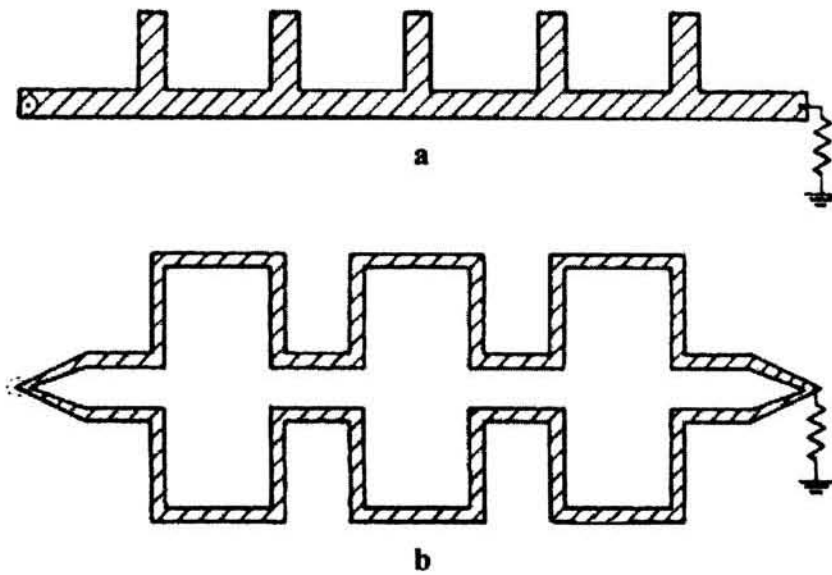


Fig. 1.8 Microstrip traveling-wave antennas

1.4.3 Microstrip slot antennas

A microstrip slot antenna comprises of a slot cut in the ground plane perpendicular to the strip conductor of a microstrip line. Energy propagating in the strip transmission line excites the slot. The slot may have the shape of a rectangle (narrow or wide), a circle or an annulus as shown in Fig. 1.9.

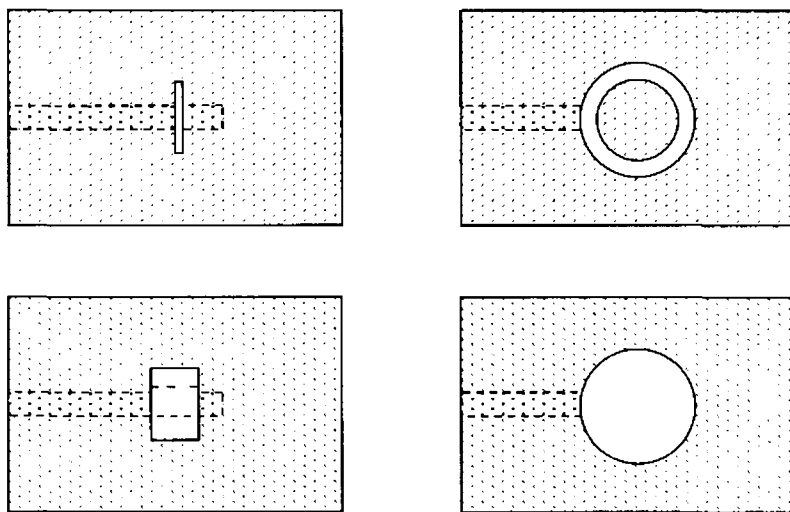


Fig. 1.9 Microstrip slot antennas

1.5 Methods of analysis of microstrip patch antennas

There are different methods of analysis for microstrip antennas. The various models include the transmission-line, cavity, the multiport network models and full-wave methods. The transmission-line model is the easiest of all, it gives good physical insight, but is less accurate and is more difficult to model coupling. A planar two-dimensional cavity model for microstrip patch antennas offers considerable improvement over the one-dimensional transmission line model. In this method of modeling, the microstrip patch is considered as a two-dimensional

resonator surrounded by a perfect magnetic wall around the periphery. In the multiport-network modeling (MNM) approach for radiating microstrip patches, the fields underneath the patch, the external fields (radiated, surface wave and fringing fields), and the fields underneath the microstrip feedlines are modeled separately in terms of multiport subnetworks. The MNM approach can conveniently incorporate the effects of the mutual coupling and the feed-junction reactances. The full-wave models are very accurate, versatile and can treat single elements, finite and infinite arrays, stacked elements, arbitrary shaped elements, and coupling. When applied to microstrip antennas, the integral equation-based full-wave analysis approach is comprised of three basic steps: (1) formulating an integral equation in terms of electric current distribution on the patch, (2) evaluating the current distribution by the moment method approach, and (3) evaluating the radiation characteristics from the current distribution. In addition to the integral equation formulation for full-wave analysis of microstrip patches, finite-difference time-domain and finite-element boundary-integral methods have also been used for these antennas. Basic formulation of the FD-TD method is as a central difference discretization of Maxwell's equations in both time and space. As in the case of FD-TD method, finite element method (FEM) can also be extended to antenna analysis by incorporating suitable absorbing boundary conditions for simulation of the infinite-external region.

1.6 Basic characteristics of rectangular and circular disk patches

A number of patch shapes can be analysed by straightforward application of the cavity model. Of these, the rectangular and the circular are basic shapes used in practice. They are considered in detail in this section.

1.6.1 Rectangular microstrip patch antenna

The rectangular patch (Fig. 1.10) is probably the most commonly used microstrip antenna. It is characterized by the length a and the width b . The electric field of a resonant mode in the cavity under the patch is given by

$$E_z = E_0 \cos(m\pi x/a) \cos(n\pi y/b) \quad (1.1)$$

Where $m, n = 0, 1, 2, \dots$

The resonant frequency is

$$f_{mn} = k_{mn} c / (2\pi \sqrt{\epsilon_r}) \quad (1.2)$$

Where

$$k_{mn}^2 = (m\pi/a)^2 + (n\pi/b)^2 \quad (1.3)$$

eqn (1.2) is based on the assumption of a perfect magnetic wall.

The resonant frequency calculation by considering the fringing fields of rectangular microstrip patch is explained in detail in chapter 5.

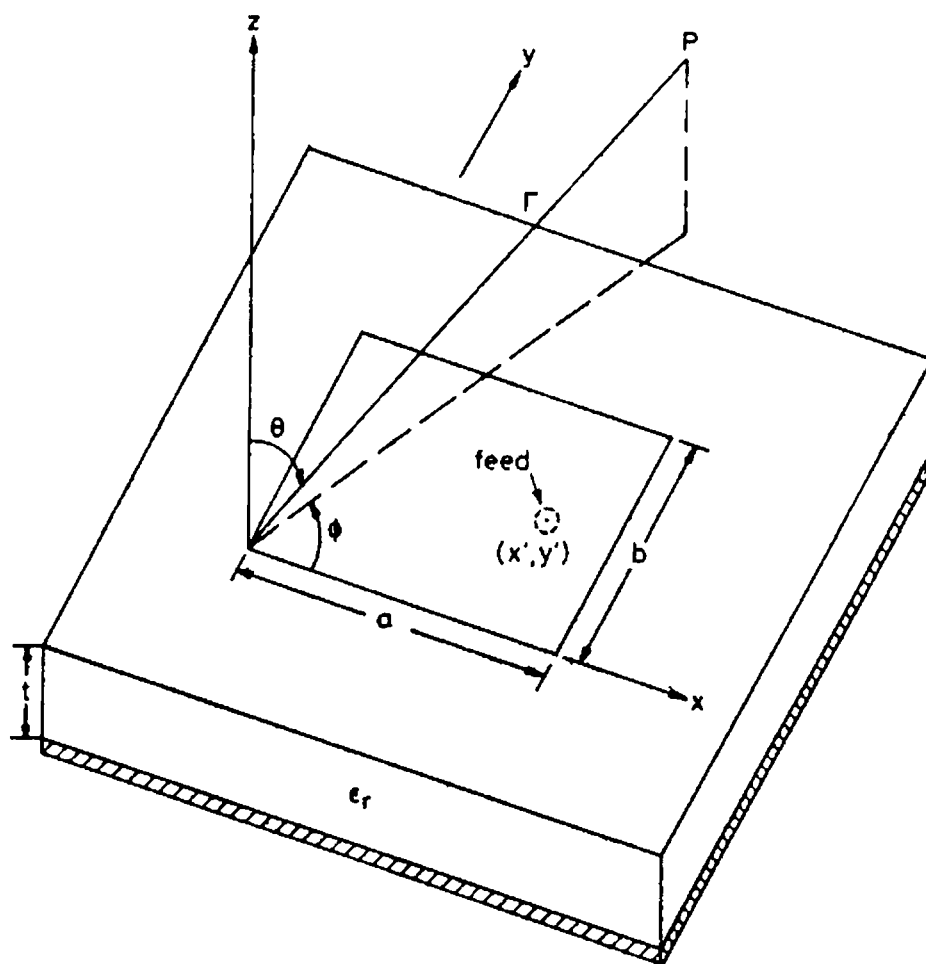


Fig. 1.10 Geometry of the rectangular patch

1.6.1.1 Magnetic current distribution

The electric field configuration of rectangular patch for TM_{10} and TM_{01} modes are shown (Fig. 1.11). The electric-field and magnetic-surface-current distributions on the side wall for TM_{10} , TM_{01} and TM_{20} modes are illustrated in fig. 1.12. For the TM_{10} mode, the magnetic currents along b are constant and in phase while those along 'a' vary sinusoidally and are out of phase. For this reason, the 'b' edge is known as the radiating edge since it contributes predominantly to the radiation. The 'a' edge is known as the non-radiating edge. Similarly, for the TM_{01} mode, the magnetic currents are constant and in phase along 'a' and are out of phase and vary sinusoidally along 'b'. The 'a' edge is thus the radiating edge for the TM_{01} mode.

1.6.1.2 Radiation Patterns

The radiation pattern represents the spatial distribution of the electromagnetic field radiated by an antenna. The patterns are broad for rectangular microstrip antenna.

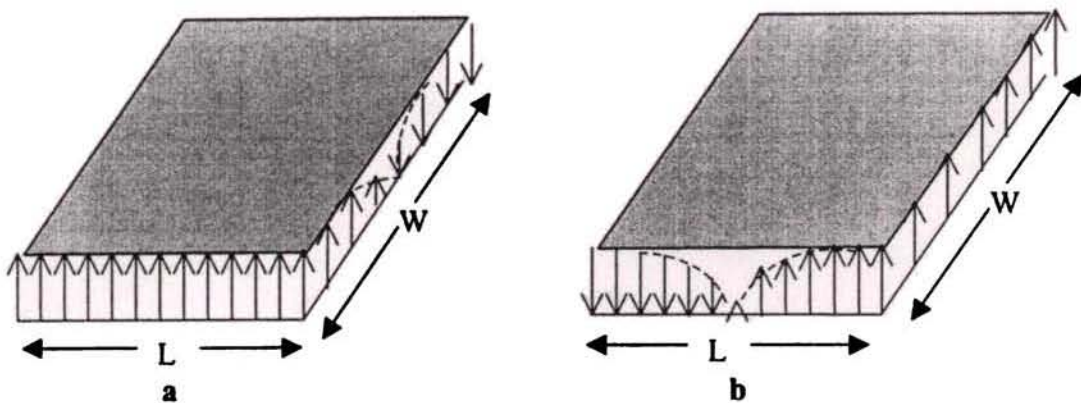


Fig. 1.11 Field configurations for rectangular microstrip patch

- a) TM_{01} mode
- b) TM_{10} mode

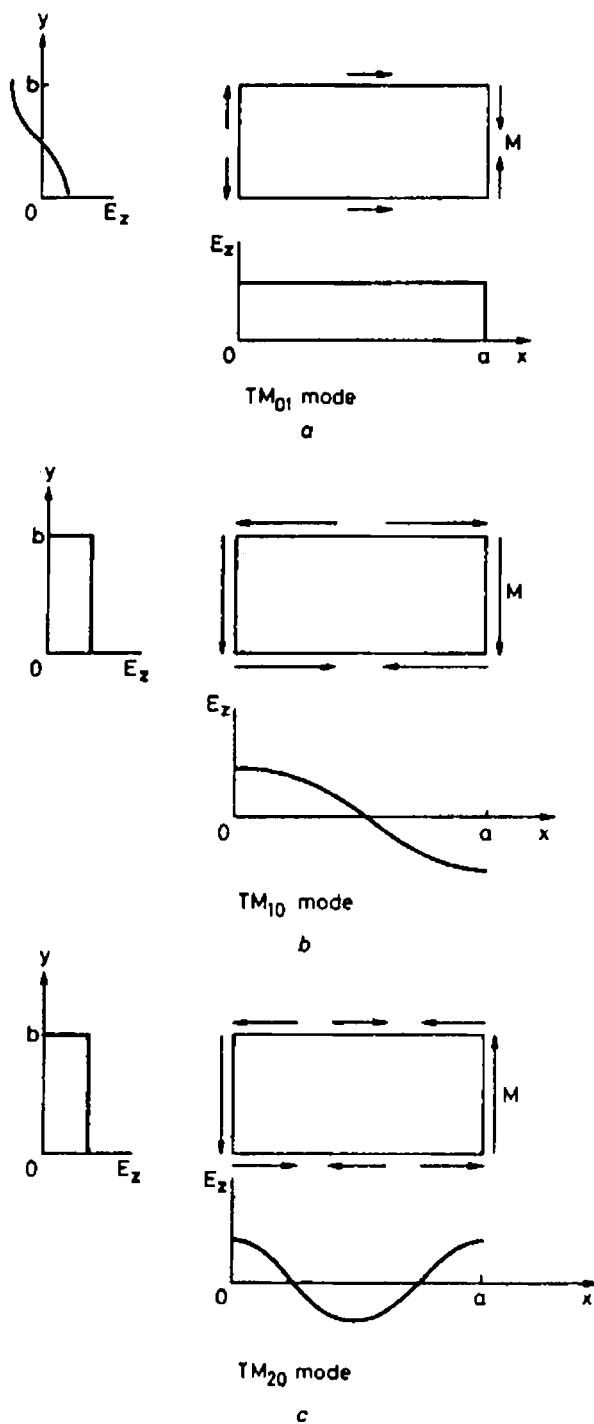


Fig 1.12 Electric field and magnetic-surface-current distributions in walls for different modes of a rectangular microstrip patch antenna

a) TM_{01} b) TM_{10} c) TM_{20}

1.6.2 Circular microstrip antenna

The geometry of the circular patch or disc (Fig.1.13) is characterised by a single parameter, namely, its radius a . Thus it may be considered the simplest geometry since other shapes require more than one parameter to describe them. The mathematical analysis of this patch involves Bessel functions.

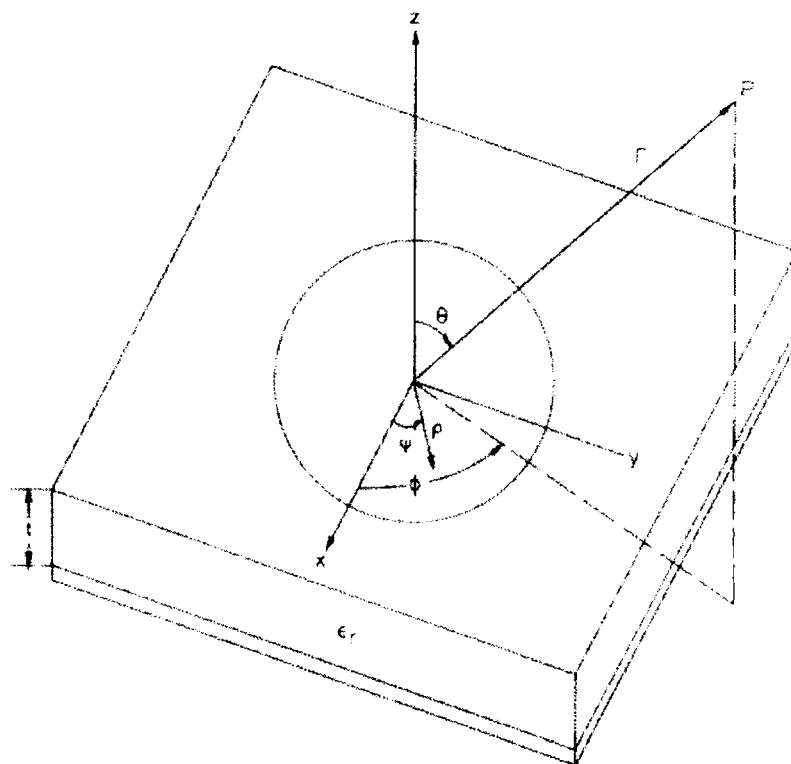


Fig. 1.13 Geometry of the circular patch antenna

The electric field of a resonant TM_{nm} mode in the cavity under the circular patch is given by

$$E_z = E_0 J_n(k_{nm}\rho) \cos n\Psi \quad (1.4)$$

Where ρ and Ψ are the radial and azimuthal co-ordinates, respectively. E_0 is an arbitrary constant, J_n is the Bessel function of the first kind of order n and

$$k_{nm} = X_{nm}/a \quad (1.5)$$

In eqn (1.5), X_{nm} are the roots of the equation $J'_n(x) = 0$, (1.6)

The resonant frequency of a TM_{nm} mode is given by

$$f_{nm} = \frac{X_{nm}}{2\pi a \sqrt{\mu_0 \epsilon}} = \frac{X_{nm} c}{2\pi a \sqrt{\epsilon_r}} \quad (1.7)$$

where c is the velocity of light in free space.

Eqn (1.7) is based on the assumption of a perfect magnetic wall and neglects the fringing fields at the open-end edge of the microstrip patch. To account for these fringing fields at the open-end edge of the microstrip patch, an effective radius a_e , which is slightly larger than the physical radius a , is considered

$$a_e = a \left[1 + \frac{2h}{\pi a \epsilon_r} \left(\ln \frac{\pi a}{2h} + 1.7726 \right) \right]^{1/2} \quad (1.8)$$

$$f_{nm} = \frac{X_{nm} c}{2\pi a_e \sqrt{\epsilon_r}} \quad (1.9)$$

Eqn (1.8) is obtained by considering the radius of an ideal circular parallel- plate capacitor which would yield the same static capacitance after fringing is taken into account.

1.6.2.1 Magnetic current distribution

The field patterns and surface currents of circular disk patch for various modes are shown Fig. 1.14. The magnetic-current distribution around the edge of the disc for the nm^{th} mode is proportional to $\cos n(\Psi - \pi)$. This is illustrated in figure 1.15. for $n=0, 1, 2$ and 3 . It is independent of Ψ for modes with $n=0$ and undergoes three sinusoidal periods for modes with $n=3$.

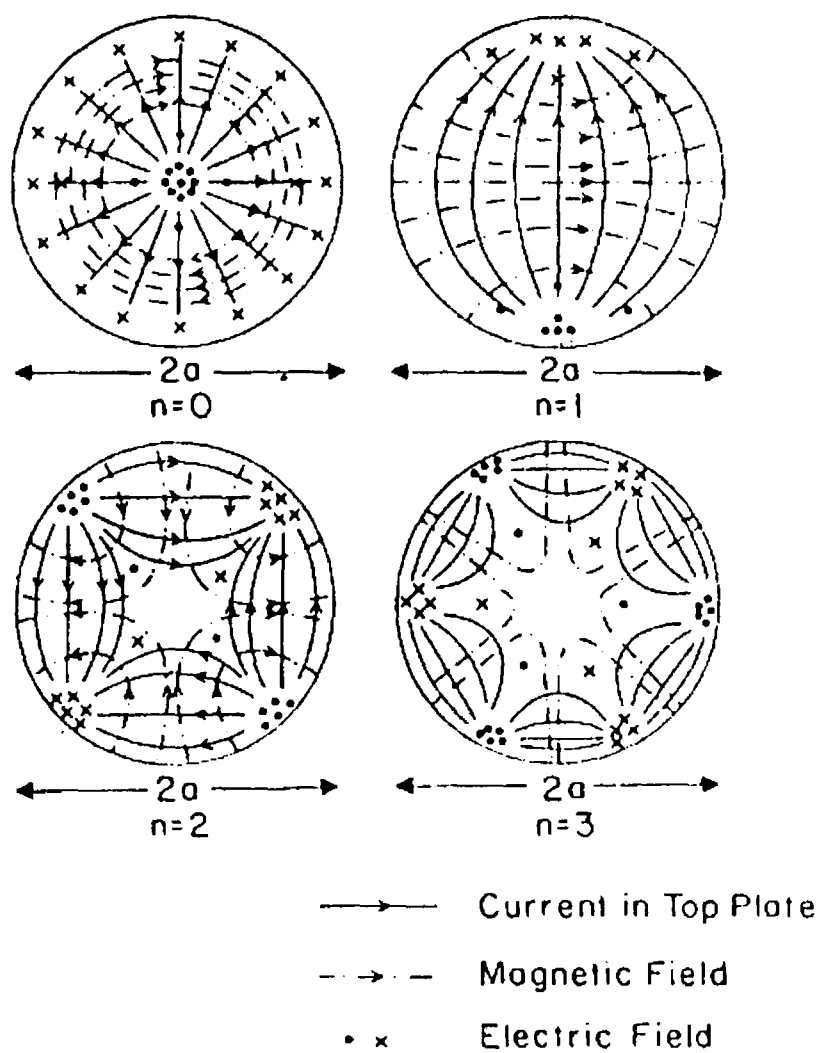


Fig. 1.14 Field patterns and surface currents for various modes

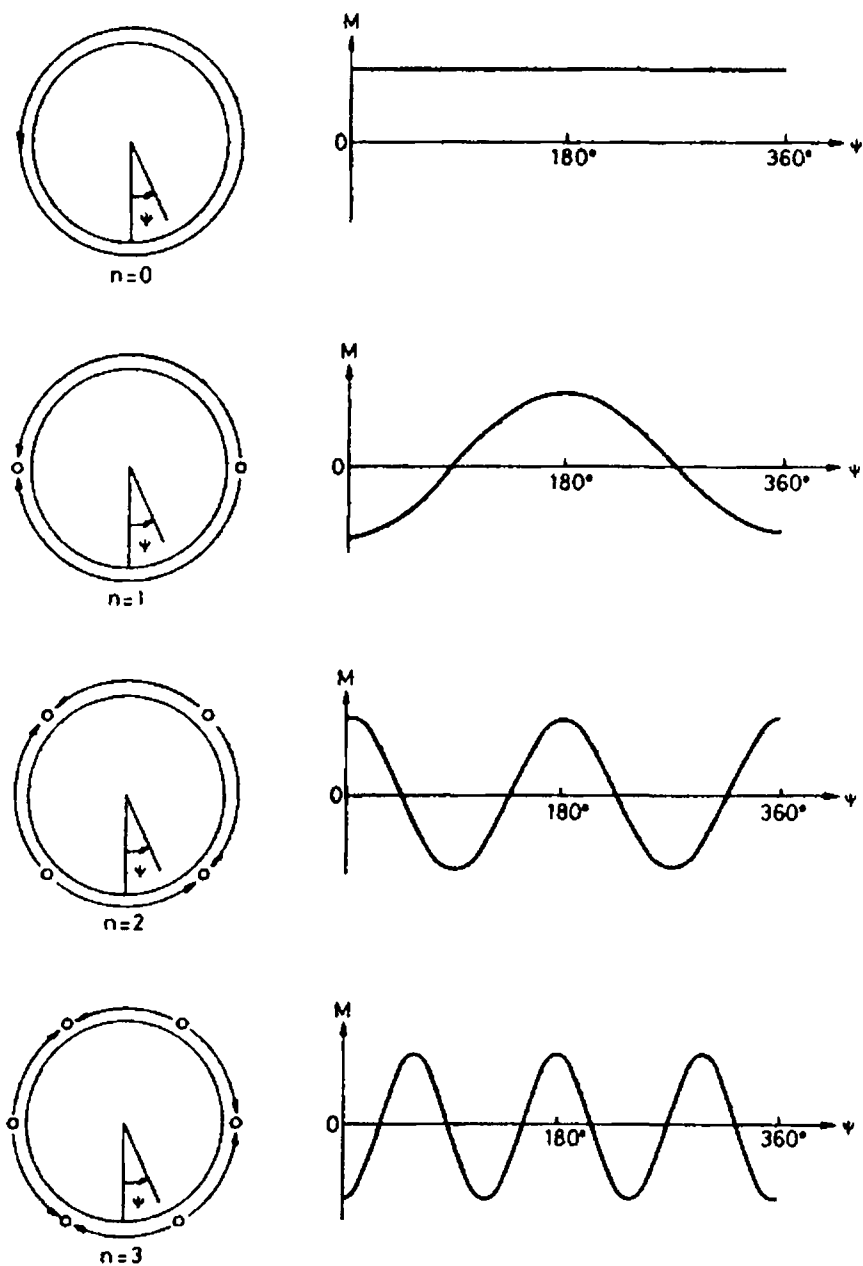


Fig. 1.15 Surface magnetic-current distribution of the various modes in the circular patch antenna

1.7 Outline of the present work

The practical applications of microstrip antennas for mobile systems are in portable or pocket-size equipment and in vehicles. Antennas for VHF/UHF hand-held portable equipment, such as pagers, portable telephones and transceivers, must naturally be small in size, light in weight and compact in structure. There is a growing tendency for portable equipment to be made smaller and smaller as the demand for personal communication rapidly increases, and the development of very compact hand-held units has become urgent.

In this thesis work, main aim is to develop a more and more reduced sized microstrip patch antenna. It is well known that the smaller the antenna size, the lower the antenna efficiency. During the period of work, three different compact circular sided microstrip patches are developed and analysed, which have a significant size reduction compared to standard circular disk antenna (the most compact one of the basic microstrip patch configurations), without much deterioration of its properties like gain, bandwidth and efficiency. In addition to this the interesting results, dual port operation and circular polarization are also observed for some typical designs of these patches. These make the patches suitable for satellite and mobile communication systems.

The theoretical investigations are carried out on these compact patches. The empirical relations are developed by modifying the standard equations of rectangular and circular disk microstrip patches, which helps to predict the resonant frequencies easily.

1.8 Organisation of the chapters

The second chapter briefly reviews the past work in the field of microstrip antennas, specifically compact microstrip antennas with enhanced properties like dual band operation and circular polarization. The methodology used for the

present work is discussed in the third chapter. It involves the detailed presentation of the experimental set up and the techniques used for the measurements of various antenna parameters. The results of the experimental investigations are presented in the fourth chapter. The measured radiation characteristics of different types of microstrip antennas like resonant frequency, return loss, bandwidth etc. are tabulated in this chapter. The fifth chapter leads us to the resonant frequency predictions of different geometries by suitably modifying the standard equations of rectangular and circular microstrip patch antennas. Resonant mode verification of the new patches are also carried out in this chapter. The conclusions drawn from experimental and theoretical studies are indicated in the sixth chapter. The chapter also gives some suggestions for future work in the field.

REVIEW OF THE PAST WORK

The rapid development of microstrip antenna technology began in the late 1970's. Recently, with the booming wireless mobile communications market, the urgency to design low volume, compact, low profile planar configuration antennas is even more pronounced. The relevant works in the field of development and analysis of microstrip antennas are reviewed in this chapter with emphasis given to compact microstrip patches.

2.1 DEVELOPMENT OF MICROSTRIP ANTENNAS

The concept of microstrip radiators was first proposed by Deschamps [11] as early as 1953.

In 1955, Gulton and Bassinot [12] in France patented a 'flat' aerial that can be used in the UHF region. Lewin [13] studied the radiation from the discontinuities in stripline.

The concept of microstrip radiator was not active until the early 1970's, when there was an immediate need for low profile conformal antennas on the emerging new generation missiles. The first microstrip radiator was constructed by Byron [14]. This antenna was a conducting strip, several wavelength long and half wavelength wide separated from a ground plane by a dielectric strip. The strip was fed at periodic intervals using co-axial connectors along the radiating edges and was used as an array. Munson [15] in 1974 demonstrated new class of microstrip wrap around antennas suitable for missiles using microstrip radiator and microstrip feed networks on the same substrate.

The basic rectangular and circular microstrip antennas were designed by Howell [16]. His low profile antenna consisted of planar resonating element separated from a ground plane by a dielectric substrate whose thickness was very small compared to the wavelength. Design procedures were presented for circularly polarized antennas and for dual frequency antennas from UHF through C band. The bandwidth obtained was very narrow and was found to be depending on permittivity and thickness of the substrate.

Sanford [17] presented the use of conformal microstrip array for L-band communication from KC-135 aircraft to the ATS-6 satellite. Weinschel [18] reported a practical pentagonal antenna in 1975.

Mathematical modeling by the application of transmission line analogies was first proposed independently by Munson [15] and Demeryd [19, 20]. This model explains the radiation mechanism and provides expressions for the radiation fields, radiation resistance, input impedance etc. for the patches of rectangular shape.

Radiation mechanism of an open circuited microstrip termination was studied by James and Wilson [21]. Theoretical and experimental pattern analysis of different radiating elements showed that they are similar to slot radiators.

Agarwal and Bailey [22] proposed the wire grid model for the evaluation of microstrip antenna characteristics. In this model, the microstrip radiating structure is modeled as a fine grid of wire segments. This method is useful for the design of microstrip antennas of different geometries like circular disc, circular segment and triangular patches.

Lo *et al.* [23, 24, 25] suggested a new mathematical technique, called cavity model, for the analysis of microstrip antennas. In this model, the region between the ground plane and the microstrip patch is viewed as a thin TM cavity bounded by magnetic wall along the edge and electric walls from above and below. Thus the fields in the antenna may be assumed to be those of a cavity. The antenna parameters of different patch geometries with arbitrary feed points can be calculated using this approach.

Carver and Coffey [26, 27, 28] formulated the modal expansion model, which is similar to cavity model. The fields between the patch and the ground plane is expanded in terms of a series of cavity resonant modes. Thus the patch is considered as a thin cavity with leaky magnetic walls. The impedance boundary conditions are imposed on the four walls and the stored and radiated energy were investigated in terms of complex wall admittances. The calculation of wall

admittance is given by Hammerstad [29] and more accurately by Alexopolus *et al.* [30].

Newman *et al.* [31, 32] proposed the method of moments for the numerical analysis of microstrip antennas. They used the Richmond's reaction method in connection with method of moments for calculating the unknown surface currents flowing on the walls forming the microstrip patch, ground plane and magnetic walls. This method can be adopted for the calculation of input impedance of microstrip antennas of nonstandard patch shapes.

Hammer *et al.* [33] developed an aperture model for calculating the radiation fields of microstrip antennas. This model accounts radiation from all the edges of the patch and can give the radiation field and the radiation resistance of any mode in a microstrip resonator antenna.

The circular microstrip patch has been rigorously treated by Butler [34]. He solved the problem of central fed circular microstrip antenna by considering the patch as a radiating annular slot, in which the radius of outer ring is very large. Butler and Yung [35] analysed the rectangular microstrip antenna using this technique.

For the numerical analysis of the patch antennas, Newman and Pozar [36, 37] developed the method of moments. They calculated the unknown surface currents flowing on the walls forming the microstrip patch, ground plane and magnetic walls using the Richmond's reaction method [38]. The reaction integral equation is solved using the method of moments.

Carver and Coffey [39] discussed a finite element approach for the numerical analysis of the fields interior to the microstrip antenna cavity.

Carver [40] analysed the circular microstrip patch and gave an accurate formulae for the resonant frequency of the patch. He showed that for the radiating patch, the resonant frequency is complex since the wall admittance is complex. A thorough investigation on the dependence of the resonant frequency on the various substrate parameters for the circular patch has been given by him.

Microstrip disc antenna has also been analysed by Derneryd [41] by calculating the radiation conductance, antenna efficiency and quality factor associated with the circular disc antenna.

Wood [42] proposed a technique for the production of circular polarization from a compact microstrip antenna based on radiation from curved microstrip transmission line supporting a single traveling wave. He has given the theoretical and experimental radiation patterns of circular sector antenna and a spiral antenna. Using these antennas he has achieved an impedance bandwidth of 40% at 10GHz. Mink [43] developed a circular microstrip antenna, which operates at a substantially low frequency compared to a circular patch antenna of the same size.

Newman and Tulyathan [44] analysed the microstrip patch antennas of different shapes using moment method. The patch is modeled by surface currents and the dielectric by volume polarization current. The theory is capable of accurately predicting antenna parameters but requires precise computation.

Chew and Kong [45] analysed the problem of circular microstrip disc antenna excited by a probe on thin and thick substrates. In the analysis unknown current was solved by vector Hankel transforms.

A full wave analysis of a circular disc conductor printed on a dielectric substrate backed by a ground plane was presented by Araki and Itoh [46]. The method was based on Galerkin's method applied in the Hankel transform domain.

Kuester *et al.* [47] reported a thin substrate approximation applied to microstrip antennas. The formulae obtained were found to be useful in simplifying the expression for the microstrip antenna parameters considerably.

Itoh and Goto [48, 49] modified the printed antenna with strips and slots to obtain dual frequency circularly polarized nature. Their antenna consisted of two different length strips and a slot excited by microstrip feed. The optimum parameters for the dual frequency operation were theoretically obtained and compared with the experimental data.

Das *et al.* [50] modified the ordinary circular patch antenna configuration by slightly depressing the patch conically into the substrate. This antenna gives a much larger bandwidth compared to ordinary antenna.

Sengupta [51] derived an expression for the resonant frequency of a rectangular patch antenna. Accuracy of the expressions for the patches of different sizes were compared with measured results.

The rectangular microstrip antenna has been extensively analysed by E. Lier *et al.* [52] for both finite and infinite ground plane dimensions.

H. Poes *et al.* [53] presented a more accurate and efficient method for the analysis of rectangular microstrip antennas. They modified transmission line model by incorporating the mutual coupling between the equivalent slots and by considering the influence of the side slots on the radiation conductance.

V. Palanisamy and R. Garg [54] presented two new geometries, which could be used as substitutes for rectangular microstrip antennas. They presented the theoretical and experimental results of rectangular ring and H-shaped antennas. Finally a comparison with the characteristics of ordinary rectangular patch antenna is also presented.

Penard and Daniel [55] used the cavity model for the analysis of open and hybrid microstrip antennas.

Das et al. [56] analysed the modal fields and radiation characteristics of microstrip ring antennas. The experiments conducted at 1.8GHz were compared with the theoretical patterns.

Richards et al. [57] analysed the annular, annular sector and circular sector microstrip antennas. The model expansion cavity model was used to predict the performance factors. The experiments done at L band for various antenna dimensions were reported.

Bhatnagar et al. [58] proposed a broadband microstrip antenna configuration for wideband operation. The configuration consists of one triangular patch placed parasitically over a driven patch.

A technique for achieving dual frequency operation in microstrip antennas was developed by Wang and Lo [59]. By placing shorting pins at appropriate locations in the patch, they were able to vary the ratio of the two band frequencies from 3 to 1.8. By introducing slots in the patch, this ratio can be made smaller.

Mahdjoubi et al. [60] constructed a dual frequency disc antenna. The input impedance and radiation patterns at both resonances were made identical by a double stub adjusting procedure. The analysis was done using cavity method.

C. K. Aanandan and K. G. Nair [61] presented the development of a compact and broadband microstrip antenna configuration. They used a number of parasitic elements, gap-coupled to a driven patch to get improvement in bandwidth.

A two-port rectangular patch antenna providing an accurate control of the radiated power is reported by A. Benella and K. C. Gupta [62]. They analysed the patch

with the input and output ports on the non radiating edges by using transmission line model.

D. M. Pozar and B. Kaufman [63] presented a broadband proximity coupled microstrip antenna configuration. The antenna consists of a microstrip patch coupled to a microstrip feed line below the patch. The antenna offered a bandwidth of 13%.

J. L. Drewniak and P.E. Mayes [64] proposed a simple, low-profile, broadband antenna with circularly polarized radiation pattern. The antenna is proposed to have 30% impedance bandwidth.

A. A. Kishk [65] presented the analysis of a spherical annular microstrip antenna. The input impedance of the patch is computed using the generalized transmission line model. Method of moments has been used for the computation of the radiation patterns. He observed that the sphere radius has significant influence on the input impedance and the resonant frequency.

T. Kashiwa et al. [66] demonstrated the analysis of rectangular microstrip antennas mounted on the curved surface using the curvilinear FDTD method. The numerical results agreed well with almost all the experimental results and this confirms the validity of the technique.

The near fields of single layer microstrip patch antennas computed through an iterative method is presented by S. A. Bokhari et al. [67]. A combination of mixed potential integral equation method, the FFT algorithm and the biconjugate gradient resulted in an efficient numerical solution. The computed results are compared with measured results.

A proximity coupled rectangular microstrip antenna giving circular polarization is demonstrated by H. Iwasaki [68]. The feeding arrangement consists of a

microstrip line placed offset from the centre of a rectangular microstrip antenna. A practical antenna suitable for applications in phased arrays with an axial ratio of less than 0.3db is realized.

A fast full-wave analysis technique that can be used to analyze the scattering and radiation from large finite arrays of microstrip antennas was presented by C. F. Wang et al. [69].

J. -Y. Sze and K. -L. Wong [70] presented a slotted rectangular microstrip antenna for bandwidth enhancement. With the loading of a pair of right -angle slots and a modified U-shaped slot in the patch, bandwidth enhancement of microstrip antennas is demonstrated.

Yen-Liang Kuo and Kin-Lu Wong [71] designed a dual band planar inverted- L patch antenna suitable for applications in Wireless Local Area Network (WLAN) and High- Performance Radio Local Area Network [HIPERLAN] systems. By using an inverted-L radiating patch, in which two additional narrow slits are inserted at the radiating edge to effectively control the excited patch surface current distributions, the proposed antenna can generate two operating frequencies at 2.4 and 5.2 GHz.

Excitation of a low-profile equilateral-triangular dielectric resonator antenna using a conducting conformal strip was described by H. Y. Lo and K. W. Leung [72]. This configuration has a wider impedance bandwidth (5.5%) and a higher front-to-back radiation ratio. The return loss, radiation patterns and antenna gain are measured and discussed.

2.2 COMPACT MICROSTRIP ANTENNAS

A tremendous amount of work has been done since 1997 to improve microstrip antennas for communication applications. Recently miniaturization of microstrip

antennas is highly desirable in portable communication equipment. A review of compact and dual band microstrip antennas is presented in this section.

V. Palanisamy and R. Garg [73] reported H-shaped and rectangular ring microstrip antennas as substitute to commonly used rectangular patch antennas. They found that the H-shaped patch antenna requires very less area compared to the rectangular patch antenna.

C. K. Aanandan and K. G. Nair [74] developed a compact broadband microstrip antenna configuration. The system uses a number of parasitic elements which are gap coupled to a driven patch. They achieved a bandwidth of 6% without deteriorating the radiation pattern.

G. Kossiavas et al. [75] presented C-shaped microstrip radiating element operating in the UHF and L bands. Its dimensions are found to be smaller than those of conventional square or circular elements.

The frequency reduction obtained through loading the patch antenna with a dielectric resonator is demonstrated by E. K. N. Yung et al. [76]. They observed that the resonant frequency of a circular microstrip antenna decreases with the position of the DR on the antenna

Supriyo Dey et al. [77] modified the geometry of an ordinary microstrip circular patch antenna by putting two sectoral slots shunted by conducting strips to get reduced resonant frequency. They were able to achieve 19% reduction in resonant frequency by this method.

By using a very small number of thin shorting posts, instead of a complete short circuit, M. Sanad [78] showed that the size of a quarter wavelength antenna could be reduced considerably without any degradation in the gain of the antenna.

Y. Zhang [79] studied the feasibility of miniaturisation of the antennas used for microcellular and personal communications by using barium titanate as superstrate in microstrip antennas designed on 900 MHz and 1800 MHz bands.

S. Dey et al. [80] proposed the design of a compact, low-cost wide band circularly polarized antenna suitable for personal communication applications. The configuration consists of four shorted rectangular patches. Two of them are fed directly and the others are fed parasitically.

M. G. Douglas and R. H. Johnston [81] demonstrated the U patch antenna. This antenna may be used as an alternative to the half wave square patch antenna, but it requires only one third to one quarter of the surface area of the square half wave antenna.

Jacob George et al. [82] proposed a broad band low profile microstrip circular patch antenna. Four sectoral slots are cut on the circular patch antenna with a uniform intersectoral angle 90° and a slot angle 8° . The antenna requires about 59.8% lesser area compared to an ordinary circular patch antenna resonating at the same frequency.

R. Waterhouse [83] presented a probe fed circular microstrip antenna which incorporates a single shorting pin. The presence of the shorting pin significantly reduces the overall size of the antenna. Experimental and theoretical impedance behaviour and radiation characteristics of the modified patch are given. Very good agreement between experiment and theory are achieved.

A broad band dual frequency circular sided microstrip antenna was proposed by M. Deepukumar et al. [84]. This antenna provides two independent ports with orthogonal polarization and gain comparable to that of a standard circular patch antenna. The structure resonates at two frequencies with large impedance bandwidth. Energy is coupled electromagnetically to these ports using two

perpendicular microstrip feedlines. The antenna offers excellent isolation between its ports which is essential in avoiding crosstalk. A formula for calculating the resonant frequencies of the two ports is also proposed.

J. George et al. [85] developed a compact drum shaped microstrip antenna with considerable reduction in size, with similar radiation characteristics to those of an equivalent rectangular patch antenna. A relationship has been suggested for finding out the resonant frequency of the new geometry, and its validity has been established by the experimental results.

D. Sanchez-Hernandez et al. [86] presented a dual-band circularly polarized microstrip antenna with a single feed by using two spur-line band-stop filters within the perimeter of the microstrip patch. This is obtained without increasing either the size or the thickness of the patch.

Z. D. Liu and P. S. Hall [87] suggested a planar dual band inverted F-antenna for hand held portable telephones. The dual-band antenna is almost the same size as a conventional inverted F-antenna operating at 0.9GHz, and has an isolation between bands of better than 17dB.

A compact microstrip antenna by loading a triangular patch antenna with a shorting pin was reported by Kin-Lu Wong and Shan-Cheng Pan [88]. This antenna can significantly reduce the antenna size at a given operating frequency. Variation of resonant frequency of the triangular microstrip patch with different shorting-pin positions are studied and comparisons of the compact and conventional triangular microstrip antenna are also discussed.

M. Sanad [89] developed a compact microstrip antenna suitable for application in cellular phones. It consists of a driven element and five small parasitic patches distributed in two stacked layers. The two layers have similar geometries and their

dimensions are almost equal. This antenna operates at two separate frequency with broad bandwidths.

A small broadband rectangular microstrip antenna with chip-resistor loading was reported by Kin-Lu Wong and Yi-Fang Lin [90]. Designs of a chip-resistor-loaded rectangular microstrip antenna fed using a probe feed or an inset microstrip-line feed are presented. These antenna designs have the advantages of small antenna size and wide antenna bandwidth, compared to a conventional rectangular microstrip antenna.

I. Park and R. Mittra [91] demonstrated a quarter-wave aperture-coupled microstrip antenna with a shorting pin. This antenna requires less than half the size of conventional microstrip antenna and hence is suitable for applications where only a limited area is available for the installation of the antenna.

Kin-Lu Wong and Jian-Yi Wu [92] developed a single-feed small circularly polarized square microstrip antenna by cutting slits in the square patch. By adjusting the length of the slits, the microstrip antenna can perform CP radiation with a reduced patch size at a fixed operating frequency. This design also provides a wide CP bandwidth and relaxed fabrication tolerances.

S. Dey and R. Mittra [93] presented the design and development of a compact microstrip patch antenna. The length of the antenna is only one eighth of the effective wavelength at resonance. They used method of moments for the analysis of the current distribution on the patch surface.

Chia-Luan Tang et al. [94] demonstrated a small circular microstrip antenna with dual frequency operation by using a single shorting pin and a single probe feed. This dual-frequency design can result in a much reduced antenna size and provide a tunable ratio of ~ 2.55 - 3.83 for the two operating frequencies.

A dual-frequency triangular microstrip antenna with a shorting pin was designed by Shan-Cheng Pan and Kin-Lu Wong [95]. By varying the shorting pin position in the microstrip patch, such a design can provide a large tunable frequency ratio of about 2.5-4.9 for the two operating frequencies. Experimental results are presented and discussed.

T. K. Lo et al. [96] used a high permittivity substrate for the design of a miniature microstrip antenna. The aperture-coupling is used for feeding power and the gain of the antenna has been increased by badding superstrates of appropriate thickness. Experimental data for the return loss, radiation pattern and measured antenna gain are presented for a 1.66GHz antenna. Here size reduction is obtained without much alterations in the electrical performance of the antenna compared to an ordinary antenna fabricated on a low dielectric constant substrate. The antenna gain is 5.3 dB, and the patch size is greatly reduced to one fifth of that of the conventional microstrip antenna.

R. B. Waterhouse [97] presented a small printed shorted antenna that significantly reduces the cross-polarised fields generated. The cross-polarised fields have been measured at more than 20dB below the co-polar levels. The shorted patch is approximately a quarter-wavelength in size and has a bandwidth comparable to a conventional microstrip patch antenna.

The design of a single-feed, reduced-size dual frequency rectangular microstrip antenna with a cross slot of equal length was presented by Kin-Lu Wong and Kai-Ping Yang [98]. The frequency ratio of the two operating frequencies is mainly determined by the aspect ratio of the rectangular patch, and the reduction in the two operating frequencies is achieved by cutting a cross slot in the microstrip patch. The experimental results for such a design are presented and discussed.

Kin-Lu Wong and Wen-Shan Chen [99] studied the characteristics of a single-feed dual-frequency compact microstrip antenna with a shorting pin are studied

experimentally. Besides the compactness of the antenna, this dual-frequency design can provide a high frequency ratio of > 3.0 between the two operating frequencies. Typical experimental results of the proposed antenna are presented and discussed.

The design of a circularly polarized broadband square microstrip antenna fed along a diagonal with a pair of suitable chip resistors located along the centerline was presented by Kin-Lu Wong and Jian-Yi Wu [100]. This design provides a wider bandwidth for circular polarization radiation about two times that of a similar design with a pair of shorting posts. The antenna design and experimental results are presented.

Circularly polarized microstrip antenna with a tuning stub was designed by Kin-Lu Wong and Yi-Fang Lin [101]. Details of the antenna designs are described and experimental results are presented and discussed.

Jui-Han Lu et al. [102] designed a compact circular polarization design for a single feed equilateral-triangular microstrip antenna with inserted spur lines at the patch edges. It is found that, with increasing spur-line length, the resonant frequency of the triangular microstrip patch is significantly lowered. Also, by further adjusting the inserted spur-lines to have a length ratio of 0.96, the proposed design can achieve CP radiation at a much lowered operating frequency, resulting in compact triangular microstrip antennas with circular polarization.

H.T. Chen [103] experimentally studied the characteristics of compact microstrip antennas and compared them with those of conventional microstrip antennas. Compactness achieved through the placement of shorting pin and through meandering are studied.

K. L. Wong and K. P. Yang [104] implemented a modified planar antenna operating in the 800 MHz band with reduced size and enhanced impedance band

suitable for applications in hand-held communication equipment. They achieved compactness through meandering the patch and bandwidth enhancement through the placement of a chip resistor.

A gain-enhanced compact broadband microstrip antenna with the loading of a high permittivity superstrate layer and a 1Ω chip resistor was presented by Chin-Yu Huang et al. [105]. Here the antenna size reduction and bandwidth improvement are mainly due to the chip-resistor loading effect, while the gain enhancement to compensate the antenna gain decrease due to patch size reduction and ohmic loss of the loading chip resistor is mainly achieved by the loading of a high permittivity superstrate layer.

A. S. Vaello and D. S. Hernandez [106] presented a bow-tie antenna similar to the drum-shaped antenna for dual frequency operation. The antenna requires very lesser size compared to conventional patch antennas and have similar radiation characteristics.

A miniaturized C-patch antenna excited by means of a coaxial probe was described by L. Zaid et al. [107]. The antenna consists of two stacked C-shaped elements connected together with a vertical conducting plane. The antenna is designed on an air substrate and offers attractive dimensions, being five times lower than those of a conventional half wavelength microstrip patch antenna operating at the same frequency. The voltage standing wave ratio, radiation patterns, and electric surface current density are presented.

Kin-Lu Wong and Ming-Huang Chen [108] implemented a design of small slot-coupled circularly polarized circular microstrip antenna with a modified cross-slot cut in the patch and a bent tuning-stub aligned along the patch boundary is proposed and experimentally studied. Results show that, for fixed circular polarization (CP) operation, the antenna proposed can have an antenna size reduction of $\sim 80\%$, as compared to a regular-size CP design.

A compact circular polarization (CP) design for a single feed equilateral-triangular microstrip antenna with inserted spur lines at the patch edges was presented by Jui-Han Lu et al. [109]. It is found that, with increasing spur-line length, the resonant frequency of the triangular microstrip patch is significantly lowered. Also, by further adjusting the inserted spur lines to have a length ratio of ~ 0.96 , the proposed design can achieve CP radiation at a much lowered operating frequency, resulting in compact triangular microstrip antennas with circular polarization.

A slot-loaded bow-tie microstrip antenna for dual-frequency operation was reported by Kin-Lu Wong and Wen-Shan Chen [110]. This is achieved by loading a pair of narrow slots close to the radiating edges of the bow-tie microstrip antenna. Various frequency ratios, within the range 2-3, of the two operating frequencies can be obtained by varying the flare angle of the bow-tie patch. Details of the antenna design and experimental results are presented and discussed.

J. George et al. [111] presented a single feed dual frequency compact microstrip antenna with a shorting pin. This antenna configuration gives a large variation in frequency ratio of the two operating frequencies, without increasing the overall size of the antenna.

A single-feed dual-band circularly polarized microstrip antenna was demonstrated by Gui-Bin Hsieh et al. [112]. By embedding two pairs of arc-shaped slots of proper lengths close to the boundary of a circular patch, and protruding one of the arc-shaped slots with a narrow slot, the circular microstrip antenna can perform dual-band CP radiation using a single probe feed. Details of the antenna design and experimental results are presented.

Kin-Lu Wong and Jia-Yi Sze [113] presented a dual-frequency slotted rectangular microstrip antenna with a pair of properly bent narrow slots close to its non-radiating edges. The two operating frequencies have parallel polarization planes and similar broadside radiation patterns, and the frequency ratio of the two frequencies is controlled by the bent angle of the embedded slots. Details of the obtained dual-frequency performance are presented and discussed.

A double U-slot rectangular patch antenna was described by Y. X. Guo et al. [114] Using a foam layer of thickness $\sim 9\%$ wavelength as the supporting substrate, an impedance bandwidth of 44% is achieved.

Kin-Lu Wong and Jen-Yea Jan [115] presented a broadband circular microstrip antenna with embedded reactive loading. The reactive loading is provided by a microstrip structure of cascaded microstrip-line sections embedded inside a slot cut in the circular patch. By this design, a bandwidth of ~ 3.2 times that of a conventional circular microstrip antenna can be obtained. Experimental results of the antenna performance are presented and discussed.

A dual-frequency planar antenna for cellular telephone handsets was designed by N. Chiba et al. [116]. This antenna operates in ~ 0.9 and 1.8 GHz bands and has almost the same size as a conventional internal antenna operating in the 0.9GHz band.

A wideband microstrip antenna with dual-frequency and dual-polarisation operation was proposed by Yeunjeong Kim et al. [117]. This enables the transmission and reception of differently polarized wideband signals simultaneously with a single antenna system. The measured bandwidths for 15dB return loss at dual frequencies are 9.02 and 12.4%, respectively.

Jui-Han Lu [118] designed a dual frequency rectangular microstrip antenna with a pair of step-slots embedded close to its non-radiating edges. The two operating

frequencies have the same polarization planes and similar broadside radiation characteristics. By adjusting the step ratio of the step-slots, the frequency ratio of the two operating frequencies is tunable in the range ~ 1.23 - 1.63 . Details of the antenna design and experimental results are presented and discussed.

A broadband stacked shorted patch antenna with significantly improved impedance behaviour was reported by R. B. Waterhouse [119]. It has a 10dB return loss bandwidth of greater than 30%. The antenna is relatively easy to manufacture and can be accommodated on a mobile communication handset terminal.

E. Lee et al. [120] presented a compact, dual-band dual polarization antenna capable of generating two distinct frequencies with different polarisation and radiation pattern characteristics: a monopolar mode for terrestrial cellular communication and a circularly polarized, upward oriented pattern for satellite mobile. Bandwidths of 2 and 4%, respectively, have been obtained in the two modes.

A small dual patch antenna was designed by R. Chair et al. [121]. Compared with a basic single layer patch antenna with the same projection area, the resonant frequency is reduced by 39%. The bandwidth is 5%; the cross-polarisation level is less than -15dB.

Manju Paulson et al. [122] demonstrated a compact microstrip antenna with circular polarization radiation. This configuration provides an area reduction of 42% compared to a standard rectangular patch antenna at the same frequency, and a 3dB CP bandwidth of $\sim 1\%$ has been obtained.

Experimental studies on a dual-band dual-polarized compact microstrip antenna were presented by S. O. Kundukulam et al. [123]. This antenna configuration provides an area reduction of 40% compared to a standard rectangular antenna

operating at the same frequency without much degradation of the gain. The antenna structure can also be modified to achieve the desired ratio between the two resonant frequencies.

Manju Paulson et al. [124] presented a compact dual-band, dual polarized microstrip antenna resonating at two frequencies with different polarizations: a linearly polarized one for terrestrial communication, and a circularly polarized one for satellite mobile communication. This antenna also provides an area reduction of 70% compared to standard rectangular patch antenna.

A slot-loaded compact arrow-shaped microstrip antenna with a pair of narrow slots close to its radiating edges for dual frequency operation was presented by Sona O Kundukulam et al. [125]. The two frequencies have parallel polarization planes and similar radiation characteristics. The ratio between the two operating frequencies can be tuned in the range (1.14-1.24), which is much smaller than that of similar designs. The antenna has an area reduction of ~75% compared to the standard rectangular patch.

A. K. Shackelford et al. [126] presented the simulated results for a small-size probe-fed notched patch antenna with a shorting post. The area of the patch has been reduced by 94%, while the antenna maintains a bandwidth of 13.2%.

A small broadband semicircular patch antenna with an L-probe feeding was presented by Y. X. Guo et al. [127]. Using a foam layer thickness $\sim 0.12\lambda_0$ as a supported substrate, an impedance bandwidth of 57% ($SWR \leq 2$) and a gain of over 4.0dBi in the whole band have been obtained.

METHODOLOGY - EXPERIMENTAL SET UP AND MEASUREMENT TECHNIQUES

The chapter describes the basic facilities and fabrication technique employed in the development of different microstrip antenna geometries. Experimental set up and measurement techniques employed for the work are explained briefly. IE3D simulation software used for the analysis of different microstrip patches is also described in this chapter.

3.1 ANTENNA FABRICATION

The microstrip antenna is fabricated using chemical etching of the patch on a substrate. The pattern to be etched is obtained either by photolithographic process or fast fabrication technique. All the measurements described in this thesis are on antennas resonating at low frequencies, which are fabricated by fast fabrication technique.

The different steps employed in this process of fabrication are shown in Fig. 3.1. Two pieces of substrates (one for the patch geometry and other for the microstrip feedline for proximity coupling) are to be used for fabrication of an antenna. Copper clad substrate of required size is taken and thoroughly cleaned (a). Drawing of the geometry is made on one side (b). The top metallised plane of the substrate is covered completely with transparent cellophane tape (c). The tape is then selectively removed from the top layer by means of a sharp tipped cutting tool in such a way that tape over the patch remains unaltered (d). The exposed top and bottom metallisation regions are etched out using concentrated nitric acid (e). After the etching process, tape is removed from top plane and cleaned once again. This method is fast and simple compared to photolithographic technique.

3.2 EXCITATION TECHNIQUE

Electromagnetic coupling is used for feeding different microstrip patches described in the remaining chapters of this thesis. The geometry is discussed in chapter 1. An SMA connector is soldered to a microstrip line of characteristic impedance of 50Ω and is placed below the patch geometry to couple electromagnetic energy. The design of microstrip feed line used for the antenna measurements is explained in chapter 5.

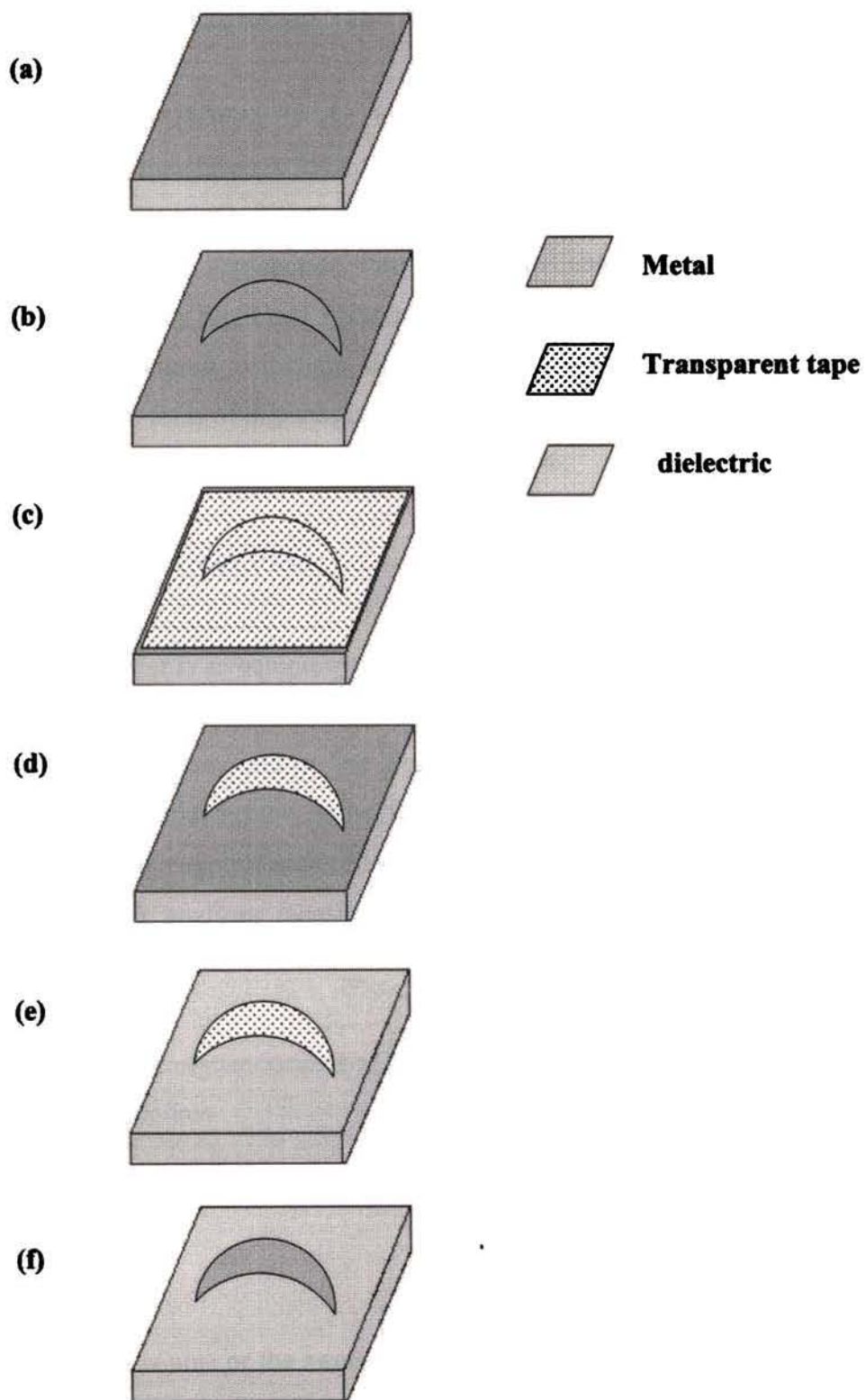


Fig. 3.1 Different steps in the fast fabrication process

3.3 ANTENNA MEASUREMENTS

Network analyzer (NWA) is the basic measuring equipment used for the measurement of impedance, VSWR, attenuation, and radiated power. It makes use of directional couplers to separate the direct and reflected waves at the input of the device under test. In conjunction with a swept frequency signal generator, the NWA can make very rapid and accurate measurements. Moreover, these devices are often manufactured to include digital processors and plotting equipment so that output in the form of a graph, (eg. Input impedance versus frequency) can be obtained either as a CRT display or in hard copy form.

3.3.1 NETWORK ANALYSER

A network analyzer is an equipment incorporating swept-frequency measurements to completely characterize the complex network parameters without any degradation of accuracy and in less time. Two types of network analysers are available, scalar and vector network analysers. A scalar network analyzer measures only the magnitudes of reflection and transmission coefficients, whereas a vector network analyzer measures both magnitude and phase of the above parameters.

A vector network analyzer consists of the following systems:

- 1) A microwave source
- 2) Test set
- 3) Signal processor
- 4) Display unit

The synthesized source or the sweep oscillator will provide the RF stimulus. The source is connected to the reflection transmission unit or S-parameter test set. Here the different scattering parameters are separated and down converted to

20MHz and fed to the IF detector. The detected signal is processed and fed to the display unit for output.

The antenna measurements are done using HP 8510C Network analyzer. Schematic diagram is shown in Fig. 3.2.

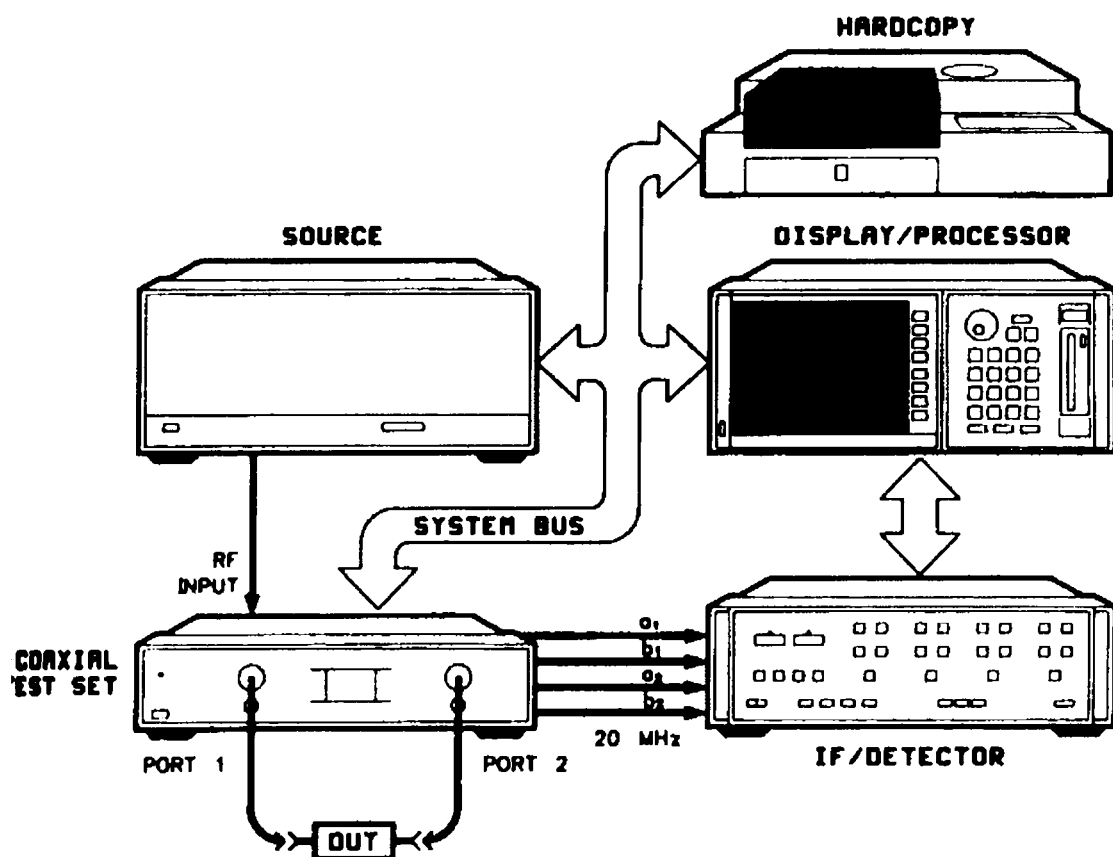


Fig. 3.2 Schematic diagram of the HP 8510C network Analyser

3.3.2 MEASUREMENT OF RETURN LOSS, RESONANT FREQUENCY AND BANDWIDTH

Network Analyser (Fig. 3.2) is calibrated for one port (port1) and the test antenna is connected to PORT1 of the S-parameter test set. The measured S_{11} LOGMAG data in the Network Analyser is acquired and stored in ASCII format in the computer interfaced with NWA (as shown in Fig. 3.3), using MERL Soft (The software for antenna studies developed by the microwave group of the Department of Electronics)

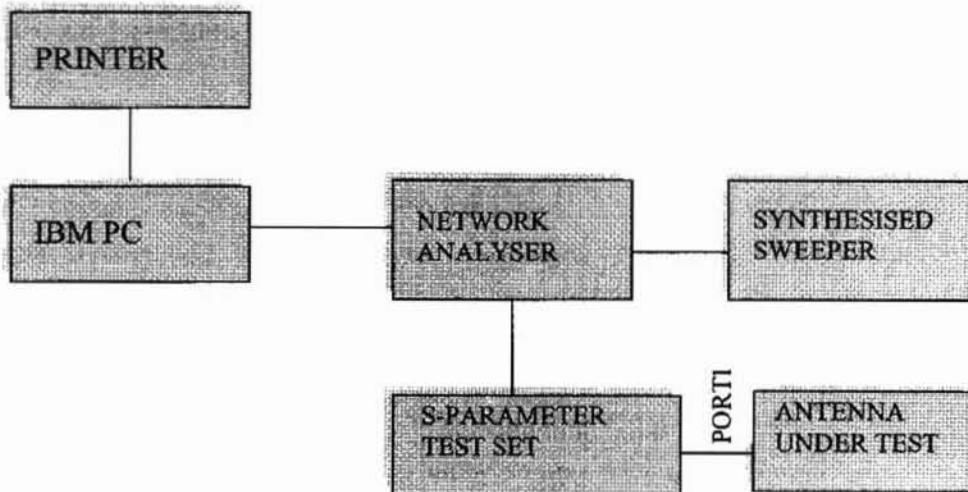


Fig. 3.3 Experimental set up for the measurement of return loss and resonant frequency

The resonant frequency of the antenna is determined from the dip of return loss curve. The impedance bandwidth can be measured by noting the range of frequencies (Δf) over which the return loss is greater than or equal to 10dB. Percentage bandwidth is calculated using the expression

$$\frac{\Delta f}{f_r} 100\%, \text{ where } f \text{ is the center frequency of the operating band.}$$

3.3.3 MEASUREMENT OF RADIATION PATTERN

The radiation pattern represents the spatial distribution of the electromagnetic field radiated by an antenna. Generally the patterns in the two principal planes are taken. The principal E-plane is the plane containing the electric field vector and the direction of maximum radiation, and the principal H-plane is the one containing the magnetic field vector and the direction of maximum radiation.

The copolar and cross-polar E-Plane and H-plane radiation patterns of the test antenna are measured by keeping the antenna inside an anechoic chamber in the receiving mode. The experimental arrangement for the measurement is shown in Fig. 3.4. A wide-band horn is used as the transmitter.

HP 8510C Network Analyzer, interfaced to an IBM PC, is used for the pattern measurement. The PC is also attached to a STIC 310C position controller. The test antenna is mounted on the antenna positioner kept inside the anechoic chamber (Fig.3.4). The test antenna and the transmitting antenna are connected to Port 2 and Port 1 respectively of the network analyzer.

The radiation patterns of the antenna at multiple frequency points can be measured in a single rotation of the test antenna positioner by using MERL Soft. The positioner will stop at each step angle and take S_{21} measurements at different frequency points in the operating band. The process is repeated till it reaches the stop angle. The entire measured data are stored in ASCII format and can be used for further processing like analysis and plotting. The different pattern characteristics like half power beam width, cross-polar level etc. are obtained after the analysis of the stored patterns.

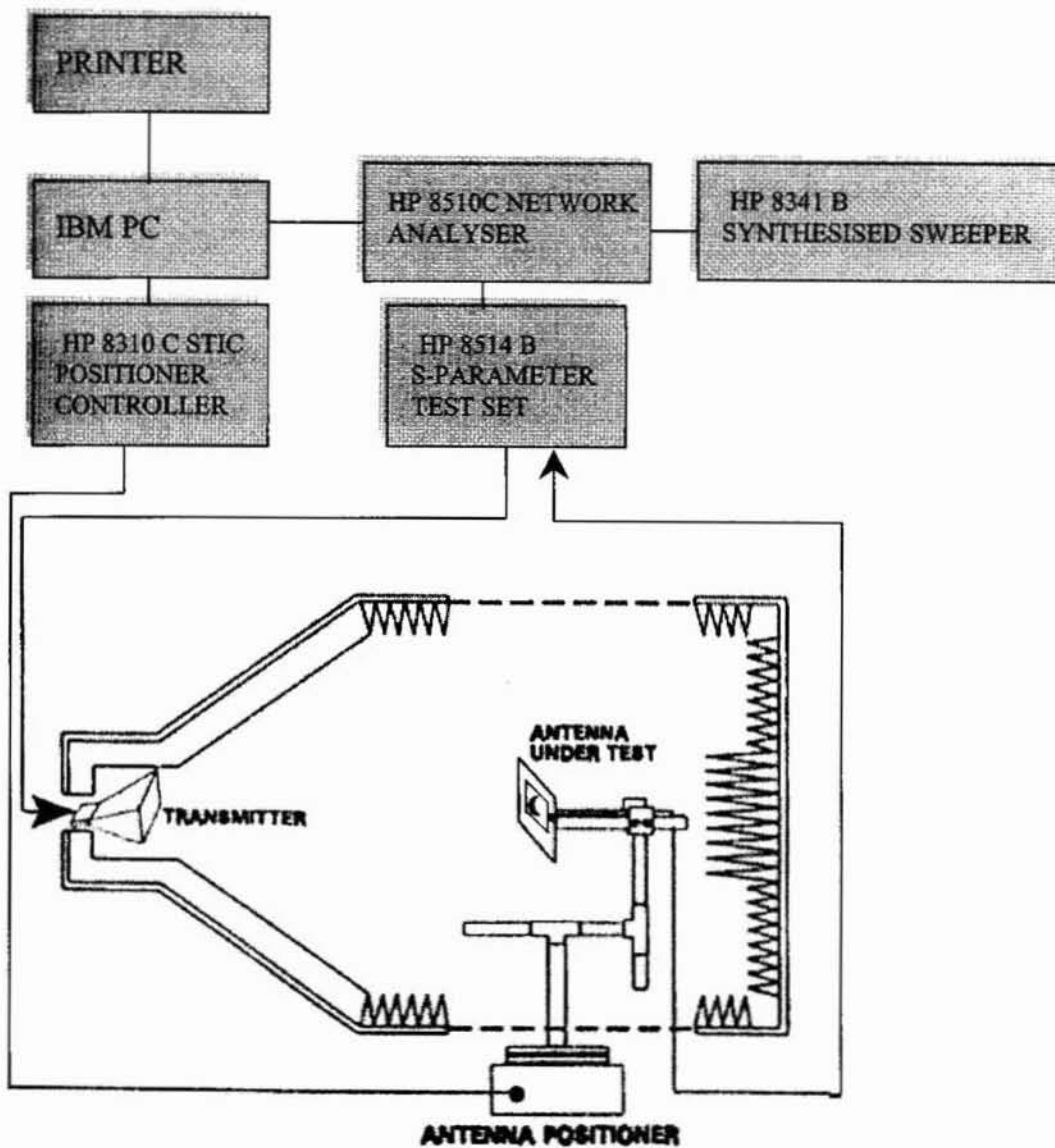


Fig. 3.4 Set up for measuring the radiation pattern of the antenna

3.3.4 MEASUREMENT OF GAIN

The setup for the measurement of gain is the same as that used for pattern measurement. The relative gain of the new antenna is measured with a standard circular patch antenna operating at the same frequency and fabricated on the same substrate.

The standard circular microstrip antenna is kept inside the anechoic chamber and connected to PORT 2 of the Network Analyzer. Port 1 is connected to the transmitting antenna. The antenna is bore-sighted and a THRU RESPONSE calibration is performed in the Network Analyzer and stored in the CAL SET. This will act as the reference gain response. The standard antenna is now replaced by the corresponding test antenna and the plot displayed on the Network Analyzer will directly give the relative gain of this antenna with respect to the circular disk.

3.3.5 MEASUREMENT OF AXIAL RATIO FOR CIRCULARLY POLARISED MICROSTRIP ANTENNA

For this measurement also, the set up is same as that used for pattern measurement. Keeping the test antenna stationary, polarization of the transmitting antenna is changed by rotating it through 360° and maximum and minimum of the power received are noted. Axial ratio at a particular frequency is calculated as follows:

$$\text{Axial Ratio} = \text{Maximum Power in dB} - \text{Minimum Power in dB}$$

The S_{21} measurements are taken for each frequency points at an interval, over a particular band, and the range of frequency over which the axial ratio is less than or equal to 3dB is noted. This is called as 3dB axial ratio band width.

3.3.6 IE3D SIMULATION TECHNIQUE

Electromagnetic simulation yields high accuracy analysis and design of complicated microwave and RF printed circuits, high speed digital circuits and antennas. IE3D is an integrated full-wave electromagnetic simulation and optimization package for the analysis and design of 3-dimensional microstrip antennas and high frequency printed circuits and digital circuits, such as microwave and millimeter-wave integrated circuits (MMICs) and printed circuit boards (PCBs).

To perform an electromagnetic simulation, a user starts from the layout editor MGRID. On MGRID, a user draws a circuit as a group of polygons. After he finishes constructing the polygons and defining the ports, he can invoke the simulation engine IE3D to perform an electromagnetic simulation.

There are mainly four window configurations as MGRID, MODUA, CURVIEW, and PATTERNVIEW for the use of our application. MGRID is a layout editor for the construction of a geometry. MODUA is the schematic editor for measured parameter display. The CURVIEW window is a post processor for display and animation of current distribution and field distribution, whereas PATTERNVIEW has a role of post processor for radiation patterns.

The IE3D simulation of a microstrip patch with an electromagnetically coupled feed is going to be explained here briefly, including the important steps during the running procedure as follows:

As the first step, run MGRID. Then select a new file from the **File** menu. Select the length unit as required. Now MGRID prompts for the **layout and grid**. Input the layout and grid as we choose and select **OK** to continue. The next step is to define the different substrate layers. A number of substrate layers can be defined easily by inputting their thickness and dielectric constant. Then we have to define the discretization parameters, highest frequency and the number of cells per

wavelength as per the requirement. Now the MGRID window is ready for a structure to be drawn, by initializing its parameters.

Next step is to draw the polygon or the desired geometry either by connecting the vertices or selecting from the **Entity** menu. For the case of electromagnetic coupling, the feed structure is also to be drawn in the lower layer of substrate. Now we need to define the port. The simulation engine will not run without any port on a structure. A port is defined on polygon edges. Select item **probe feed to patch** from the entity menu and input the coordinates. Electromagnetically fed microstrip patch geometry in MGRID window is shown in Fig. 3.5.

The next necessary step is to save the geometry. For this, select **Save** in **File** menu. Now the geometry is saved as a **.geo** file.

Select item **Gridding** in menu **Process**. This process is not necessary for a simulation. The gridding process here is just to give the user an idea how a circuit is meshed. Now the meshed circuit will be displayed on the window, as shown in Fig. 3.6.

We have constructed the circuit now. The next step is to perform an electromagnetic simulation. Select **Set Simulation** in **Process** menu. The Simulation Setup dialog box is invoked as shown in figure Fig. 3.7. Enter start, stop and no. of frequencies. Select **OK** to continue. Checking of **Adaptive Intelli-Fit** will make the simulation more faster. This scheme yields accurate results over a wide bandwidth by just simulating a few frequency points.

After the simulation is finished, the MODUA simulator is invoked automatically to display the data in Smith chart as shown in Figure 3.8(a). We can select the **Define Display Data** or **Define Display Graph** in **Control** menu for displaying the **dB and Phase of S-Parameters** like S_{11} , S_{22} and S_{21} (Fig. 3.8(b)).

For the calculation and display of radiation patterns and current density distribution, the running procedure is similar to that explained above. In the Set Simulation Dialog box, disable **Adaptive Intelli-Fit**. Check the **Radiation Pattern File** check box and **Current Distribution File** will be checked automatically. Then select **OK** to continue. The calculated data of radiation pattern and current distribution are saved as **.pat** and **.cur** extension files. The display of radiation pattern and current distribution of a particular geometry can be observed in **PATTERNVIEW** and **CURVIEW** windows respectively as shown in figure 3.10.

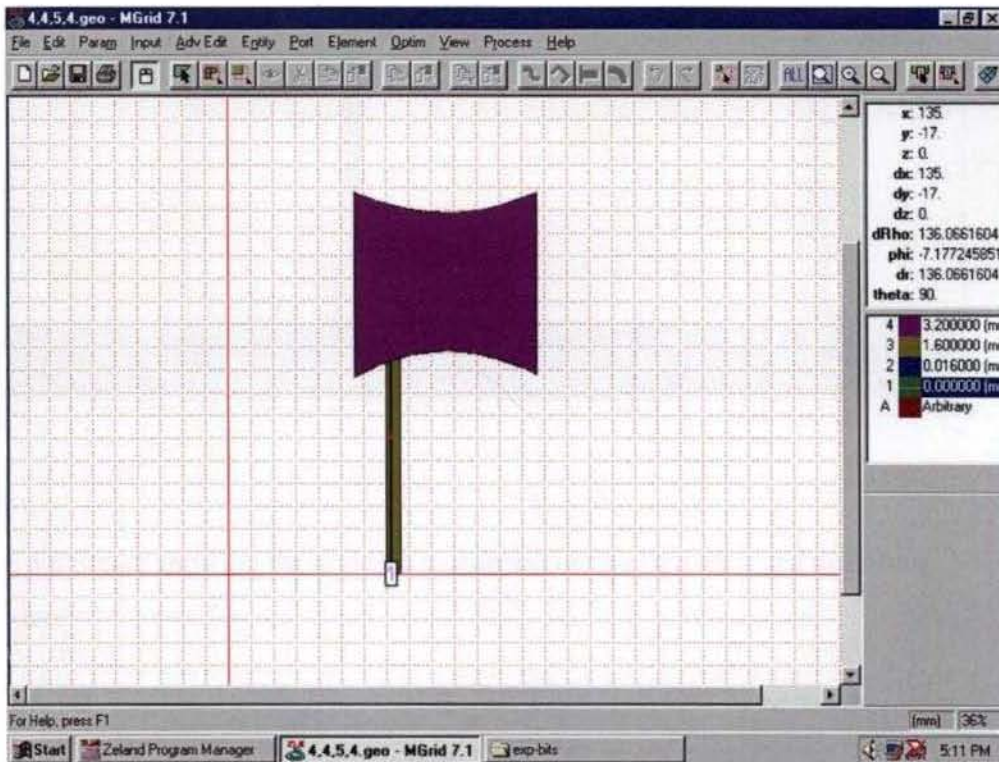


Fig. 3.5 MGRID window with circular sided structure with an electromagnetically coupled feed

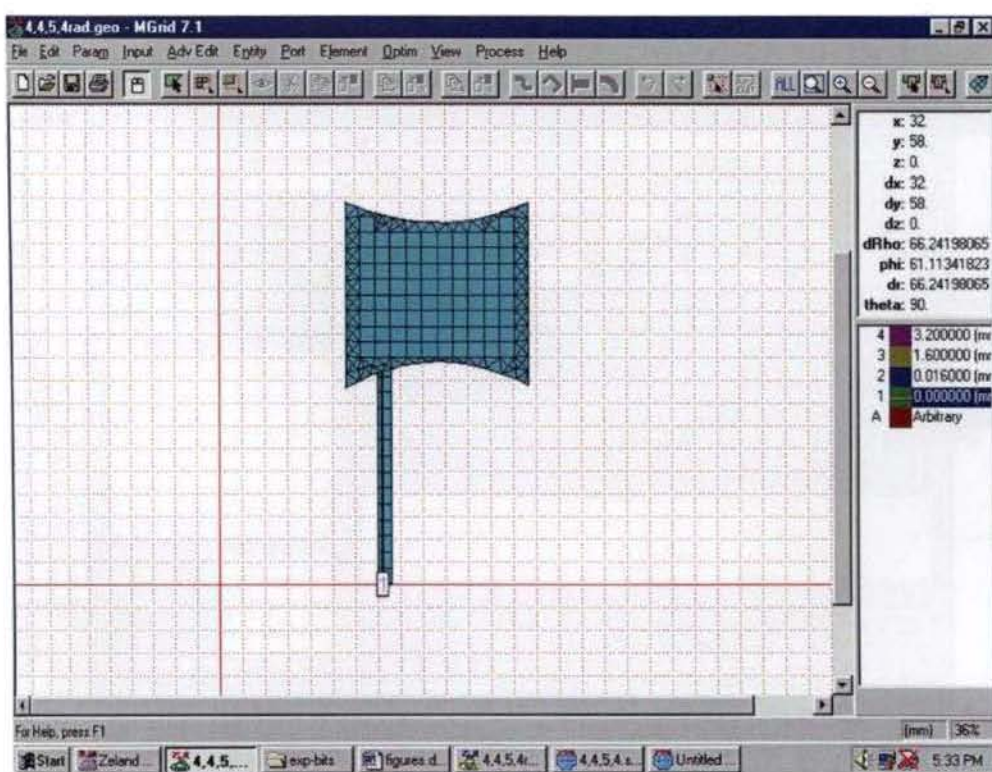


Fig. 3.6 Figure showing the gridding performed on the circular sided microstrip antenna

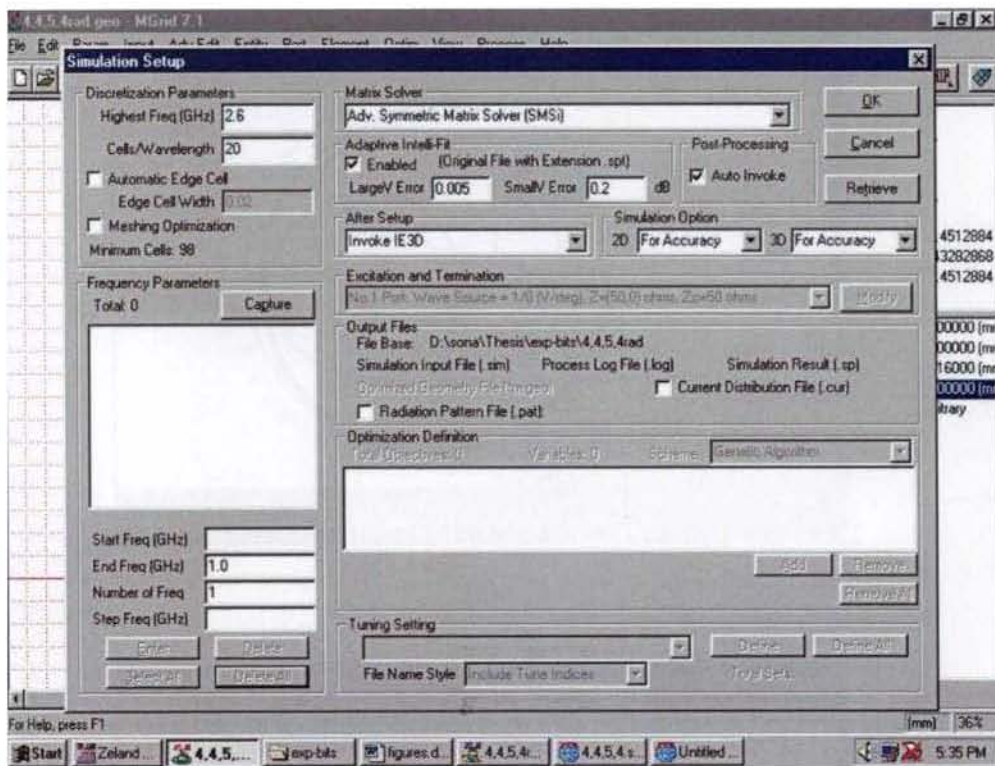
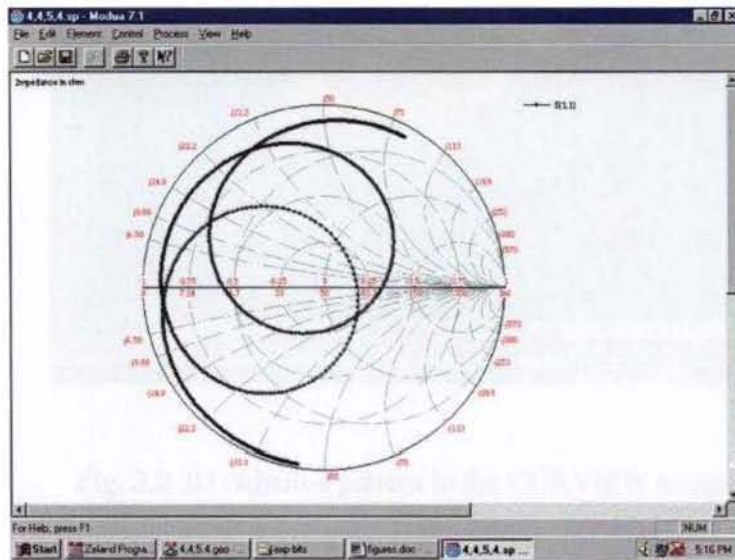
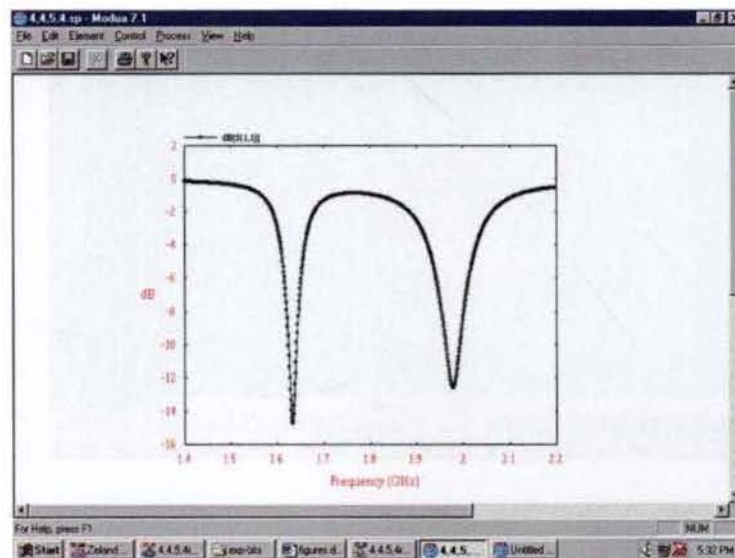


Fig. 3.7 The simulation setup dialog on MGRID



(a)



(b)

Fig. 3.8 The a) smith chart and b) return loss graphs in the IE3D MODUA window after simulation.

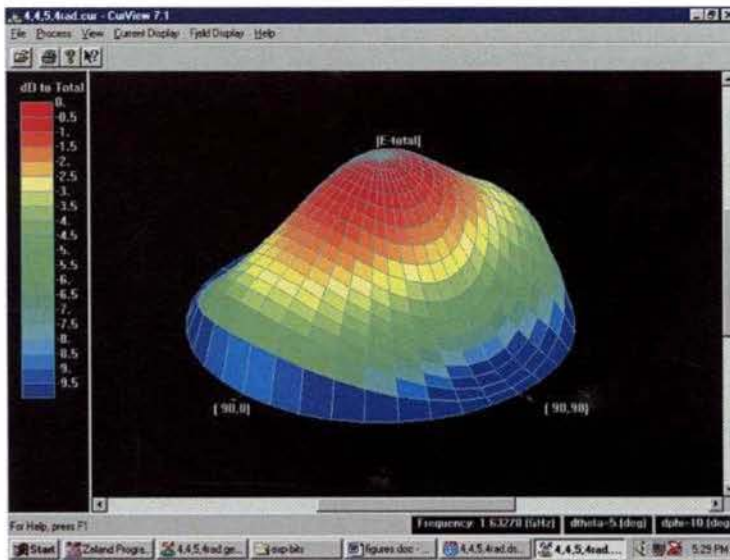


Fig. 3.9 3D radiation pattern in the CURVIEW window

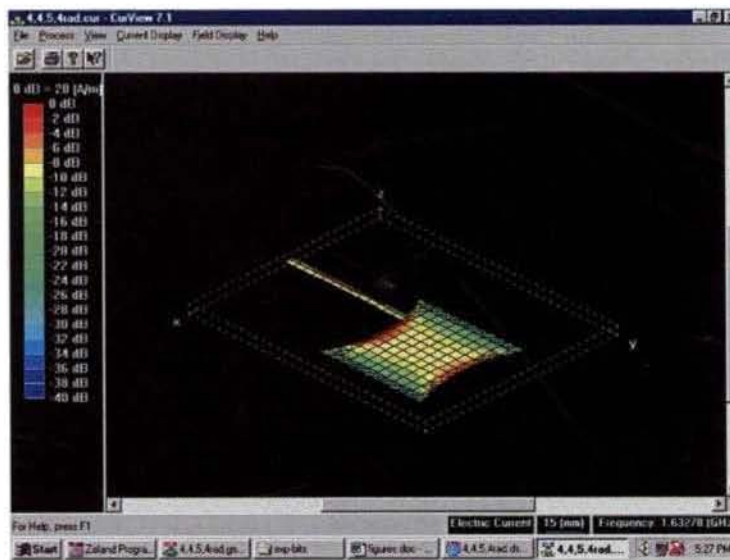


Fig. 3.10 3D average current density in the CURVIEW window.

EXPERIMENTAL OBSERVATIONS

One of the basic developmental trends in electronics is miniaturization, particularly in antennas where it is of paramount significance for modern aircraft, spacecraft and mobile radio- electronic equipment. Compact microstrip antennas have recently received much attention due to the increasing demand of small antennas for personal communication systems. Various small microstrip antenna designs have been reported in the literature to overcome the size problem of a conventional microstrip patch antenna, by different techniques such as using substrate with high dielectric constant, shorting pins placed between the radiating element and the ground plane, slots etched directly on the radiating element or modifications to the shape of a half wavelength patch antenna. This chapter presents the results of experimental investigations carried out on different patch geometries obtained by modifying standard rectangular and circular microstrip patches for developing a compact microstrip antenna. Characteristics of antennas having dual band operation, circular polarization etc. are also discussed in this chapter.

4.1 INTRODUCTION

Since the basic configurations for standard microstrip antennas are rectangular and circular disk patches, the work presented here is based on those simple geometries. The idea was to develop new configurations by modifying these patches. Before going into the experimental results, a brief review of the characteristics of the standard rectangular and circular disk microstrip patches, is given.

4.2 CHARACTERISTIC PROPERTIES OF RECTANGULAR AND CIRCULAR DISK MICROSTRIP ANTENNAS

For an operating frequency of 2 GHz, the characteristics of rectangular and circular antennas fabricated on a low dielectric constant substrate having $\epsilon_r=2.32$ and $h=0.159\text{cm}$ are shown in the Table 4.1 [1].

Table 4.1 The characteristics of rectangular and circular microstrip patches designed for 2 GHz

Characteristic	Configuration	
	Rectangular	Circular disk
Directivity	7.14 dB	7.1 dB
Efficiency	91.2 %	91 %
Gain	7.07 dB	6.8 dB
2:1 VSWR Bandwidth	2 %	1.14 %
Area of patch	28.2 cm ²	24.3 cm ²

It is seen the directivity and efficiency are almost the same for both antennas, but the rectangular antenna has a better value for the VSWR bandwidth. The physical area of the rectangular configuration, however, is 16% percent greater than that of

the circular disk. Since the aim was to develop a compact microstrip antenna, without deteriorating the radiation characteristics, the research work was concentrated on developing a more compact antenna retaining the properties of a rectangular patch antenna.

The basic geometry investigated for developing a more compact patch is the drum-shaped antennas already reported in the literature. Straight edges of the drum shaped patch of Fig. 4.1(b) is modified into curved one as shown in Fig. 4.1(c). This circular-sided patch is found to be more compact than straight edged ones because of the curved resonating edges. Larger resonating edge reduces the frequency excited by that side and thus becomes 'compact'.

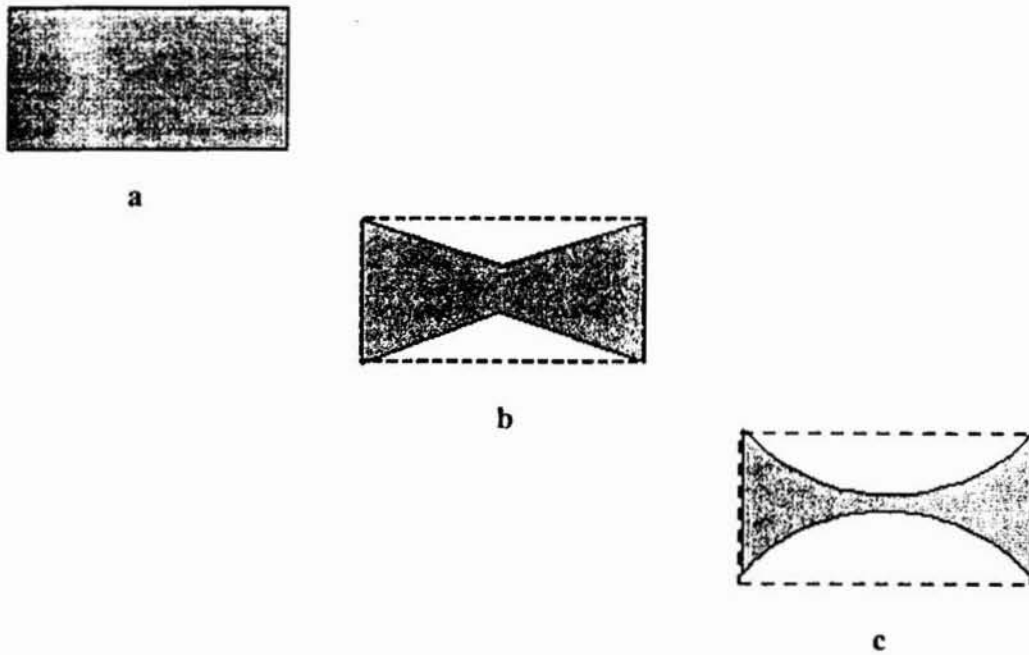


Fig. 4.1 a) rectangular b) drum-shaped and c) circular-sided patch geometries

Numerous antenna structures are designed and analysed using IE3D simulation package. Few patches with optimum parameters having the desired characteristics are fabricated for experimentation. Antenna measurements generally lie within two basic categories: impedance measurements and pattern

measurements. The first category deals with one of the most important antenna parameters- the resonant frequency and the return loss. The second category is a very broad and equally important one, with many subcategories, such as measurements of beamwidth, gain, polarization etc. Measurements are taken using Network Analyser which facilitates rapid measurements, as explained in the previous chapter. Characteristics of different compact circular-sided patches were studied in detail and results are shown in figures and tables.

4.3. CIRCULAR-SIDED COMPACT MICROSTRIP ANTENNA (WITH TWO CONCAVE SIDES)

4.3.1 Geometry

Schematic diagram of the antenna geometry is shown in Fig. 4.2. The antenna structure is based on a rectangular geometry and it incorporates two circular arcs of radii r_1 and r_2 on two sides of it. The substrate has a thickness 'h' and relative permittivity ϵ_r . The antenna is excited by electromagnetic coupling using a 50Ω microstrip feed line.

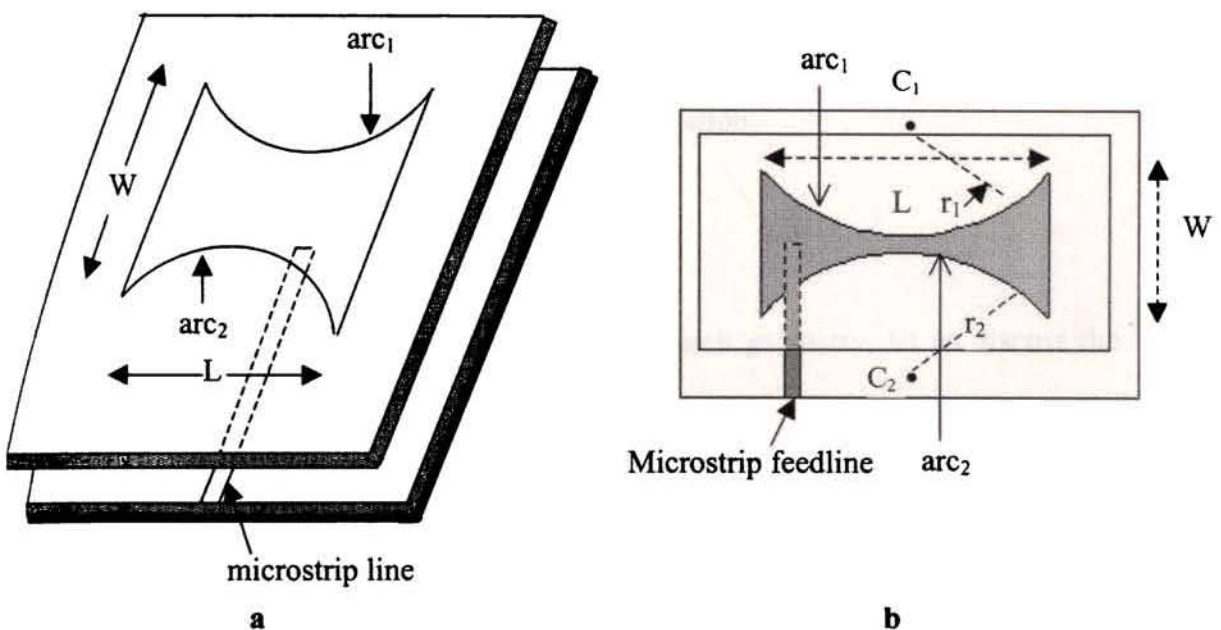


Fig. 4.2 (a) Geometry of the microstrip patch antenna (b) Top view of the patch

This geometrical shape is a modified form of a drum shaped structure, in which the straight edged sides are replaced by circular arcs. This antenna geometry exhibits the compactness due to its circular sides.

4.3.2 Excitation technique

Electromagnetic coupling

The feed system is a covered microstrip network, and the radiating elements are etched on the covering substrate immediately above the open-ended feedline. A microstrip feedline etched on a substrate of same dielectric constant (ϵ_r) and thickness h as used for the construction of the patch is placed beneath the patch. As explained in chapter 1, this electromagnetically coupled patch allows reduction in feed radiation by locating it closer to the ground plane than the patch. Moreover it is very easy to adjust the position of the patch on this feed substrate to locate the optimum impedance matching location. So this feeding technique is used for this patch as well as all other types of patches discussed throughout this thesis. The design equation of the microstrip feedline for the electromagnetic coupling will be discussed in detail in the chapter 5. The position of the feedline can also be easily adjusted to get the proper matching point for the excitation of two modes simultaneously for the dual band operation.

4.3.3 Characteristics of a typical structure

Before going into a detailed study of the patch geometry, let us discuss the basic characteristics of a typical patch.

The patch has dimensions of length $L=7\text{cm}$, Width $W=4\text{cm}$, radii of curvature $r_1=r_2=6\text{cm}$ with substrate thickness $h=0.16\text{cm}$ and dielectric constant $\epsilon_r = 4.28$. The lower layer substrate containing the microstrip feedline also has the same 'h' and ' ϵ_r '.

4.3.3.1 Resonant modes

The dominant modes of excitation of the patch are found to be similar to those of a rectangular patch. In this thesis experimental and theoretical observations are concentrated on the TM_{10} and TM_{01} modes. In rectangular microstrip antennas, the length of the patch element excites one frequency and the width the other frequency. These are the TM_{10} and TM_{01} modes, respectively. In this circular sided patch, the resonating length will not be the physical length of the patch, but will be the effective length of it. Here the effective length will be longer due to the curvature which accounts for its compactness compared to the standard rectangular patch. S_{11} plot for the typical antenna is shown in Fig. 4.3. Since the length of the patch is greater than the width ($L > W$) for this particular case, $f_{10} = 0.8667$ GHz shown in the figure is in the TM_{10} mode.

Since TM_{10} is the lowest order mode of this structure, area reduction is maximum for this frequency. Naturally the studies are concentrated on this mode of resonance. Different radiation properties of TM_{10} mode are discussed below.

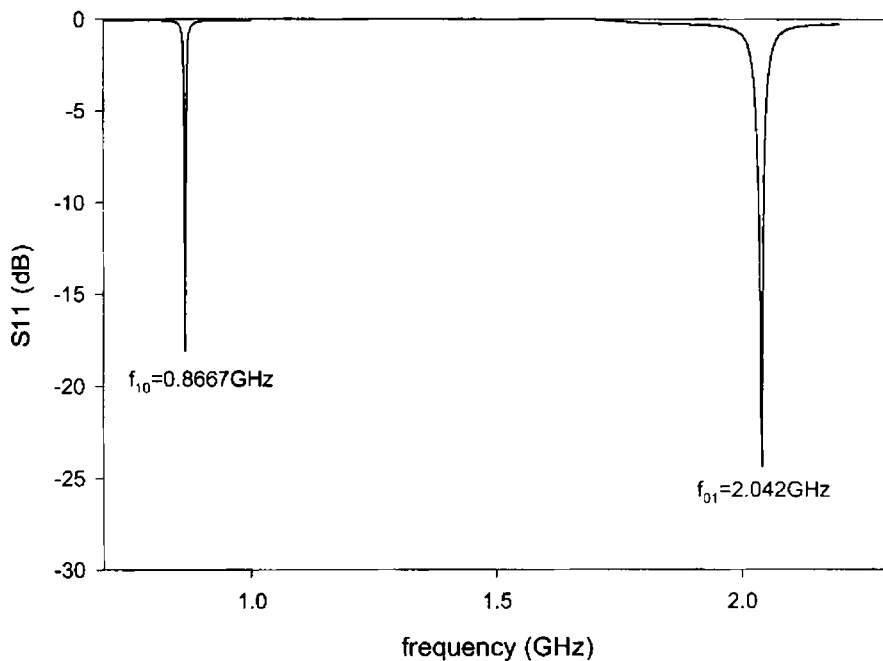


Fig. 4.3 Measured return loss against frequency

4.3.3.2 Gain

Gain of a patch for a particular frequency is measured by comparing it to that of a standard microstrip geometry. Here relative gain is determined with respect to the gain of a circular microstrip patch designed for the same frequency. The result is shown in Fig. 4.4. As indicated in the figure, the gain of the patch for f_{10} is slightly less (<1dB) than that of a circular patch.

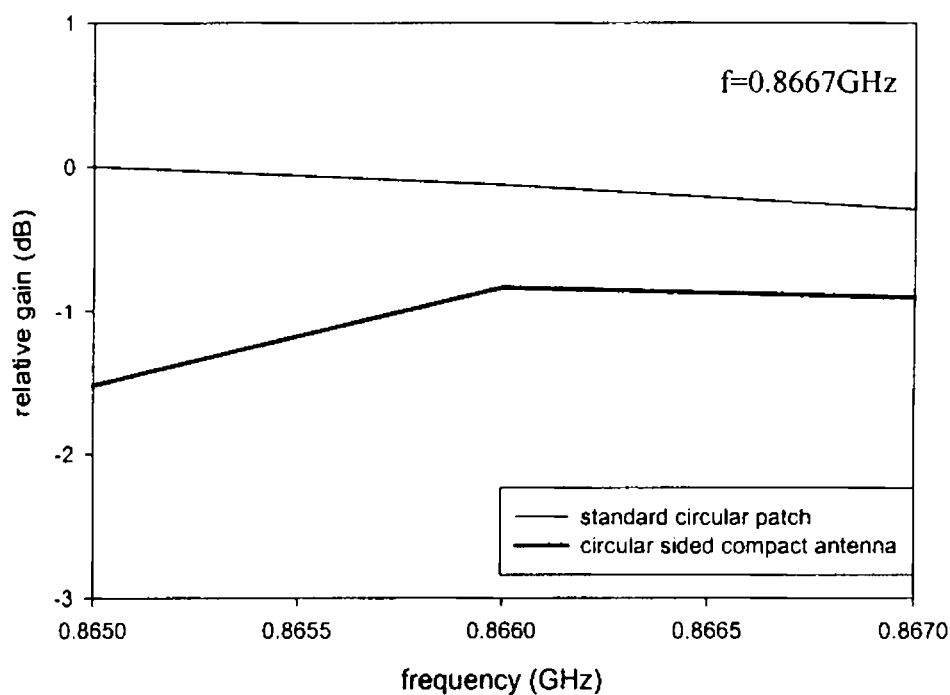


Fig. 4.4 Variation of relative gain for the patch

4.3.3.4 Radiation patterns

E and H plane radiation patterns of the circular sided patch are plotted in Fig. 4.5. They are broad and symmetric as in the case of a rectangular microstrip antenna with good cross polarization levels (better than 25 dB).

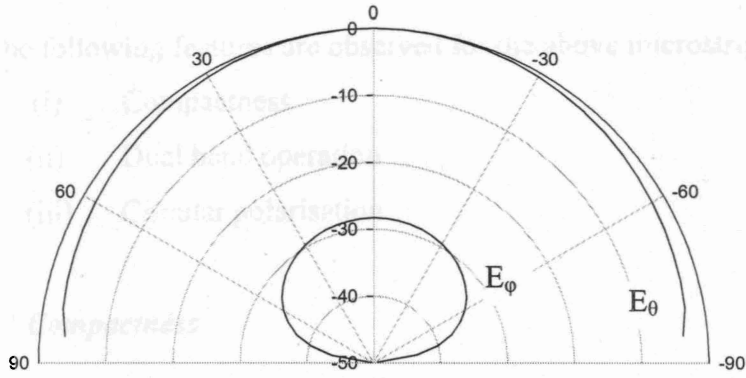
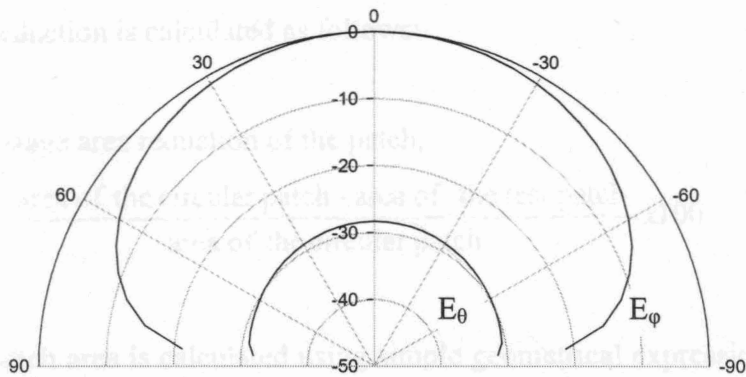
a) $\varphi=0$ b) $\varphi=90$

Fig. 4.5 Radiation patterns for TM_{10} mode frequency ($f=0.8667\text{GHz}$)

4.3.4 Characteristic features

The following features are observed for the above microstrip patch antenna:

- (i) Compactness
- (ii) Dual band operation
- (iii) Circular polarisation

4.3.4.1 Compactness

Compactness of a particular geometry is determined by comparing its patch area with a standard circular microstrip patch because circular patch is the standard compact basic geometry. The circular-sided patch explained above has a reduced surface area compared to standard circular geometry designed for same frequency. Comparisons of patch areas are done here for TM_{10} mode resonant frequency. The size reduction is calculated as follows:

Percentage area reduction of the patch,

$$A = \frac{\text{area of the circular patch} - \text{area of the test patch}}{\text{area of the circular patch}} \times 100$$

The patch area is calculated using simple geometrical expressions as explained in section 5.9. The percentage area reduction of this patch is obtained as ~77 according to the calculation.

4.3.4.2 Dual band operation and circular polarization

The TM_{10} and TM_{01} mode frequencies are excited simultaneously for this patch antenna by slightly adjusting the position of microstrip feed line under the patch, as explained in the previous section. As these orthogonally polarized frequencies are controlled by the length and width of the patch respectively, they can be made closer and merged to get circular polarization by adjusting the parameters of the

patch. The experimental results of a typical patch for circular polarization will be discussed in section 4.3.9.

4.3.5 Characteristics of TM_{10} and TM_{01} mode frequencies (f_{10} and f_{01})

The dependence of various parameters of the antenna on its characteristics is discussed in the following sections.

4.3.5.1 Resonant frequency variation with respect to the length

TM_{10} mode frequency (f_{10}) and TM_{01} mode frequency (f_{01}) are excited by the effective length and width of the patch, respectively. It is evident from the table 4.2 that for a constant width and radius, f_{10} decreases as length increases whereas f_{01} remains almost constant.

Also the effect of radii of curvatures can be observed from the results. Fig 4.6 plots the variation of TM_{10} and TM_{01} mode frequencies for various lengths of the patch. It is very clear from the figure that f_{10} extends to a wide range whereas f_{01} confined to a narrow region.

Variation of size reduction with length of the patch is also tabulated [Table 4.2]. It is observed from the table that area reduction increases with length. The percentage area reduction varies in a wide range as from 18 to 88 for variation of the length.

Table 4.2 Resonant frequencies and area reduction with length for patches of different radii ($W=4\text{cm}$)

Length L (cm)	Radii r_1, r_2 (cm)	Frequency (GHz)		Area reduction (%)
		f_{10}	f_{01}	
4	9,9	1.699	2.104	24.63
	8,8	1.688	1.95	26.38
	7,7	1.66	1.923	29.8
	6,6	1.672	1.978	30.15
	5,5	1.654	1.902	33.6
	4,4	1.609	2.168	40.15
5	9,9	1.363	1.98	42.22
	8,8	1.356	2.202	43.84
	7,7	1.345	2.052	46.06
	6,6	1.327	2.244	49.28
	5,5	1.301	2.23	53.81
	4,4	1.256	2.225	61.02
6	8,8	1.15	2.089	55.00
	7,7	1.14	2.234	57.50
	6,6	1.12	2.22	61.33
	5,5	1.05	2.27	69.24
	4,4	1.00	2.31	77.54
7	9,9	0.9574	2.027	65.52
	8,8	0.9343	2.021	68.61
	7,7	0.9055	2.025	72.35
	6,6	0.8667	2.042	77.13
	5,5	0.8105	2.027	83.52
	4.5,4.5	0.7595	2.059	88.09

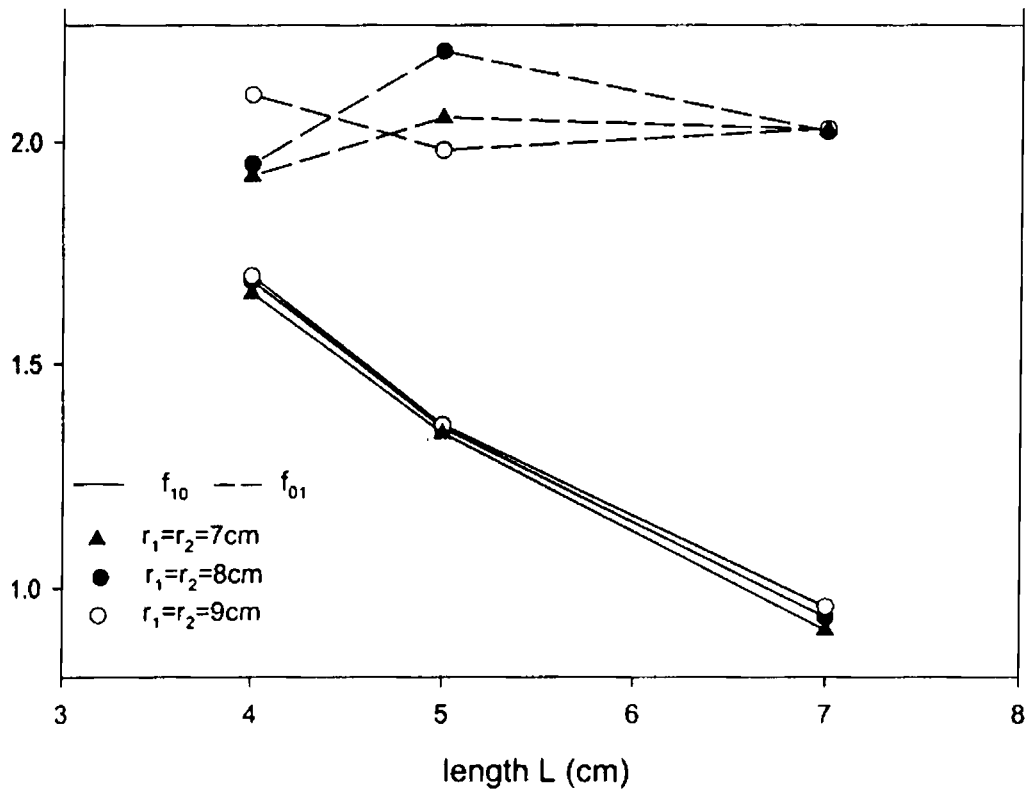


Fig. 4.6 Variation of TM_{10} and TM_{01} frequencies with length ($W=4\text{cm}$, $\epsilon_r=4.28$, $h=0.16\text{cm}$)

4.3.5.2 Resonant frequency variation with respect to the width.

The TM_{01} mode frequency (f_{01}) is determined by the effective width as shown in table 4.3. Hence the effect of variation of width keeping a constant length and radius is studied. The results plotted in Fig.4.7 show a variation of frequency (f_{01}), retaining f_{10} almost constant.

From the table it can be seen that as the width increases, the TM_{01} mode frequency decreases drastically, whereas the TM_{10} mode frequency remains almost constant. Thus it is obvious that the f_{01} is due to the excitation of width side of the patch.

Table 4.3 The variation of frequencies with width for patches of different radii ($L=4\text{cm}$, $h=0.16\text{cm}$, $\epsilon_r=4.28$)

Width W(cm)	Radii r_1, r_2 (cm)	Frequency (GHz)	
		f_{10}	f_{01}
4	4,4	1.609	2.168
	5,5	1.654	1.902
	6,6	1.672	1.978
	7,7	1.66	1.923
	8,8	1.688	1.95
	9,9	1.699	2.104
5	4,4	1.627	1.683
	5,5	1.676	1.676
	6,6	1.658	1.601
	7,7	1.648	1.5
	8,8	1.679	1.552
	9,9	1.688	1.574
6	4,4	1.63	1.382
	5,5	1.664	1.362
	6,6	1.667	1.319
	7,7	1.648	1.249
	8,8	1.673	1.286
	9,9	1.685	1.301
7	4,4	1.635	1.168
	5,5	1.663	1.155
	6,6	1.656	1.122
	7,7	1.647	1.073
	8,8	1.669	1.1
	8.5,8.5	1.677	1.099

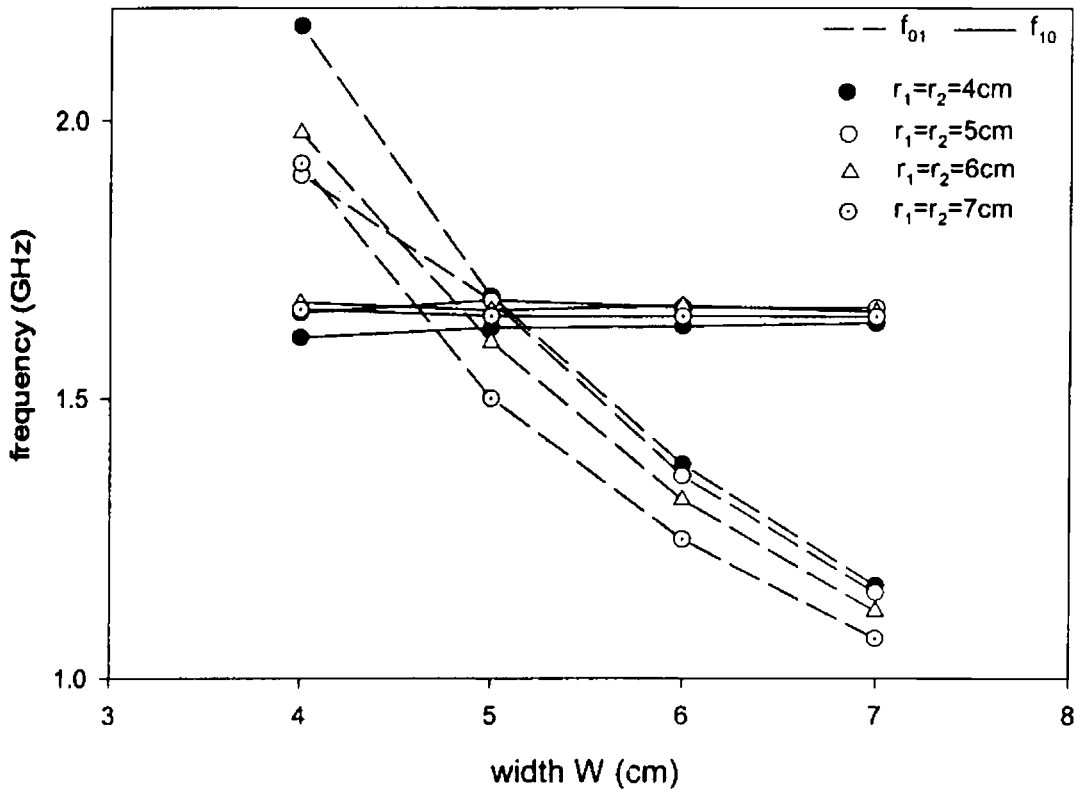


Fig 4.7 Variation of frequencies for the patches of different width ($L=4\text{cm}$, $h=0.16\text{cm}$, $\epsilon_r=4.28$)

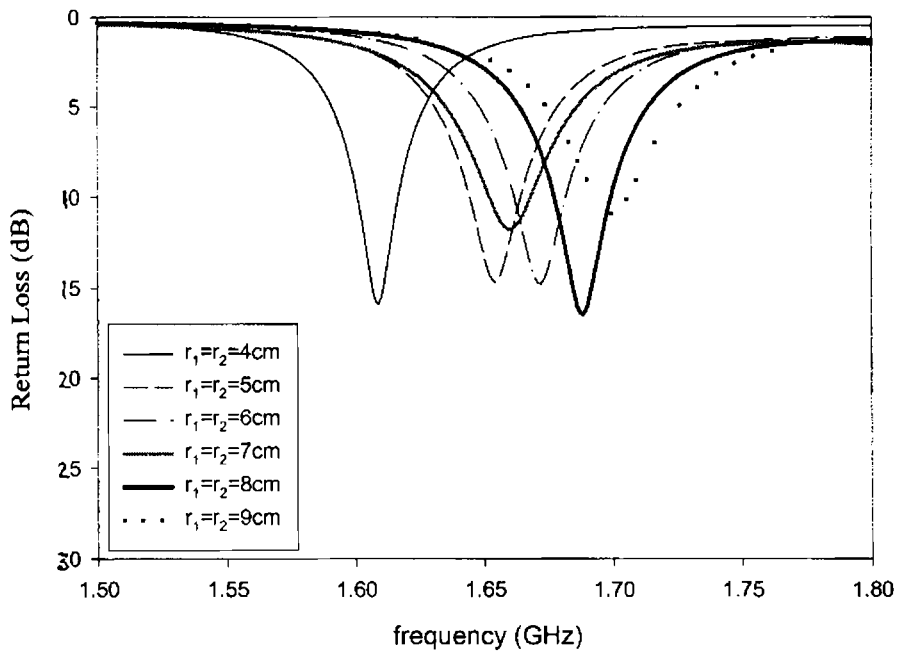
4.3.5.3 Variation of frequencies with respect to radii of curvature

For different sets of length and width as radii of arcs decrease, the frequency (f_{10}) decreases in general. This is because of the fact that as the radii decrease, the effective length of the curve increases which results in a decrease in frequency. Variation of return loss for patches of different aspect ratios are plotted in Fig. 4.8. Also it is clear that as the radii of curvatures decrease, the area reduction increases correspondingly.

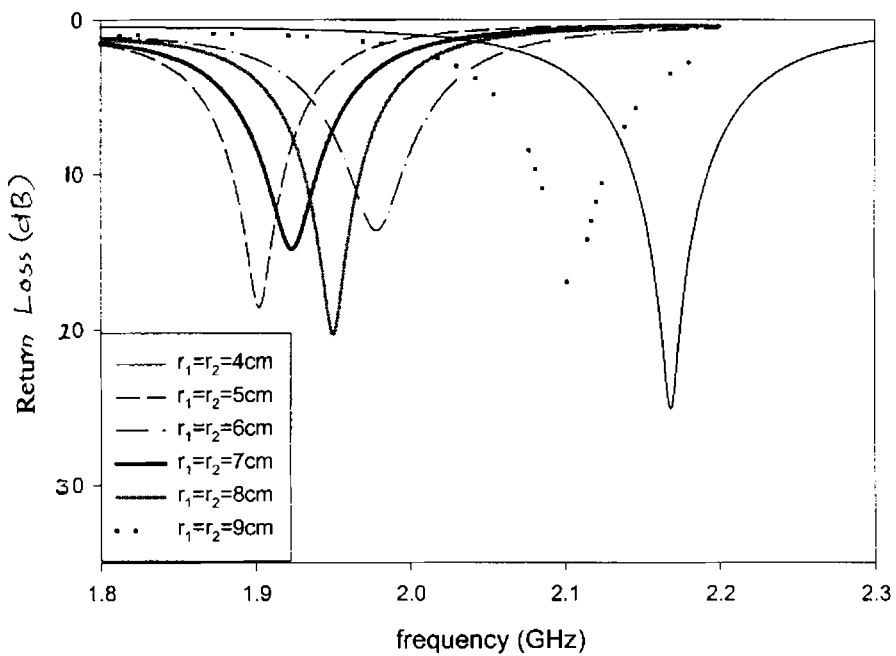
Another possible geometry for this type of patch is with different radii r_1 and r_2 . Resonant characteristics are studied for patches with different radii of curvature and the variation of f_{10} and f_{01} is shown in Table 4.4. It can be observed that as the radius r_1 or r_2 is decreased keeping other one a constant, f_{10} is decreasing and f_{01} is increasing gradually. It can also be noted from the table, that a decrease in either r_1 or r_2 , results in an increase in area reduction. Fig. 4.9 shows the variation of area reduction with radii of curvatures of the patch for different sets of length and width.

Table 4.4 The variation of frequencies for sets of different radii and corresponding area reduction

Length L (cm)	Width W(cm)	Radii r_1, r_2 (cm)	Frequency (GHz)		Percentage area reduction
			f_{10}	f_{01}	
4	4	4,9	1.662	1.927	32.01
		4,8	1.671	1.954	31.65
		4,7	1.657	1.965	33.29
		4,6	1.641	1.982	35.23
		4,5	1.645	1.99	35.88
		4,4	1.609	2.168	40.15
4	4	9,4	1.675	1.975	30.94
		8,4	1.676	1.957	31.24
		7,4	1.657	1.978	33.29
		6,4	1.647	1.998	34.76
		5,4	1.633	1.979	36.82
		4,4	1.609	2.168	40.15

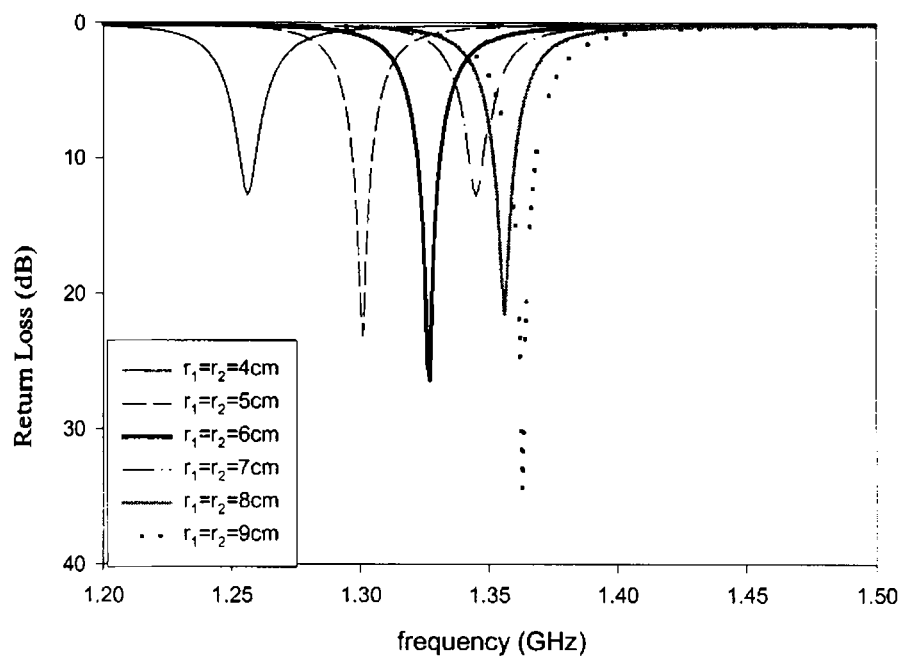


(a)

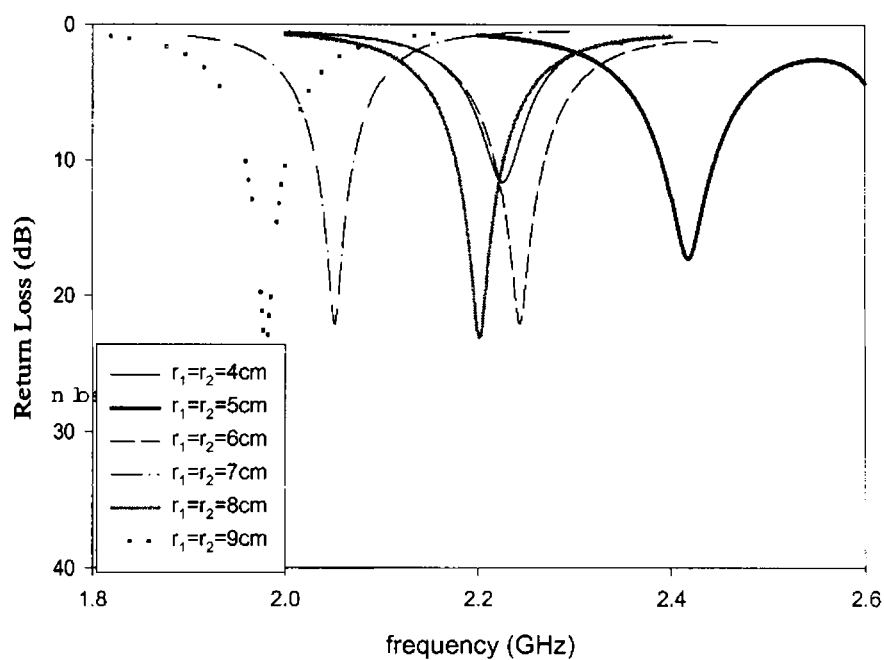


(b)

Fig 4.8 (i) Variation of return loss with frequencies for the case $L=W$ ($L=W=4\text{cm}$, $h=0.16\text{cm}$, $\epsilon_r=4.28$) (a) f_{10} (b) f_{01}

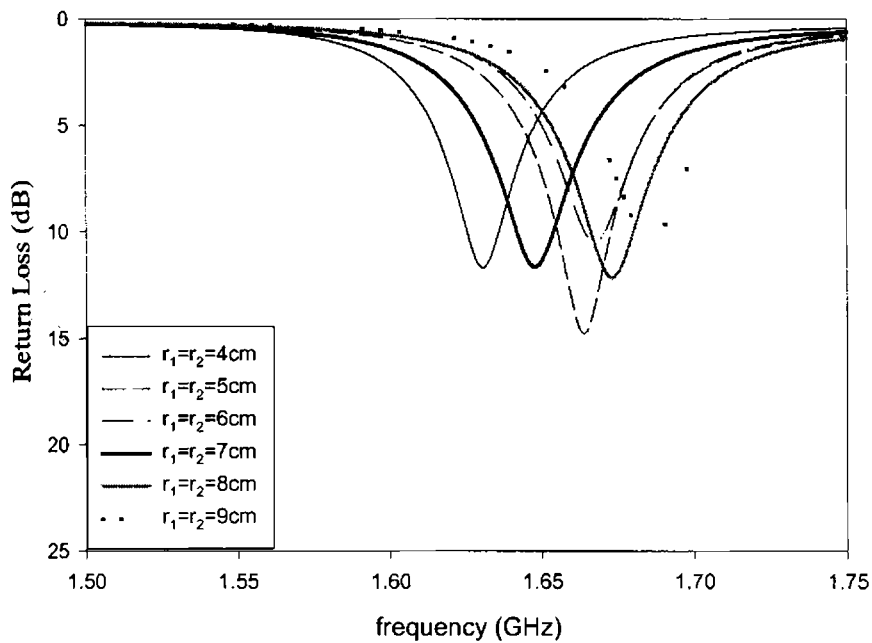


(a)

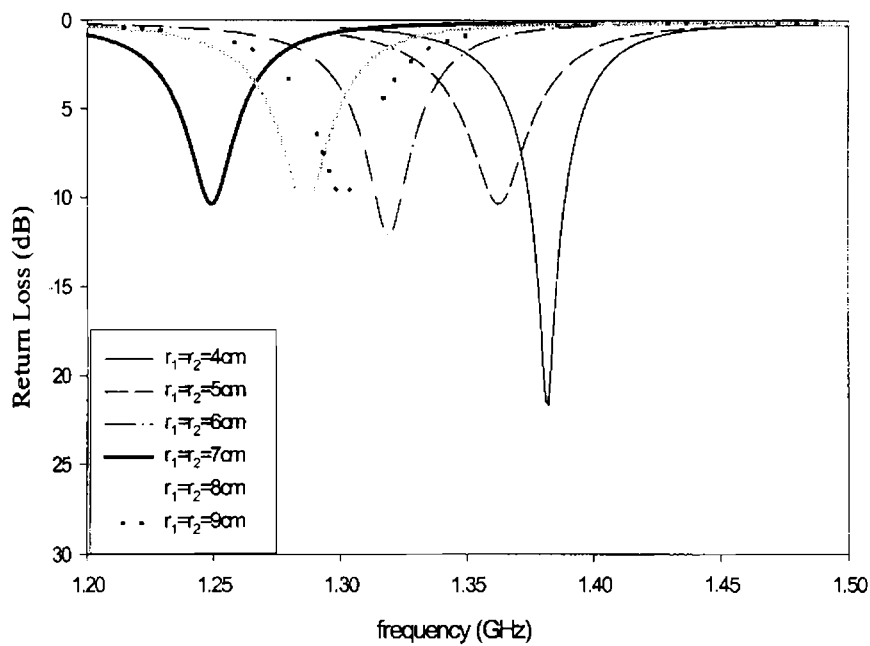


(b)

Fig 4.8 (ii) Variation of return loss with frequencies for the case $L > W$ ($L=5$, $W=4$, $h=0.16\text{cm}$, $\epsilon_r=4.28$) (a) f_{10} (b) f_{01}



(a)



(b)

Fig 4.8 (iii) Variation of return loss with frequencies for the case $L < W$ ($L=4$, $W=6$, $h=0.16\text{cm}$, $\epsilon_r=4.28$)

(a) f_{10} (b) f_{01}

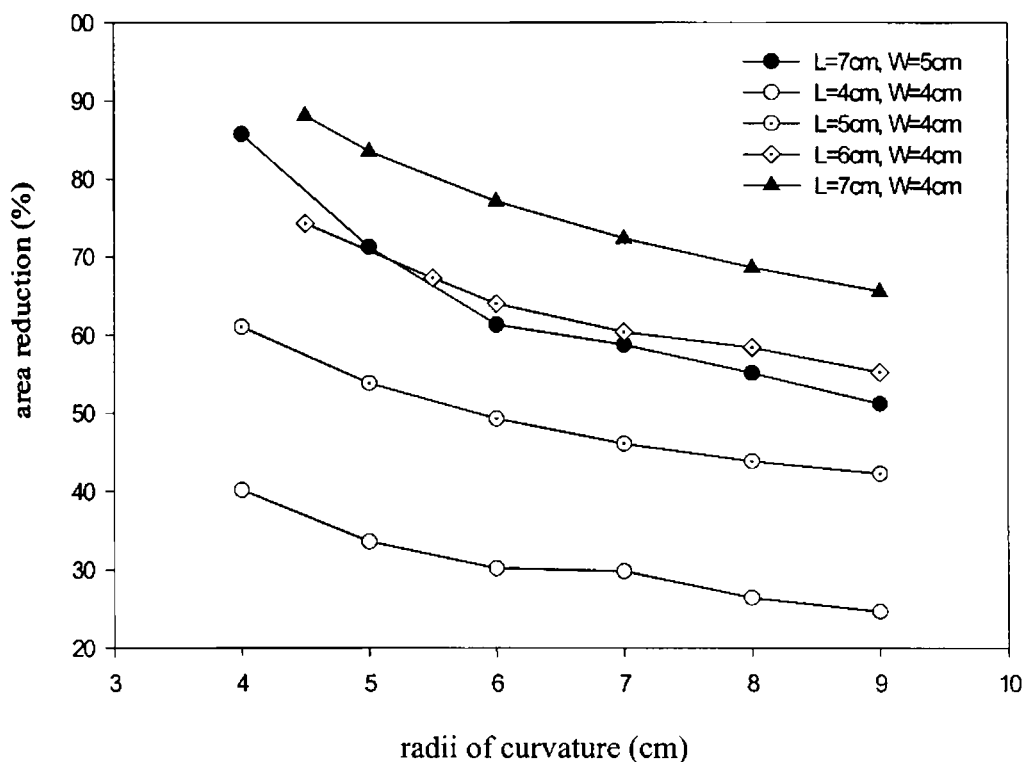


Fig 4.9 Variation of area reduction compared to that of a circular patch with radii of the two arcs

4.3.5.4 Variation of frequencies for patches of different h and ϵ_r

Variation of frequencies for circular sided patches with different h and ϵ_r are studied and the results are tabulated [Table 4.5]. Here it is obvious from the table that as the thickness h of the antenna is increased, keeping other parameters of the patch constants, the resonant frequencies decrease gradually. When the value of dielectric constant ϵ_r is increased, both the TM_{10} and TM_{01} mode resonant frequencies are decreased. The effect of radii of curvature is same as in the case of previous studies. As they are decreased keeping other parameters constant, f_{10} decreases whereas f_{01} increases.

Table 4.5 Resonant frequencies of patches fabricated on substrates of different thickness and dielectric constant (L=5cm, W=4cm)

radii (cm)	r_1, r_2	h (cm)	ϵ_r	frequency f_{10} (GHz)	frequency f_{01} (GHz)
9,9 8,8 7,7 6,6 5,5 4,4		0.08	2.2	1.883 1.877 1.859 1.806 1.784 1.724	2.648 2.693 2.768 2.893 2.995 3.152
9,9 8,8 7,7 6,6 5,5 4,4		0.318	2.2	1.766 1.752 1.73 1.728 1.703 1.626	2.375 2.441 2.501 2.529 2.67 2.773
9,9 8,8 7,7 6,6 5,5 4,4		0.16	4.28	1.363 1.356 1.345 1.327 1.301 1.256	1.98 2.202 2.052 2.244 2.418 2.225
8,8 7,7 6,6 5,5 4,4		0.066	10.2	0.9035 0.8995 0.8854 0.8693 0.8263	1.343 1.348 1.378 1.429 1.583

4.3.6 Impedance bandwidth and VSWR

The bandwidth of an antenna is the range of frequencies within which the performance of the antenna, with respect to some characteristic, conforms to a specific standard. In the case of the microstrip patch antenna which is basically a resonant device, it is usually the variation of impedance, rather than pattern, which limits the standard of performance. The impedance bandwidth can be defined simply as the range of frequencies over which the VSWR is less than 2 (return loss greater than 10 dB).

Impedance bandwidth of this antenna for both the frequency bands are found to be in the range of 1-2%. This property is similar to that of a general microstrip patch antenna. Percentage bandwidths for different cases is shown in Table 4.6.

4.3.7 Radiation characteristics

The radiation characteristics of the patch with different parameters are analysed and the results are shown in Table 4.7. It is observed that the efficiency of these patches are nearly 80%. The gain and directivity values are comparable to that of standard rectangular microstrip patch and thus the patch attains the compactness without deteriorating the radiation characteristics. These parameters are studied for the TM_{10} mode resonant frequency, where the antenna offers area reduction.

Table 4.6 Impedance bandwidth percentage with frequency for the patch

patch parameters			frequency (GHz)		frequency (GHz)	
L (cm)	W (cm)	r ₁ , r ₂ (cm)	f ₁₀	%bandwidth	f ₀₁	%bandwidth
3.4	4	2,2	1.746	0.60	2.404	1.21
		2.5,2.5	1.858	1.24	2.172	1.00
		3,3	1.914	2.56	1.986	2.06
		4,4	1.927	1.66	1.961	1.84
		5,5	1.943	1.80	1.943	1.80
4	4	4,4	1.609	1.00	2.168	1.62
		5,5	1.654	1.21	1.902	1.74
		6,6	1.672	1.14	1.978	1.67
		7,7	1.66	0.96	1.923	1.72
		8,8	1.688	1.30	1.95	1.79
4	3.4	4,4	1.659	0.96	2.491	2.77
		5,5	1.662	0.96	2.278	2.33
		6,6	1.662	1.08	2.286	2.36
		7,7	1.667	1.14	2.216	2.21
		8,8	1.698	1.09	2.199	2.14
4	4	4,5	1.645	1.22	1.99	1.61
		4,6	1.641	1.1	1.982	1.82
		4,7	1.657	0.84	1.965	1.58
		4,8	1.671	1.02	1.954	1.28
		4,9	1.662	1.14	1.927	1.56
4	4	5,4	1.633	1.1	1.979	1.57
		6,4	1.647	1.12	1.998	1.60
		7,4	1.657	1.27	1.978	1.77
		8,4	1.676	1.16	1.957	1.53
		9,4	1.675	1.25	1.975	1.47

Table 4.7 showing the radiation characteristics (IE3D)

Parameters L,W, r ₁ , r ₂ (cm)	Radiation properties				
	f ₁₀ (GHz)	Antenna Efficiency (%)	Gain (dBi)	Directivity (dBi)	3dBbeamwidth (deg.)
4,4,4,4	1.609	79.37	5.3299	6.333	87.677,149.51
4,4,5,5	1.654	77.55	5.248	6.352	87.69,147.92
4,4,6,6	1.672	79.4	5.377	6.379	86.67,148.18
4,5,4,4	1.627	78.50	5.340	6.391	87.528,144.28
4,5,5,5	1.676	79.39	5.365	6.367	55.32,110.26
4,5,6,6	1.658	76.35	5.233	6.404	91.11,131.85
5,4,4,4	1.256	74.70	4.979	6.246	88.81,154.42
5,4,5,5	1.301	78.58	5.208	6.254	88.859,153.42
5,4,6,6	1.327	80.50	5.333	6.275	88.478,152.7

4.3.8 Antenna fabrication and measurement

A circular sided microstrip antenna with optimum parameters giving area reduction as well as enhanced gain is constructed and experimental results are presented.

4.3.8.1 Geometry and design

The geometry shown in Fig. 4.2 is fabricated on a glass-epoxy substrate with dielectric constant $\epsilon_r=4.28$ and thickness $h=0.16\text{cm}$. Here, $L=6\text{cm}$, $W=4\text{cm}$, $r_1=r_2=6\text{cm}$. Energy is electromagnetically coupled using microstrip feedline of impedance 50Ω .

4.3.8.2 Experimental results

The measured return loss against frequency for this patch is plotted in Fig. 4.10. The 2:1 VSWR bandwidth is around 2%. This configuration provides an area reduction of 64% compared to standard circular disk microstrip antenna, with a slight gain enhancement compared to the circular disk.

E-plane and H-plane radiation patterns of the antenna at TM_{10} mode resonant frequency are shown in Fig. 4.11. They are broad as in the case of standard rectangular microstrip patches.

Relative gain of the patch with respect to that of standard circular patch is plotted in the Fig. 4.12. Gain measurement is done using network analyzer as explained in

the previous chapter. The plot shows that the gain of the patch is better compared to that of a standard circular disk patch.

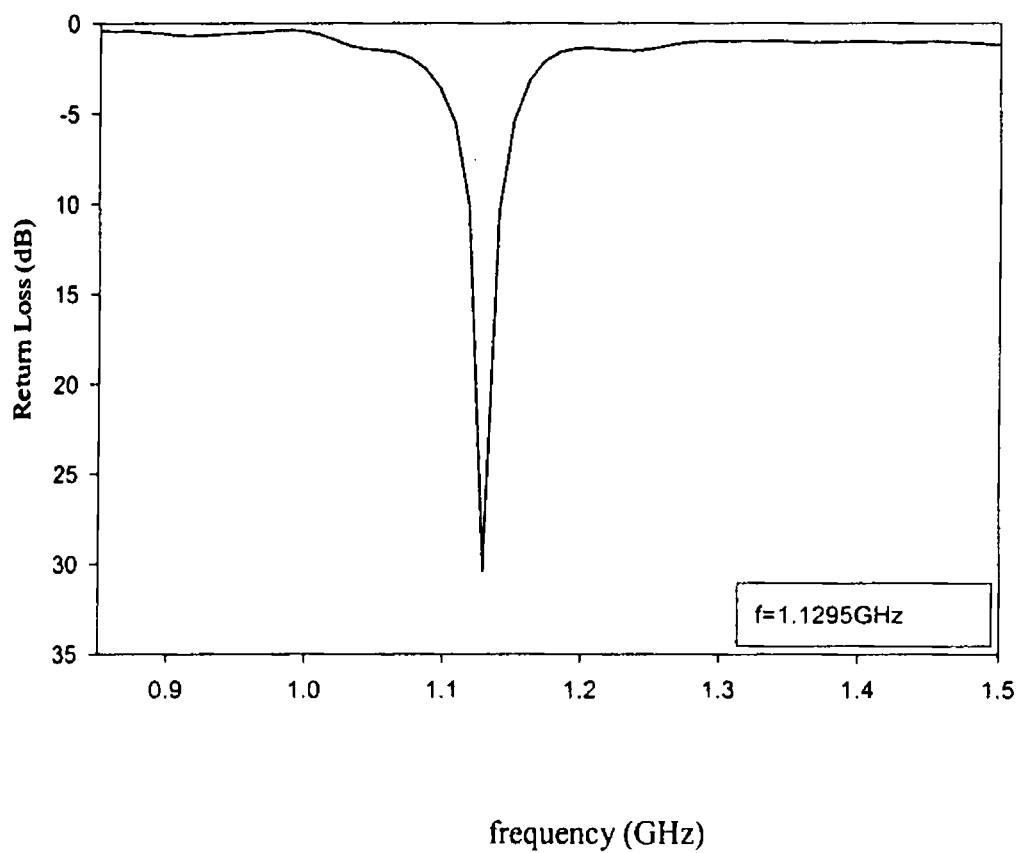


Fig. 4.10 Variation of return loss with frequency

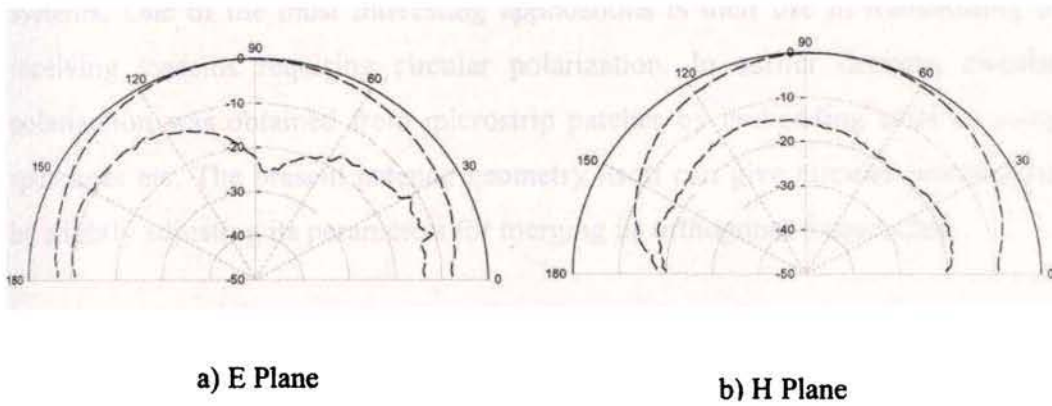


Fig. 4.11 E and H plane radiation patterns for frequency $f=1.1295\text{GHz}$

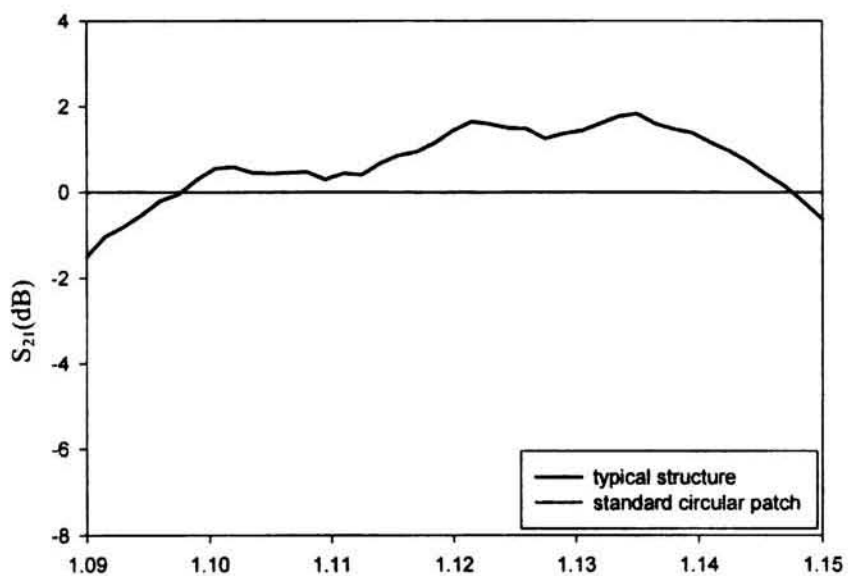


Fig 4.12 Relative gain of the patch with respect to standard circular disk

4.3.9 Circularly polarized compact microstrip antenna

Microstrip antenna is widely used as an efficient radiator in many communication systems. One of the most interesting applications is their use in transmitting or receiving systems requiring circular polarization. In earlier designs, circular polarization was obtained from microstrip patches by embedding slots or using spur lines etc. The present antenna geometry itself can give circular polarization by slightly adjusting its parameters for merging its orthogonal frequencies.

4.3.9.1 Geometry and design

Geometry is already explained in the previous section. In this case, the width of the patch is taken to be greater than the length so that the length and width will excite two closely spaced orthogonal frequencies. The antenna structure shown in Fig. 4.13, having $L = 3.4\text{cm}$, $W = 4.6\text{cm}$, $r_1 = r_2 = 2\text{cm}$ is etched on glass epoxy substrate of $h = 0.16\text{cm}$ and $\epsilon_r = 4.28$. A 50Ω microstrip feedline etched on the same substrate is used for electromagnetic coupling.

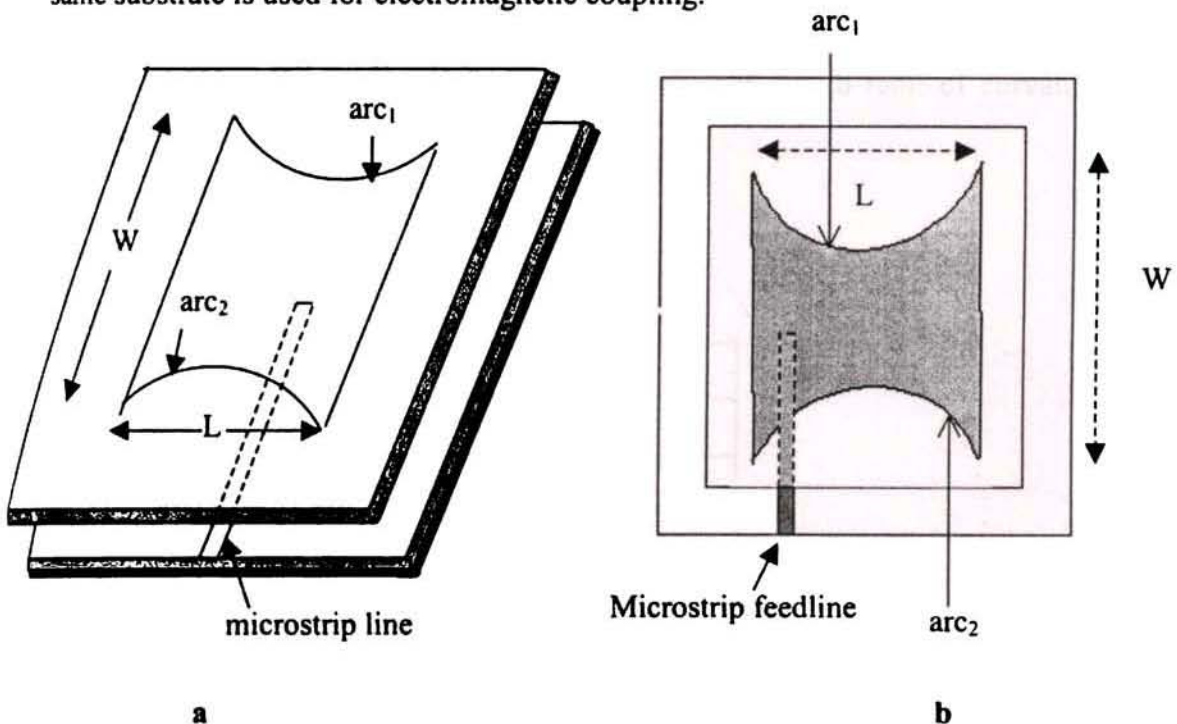


Fig 4.13 a) Geometry of the patch for circular polarization b) Top view

4.3.9.2 Experimental results:

Keeping L and W constant, the radii of curvature r_1 and r_2 are varied to merge two closely spaced orthogonal resonant frequencies to get circular polarisation as shown in Table 4.8. Variation of return loss against frequency for the typical antenna structure is shown in Fig. 4.14.

The axial ratio of the CP antenna is measured in the particular frequency band as explained in section 3.3.5. and is plotted in Fig. 4.15. The 3dB axial ratio bandwidth is 28MHz. By considering the center frequency at 1.885GHz, where a minimum axial ratio is observed, the proposed design has an axial ratio bandwidth of 1.5%.

E-plane and H-plane radiation patterns of the antenna at the center frequency are shown in Fig. 4.16. The copolar and crosspolar radiation patterns are almost identical in the entire radiating angular region.

Table 4.8 Variation of orthogonal resonant frequencies with radii of curvature ($L=3.4\text{cm}$, $W=4.6\text{cm}$, $h=0.16\text{cm}$ and $\epsilon_r=4.28$)

r_1, r_2 (cm)	frequencies (GHz)	
	f_1	f_2
5, 5	1.641	1.945
4, 4	1.681	1.931
3, 3	1.732	1.904
2, 2	1.88	

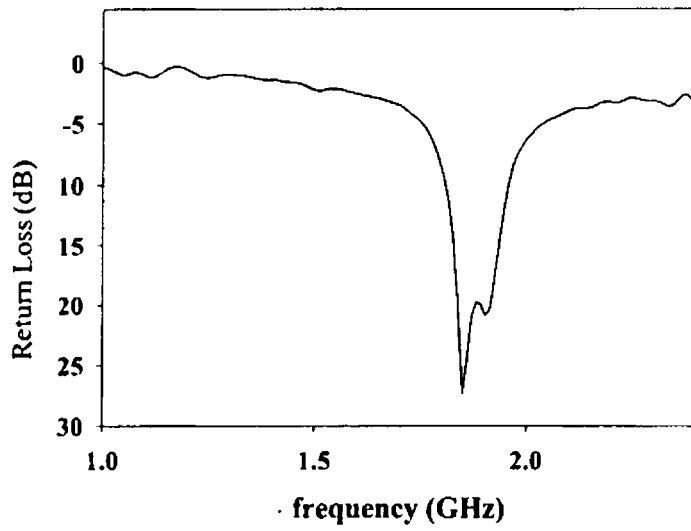


Fig. 4.14 Variation of return loss with frequency

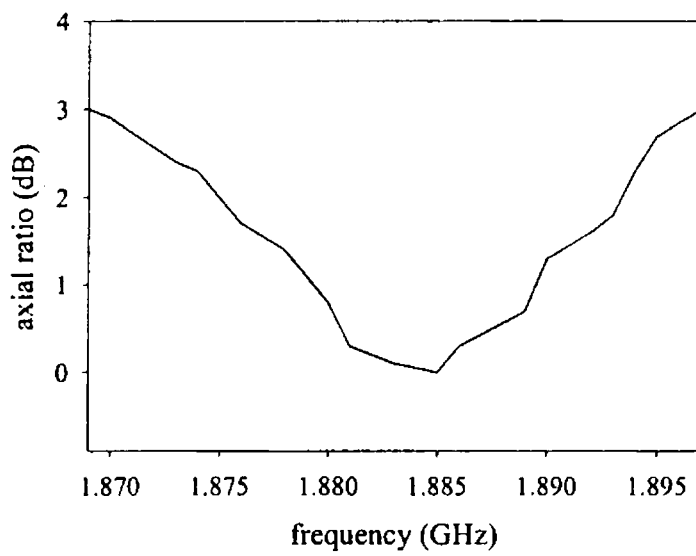
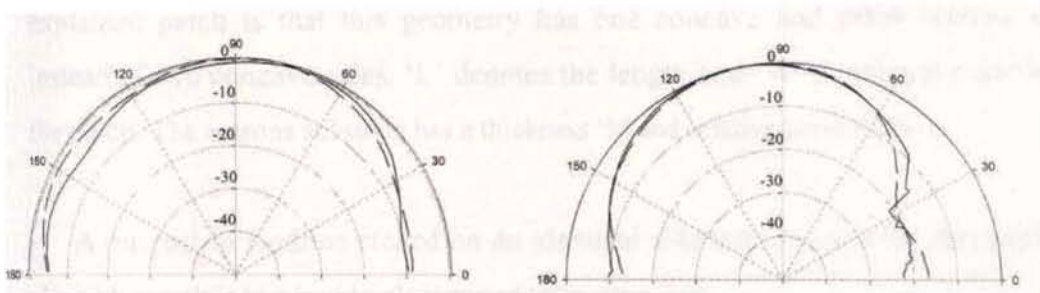


Fig 4.15 Measured axial ratio against frequency



a) E-Plane pattern

b) H-Plane pattern

Fig 4.16 Radiation patterns of the CP antenna at the centre frequency $f=1.885\text{GHz}$

4.4. CIRCULAR-SIDED PATCH (with one convex and other concave side)

4.4.1 Geometry and excitation technique

Geometry of the antenna is as shown in Fig. 4.17. The antenna structure incorporates two circular arcs of radii r_1 and r_2 . Only difference from previously explained patch is that this geometry has one concave and other convex side instead of two concave sides. 'L' denotes the length and 'W' denotes the width of the patch. The antenna substrate has a thickness 'h' and relative permittivity ϵ_r .

A microstrip feedline etched on an identical substrate as used for the patch is placed beneath it to provide electromagnetic coupling.

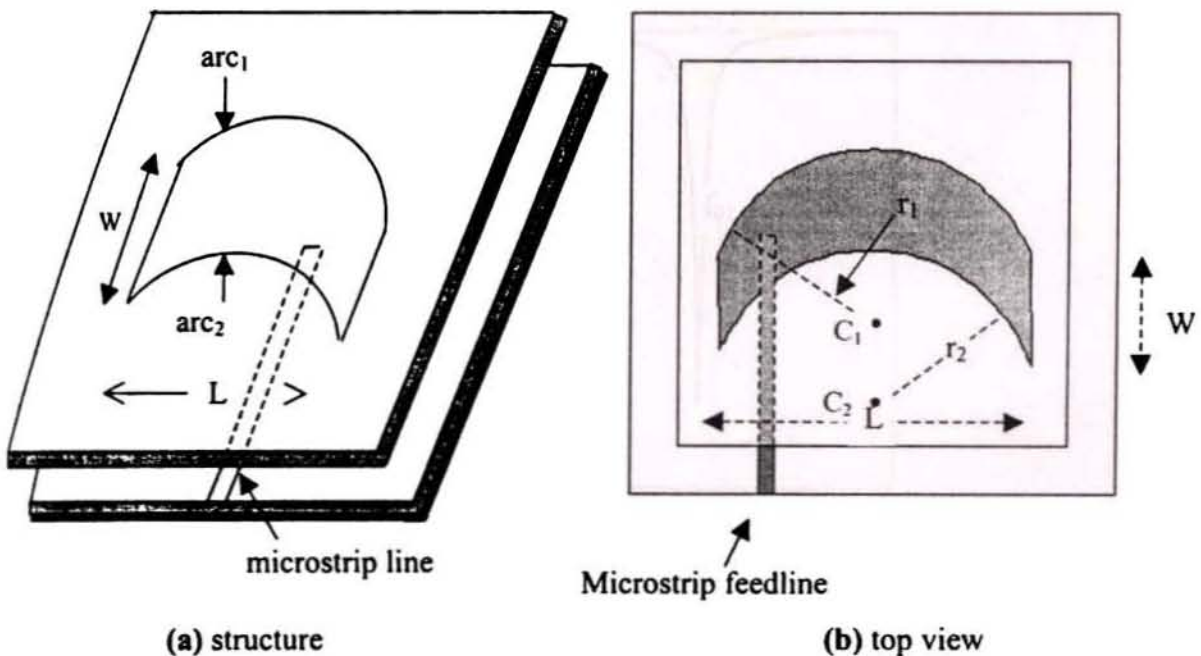


Fig 4.17 Geometry of the compact microstrip antenna

Let us discuss the characteristic properties of a typical patch as an example before going into detailed study on variation of its different parameters.

4.4.2 Characteristics of a typical example

The patch has dimensions of length $L=6\text{cm}$, Width $W=4\text{cm}$, radii of curvature $r_1=r_2=6\text{cm}$ with thickness $h=0.16\text{cm}$ and dielectric constant $\epsilon_r = 4.28$. The lower layer substrate containing the 50Ω microstrip feedline also has the same h and ϵ_r .

4.4.2.1 Resonant modes

In this geometry also, it is observed that two resonant modes TM_{10} and TM_{01} are excited as shown in Fig. 4.18. Size reduction is achieved for TM_{10} mode frequency. Different properties of TM_{10} mode are discussed below.

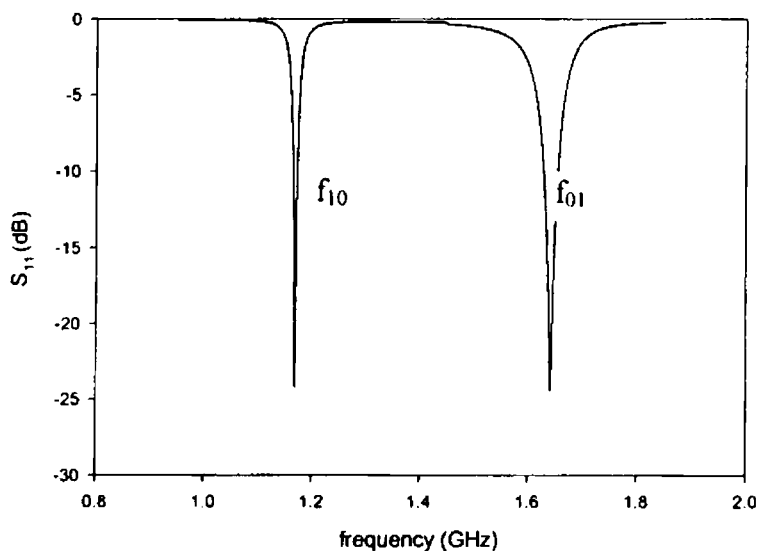


Fig. 4. 18 Variation of return loss against frequency

$$f_{10}=1.169\text{GHz}$$

$$f_{01}=1.641\text{GHz}$$

4.4.2.2 Gain

Gain of a patch for a particular frequency is measured comparing it to that of a standard circular microstrip patch designed for the same frequency. Fig. 4.19 shows the S_{21} plot showing the relative gain of the patch. As indicated in the figure, the gain of the patch for f_{10} is slightly greater than that of a standard circular patch.

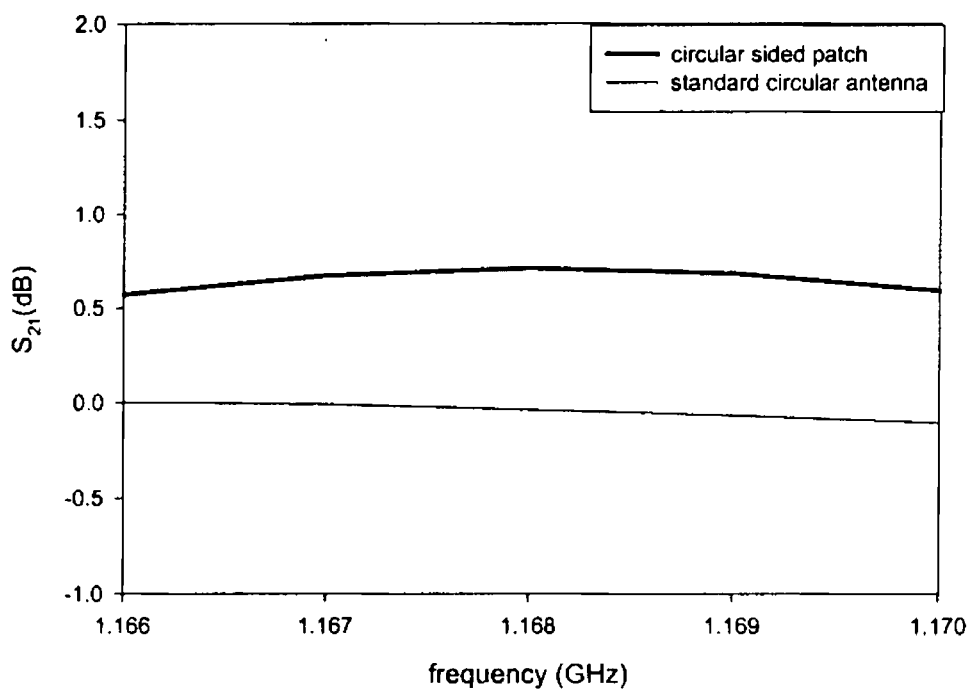


Fig. 4.19 Variation of gain of the patch compared to standard circular disk

4.4.2.3 Radiation patterns

Radiation patterns for $f_{10}=1.169$ GHz are plotted in Fig.4.20. They are broad like those of a rectangular patches and the cross polar levels are better than 20 dB, in both planes.

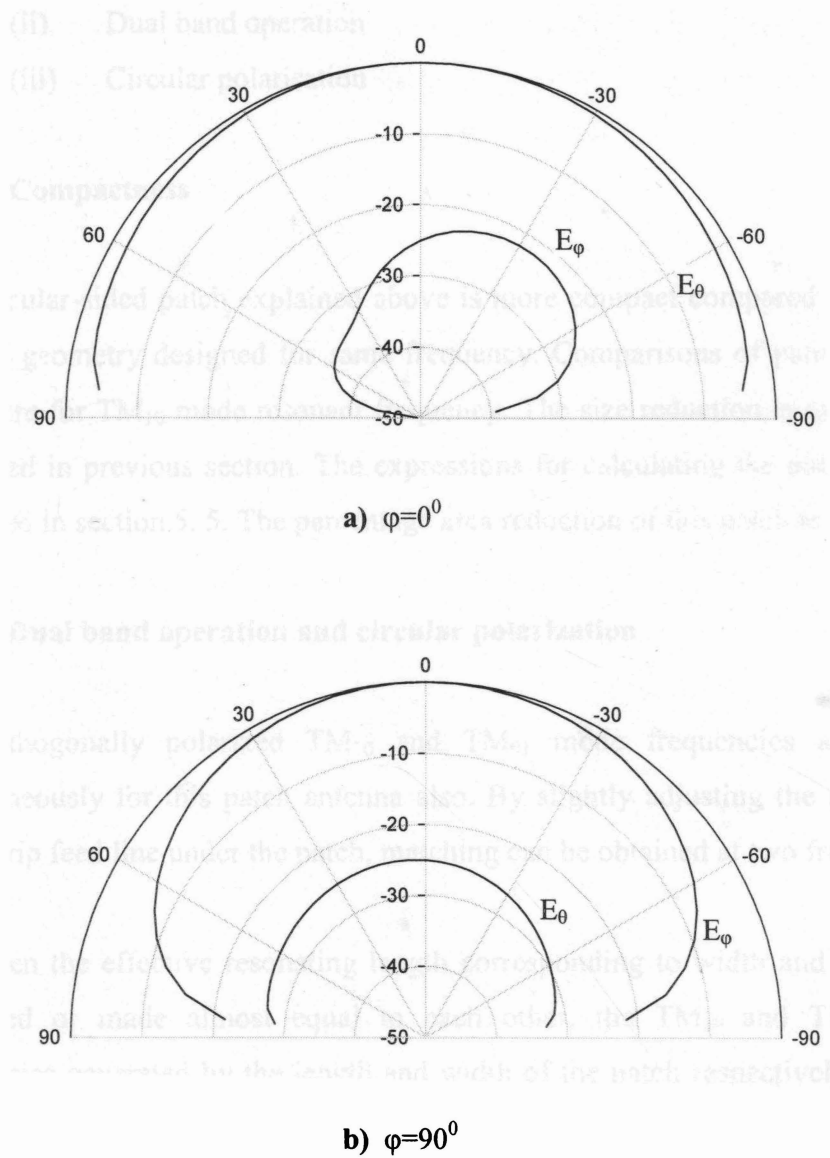


Fig. 4.20 Radiation patterns for TM_{10} mode frequency ($f_{10} = 1.169$ GHz)

4.4.3 Characteristic features

The following features are observed for this circular sided microstrip patch:

- (i) Compactness
- (ii) Dual band operation
- (iii) Circular polarisation

4.4.3.1 Compactness

The circular-sided patch explained above is more compact compared to standard circular geometry designed for same frequency. Comparisons of patch areas are done here for TM_{10} mode resonant frequency. The size reduction is calculated as explained in previous section. The expressions for calculating the patch area are discussed in section 5.5. The percentage area reduction of this patch is ~40%.

4.4.3.2 Dual band operation and circular polarization

The orthogonally polarized TM_{10} and TM_{01} mode frequencies are excited simultaneously for this patch antenna also. By slightly adjusting the position of microstrip feed line under the patch, matching can be obtained at two frequencies.

When the effective resonating length corresponding to width and length are coincided or made almost equal to each other, the TM_{10} and TM_{01} mode frequencies generated by the length and width of the patch respectively, are also very close to each other. These orthogonally polarized frequencies can be merged to a single frequency band with circular polarization by suitably modifying the parameters of the patch.

4.4.4 Characteristics of TM_{10} and TM_{01} mode frequencies (f_{10} and f_{01})

4.4.4.1 Resonant frequency variation with respect to the length

From the table 4.9, it is clear that for a constant width W , as the length increases, the TM_{10} mode frequency (f_{10}) decreases gradually. It is due to the increase in the effective resonating length for this mode. Area reduction for patches of different length are also included in Table 4.9. As the length increases, size reduction also increases.

Fig 4.21 plots the variation of frequencies with Length. The TM_{10} mode frequency changes in a wide range whereas the TM_{01} mode frequency spreads only into a small region or it is almost constant, since the width of the patch remains constant.

Fig 4.22 shows the return loss curves for a typical patch.

Table 4.9 The resonant frequency variation with length for patches of different radii ($W=4\text{cm}$, $h=0.16\text{cm}$, $\epsilon_r=4.28$)

length L (cm)	radii r_1, r_2 (cm)	frequency (GHz)		percentage area reduction
		f_{10}	f_{01}	
4	9,9	1.638	1.732	20.45
	8,8	1.657	1.74	18.6
	7,7	1.652	1.716	19.09
	6,6	1.649	1.735	19.39
	5,5	1.636	1.719	20.66
	4,4	1.661	1.723	18.21
5	9,9	1.404	1.706	30.45
	8,8	1.406	1.699	30.25
	7,7	1.397	1.725	31.14
	6,6	1.389	1.705	31.93
	5,5	1.365	1.678	34.26
	4,4	1.369	1.659	33.87
6	9,9	1.172	1.673	41.85
	8,8	1.167	1.671	42.35
	7,7	1.179	1.683	41.16
	6,6	1.169	1.641	42.15
	5,5	1.168	1.655	42.25
	4,4	1.141	1.604	44.89

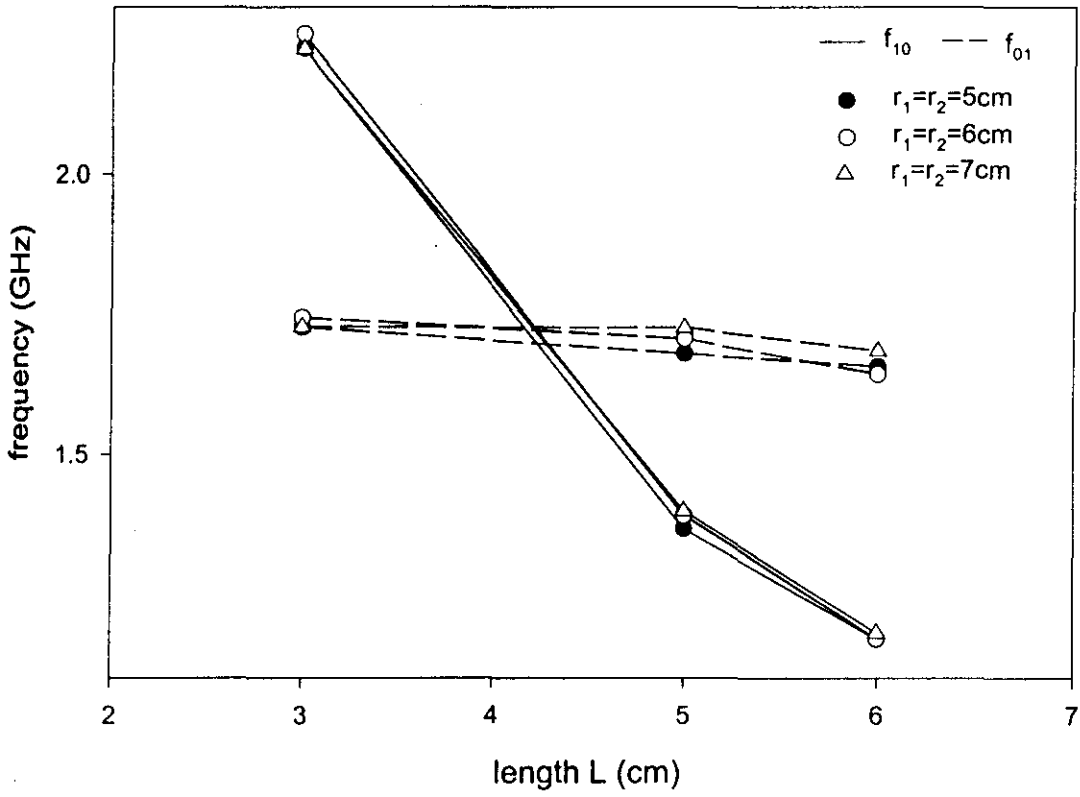
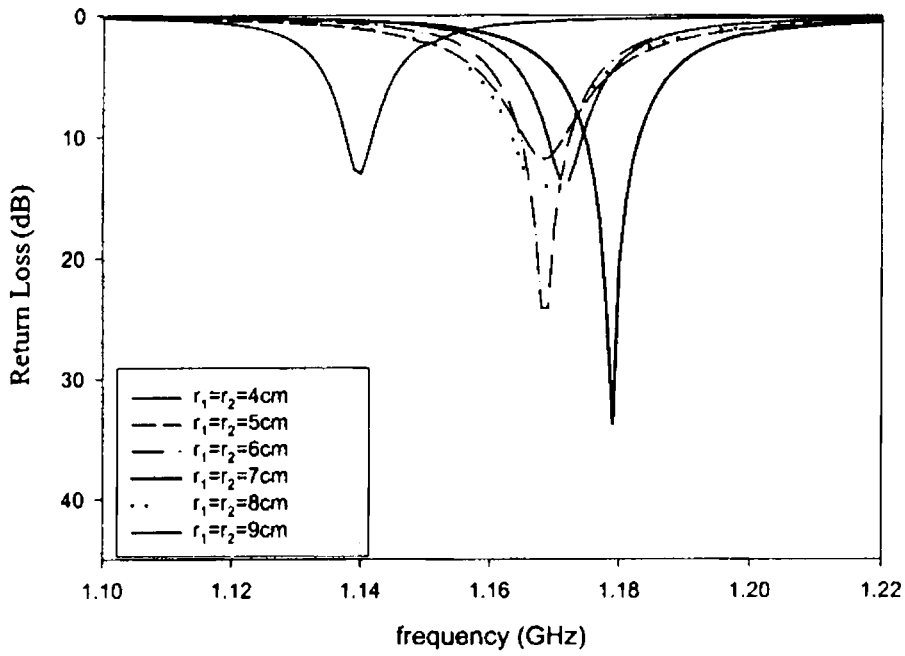
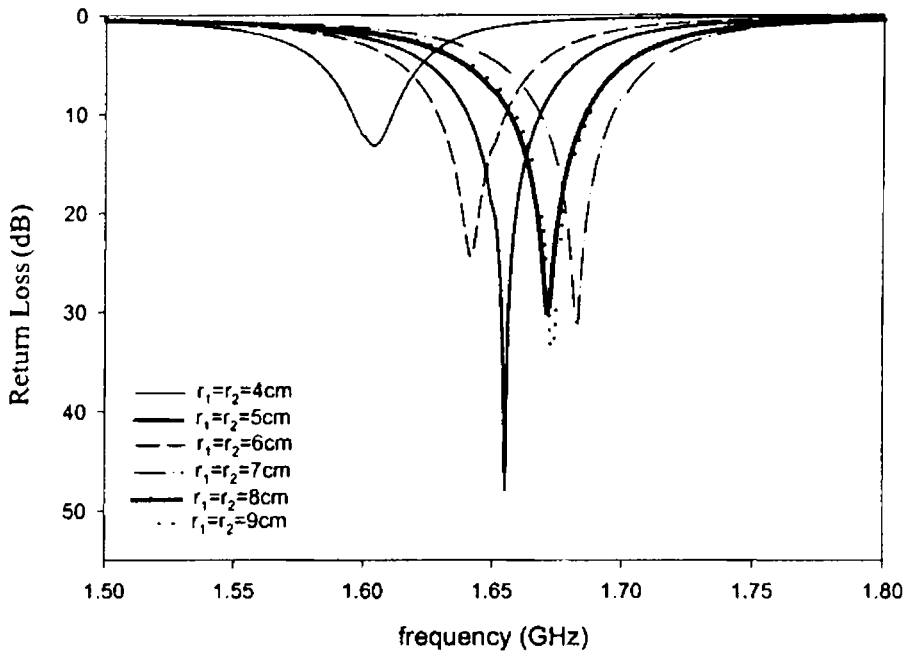


Fig. 4.21 Variation of TM_{10} and TM_{01} frequencies with radii for patches of different lengths ($W=4\text{cm}$, $h=0.16\text{cm}$, $\epsilon_r=4.28$)



(a)



(b)

Fig 4.22 Variation of return loss with frequencies ($L=6, W=4, h=0.16\text{cm}, \epsilon_r=4.28$) (a) f_{10} (b) f_{01}

4.4.4.2 Resonant frequency variation with respect to the width

The effective width of the patch excites the TM_{01} mode frequency (f_{01}). As shown in Table 4.10, the variation of width keeping a constant length and radius results in a change of frequency (f_{01}), retaining f_{10} almost constant. Fig 4.23 plots the variation of frequencies with width.

Table 4.10 The variation of frequencies with width for patches of different radii ($L=4\text{cm}$, $h=0.16\text{cm}$, $\epsilon_r=4.28$)

width W(cm)	radii r_1, r_2 (cm)	frequency (GHz)	
		f_{10}	f_{01}
2	9,9	1.787	3.172
	8,8	1.769	3.185
	7,7	1.755	3.094
	6,6	1.764	3.135
	5,5	1.787	3.084
	4,4	1.775	3.026
3	8,8	1.743	2.258
	7,7	1.723	2.212
	6,6	1.732	2.247
	5,5	1.755	2.218
	4,4	1.751	2.221
4	9,9	1.732	1.638
	8,8	1.74	1.657
	7,7	1.716	1.652
	6,6	1.735	1.649
	5,5	1.719	1.636
	4,4	1.723	1.661

621 396.57
SON

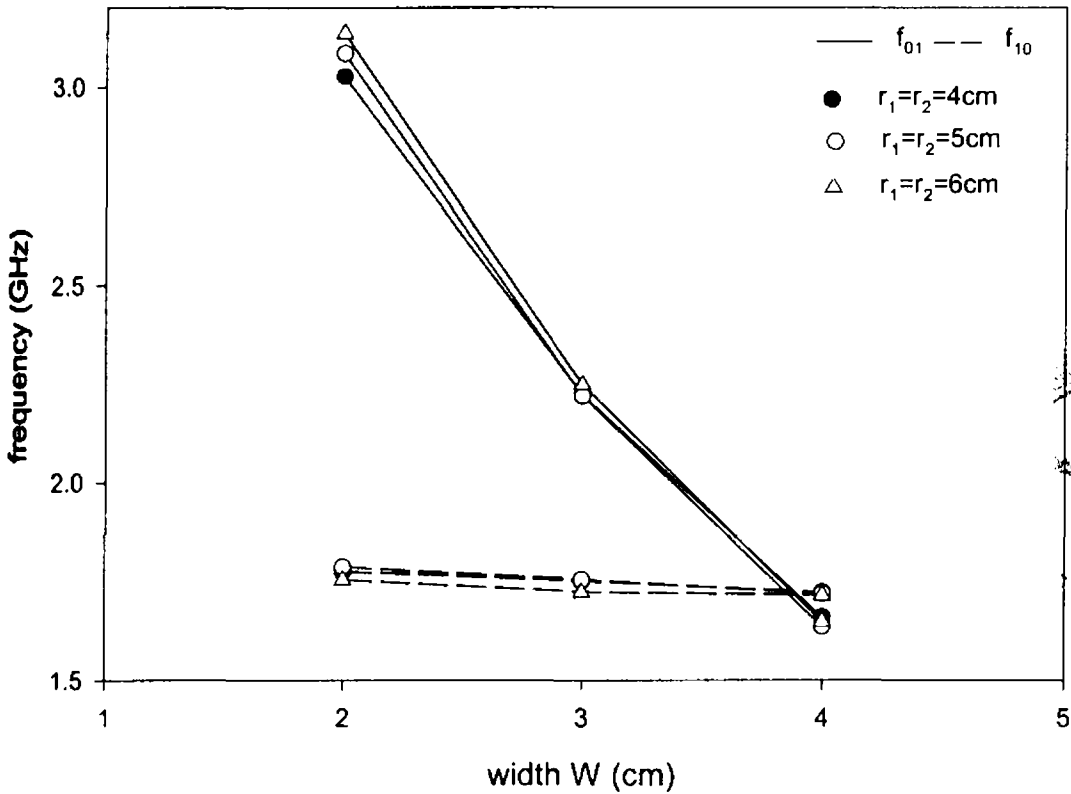


Fig 4.23 Variation of TM_{10} and TM_{01} frequencies with width ($L=4$ cm, $h=0.16$ cm, $\epsilon_r=4.28$)

4.4.4.3 Variation of frequencies with radii of curvature

It can also be noted from Table 4.9 and 4.10 that a decrease in the radii of the patch gives a decrease in the frequencies for constant length and width. This is because of the increase in effective resonating length of the patch. Fig. 4.24 shows the percentage area reduction with radii of curvature for different length of the patch.

G8521

Variation of frequencies (f_{10} and f_{01}) for circular sided patches of unequal radii of curvatures are shown in Table 4.11. It is seen from the table that when the radius of curvature of outer arc increases, f_{10} decreases and f_{01} increases. Whereas for the inner arc, as it increases f_{10} increases and f_{01} decreases, keeping other parameters constant.

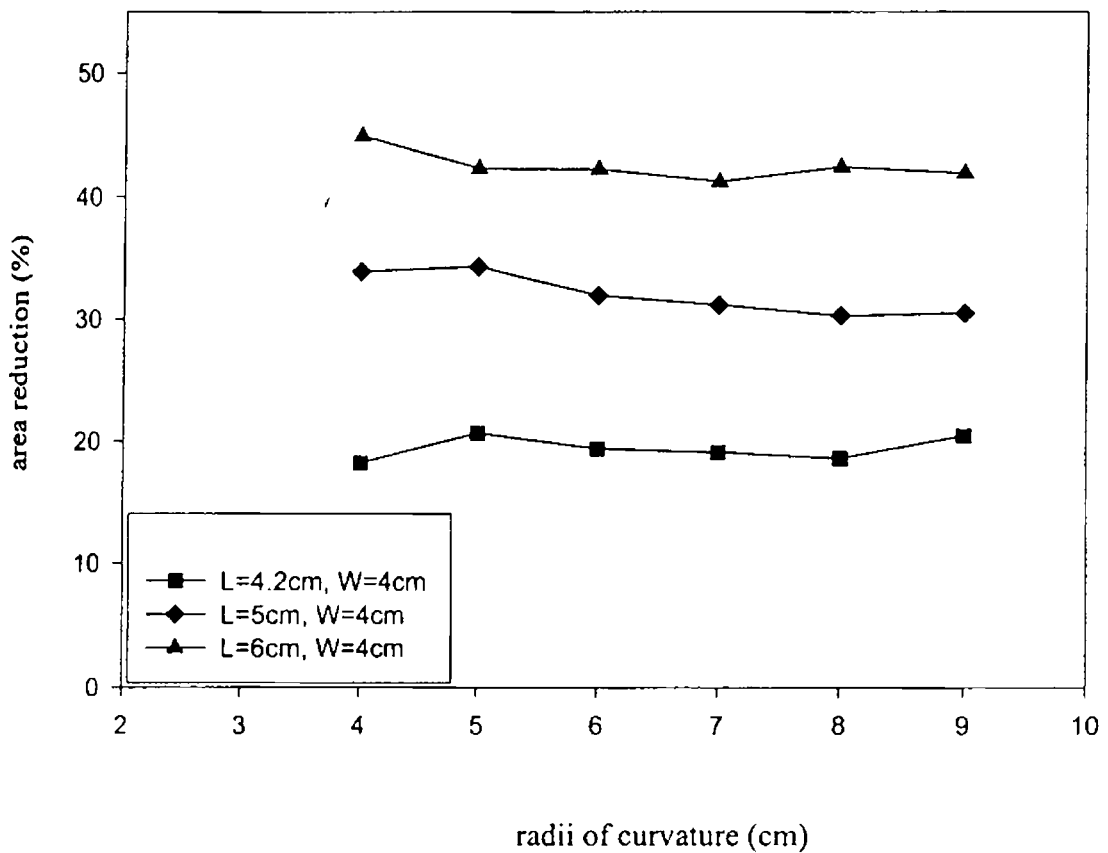


Fig. 4.24 Variation of area reduction compared to that of a circular patch with radii of the two arcs

Table 4.11 Variation of frequencies for patches of different radii (L=4cm, W=3cm, h=0.16cm, $\epsilon_r=4.28$)

radii r_1, r_2 (cm)	frequency f_{10} (GHz)	frequency f_{01} (GHz)
4,4	1.751	2.221
4,5	1.751	2.13
4,6	1.744	2.082
4,7	1.755	2.093
4,8	1.768	2.102
4,9	1.767	2.107
4,4	1.751	2.221
5,4	1.707	2.282
6,4	1.722	2.26
7,4	1.697	2.352
8,4	1.718	2.317
9,4	1.714	2.324

4.4.4.4 Variation of TM_{10} mode frequency for patches of different h and ϵ_r

The variation of f_{10} is studied for antennas on different types of substrates and the results are shown in Table 4.12. It is obvious from the table that, as thickness of the patch increases, f_{10} decreases correspondingly. An increase in dielectric constant also causes reduction in frequency. This behaviour is similar to that of standard microstrip patches.

Table 4.12 Variation of TM_{10} mode frequency with patches of different thickness and dielectric constant

length L (cm)	Width W(cm)	Radii r_1, r_2 (cm)	h (cm)	ϵ_r	Frequency f_{10} (GHz)
5	2	4, 4	0.08	2.2	1.95
6	2	4, 4			1.597
7	2	4, 4			1.335
5	2	4, 4	0.318	2.2	1.835
6	2	4, 4			1.53
7	2	4, 4			1.294
5	2	4, 4	0.16	4.28	1.406
6	2	4, 4			1.16
7	2	4, 4			0.977

4.4.5 Impedance bandwidth and VSWR

Impedance bandwidth and VSWR have similar variations as in the case of the patch discussed in section 4.3. Table 4.13 shows percentage bandwidth values for typical patches. Good matching with desired dual resonant frequencies (f_{10} and f_{01}) can be obtained by adjusting the antenna parameters.

Table 4.13 Impedance bandwidth percentage with frequency for the patch
($h=0.16\text{cm}$, $\epsilon_r=4.28$)

patch parameters (cm)			frequency (GHz)			
L	W	r_1, r_2	f_{10}	%bandwidth	f_{01}	%bandwidth
4	2	4,4	1.775	0.93	3.026	0.5
		5,5	1.787	0.8	3.084	1.3
		6,6	1.764	0.5	3.135	1.0
		7,7	1.755	1.03	3.094	1.16
		9,9	1.787	1.01	3.172	0.8
4	3	4,4	1.751	1.2	2.221	2.21
		5,5	1.755	1.17	2.218	2.19
		6,6	1.732	1.3	2.247	2.27
		7,7	1.723	1.6	2.212	2.26
		8,8	1.743	1.0	2.258	2.3
4	3	4,4	1.751	1.2	2.221	2.21
		4,5	1.751	1.37	2.13	2.02
		4,6	1.744	1.06	2.082	1.97
		4,7	1.755	1.14	2.093	1.89
		4,8	1.768	0.96	2.102	1.95
		4,9	1.767	0.71	2.107	1.97
4	3	4,4	1.751	1.2	2.221	2.21
		5,4	1.707	1.17	2.282	2.30
		6,4	1.722	1.19	2.26	2.26
		7,4	1.697	1.18	2.352	2.47
		8,4	1.718	0.84	2.317	2.37
		9,4	1.714	1.17	2.324	2.45

4.4.6 Radiation characteristics

The radiation characteristics of some typical patches are shown in the Table 4.14. The antenna efficiency is ~75% for all the patches. The gain and directivity values are similar to those of conventional microstrip antennas. In this case also, the patch attains compactness without deteriorating the radiation characteristics.

The gain of patches are almost equal to that of standard circular patches as in the case of circular sided patch which was discussed in the previous section.

Table 4.14 The radiation characteristics of the circular sided antenna

Parameters	Radiation properties				
	f_{10} (GHz)	Antenna Effic.(%)	Gain (dBi)	Directivity (dBi)	3dB beamwidth (deg.)
4, 2, 4, 4	1.661	76.75	5.272	6.42	90.66, 132.30
4, 2, 4, 5	1.635	72.361	5.019	6.424	89.152, 136.23
4, 2, 4, 6	1.649	75.245	5.192	6.427	88.79, 137.22
3, 4, 4, 4	1.725	75.169	4.886	6.125	77.675, 158.992
3, 4, 5, 5	1.726	74.779	4.86	6.125	77.68, 159.02
3, 4, 6, 6	1.743	74.618	4.846	6.118	77.618, 159.076
4, 2, 4, 4	1.775	78.652	5.296	6.339	88.726, 147.212
4, 2, 5, 5	1.787	75.558	5.13	6.348	88.62, 146.65
4, 2, 6, 6	1.764	73.673	5.014	6.341	88.73, 146.814

4.4.7 Antenna fabrication and measurement

4.4.7.1 Geometry and design:

Geometry and various parameters of the patch are as shown in Fig. 4.17.

The antenna with $L=6\text{cm}$, $W=2\text{cm}$, $r_1=4\text{cm}$, $r_2=4\text{cm}$ is fabricated on glass epoxy substrate of thickness $h=0.16\text{cm}$, and dielectric constant $\epsilon_r=4.28$. A 50Ω microstrip feedline on an identical substrate is used for electromagnetic coupling.

4.4.7.2 Experimental results

Variation of return loss against frequency for the fabricated antenna structure is shown in Fig. 4.25. E and H Plane radiation patterns of the antenna at the resonance frequency are shown in Fig. 4.26. The cross polarisation levels are better than 25 dB.

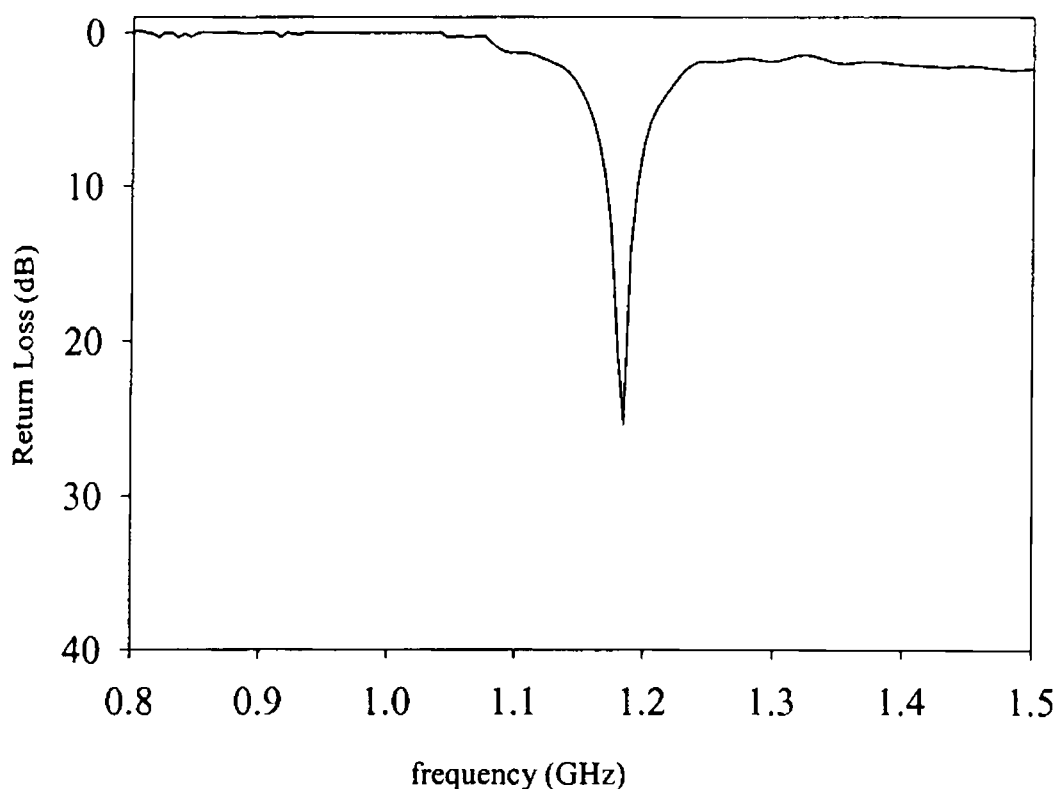


Fig. 4.25 Variation of return loss with frequency

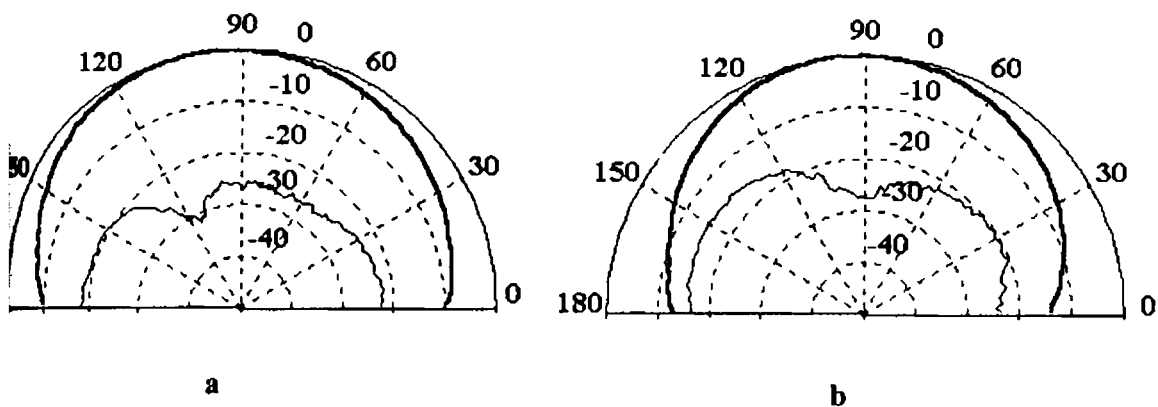


Fig. 4.26 (a) E- Plane Patterns and (b) H- Plane Patterns, for 1.185GHz

———— Copolar ———— Crosspolar

Area reduction of the patch compared to standard circular disk designed for the same frequency is 70% with a small reduction in gain (Fig. 4.27).

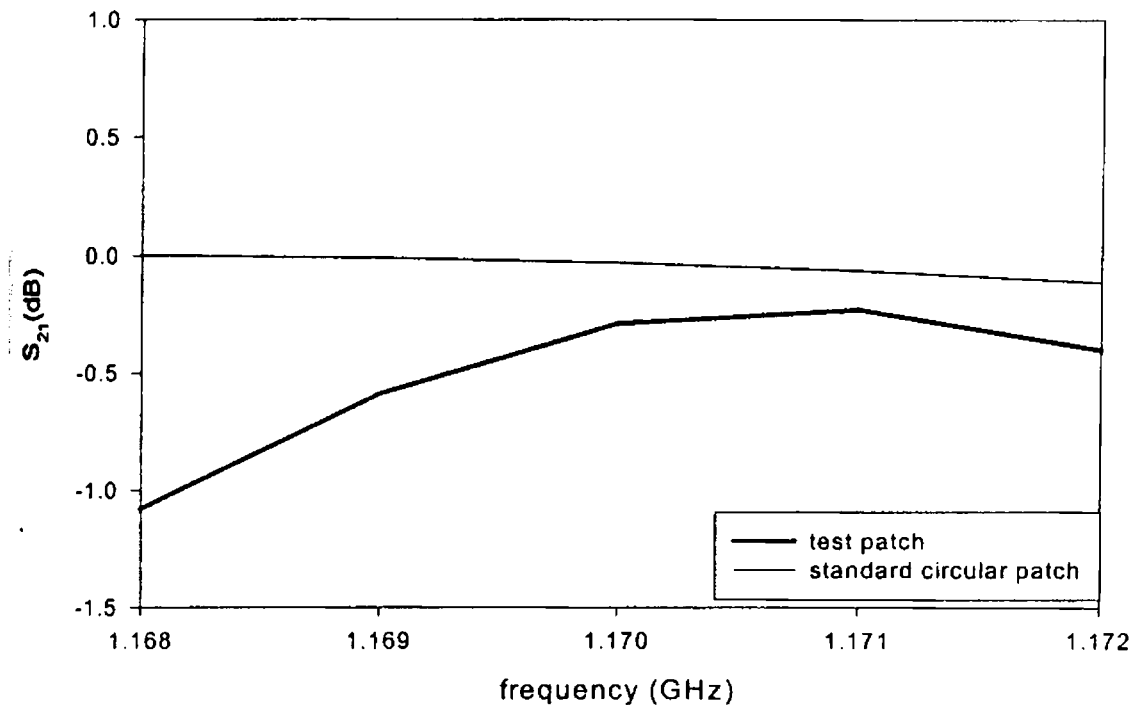


Fig. 4.27 Gain plot (IE3D)

4.5 CRESCENT SHAPED MICROSTRIP ANTENNA

4.5.1 Antenna geometry and excitation technique

Geometry of the patch is a half moon shaped one and hence its name 'crescent-shaped' patch (Fig. 4.28). The patch is formed by two circular arcs of different radii of curvature (r_1 and r_2) displaced by a distance 'd' between their centres of curvature. The structure is on a substrate of dielectric constant ϵ_r and thickness h. A microstrip feed line on the substrate of same ϵ_r and h is used to provide electromagnetic coupling for the patch.

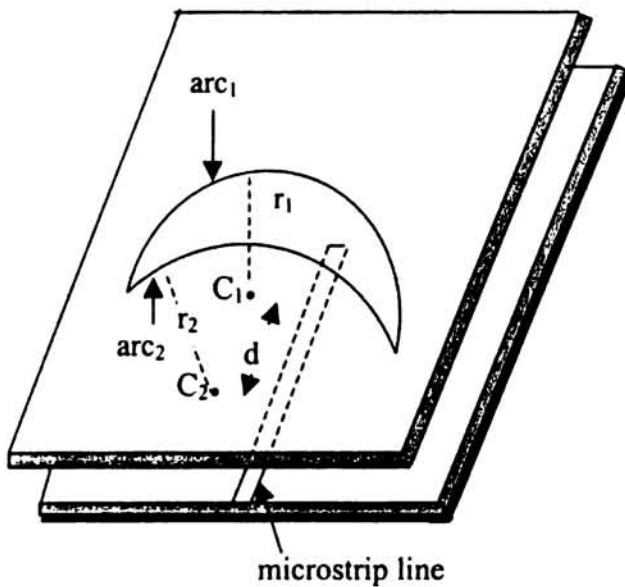


Fig. 4.28 Geometry of the crescent shaped patch

4.5.2 Characteristics of a typical example

Frequency properties of a typical example of $r_1=4\text{cm}$, $r_2=6\text{cm}$ and $d=5\text{cm}$ are discussed below.

4.5.2.1 Resonant modes

The dominant modes of this crescent shaped patch are TM_{11} and TM_{21} (Fig. 4.29) as in the case of standard circular microstrip patch geometries. These modes can be excited using electromagnetic coupling by slightly altering the position of the feed.

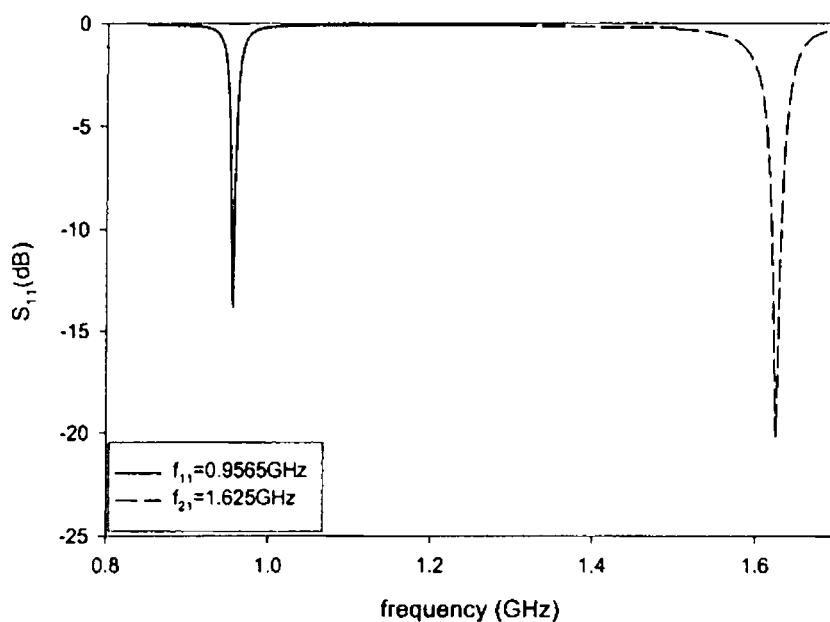


Fig. 4.29 Variation of return loss against frequency

4.5.2.2 Radiation patterns and gain

E plane and H plane radiation patterns of the above structure are shown in Fig. 4.30. The patterns are broad with good cross polar levels (20dB).

Gain of the patch is compared with that of a standard circular microstrip antenna and is plotted in Fig. 4.31. The plot shows a slight decrease in gain.

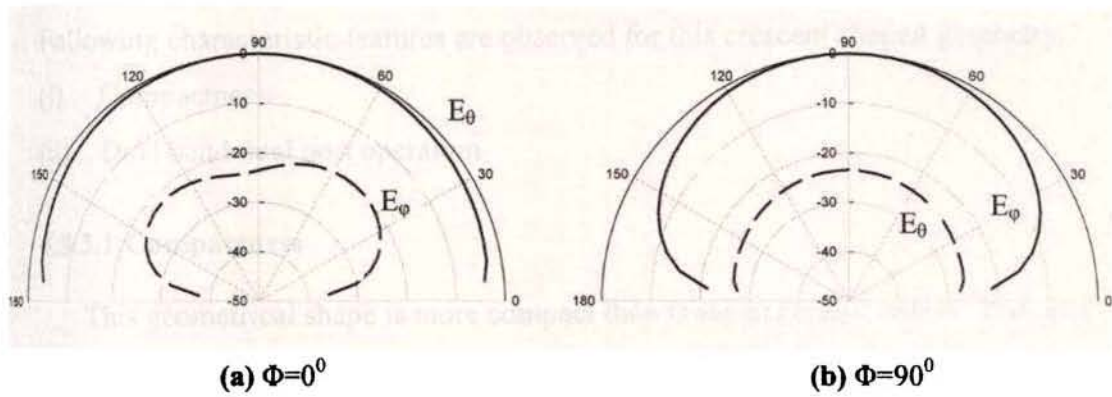


Fig. 4.30 Radiation patterns for $f_{11} = 0.9565 \text{ GHz}$

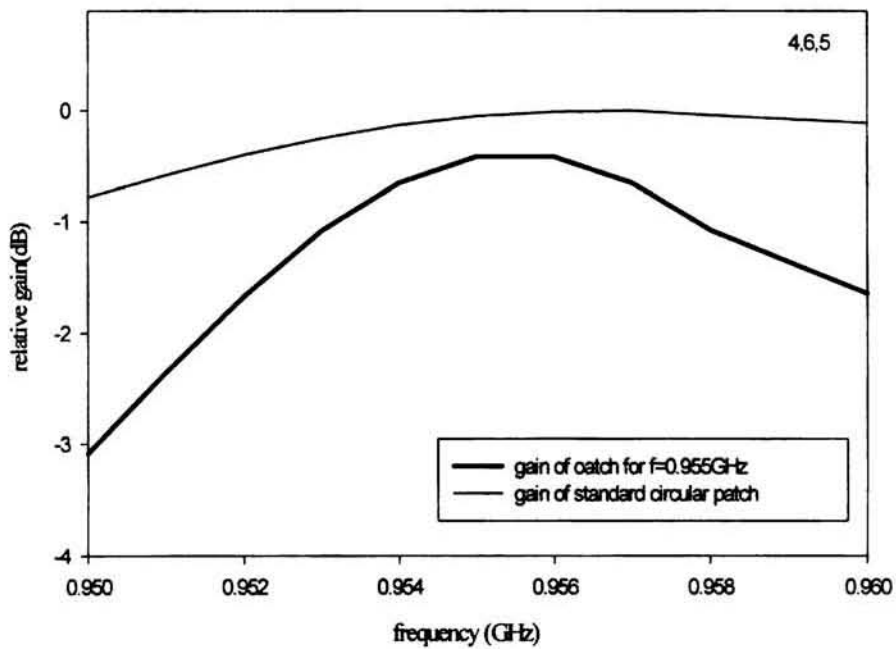


Fig. 4.31 Relative gain of the patch with respect to a circular disk micro strip antenna.

4.5.3 Characteristic features

Following characteristic features are observed for this crescent shaped geometry.

- (i) Compactness
- (ii) Dual band dual port operation

4.5.3.1 Compactness

This geometrical shape is more compact than those explained before. The area reduction of this shape compared to standard circular disk patch designed for the same frequency are expressed in table 4.15. It can be observed from the table that with the increase of distance between the centres of arcs, the area reduction decreases.

4.5.3.2 Dual band dual port operation

The antenna is resonating at TM_{11} and TM_{21} modes. Both these modes can be excited by a single feed suitably located for matching. Also the two modes can be excited independently by two orthogonal feed lines.

4.5.4 Variation of TM_{11} and TM_{21} mode frequencies

The Table 4.15 shows a clear view of the variation of frequencies with different parameters of the patch geometry. As the distance between the centres of curvature 'd' increases, the frequencies f_{11} and f_{21} are decreased, since both the frequencies are dependent on the parameter d. Other effects to be studied are those of radii of curvature of inner and outer circular arcs (r_1 and r_2). It can be seen from the table that as the radius of the inner arc increases, both the frequencies decrease drastically. Whereas with the increase of the radius of the outer arc, the frequencies increase. Thus it can be concluded that the antenna is having an 'effective radius' depending on r_1 and r_2 . The more detailed analysis

Table 4.15 Variation of dual frequencies with d of the crescent shaped microstrip antenna

r_1, r_2 (cm)	d (cm)	f_{11} (GHz)	f_{21} (GHz)	Area reduction (%)
4, 5	2	1.093	1.932	87.23
	2.5	0.9985	1.763	82.49
	3	0.9535	1.659	77.49
	3.5	0.9296	1.597	78.35
	4	0.9278	1.579	77.9
4, 6	3	1.222	2.167	85.91
	3.5	1.099	1.937	80.68
	4	1.016	1.775	76.37
	4.5	0.9833	1.702	71.44
	5	0.9565	1.625	72.65
4, 7	4	1.343	2.383	84.52
	4.5	1.159	2.04	79.76
	5	1.073	1.885	74.84
	5.5	1.017	1.755	70.18
	6	0.9859	1.681	68.45
5, 6	2	0.8904	1.581	89.58
	2.5	0.8134	1.433	85.69
	3	0.7768	1.362	81.88
	3.5	0.7514	1.309	79.66
	4	0.7386	1.278	79.86
5, 7	3	1.01	1.801	88.32
	3.5	0.9067	1.607	84.01
	4	0.8447	1.487	80.07
	4.5	0.802	1.395	76.42
	5	0.7788	1.349	73.49
5, 8	4	1.092	1.957	87.46
	4.5	0.97	1.723	82.91
	5	0.8889	1.563	79.11
	5.5	0.84	1.47	75.29
	6	0.8071	1.401	71.47
6, 7	2	0.7528	1.341	91.17
	2.5	0.6867	1.22	87.89
	3	0.6547	1.154	84.53
	3.5	0.631	1.107	81.43
	4	0.6183	1.076	81.16
6, 8	3	0.8628	1.541	90
	3.5	0.77	1.363	86.44
	4	0.7148	1.264	83.18
	4.5	0.68	1.19	80.00
	5	0.6576	1.147	76.73

and the equations for predicting the resonant frequency of the patch are discussed in the next chapter.

Fig. 4.32 plots the variation of frequencies with 'd' for different values of r_2 and Fig. 4.33 shows those variations for different values of r_1 . The frequencies of the crescent shaped patches on different substrates is given in Table 4.16. The return loss curves for some typical patches are plotted in Fig. 4.34. The variation of area reduction is plotted in Fig. 4.35.

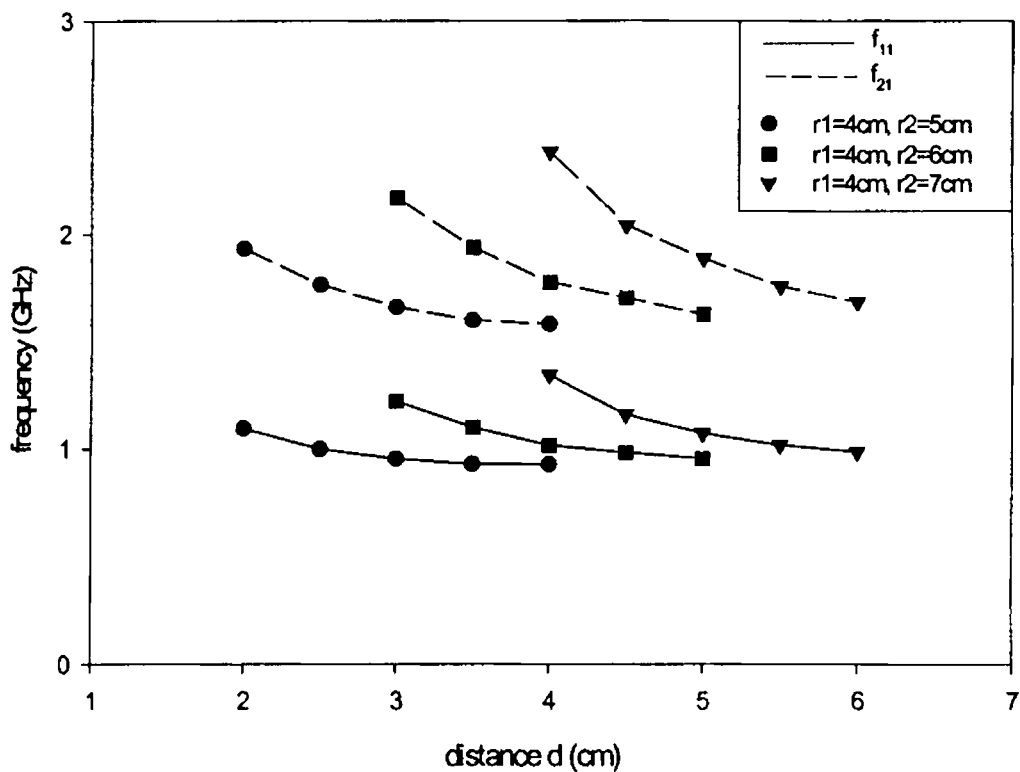


Fig. 4.32 Variation of frequencies for different d and radius of outer arc r_2

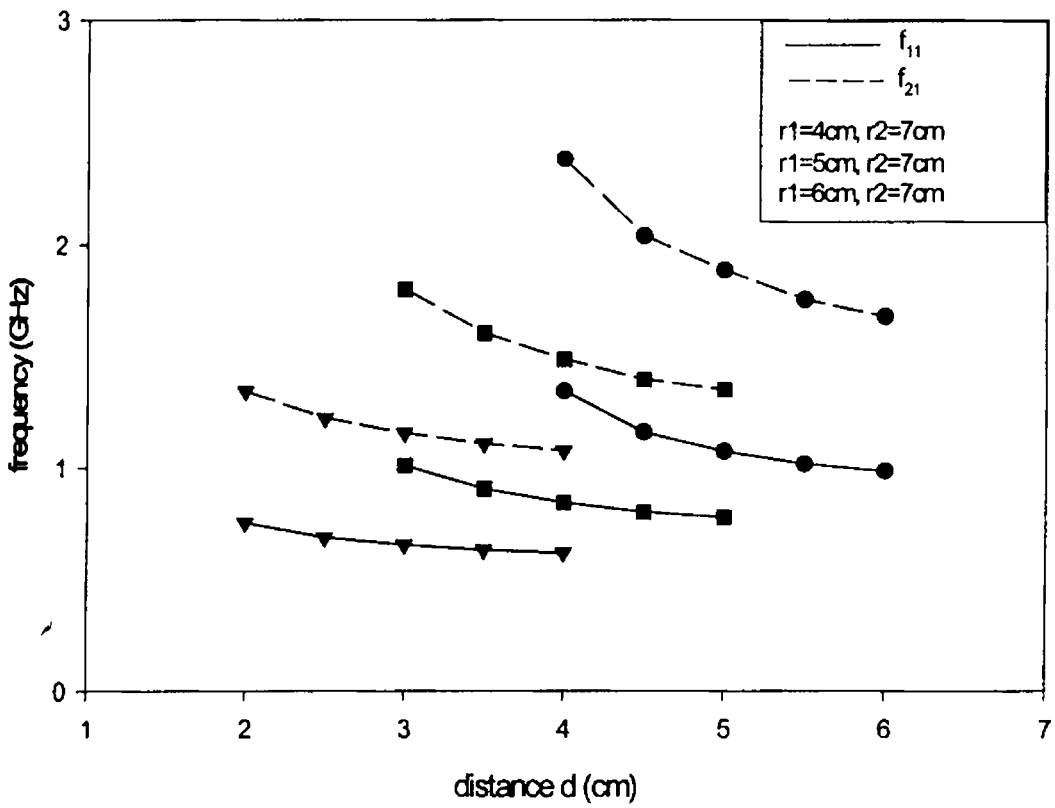
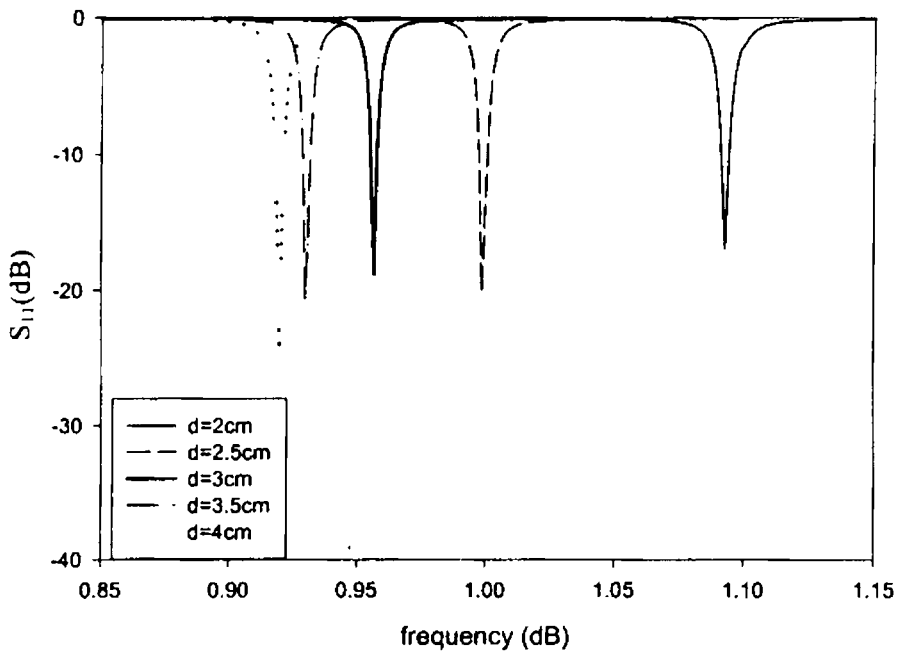


Fig. 4.33 Variation of frequencies for different d and radius of curvature of inner arc ($r_2 = 7$ cm)

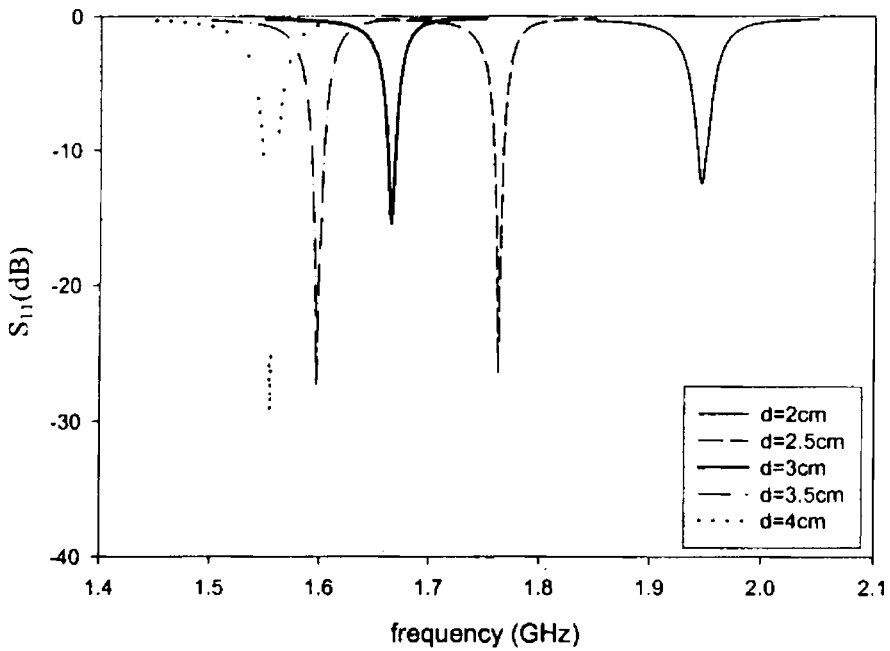
● $r_1 = 4$ cm ■ $r_1 = 5$ cm ▲ $r_1 = 6$ cm

Table 4.16 showing the variation of frequencies with h and ϵ_r ($r_1 = 4$ cm, $r_2 = 6$ cm)

d (cm)	h	ϵ_r	f_{11} (GHz)	f_{21} (GHz)
3	0.08	2.2	1.702	3.03
4			1.4	2.457
5			1.316	2.249
3	0.318	2.2	1.583	2.875
4			1.335	2.326
5			1.26	2.121
3	0.16	4.28	1.222	2.167
4			1.016	1.775
5			0.9565	1.625
3	0.066	10.2	0.832	1.445
4			0.6777	1.189
5			0.6287	1.079



(a)



(b)

Fig. 4.34 Return loss variation with frequency (for different d)

($r_1=4\text{cm}$, $r_2=5\text{cm}$, $h=0.16\text{cm}$, $\epsilon_r=4.28$)

(a) f_{11}

(b) f_{21}

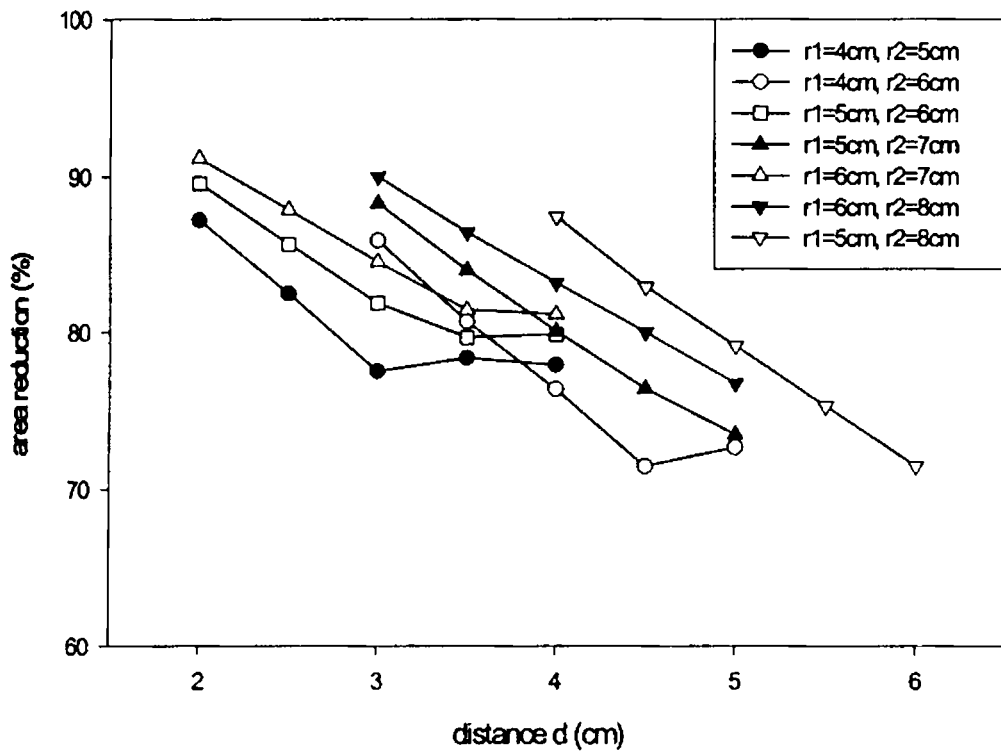


Fig. 4.35 Plot of percentage area reduction versus distance d

4.5.5 Radiation characteristics

Table shows the radiation characteristics of the crescent shaped patch. The efficiency and gain are slightly less than those of the previous patches but the directivity remains the same. Area reduction achieved is as high as 90% for some designs and this is the reason for the reduction in its gain.

Table 4.17 Radiation characteristics of the crescent shaped antenna

Parameters r_1, r_2, d (cm)	Radiation properties				
	f_{11} (GHz)	Antenna Effic.(%)	Gain (dBi)	Directivity (dBi)	3dB beamwidth (deg.)
4, 5, 2	1.093	62.74	4.199	6.224	89.76, 152.93
4, 5, 3	0.9535	68.12	4.521	6.188	89.45, 157.13
4, 5, 4	0.9278	72.99	4.817	6.185	89.036, 158.755
4, 6, 3	1.222	69.79	4.69	6.25	89.82, 150.48
4, 6, 4	1.016	68.035	4.54	6.21	89.44, 154.99
4, 6, 5	0.9565	71.51	4.74	6.20	89.01, 157.32
5, 6, 2	0.8904	54.26	3.535	6.19	89.78, 156.32
5, 6, 3	0.7768	57.29	3.74	6.15	89.54, 160.16
5, 6, 4	0.7386	61.27	4.02	6.15	89.28, 161.35

4.5.6 Compact dual frequency microstrip antenna with dual port

Simultaneous transmit and receive operations can be performed in radar and satellite communication applications using dual port dual polarized microstrip antennas. A good level of isolation is necessary for these antennas to eliminate crosstalk between the two polarizations. The crescent shaped patch is fed with two feedlines, each exciting one frequency. Excellent isolation is achieved between the ports.

4.5.6.1 Geometry and design

Geometrical structure is shown in Fig. 4.36. The patch geometry is already explained in the previous section. Here two perpendicular microstrip feedlines are used to extract the two frequencies independently.

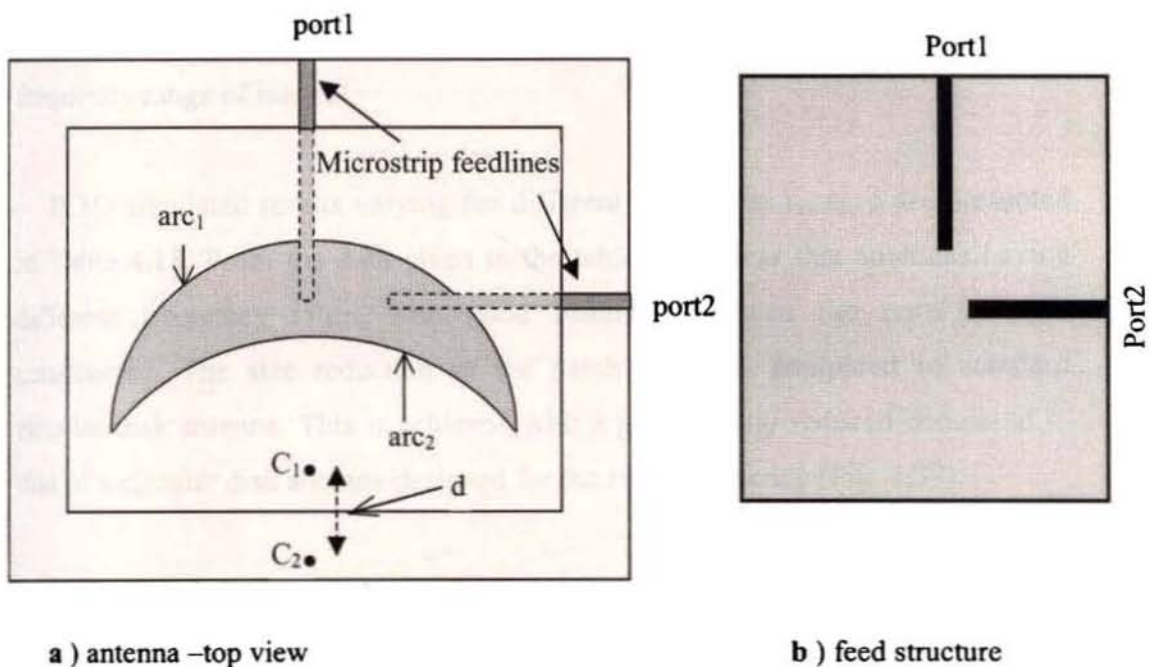


Fig. 4.36 Geometry of the dual port antenna

A crescent shaped antenna with $r_1=4\text{cm}$, $r_2=7\text{cm}$ and $d=6\text{cm}$ is fabricated on a substrate with dielectric constant $\epsilon_r=4.28$ and thickness $h=0.16\text{cm}$. Antenna is excited by electromagnetic coupling using two perpendicular 50 ohm microstrip feedlines of length 6.3cm each etched on a substrate of same thickness and dielectric constant.

4.5.6.2 Experimental and Simulated Results

The antenna resonates at two frequencies 0.9825 GHz and 1.7 GHz for ports 1 and 2 respectively. Variation of return loss with frequency is shown in Fig. 4.37. S_{21} measurements between port1 and port2 in the operating band is shown in Fig. 4.38. It shows that the antenna offers an isolation ~ 30 dB between the ports in the frequency range of interest.

IE3D simulated results varying the different parameters r_1 , r_2 , d are presented in Table 4.18. From the data given in the table, it is clear that antennas having different frequency ratios with good isolation between the ports can be constructed. The size reduction of the patch is $\sim 68\%$ compared to standard circular disk antenna. This is achieved with a gain slightly reduced compared to that of a circular disk antenna designed for the same frequency (Fig. 4.39).

E-Plane and H-Plane patterns of the antenna are taken at TM_{11} and TM_{21} mode frequencies. For taking the radiation patterns, the antenna is kept in the receiving mode with port1 receiving the signal at f_{11} and port2 with the signal at f_{21} . The radiation patterns are broad as in the case of ordinary microstrip antennas and offers excellent cross polar performance (Fig. 4.40).

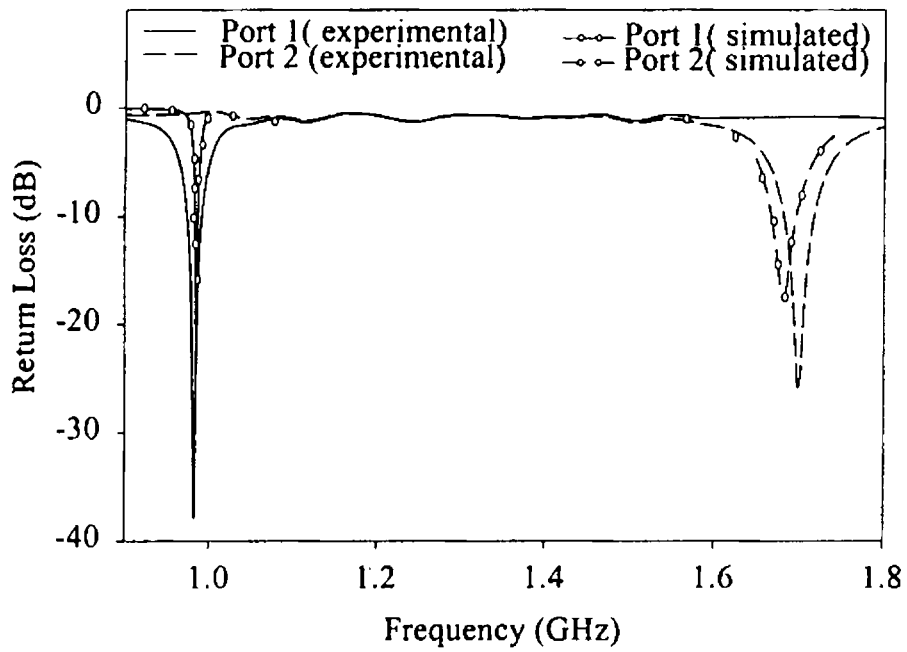


Fig. 4.37 Variation of return loss against frequency

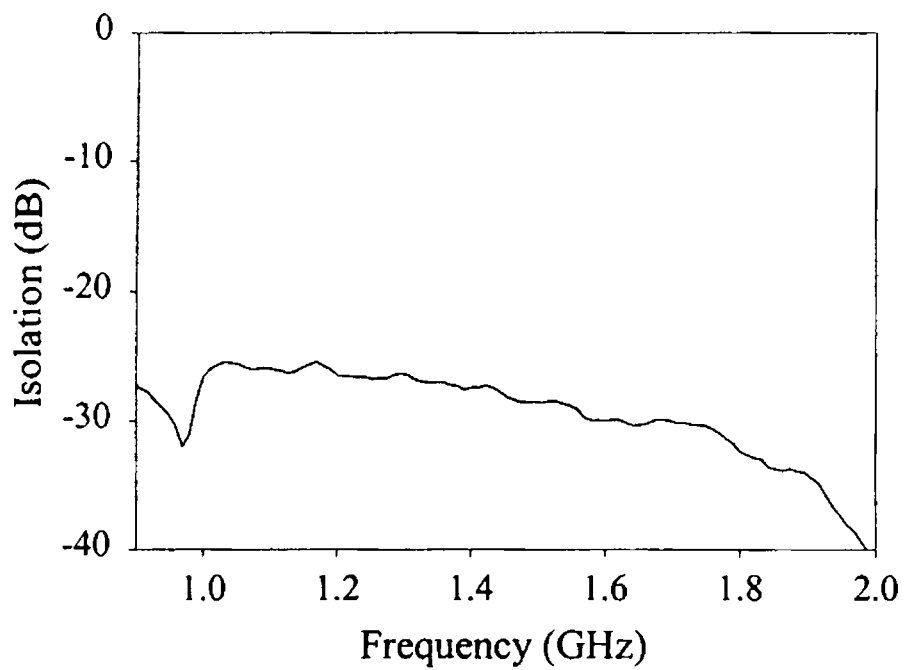
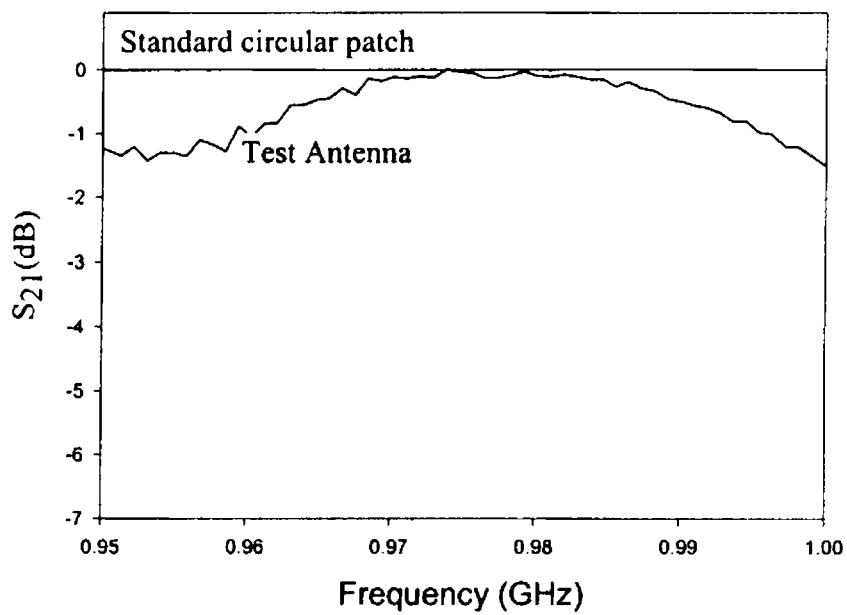


Fig. 4.38 Measured isolation between port1 and port2

Table 4.18 IE3D results for the dual port antenna

r1 (m)	r2 (m)	d (m)	Frequency (GHz)	
			Port1	Port2
0.03	0.06	0.05	1.374	2.369
0.04	0.06	0.04	1.050	1.788
0.05	0.07	0.05	1.352	1.906
0.06	0.07	0.04	1.080	1.521

**Fig. 4.39** Relative gain of the antenna

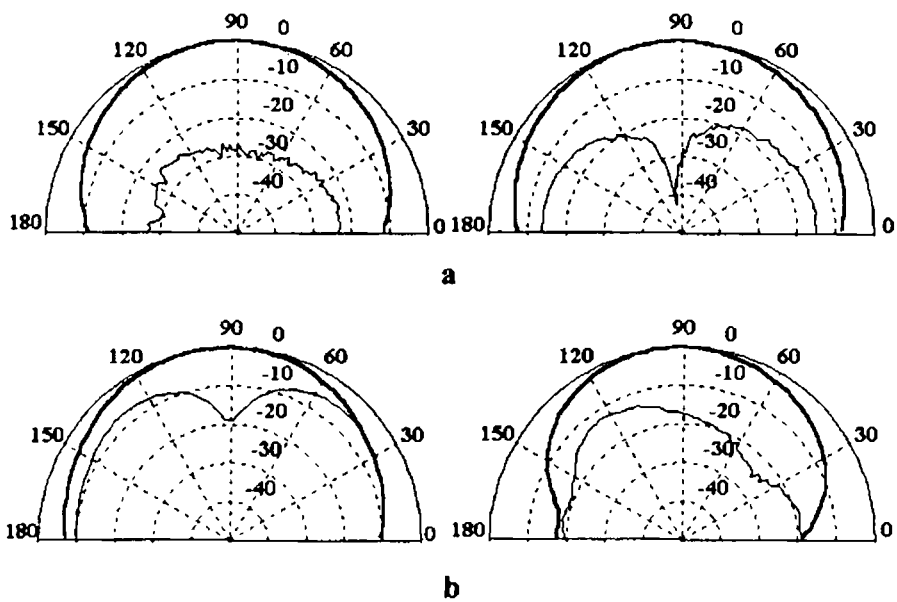


Fig. 4.40 E- and H- plane radiation patterns at the centre frequencies of the two ports

a Port1 (0.9825 GHz)

b Port2 (1.7 GHz)

— copolar
 - - - crosspolar


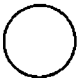
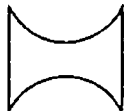


4.6 COMPARISON OF CHARACTERISTICS OF THE RECTANGULAR, CIRCULAR, AND PRESENTED CIRCULAR SIDED PATCHES

It is very useful at this point to compare the characteristics of the standard microstrip antennas with the circular sided patches developed here. Let us take the operating frequency to be 2GHz and design the patches on a substrate material of thickness $h=0.16\text{cm}$ and $\epsilon_r=4.28$. The characteristics of the lowest mode for all the five patches are shown in Table 4.19. If the patches are designed to operate in the lowest mode, a rectangular patch has dimensions $L=3.4\text{cm}$, $W=4.6\text{cm}$ and a circular patch has radius 2cm . The dimensions of different types of circular sided patches are also shown in the table.

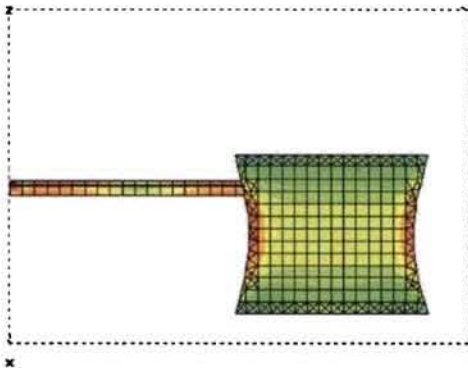
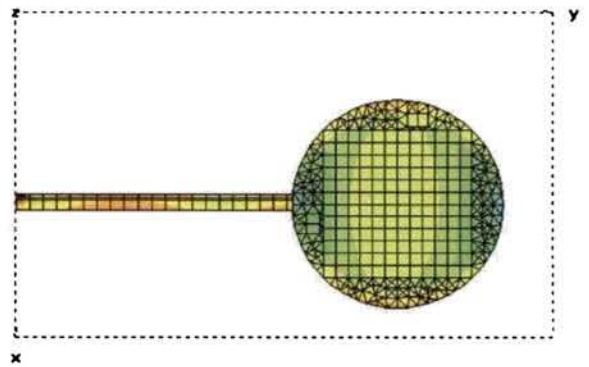
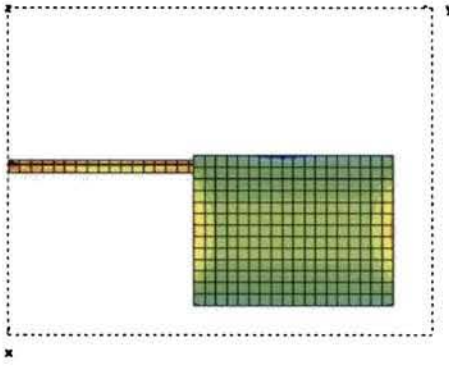
It is seen that all patches radiate in the broadside direction. Directivity is largest for rectangular patch, whereas the antenna efficiency is maximum for the circular disk. The gain of the antenna is the greatest for the circular sided patch with one concave and other convex side.

Fig. 4.41 shows the current density distribution of the various patches simulated using IE3D simulation software. The detailed study of current distribution for identifying the modes of the patches is discussed in next chapter.

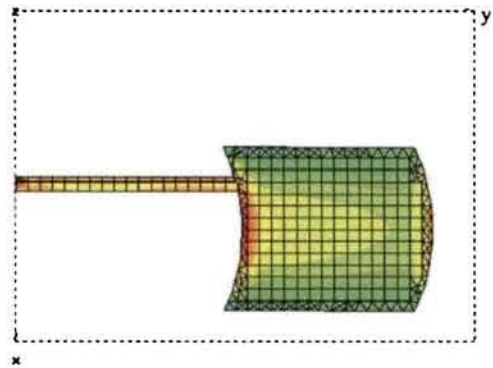
Table 4.19 Comparison of characteristics of rectangular, circular disk and other circular sided compact patches ($h=0.16\text{cm}$, $\epsilon_r=4.28$, $f=2\text{GHz}$)

Characteristics	Rectangular	Circular disk	Circular sided(two concave sides)	Circular sided(one concave and one convex side)	Crescent shaped patch
1. Geometry					
2. Radiation	TM ₁₀	TM ₁₁	TM ₁₀	TM ₁₀	TM ₁₁
Beam position	Broadside	Broadside	Broadside	Broadside	Broadside
Directivity (dBi)	6.61	6.22	6.57	6.55	6.36
Antenna efficiency (%)	78.14	81.00	77.91	80.81	75.94
Gain (dBi)	5.54	5.308	5.49	5.63	5.17
3. Bandwidth (2:1 VSWR)	1.25%	1.75%	1.17%	1.49%	0.6%
4.dimensions (cm)	L=3.4, W=4.6	r=2	L=3.2,W=4, r1=r2=4	L=3.4,W=4, r1=r2=4	r1=2,r2=3, d=2
Area (cm ²)	15.64	12.56	11.36	13.6	3.24

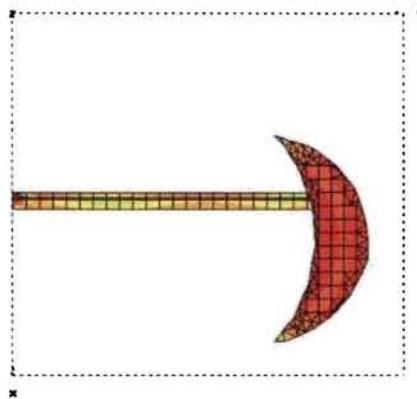
$I_{dB} = 17 \text{ (A/m)}$



c



d



e

Fig. 4.48 Surface current distribution on the different patches.

4.7 CONCLUDING REMARKS

The detailed study of characteristics of three different compact microstrip patches are carried out in this chapter. The frequency variations by varying each parameter are studied. The radiation characteristics and E plane, H plane patterns are discussed for typical patches. Some typical designs with attractive features are studied in detail and the results are presented. Finally comparison of the characteristics of different patches is done using IE3D simulation software.

The aim was to develop a more compact microstrip antenna. Here two circular sided patches with a good size reduction have been achieved. The third patch is of crescent shaped one and it has an excellent size reduction compared to other patches. In this case, gain and efficiency are slightly reduced but almost equal with that of standard rectangular and circular microstrip patches.

THEORETICAL INVESTIGATIONS

The results of theoretical investigations on the different compact microstrip antenna structures are reported in this chapter. The dominant resonant frequency modes of the patches are identified by analyzing the magnetic current distribution of the patches using electromagnetic simulation. Simple design equations are developed for calculating the resonant frequencies of different microstrip shapes by modifying the standard equations for rectangular and circular microstrip patches. This is a fast method for the resonant frequency prediction compared to the complex simulation softwares. The validity of these equations are established by the experimental results.

5.1 IDENTIFICATION AND VERIFICATION OF DOMINANT MODES OF COMPACT MICROSTRIP PATCHES

Here the lower order modes excited by each of the new microstrip patch antenna are studied by analyzing these shapes using IE3D electromagnetic simulation software. The magnetic current distribution plots clearly shows the different excited modes of the patches.

5.1.1 Discussion on different modes of a rectangular microstrip antenna

Before going into the circular sided patches, let us discuss the dominant modes of a rectangular patch geometry. The dominant lower order modes of rectangular microstrip patch, which we are discussing here are TM_{01} , TM_{10} and TM_{11} modes. Conventionally the mode corresponding to the length is TM_{10} , and that excited by width is TM_{01} , while for TM_{11} , there is current variation along both the length and width of the patch. This can be clearly observed from the simulated current distribution plots (Fig. 5.1). The magnetic current distribution graphs for the first three resonant modes of a rectangular microstrip patch with Length $L=7\text{cm}$ and width $W=4\text{cm}$ are shown in Fig. 5.1.a. The plot for the first frequency ($f_1=1.035\text{GHz}$) shows that the current variation is along the length of the patch whereas along the width, it is constant, which represents a TM_{10} mode. Similarly the current distribution for the frequency ($f_2=1.716\text{GHz}$) plotted in fig. 5.1.b, has a current variation along the width of the patch whereas it remains constant along the length, which is TM_{01} mode. Now the current distribution shown in Fig. (5.1.c) for the third frequency ($f_3=2.067\text{GHz}$) clearly indicates that the mode is TM_{11} .

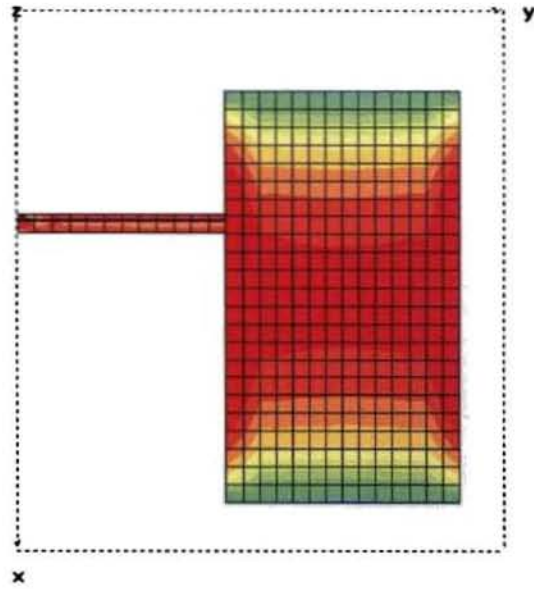
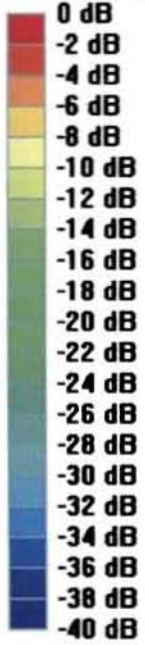
5.1.2 Resonating modes of the circular sided patch (with two concave sides)

The resonant frequencies of the circular sided patch (with two concave sides) are less than those of a rectangular patch for the same length and width. The modifications are due to the circular arcs of the geometry as explained in chapter 4. The magnetic current distribution graphs for a typical circular sided patch geometry with length $L=7\text{cm}$, width $W=4\text{cm}$, and radii of curvature $r_1=r_2=10\text{cm}$, are shown in Fig. 5.2. The current variation for first frequency ($f_1=0.9589\text{GHz}$), the second frequency ($f_2=2.085\text{GHz}$) and the third frequency ($f_3=2.214\text{GHz}$) are similar to those of a rectangular patch. Hence f_1 , f_2 , and f_3 are identified to be resonant frequencies of the modes TM_{10} , TM_{01} and TM_{11} respectively.

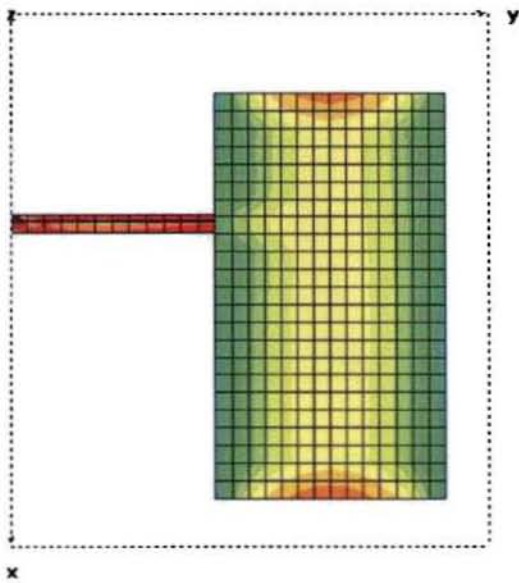
5.1.3 Resonant modes of the circular sided patch (with one concave and other convex side)

The resonant frequencies of the circular sided patch (with one concave and other convex side) are also studied using IE3D simulation software. Magnetic current distribution graphs for a typical circular sided patch geometry with length $L=7\text{cm}$, width $W=4\text{cm}$, and radii of curvature $r_1=r_2=10\text{cm}$, are shown in Fig. 5.3. The current variation for first frequency ($f_1=1.018\text{GHz}$), second frequency ($f_2=1.651\text{GHz}$) and the third frequency ($f_3=2.027\text{GHz}$) are similar to those of rectangular and the circular sided (with two concave sides) patches. The current varies along the length for f_1 , the width for f_2 , and both length and width for f_3 .

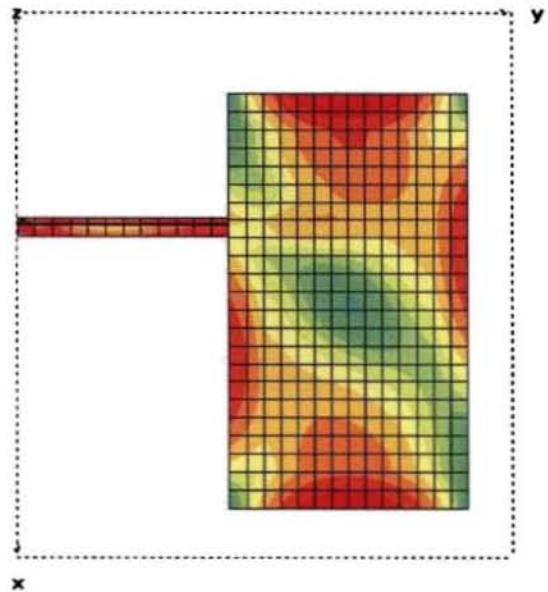
0 dB = 10 [A/m]



a) $f_1=1.035\text{GHz}$

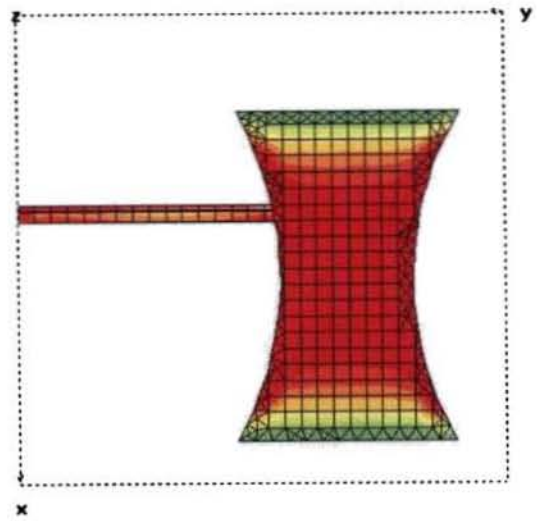
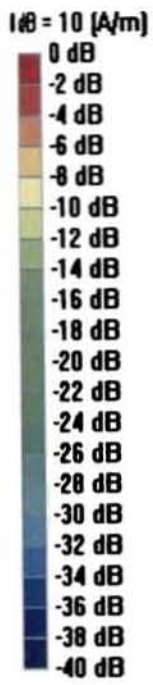


b) $f_2=1.716\text{GHz}$

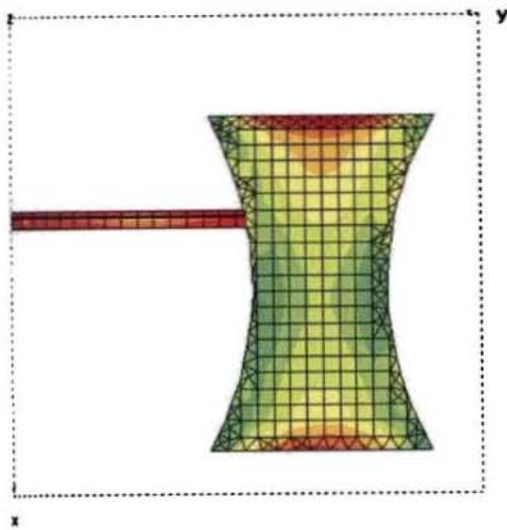


c) $f_3=2.067\text{GHz}$

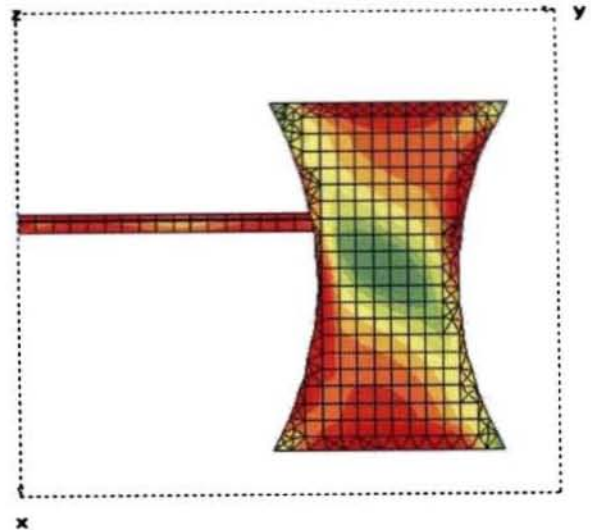
Fig 5.1 3D average current density on the surface of the rectangular patch ($L=7\text{cm}$, $W=4\text{cm}$)



a) $f_1=0.9589\text{GHz}$

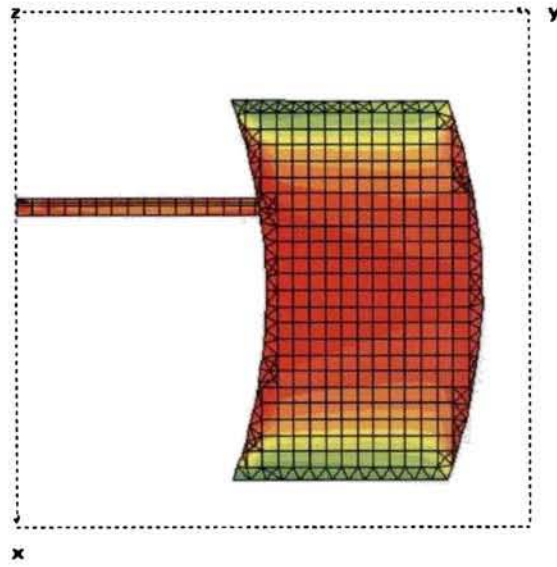
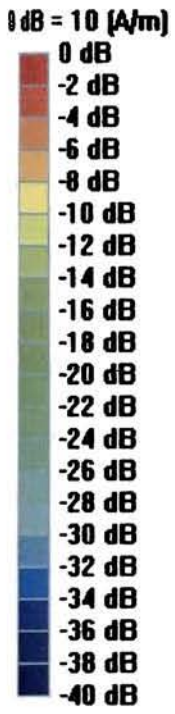


b) $f_2=2.085\text{GHz}$

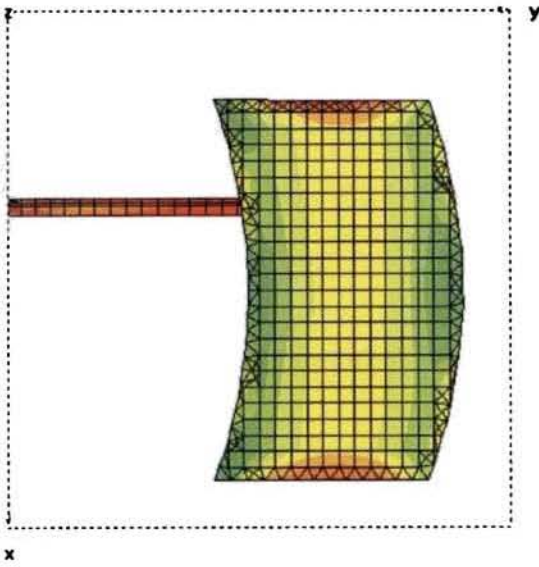


c) $f_3=2.214\text{GHz}$

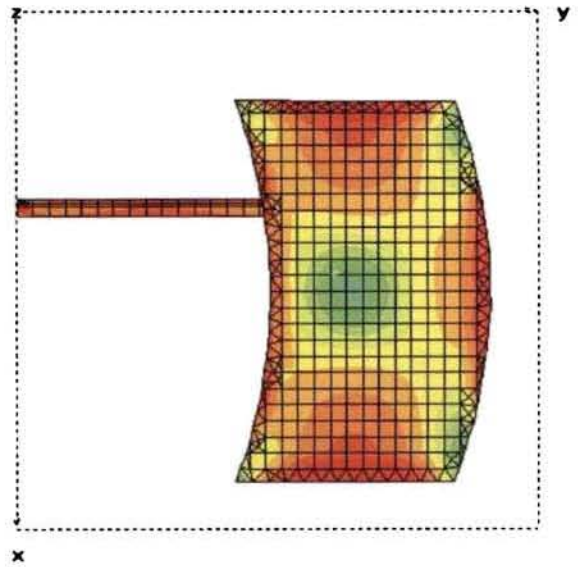
Fig. 5.2 3D average current density on the surface of the circular sided patch ($L=7\text{cm}$, $W=4\text{cm}$, $r_1=r_2=10\text{cm}$)



a) $f_1 = 1.018 \text{ GHz}$



b) $f_2 = 1.651 \text{ GHz}$



c) $f_3 = 2.027 \text{ GHz}$

Fig. 5.3 3D average current density on the patch surface ($L=7\text{cm}$, $W=4\text{cm}$, $r_1=r_2=10\text{cm}$)

5.1.4 Discussion on different modes of a circular disk microstrip antenna

The lower order modes of a circular disk patch are TM_{11} , TM_{21} and TM_{02} respectively, as explained in chapter 1. Since the circular patch has only one varying parameter (the radius), its mode prediction is more simple compared to that of a rectangular microstrip patch. The magnetic current distribution of the circular disk patch with radius $r=4\text{cm}$, for the three modes ($f_1=1.026\text{GHz}$, $f_2=1.748\text{GHz}$ and $f_3=2.091\text{GHz}$) is illustrated in Fig. 5.4.

The resonant modes of a half-disk microstrip antenna are the same as that for the circular-disk. Here also the single parameter that affects the frequency is the radius of the circle. The magnetic current distribution for the half disk antenna is however, somewhat different from that of a circular disk antenna. The current variation graphs of a typical half-disk microstrip with $r=4\text{cm}$ for $f_1=1.05\text{GHz}$ (TM_{11}), $f_2=1.706\text{GHz}$ (TM_{21}) and $f_3=2.365\text{GHz}$ (TM_{02}) modes are shown in the Fig. 5.5.

5.1.5 Modes of the crescent-shaped microstrip antenna

Since the geometrical shape of the crescent-shaped patch is more closer to that of a half-disk, the current distribution of it is similar to that of a half-disk. The current distribution of the crescent-shaped patch for $f_1=1.016\text{GHz}$, $f_2=1.745\text{GHz}$, and $f_3=2.472\text{GHz}$ are illustrated in Fig. 5.6. These frequencies are very close to the TM_{11} , TM_{21} , and TM_{02} mode frequencies of circular and half-disk microstrips. The resonant frequency calculation of this crescent-shaped patch will be discussed in the coming sections. It is also clear from the figure that the current distribution of the crescent-shaped patch is similar to that of a half-disk and thus the TM_{11} , TM_{21} and TM_{02} modes identified.

θ dB = 5 (A/m)

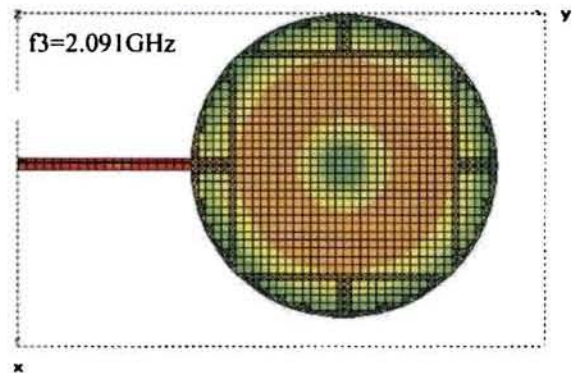
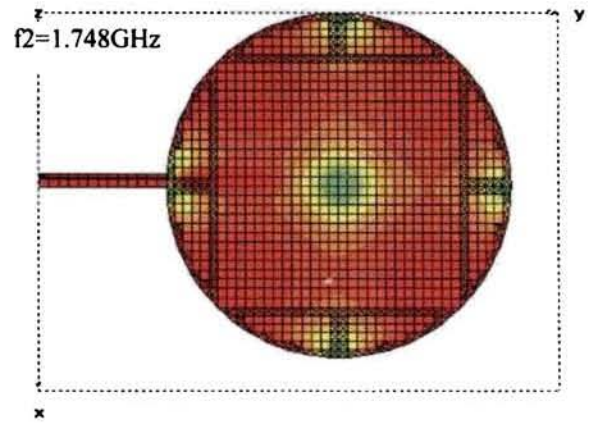
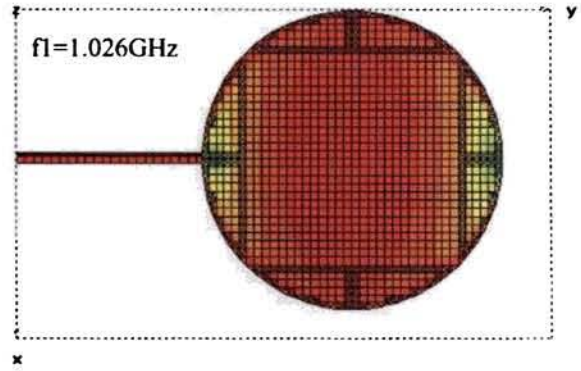


Fig. 5.4 Current distribution on the circular patch ($r=4\text{cm}$)

0 dB = 11 (A/m)

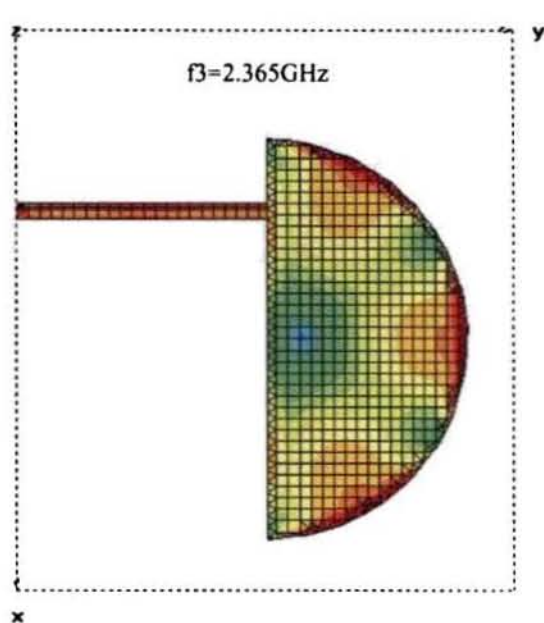
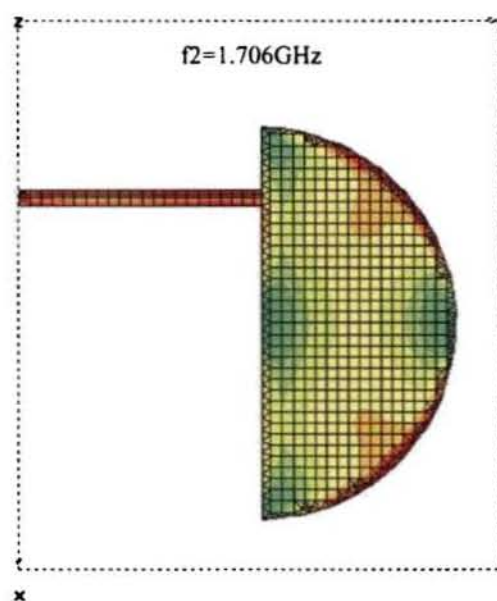
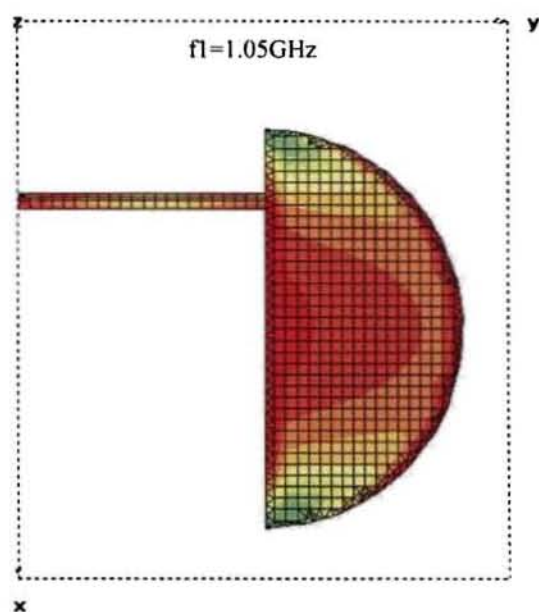


Fig. 5.5 Current distribution on the half disk ($r=4\text{cm}$)

0 dB = 11 (A/m)

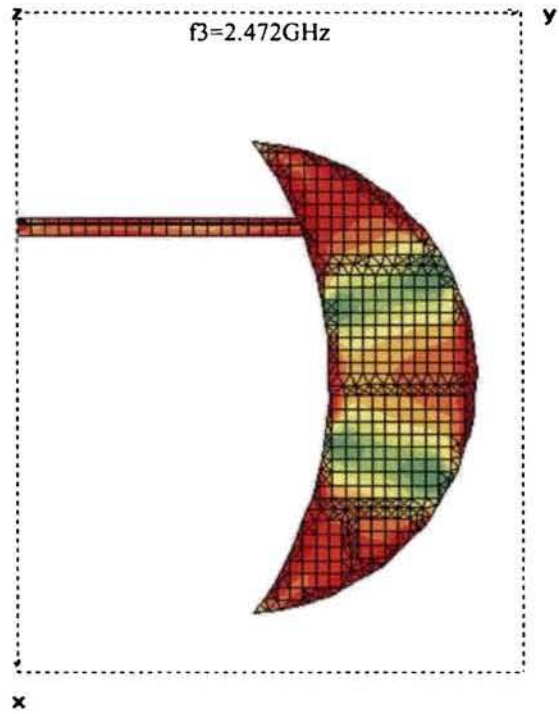
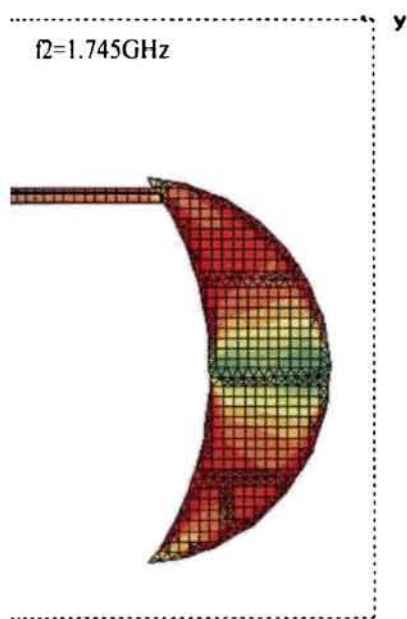
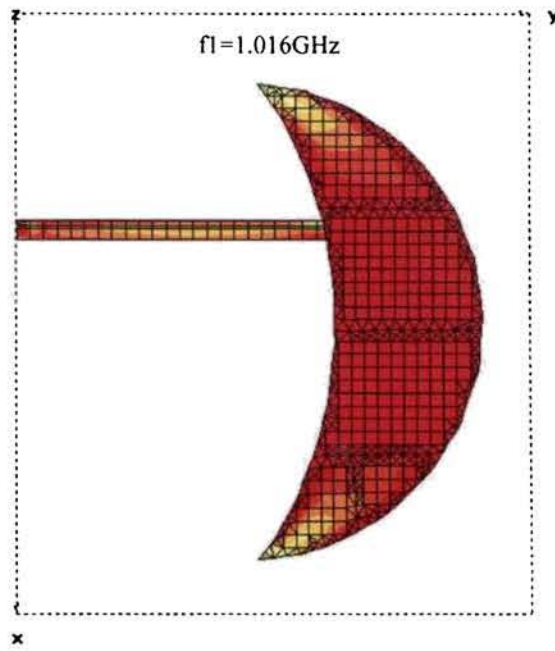


Fig. 5.6 Current distribution on the crescent shaped patch ($r_1=4\text{cm}$, $r_2=7\text{cm}$ and $d=5.5\text{cm}$)

$$Z_c \sim \frac{Z_0}{\sqrt{\epsilon_r}} \left(\frac{w}{h} + 1.393 + 0.667 \ln \left(\frac{w}{h} + 1.444 \right) \right)^{-1} \Omega \quad w/h > 1 \quad (5.2)$$

where $Z_0 = 120\pi = 376.6 \Omega$ is the characteristic impedance of free space.

These expressions are used to determine C_c and Z_c in terms of the line dimensions and the substrate permittivity.

5.2.2 Microstrip line synthesis

The determination of the w/h ratio for a required characteristic impedance Z_c , is carried out using the following relations:

For $w/h < 2$:

$$\frac{w}{h} \cong 4 \left[\frac{1}{2} \exp(A) - \exp(-A) \right]^{-1} \quad (5.3)$$

with

$$A = \pi \sqrt{2(\epsilon_r + 1)} (Z_c / Z_0) + \frac{\epsilon_r - 1}{\epsilon_r + 1} (0.23 + 0.11 / \epsilon_r) \quad (5.4)$$

while for $w/h \geq 2$

$$\frac{w}{h} \cong \frac{\epsilon_r - 1}{\pi \epsilon_r} (\ln(B - 1) + 0.39 - 0.61 / \epsilon_r) + \frac{2}{\pi} (B - 1 - \ln(2B - 1)) \quad (5.5)$$

with

$$B = \frac{\pi}{2\sqrt{\epsilon_r}} \frac{Z_0}{Z_c} \quad (5.6)$$

Most of the antennas for the present work were fabricated on glass epoxy substrates with $h=0.16\text{cm}$ and $\epsilon_r = 4.28$. For this substrate, the width of the line corresponding to a characteristic impedance 50Ω is calculated as 3mm .

5.3 RESONANT FREQUENCY CALCULATION OF A RECTANGULAR MICROSTRIP ANTENNA

Microstrip antennas resemble dielectric loaded cavities, and they exhibit higher order resonances. In the cavity model analysis, the normalized fields within the dielectric substrate (between the patch and the ground plane) can be found accurately by treating that region as a cavity bounded by electric conductors (above and below it) and by magnetic walls along the perimeter of the patch [23, 24, 25].

Referring to Fig. 5.8, the volume beneath the patch can be treated as a rectangular cavity loaded with a dielectric material with permittivity ϵ_r .

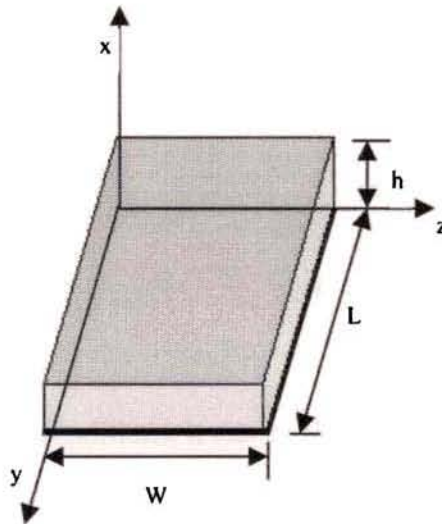


Fig 5.8 Rectangular microstrip patch geometry

The field configurations within the cavity can be found using the vector potential approach.

The vector potential A_x must satisfy the homogeneous wave equation of

$$\nabla^2 A_x + k^2 A_x = 0 \quad (5.7)$$

Whose solution is written in general, using the separation of variables as

$$A_x = [A_1 \cos(k_x x) + B_1 \sin(k_x x)] \cdot [A_2 \cos(k_y y) + B_2 \sin(k_y y)] \\ \cdot [A_3 \cos(k_z z) + B_3 \sin(k_z z)] \quad (5.8)$$

Where k_x , k_y and k_z are the wave numbers along the x , y , and z directions, respectively. These will be determined subject to the boundary conditions. The electric and magnetic fields within the cavity are related to the vector potential A_x by

$$E_x = -j \frac{1}{\omega \mu \epsilon} \left(\frac{\partial^2}{\partial x^2} + k^2 \right) A_x, \quad H_x = 0 \quad (5.9)$$

$$E_y = -j \frac{1}{\omega \mu \epsilon} \frac{\partial^2 A_x}{\partial x \partial y}, \quad H_y = \frac{1}{\mu} \frac{\partial A_x}{\partial z}$$

$$E_z = -j \frac{1}{\omega \mu \epsilon} \frac{\partial^2 A_x}{\partial x \partial z}, \quad H_z = \frac{1}{\mu} \frac{\partial A_x}{\partial y}$$

Applying the boundary conditions, it can be shown that

$$B_1 = B_2 = B_3 = 0 \quad (5.10)$$

and the wave numbers are given by

$$\left. \begin{aligned} k_x &= \left(\frac{m\pi}{h} \right), \quad m = 0, 1, 2, \dots \\ k_y &= \left(\frac{n\pi}{L} \right), \quad n = 0, 1, 2, \dots \\ k_z &= \left(\frac{p\pi}{W} \right), \quad p = 0, 1, 2, \dots \end{aligned} \right\} m = n = p \neq 0 \quad (5.11)$$

where m, n, p represent, the number of half-cycle field variations along the x, y, z directions, respectively.

Thus the final form for the vector potential A_x within the cavity is

$$A_x = A_{mnp} \cos(k_x x') \cos(k_y y') \cos(k_z z') \quad (5.12)$$

Since the wave numbers $k_x, k_y,$ and k_z are subject to the constraint equation

$$k_x^2 + k_y^2 + k_z^2 = \left(\frac{m\pi}{h}\right)^2 + \left(\frac{n\pi}{L}\right)^2 + \left(\frac{p\pi}{W}\right)^2 = k_r^2 = \omega_r^2 \mu \epsilon \quad (5.13)$$

The resonant frequencies for the cavity are given by

$$(f_r)_{mnp} = \frac{1}{2\pi\sqrt{\mu\epsilon}} \sqrt{\left(\frac{m\pi}{h}\right)^2 + \left(\frac{n\pi}{L}\right)^2 + \left(\frac{p\pi}{W}\right)^2} \quad (5.14)$$

For all microstrip antennas $h \ll W$.

If $L > W > h$, the mode with the lowest frequency (dominant mode) is the TM_{010}^x whose resonant frequency is given by

$$(f_r)_{010} = \frac{1}{2L\sqrt{\mu\epsilon}} = \frac{c}{2L\sqrt{\epsilon_r}} \quad (5.15)$$

If $W > L > h$, the dominant mode is the TM_{001}^x whose resonant frequency is given by

$$(f_r)_{001} = \frac{c}{2W\sqrt{\epsilon_r}} \quad (5.16)$$

For a microstrip line shown in figure, typical electric field lines are shown in fig. As can be seen, most of the electric field lines reside in the substrate and parts of

some lines exist in air. Since some of the waves travel in the substrate and some in air, an effective dielectric constant ϵ_{eff} is introduced to account for fringing and the wave propagation in the line and is calculated as

$$\epsilon_e = \frac{\epsilon_r + 1}{2} + \frac{\epsilon_r - 1}{2} (1 + 12h/W)^{-1/2} \quad (5.17)$$

Because of the fringing effects, electrically the patch of the microstrip antenna looks larger than its physical dimensions. The dimensions of the patch along its length have been extended on each end by a distance Δl , which is a function of the effective dielectric constant ϵ_e and the width-to-height ratio (W/h). A very popular and practical relation for the normalized extension of the length is

$$\Delta l = \frac{0.412h(\epsilon_e + 0.3)(W/h + 0.264)}{(\epsilon_e - 0.258)(W/h + 0.8)} \quad (5.18)$$

Since the length of the patch has been extended by Δ on each side, the effective length of the patch is now

$$L_{\text{eff}} = L + 2 \Delta l \quad (5.19)$$

Since equation (5.15) for calculating the resonant frequency of the dominant mode does not account for fringing, it must be modified to include edge effects as

$$f_{10} = \frac{c}{2(L + 2\Delta l)\sqrt{\epsilon_e}} \quad (5.20)$$

5.4 RESONANT FREQUENCY CALCULATION OF CIRCULAR SIDED MICROSTRIP ANTENNA (with one concave and other convex side)

Geometry of the antenna is as shown in Fig.5.9. The antenna structure incorporates two circular arcs of radii r_1 and r_2 . As explained in chapter4, this structure resonates at a frequency lower than that of a rectangular patch because of the curved edges.

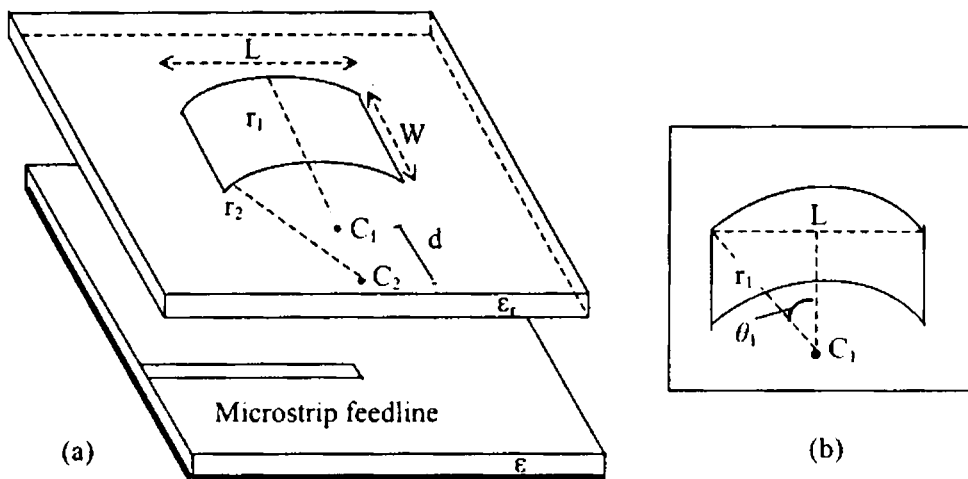


Fig. 5.9. (a) Geometry of the new compact microstrip antenna (b) Top view

The standard equations for computing the resonant frequency of a rectangular patch antenna explained in the previous section are modified to take into account the effects of the radii of first and second circular arcs and separation between the centers. The resonant frequency of this structure is calculated using eqns.(5.20), but the eqns (5.17) and (5.18) are modified as follows:

For the present geometry two layers of glass epoxy substrate of dielectric constant $\epsilon_r = 4.28$ are used. Hence the effective thickness of the substrate used here is $h_{\text{eff}} = h_1 + h_2$.

The modified equations are

$$\varepsilon_e = \frac{\varepsilon^r + 1}{2} + \frac{\varepsilon^r - 1}{2} \left(1 + 12h_{eff} / W\right)^{-1/2} \quad (5.21)$$

$$\Delta l = \frac{0.412h_{eff} (\varepsilon_e + 0.3)(W / h_{eff} + 0.264)}{(\varepsilon_e - 0.258)(W / h_{eff} + 0.8)} \quad (5.22)$$

The length L is replaced by L_{eff} , which is the effective length of the patch, by considering the effect of arc length and the radius of curvature of the arcs, which is calculated by the following relations.

for $r_1 = r_2$

$$L_{eff} = l_1 - 0.35(l_1 - L) - 0.04(L - r_1), \quad (5.23)$$

where the length of the arc, $l_1 = 2r_1 \theta_1$, and $\theta_1 = \sin^{-1}(L/2r_1)$, as shown in the figure 1(b).

$$(5.24)$$

for $r_1 > r_2$

$$L_{eff} = l_1 + 0.05(l_1 - L) + 0.1(r_1 - r_2) \quad (5.25)$$

for $r_1 < r_2$

$$L_{eff} = l_1 - 0.7(l_1 - L) + 0.05(d - 0.03) \quad \text{for } (r_2 - r_1) \leq 0.02 \quad (5.26)$$

$$L_{eff} = l_1 - 1.06(l_1 - L) + 0.15(d - 0.04) \quad \text{for } (r_2 - r_1) > 0.02 \quad (5.27)$$

Where d is the distance between the centres of curvature of inner and outer arcs of the patch.

5.4.1 Comparison between the measured and calculated results

The TM_{10} mode resonant frequency of the circular sided microstrip patch are determined by varying different parameters of the antenna using IE3D. The results are compared with the values calculated using the equations developed here. The three different cases which are taken into consideration here are (1) $r_1=r_2$, (2) $r_1<r_2$, and (3) $r_1>r_2$. The comparison between the measured and calculated results for these cases are shown in Tables 5.1, 5.2 and 5.3 respectively. From the tabulated results, it is obvious that the percentage error is less than two for almost all cases. The plots corresponding to the different cases are shown in Fig. 5.10, 5.11 and 5.12. Frequency variation of the patch geometry with different substrates for various combinations of thickness and dielectric constant is also studied for validating the equation. The results shown in Table 5.4 and Fig. 5.13 also show close agreement with the simulated values.

Table 5.1 Variation of frequency for different values of L, r_1 , r_2 and W ($\epsilon_r=4.28$, $h=0.16\text{cm}$)

L, r_1, r_2 (cm)	W (cm)	frequency (GHz)		% error
		Measured	Calculated	
6,4,4	1	1.198	1.217	1.59
	2	1.16	1.1775	1.51
	3	1.148	1.156	0.70
	4	1.143	1.143	0.00
7,4,4	1	1.004	1.0017	0.23
	2	0.977	0.9695	0.77
	3	0.9667	0.9523	1.49
	4	0.959	0.9412	1.86
5,5,5	1	1.484	1.503	1.28
	2	1.44	1.454	0.97
	3	1.403	1.427	1.71
	4	1.394	1.41	1.15
6,5,5	1	1.229	1.252	1.87
	2	1.194	1.211	1.42
	3	1.177	1.189	1.02
	4	1.156	1.175	1.64
7,5,5	1	1.045	1.061	1.53
	2	1.012	1.028	1.58
	3	1.004	1.009	0.50
	4	0.9838	0.9975	1.39
5,6,6	1	1.488	1.506	1.21
	2	1.434	1.457	1.6
	3	1.418	1.43	0.85
	4	1.393	1.413	1.44
6,6,6	1	1.238	1.263	2.02
	2	1.205	1.22	1.24
	3	1.183	1.2	1.44
	4	1.172	1.186	1.19
7,6,6	1	1.063	1.081	1.69
	2	1.031	1.046	1.45
	3	1.017	1.028	1.08
	4	1.009	1.016	0.69

Table 5.2 The variation of frequency for different values of L, r_1, r_2 and W ($r_1 < r_2$)

L, r_1,r_2 (cm)	W (cm)	frequency f ₁₀ (GHz)		
		measured	calculated	% error
5,5,7	0.79	1.542	1.544	0.16
	1.79	1.467	1.470	0.22
	2.79	1.422	1.427	0.39
6,5,7	0.68	1.321	1.298	1.76
	1.68	1.247	1.233	1.13
	2.68	1.209	1.197	0.94
7,5,7	0.51	1.142	1.122	1.74
	1.51	1.08	1.059	1.93
	2.51	1.043	1.028	1.44
5,4,5	0.79	1.519	1.544	1.66
	1.79	1.443	1.470	1.86
	2.79	1.411	1.427	1.16
6,4,5	0.65	1.279	1.290	0.85
	1.65	1.21	1.224	1.13
	2.65	1.188	1.188	0.02
7,4,5	0.37	1.125	1.112	1.21
	1.37	1.046	1.040	0.61
	2.37	1.022	1.010	1.49
6,6,7	1.87	1.234	1.245	0.89
	2.87	1.195	1.212	1.38
	3.87	1.182	1.187	0.47
7,6,7	1.81	1.058	1.069	1.08
	2.81	1.032	1.041	0.91
	3.81	1.019	1.021	0.25
5,6,8	0.86	1.524	1.545	1.4
	1.86	1.455	1.474	1.31
	2.86	1.430	1.432	0.16
6,6,8	0.78	1.309	1.298	0.80
	1.78	1.231	1.238	0.59
	2.78	1.207	1.204	0.24
7,6,8	0.68	1.132	1.120	1.04
	1.68	1.068	1.066	0.18
	2.68	1.048	1.036	1.09
6,5,8	0.58	1.346	1.34	0.45
	1.58	1.248	1.247	0.04
	2.58	1.213	1.192	1.8
7,5,8	0.38	1.202	1.180	1.86
	1.38	1.096	1.089	0.65
	2.38	1.053	1.040	1.2

Table 5.3 The variation of frequency for different values of L, r₁, r₂ and W (r₁>r₂)(h=0.16cm, $\epsilon_r = 4.28$)

L,r ₁ ,r ₂ (cm)	W (cm)	frequency f ₁₀ (GHz)		
		measured	calculated	% error
5,7,5	2.21	1.406	1.404	0.09
	3.21	1.399	1.382	1.26
	4.21	1.378	1.366	0.83
6,7,5	2.32	1.164	1.173	0.75
	3.32	1.159	1.155	0.37
	4.32	1.153	1.143	0.90
7,7,5	2.49	0.985	0.999	1.41
	3.49	0.983	0.985	0.19
	4.49	0.976	0.975	0.12
5,7,6	1.08	1.457	1.479	1.55
	2.08	1.422	1.434	0.83
	3.08	1.410	1.409	0.07
6,7,6	1.13	1.213	1.232	1.53
	2.13	1.198	1.195	0.23
	3.13	1.173	1.175	0.19
7,7,6	1.19	1.041	1.048	0.67
	2.19	1.017	1.018	0.14
	3.19	1.015	1.002	1.32
6,7,4	3.68	1.124	1.133	0.79
	4.68	1.113	1.122	0.80
	5.68	1.126	1.115	0.99

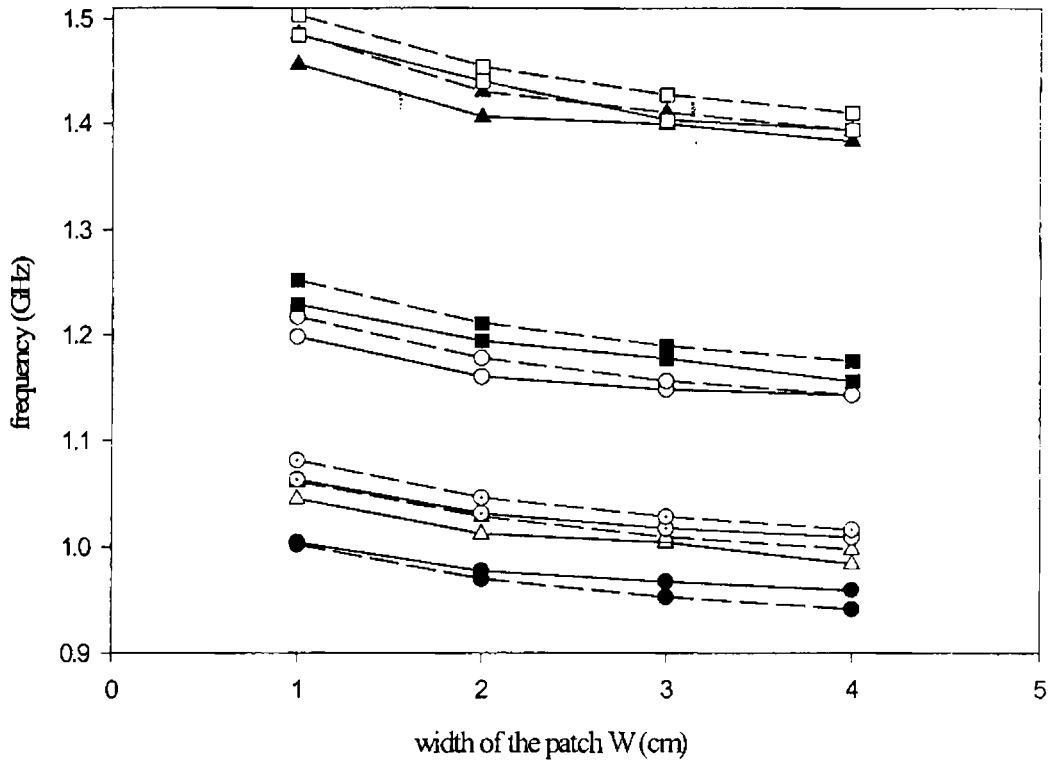


Fig 5.10 Measured and calculated TM_{10} mode frequency (case $r_1=r_2$)

----- experimental ——— theoretical

$L=7\text{cm}, r_1=r_2=4\text{cm}$ ●

$L=6\text{cm}, r_1=r_2=5\text{cm}$ ■

$L=6\text{cm}, r_1=r_2=4\text{cm}$ ○

$L=5\text{cm}, r_1=r_2=5\text{cm}$ □

$L=5\text{cm}, r_1=r_2=4\text{cm}$ ▲

$L=7\text{cm}, r_1=r_2=6\text{cm}$ ⊙

$L=7\text{cm}, r_1=r_2=5\text{cm}$ △

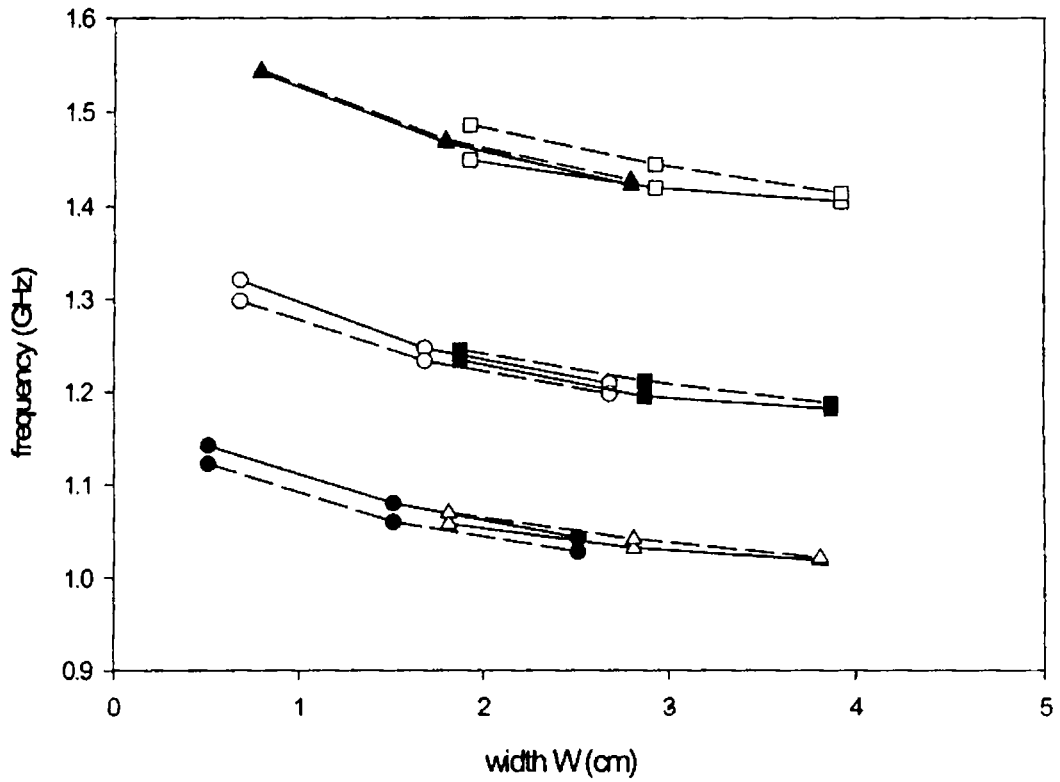


Fig 5.11 Measured and calculated TM_{10} mode frequency (case $r_1 < r_2$)

----- experimental ——— theoretical

- | | |
|--|--|
| ● $L=7\text{cm}, r_1=5\text{cm}, r_2=7\text{cm}$ | △ $L=7\text{cm}, r_1=6\text{cm}, r_2=7\text{cm}$ |
| ○ $L=6\text{cm}, r_1=5\text{cm}, r_2=7\text{cm}$ | ■ $L=6\text{cm}, r_1=6\text{cm}, r_2=7\text{cm}$ |
| ▲ $L=5\text{cm}, r_1=5\text{cm}, r_2=7\text{cm}$ | □ $L=5\text{cm}, r_1=6\text{cm}, r_2=7\text{cm}$ |

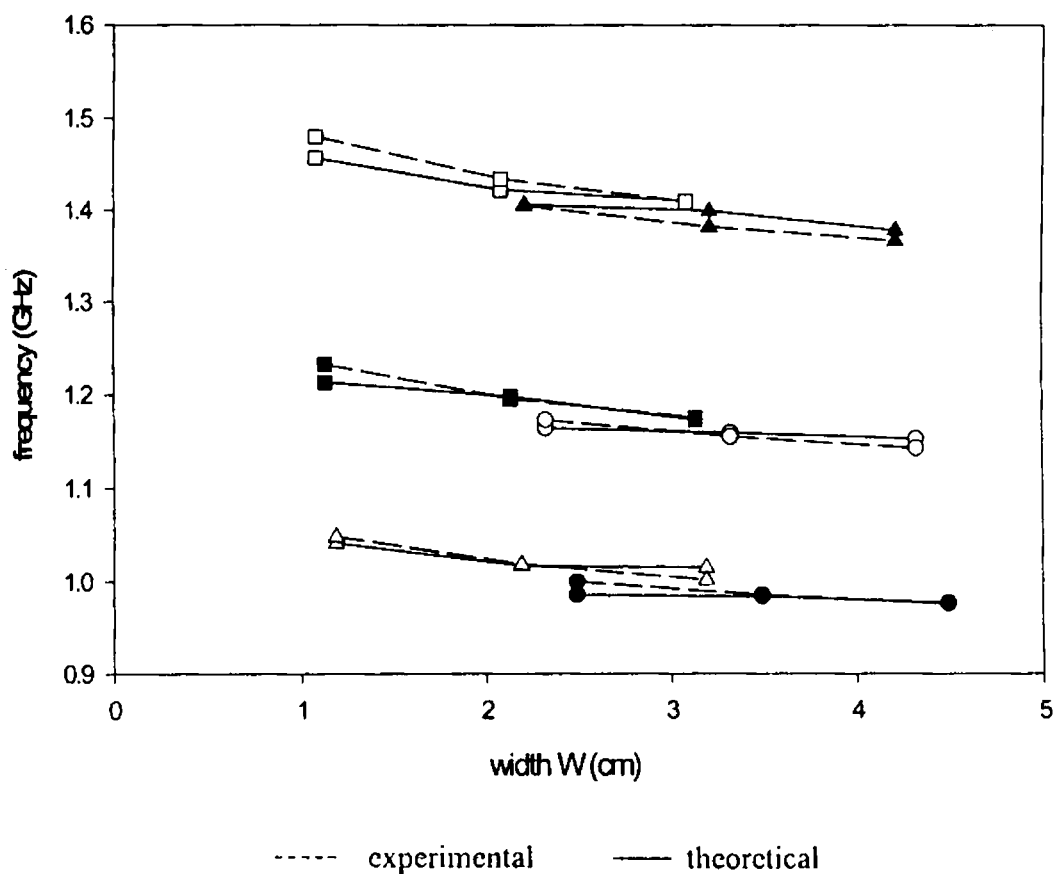


Fig 5.12 Measured and calculated TM_{10} mode frequency (case $r_1 > r_2$)

$L=7\text{cm}, r_1=7\text{cm}, r_2=5\text{cm}$

$\triangle L=7\text{cm}, r_1=7\text{cm}, r_2=6\text{cm}$

$L=6\text{cm}, r_1=7\text{cm}, r_2=5\text{cm}$

$\blacksquare L=6\text{cm}, r_1=7\text{cm}, r_2=6\text{cm}$

$L=5\text{cm}, r_1=7\text{cm}, r_2=5\text{cm}$

$\square L=5\text{cm}, r_1=7\text{cm}, r_2=6\text{cm}$

Table 5.4 showing the variation of frequency (for different h and ϵ_r)

L, W, r1, r2 cm	h cm	ϵ_r	Frequency (GHz)		% error
			Measured	Calculated	
5, 2, 4, 4	0.08	2.2	1.95	1.955	0.26
6, 2, 4, 4			1.597	1.5966	0.06
7, 2, 4, 4			1.335	1.31	1.87
5, 2, 4, 4	0.318	2.2	1.835	1.87	1.91
6, 2, 4, 4			1.53	1.556	1.7
7, 2, 4, 4			1.294	1.292	0.15
5, 2, 4, 4	0.16	4.28	1.406	1.43	1.71
6, 2, 4, 4			1.16	1.1775	1.51
7, 2, 4, 4			0.977	0.9695	0.77

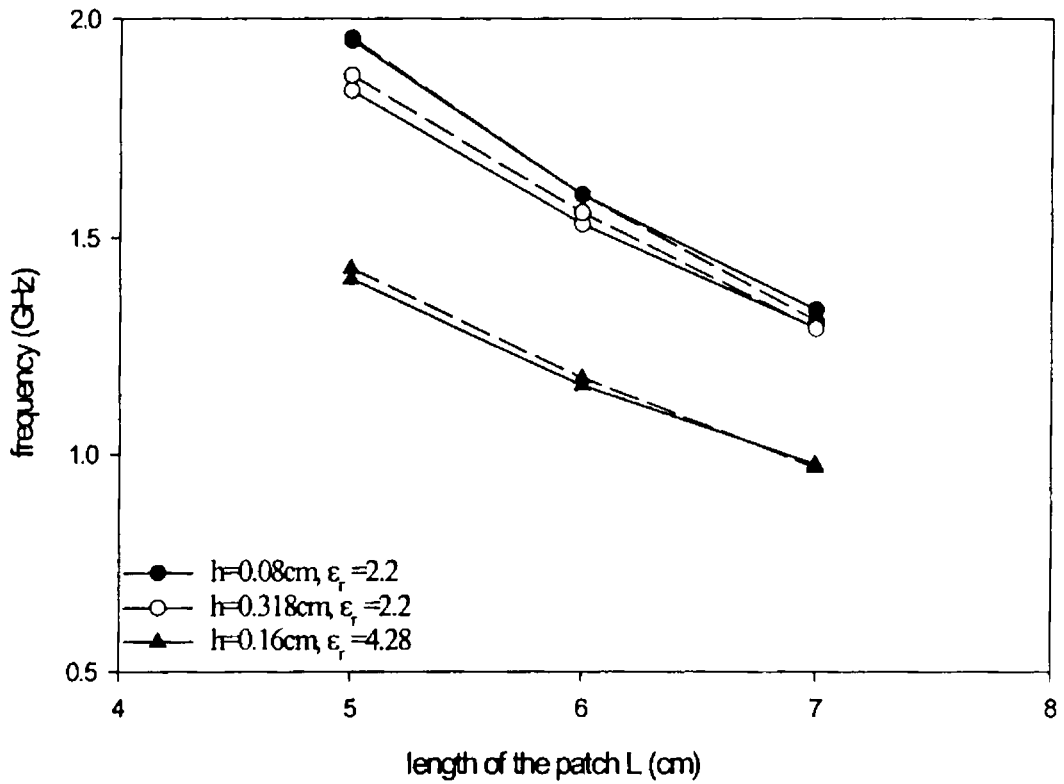


Fig. 5.13 Variation of TM_{10} with length L for different ϵ_r and h ($r_1=r_2=4\text{cm}$, $W=2\text{cm}$)

5.5 PATCH AREA CALCULATION OF CIRCULAR SIDED PATCH (with one concave and other convex side)

Using simple geometrical relations, area of the circular sided patch can be calculated as follows:

From Figure 5.14(a),

$$d_1 = \sqrt{r_1^2 - \left(\frac{L}{2}\right)^2} \quad (5.28)$$

$$d_2 = \sqrt{r_2^2 - \left(\frac{L}{2}\right)^2} \quad (5.29)$$

where d_1 and d_2 are the distance between the centres C_1 and C_2 to the corresponding chords, respectively.

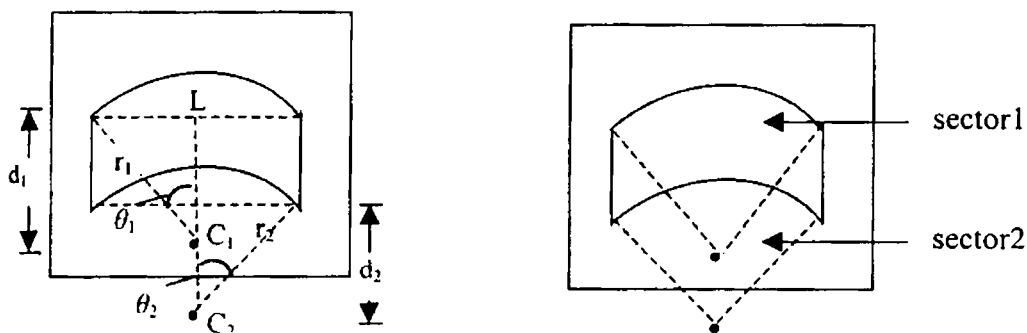


Fig. 5.14 Geometry of the patch

$$\theta_1 = \sin^{-1} (L/2r_1) \quad (5.30)$$

$$\theta_2 = \sin^{-1} (L/2r_2)$$

Area of upper sector, $A_{sec1} = r_1^2 \theta_1$

Area of lower sector, $A_{sec2} = r_2^2 \theta_2$

Area of extension due to the outer curve $a_1 = A \sec_1 - L d_1 / 2$

Area of reduction due to the inner curve $a_2 = A \sec_2 - L d_2 / 2$

Patch area, $A = L * W + a_1 - a_2$

5.6 RESONANT FREQUENCY CALCULATION OF CIRCULAR DISK MICROSTRIP ANTENNA

The electric field of a resonant TM_{nm} mode in the cavity under the circular patch is given by

$$E_z = E_0 J_n(k_{nm} \rho) \cos n\Psi \quad (5.31)$$

Where ρ and Ψ are the radial and azimuthal co-ordinates, respectively (Fig. 1.13).

E_0 is an arbitrary constant, J_n is the Bessel function of the first kind of order n and

$$k_{nm} = X_{nm} / a \quad (5.32)$$

$$X_{nm} \text{ are the roots of the equation } J'_n(x) = 0 \quad (5.33)$$

The first five non-zero roots are shown in Table 5.5. The resonant frequency of TM_{nm} mode is given by

$$f_{nm} = \frac{X_{nm}}{2\pi a \sqrt{\mu_0 \epsilon}} = \frac{X_{nm} c}{2\pi a \sqrt{\epsilon_r}} \quad (5.34)$$

Eqn (5.34) is based on the assumption of a perfect magnetic wall and neglects the fringing fields at the open-end edge of the microstrip patch. To account for these fringing fields at the open-end edge of the microstrip patch. To account for these fringing fields, an effective radius a_e , is calculated as

$$a_e = a \left[1 + \frac{2h}{\pi a \epsilon_r} \left(\ln \frac{\pi a}{2h} + 1.7726 \right) \right]^{1/2} \quad (5.35)$$

$$f_{nm} = \frac{X_{nm}c}{2\pi a_e \sqrt{\epsilon_r}} \quad (5.36)$$

Eqn (5.35) is obtained by considering the radius of an ideal circular parallel- plate capacitor which would yield the same static capacitance after fringing is taken into account.

Table 5.5 the first five non-zero roots of $J_n(x) = 0$

(n, m)	X
(1,1)	1.841
(2,1)	3.054
(0,2)	3.832
(3,1)	4.201
(1,2)	5.331

5.7 RESONANT FREQUENCY CALCULATION OF CRESCENT-SHAPED MICROSTRIP ANTENNA

The schematic diagram of the antenna is shown in Fig. 5.15. As explained earlier, the antenna geometry is defined by two circular arcs of radii r_1 and r_2 with their centers C_1 and C_2 displaced by a distance d . The patch is etched on a substrate of thickness h and dielectric constant ϵ_r .

The standard equations for computing the resonant frequencies of a circular patch antenna are modified to take into account the effect of different arc radii and the displacement between the centers of circular arcs in the present geometry.

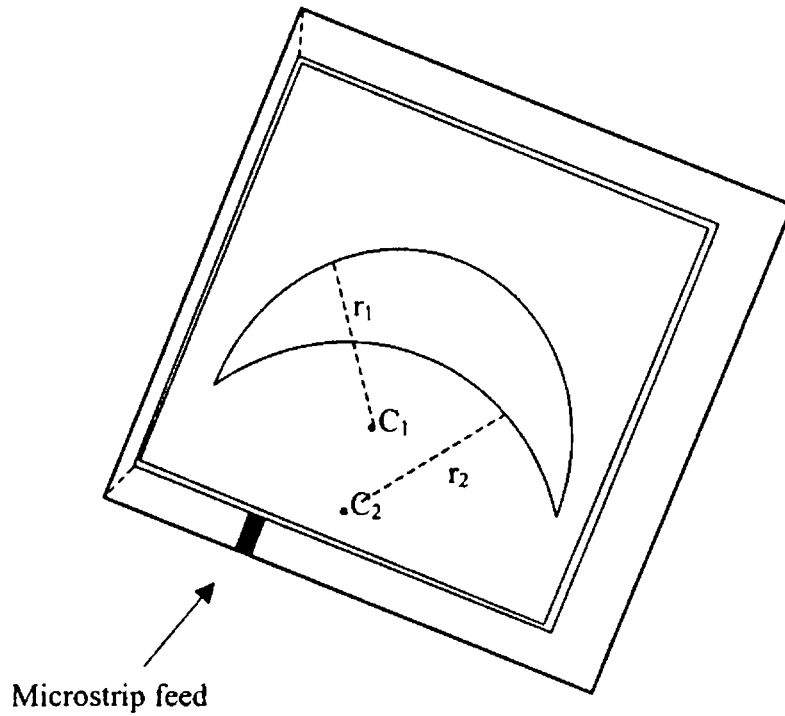


Fig. 5.15 Geometry of the crescent-shaped microstrip antenna

The TM_{11} and TM_{21} resonant frequencies of a circular microstrip antenna of radius r fabricated on a substrate of dielectric constant ϵ_r and thickness h are given by [3]:

$$\text{For } TM_{11} \text{ mode, } f_1 = \frac{1.84118 c}{2 \pi r_e \sqrt{\epsilon_r}} \quad (5.37)$$

$$\text{For } TM_{21} \text{ mode, } f_2 = \frac{3.05424 c}{2 \pi r_e \sqrt{\epsilon_r}} \quad (5.38)$$

$$\text{where } r_e = r \left[1 + \frac{2h}{\pi r \epsilon_r} \left(\ln \frac{\pi r}{2h} + 1.7726 \right) \right]^{1/2} \quad (5.39)$$

The two resonant frequencies of the crescent shaped patch are calculated as

$$f_{11} = f_1 + df_1 \quad (5.40)$$

$$f_{2l} = f_2 + df_2 \quad (5.41)$$

When the distance between the centres of the two arcs of the crescent shaped geometry is large, (i.e. $d > 0.04$) the values of f_1 and f_2 are calculated using equations (5.37), (5.38) and (5.39) with ' r ' replaced by ' r_1 '. If the centres are close, (i.e. $d \leq 0.04$), r is replaced by

$$r = (3/2)r_1 - (1/2)r_2 \text{ to take into account the effect of } r_2.$$

The correction terms df_1 and df_2 are calculated as follows:

For $r_2 - r_1 < 0.02$,

$$\left. \begin{aligned} df_1 &= \frac{-0.84f_1d}{r_1 + r_2} + \frac{0.17f_1(r_2 - r_1)}{d} \\ df_2 &= \frac{-0.78f_2d}{r_1 + r_2} + \frac{0.23f_2(r_2 - r_1)}{d} \end{aligned} \right\} \text{ for } d < 0.04 \quad (5.42)$$

$$\left. \begin{aligned} df_1 &= -0.175f_1 - \frac{0.01f_1(r_1 + r_2)}{r_2 - r_1} + \frac{0.019f_1(r_1 + r_2)}{d} \\ df_2 &= -0.17f_2 - \frac{0.16f_2(r_2 - r_1)}{r_1 + r_2} + \frac{0.01f_2(r_1 + r_2)}{d} \end{aligned} \right\} \text{ for } d \geq 0.04 \quad (5.43)$$

For $r_2 - r_1 \geq 0.02$,

$$\left. \begin{aligned} df_1 &= \frac{-0.27f_1d}{r_2 - r_1} + \frac{0.082f_1(r_1 + r_2)}{d} - \frac{0.245f_1(r_2 - r_1)}{r_1 + r_2} \\ df_2 &= \frac{-0.275f_2d}{r_2 - r_1} + \frac{0.1f_2(r_1 + r_2)}{d} - \frac{0.22f_2(r_2 - r_1)}{r_1 + r_2} \end{aligned} \right\} \text{ for } d \leq 0.04 \quad (5.44)$$

$$\left. \begin{aligned}
 df_1 &= \frac{-0.49 f_1 d}{r_1 + r_2} + \frac{0.442 f_1 (r_2 - r_1)}{d} - \frac{0.005 f_1 (r_1 + r_2)}{r_2 - r_1} \\
 df_2 &= \frac{-0.465 f_2 d}{r_1 + r_2} + \frac{0.48 f_2 (r_2 - r_1)}{d}
 \end{aligned} \right\} \text{for } d > 0.04 \quad (5.45)$$

5.7.1 Comparison of theory and experiment

The theoretical variation of the two resonant frequencies f_{1l} and f_{2l} with different values of r_1 , r_2 and d are given in Table 5.6 and Fig. 5.16. The experimental results are also plotted in the same figure for comparison. To further check the validity, the antennas are fabricated on substrates with different dielectric constants and thickness. These results are shown in Table 5.7 and Fig. 5.17. In all these cases the theoretical results are found to be in good agreement with experimental values with a maximum error of 2%.

Table 5.6: Variation of the two resonant frequencies f_{11} and f_{21} with different values of r_1 , r_2 and d ($h=0.16\text{cm}$, $\epsilon_r=4.28$)

r_1, r_2 (cm)	d (cm)	frequency (GHz)					
		f_{11}			f_{21}		
		Meas- ured	Calcul- ated	% error	Meas- ured	Calcul- ated	% error
4,5	2	1.093	1.0956	0.24	1.932	1.933	0.05
	3	0.9535	0.93	2.11	1.659	1.641	1.08
	4	0.9278	0.9528	2.15	1.579	1.608	1.84
4,6	3	1.222	1.224	0.16	2.167	2.162	0.23
	4	1.016	1.017	0.09	1.775	1.783	0.45
	5	0.9565	0.938	1.93	1.625	1.645	1.23
4,7	4	1.343	1.371	2.08	2.383	2.411	1.17
	5	1.073	1.059	1.3	1.885	1.847	2.02
	6	0.9859	0.967	1.92	1.681	1.691	0.59
5,6	2	0.8904	0.891	0.06	1.581	1.565	1.01
	3	0.7768	0.7785	0.22	1.362	1.363	0.07
	4	0.7386	0.7415	0.39	1.278	1.274	0.31
5,7	3	1.01	0.9967	1.32	1.801	1.769	1.78
	4	0.8447	0.8259	1.67	1.487	1.455	2.01
	5	0.7788	0.783	0.54	1.349	1.375	1.85
6,7	2	0.7528	0.7514	0.19	1.341	1.315	1.94
	3	0.6547	0.668	1.98	1.154	1.164	0.87
	4	0.6183	0.606	1.94	1.076	1.057	1.77
6,8	3	0.8628	0.855	0.9	1.541	1.527	0.91
	4	0.7148	0.7062	1.2	1.264	1.25	1.11

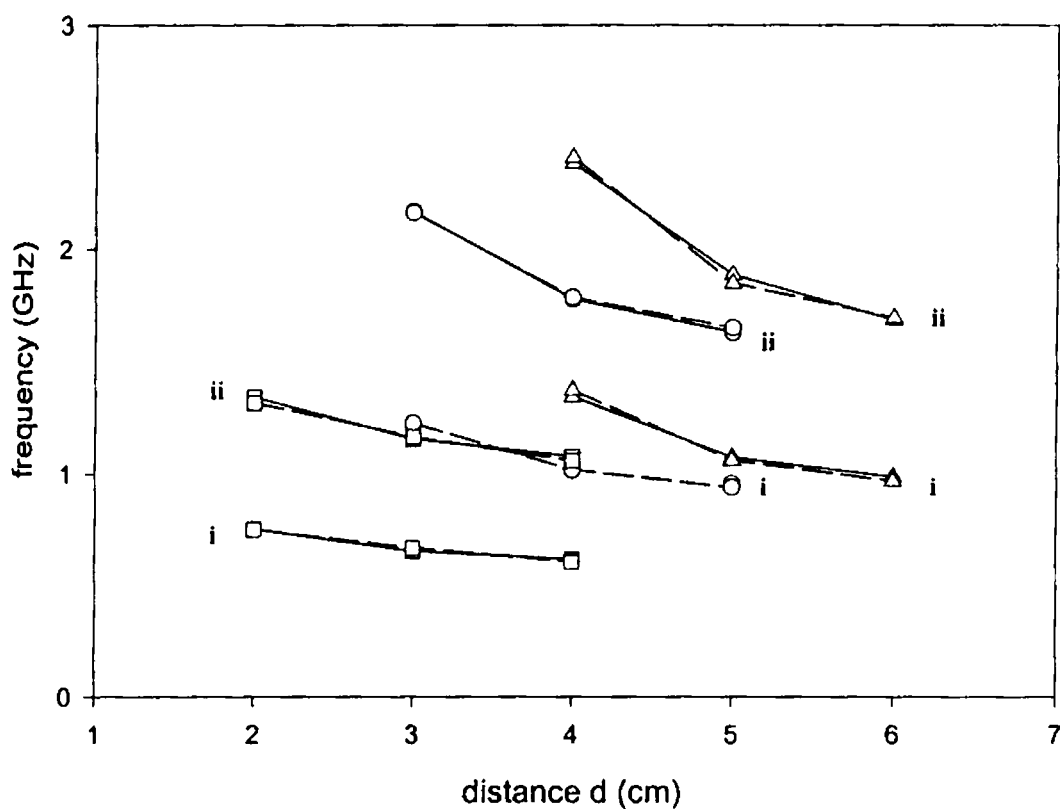


Fig. 5.16 Variation of TM_{11} and TM_{21} mode frequencies with distance between centers of arcs for different r_1 and r_2 ($\epsilon_r=4.28$, $h=0.16\text{cm}$)

----- experimental ——— theoretical

o : $r_1=4\text{cm}, r_2=6\text{cm}$ Δ : $r_1=4\text{cm}, r_2=7\text{cm}$ \square : $r_1=6\text{cm}, r_2=7\text{cm}$

i : f_{11} ii : f_{21}

Table 5.7 Variation of the two resonant frequencies f_{11} and f_{21} with different values of ϵ_r and h ($r_1=4\text{cm}$, $r_2=6\text{cm}$)

d (cm)	h (cm)	ϵ_r	f_{11} (GHz)			f_{21} (GHz)		
			IE3D	calculated	% error	IE3D	calculated	% error
3	0.08	2.2	1.702	1.701	0.05	3.03	3.003	0.99
4			1.4	1.413	0.93	2.457	2.477	0.81
5			1.316	1.304	0.91	2.249	2.288	1.73
3	0.318	2.2	1.583	1.593	0.63	2.87	2.812	2.02
4			1.335	1.323	0.90	2.326	2.319	0.30
5			1.26	1.234	2.06	2.121	2.165	2.07
3	0.16	4.28	1.244	1.2248	1.54	2.207	2.162	1.82
4			1.031	1.0173	1.26	1.802	1.7833	1.05
5			0.9568	0.9377	1.99	1.623	1.6458	1.42
3	0.066	10.2	0.832	0.815	2.04	1.445	1.4387	0.44
4			0.6777	0.6769	0.12	1.189	1.1867	0.25
5			0.6287	0.6207	1.27	1.079	1.089	0.93

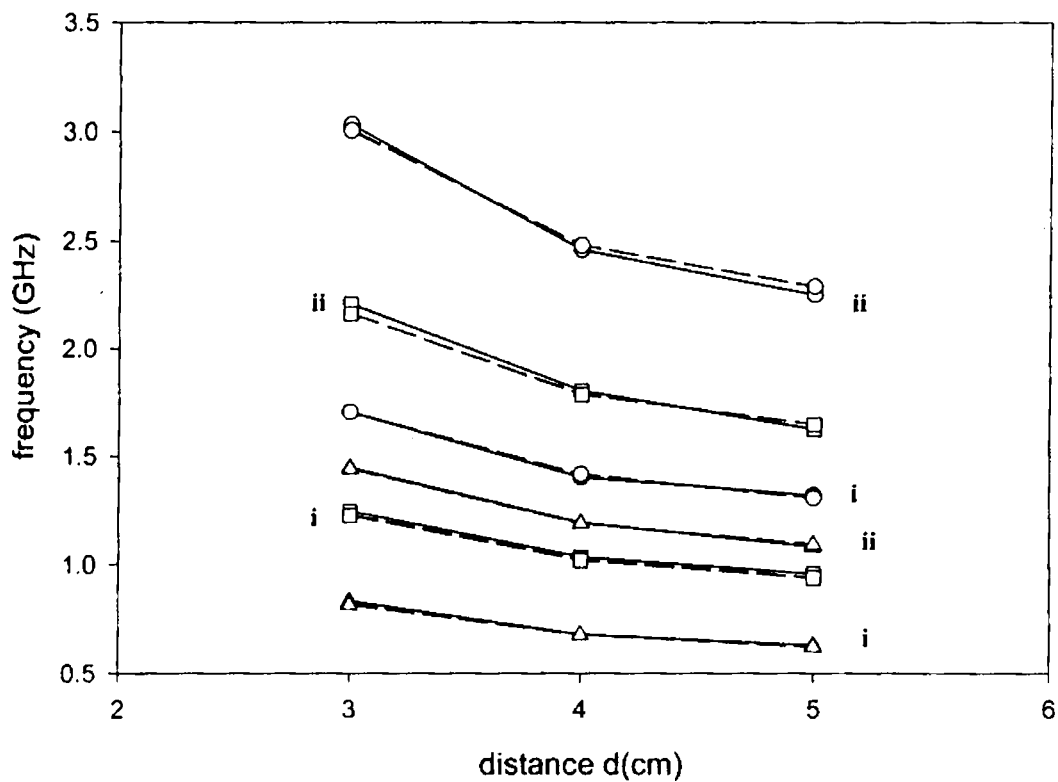


Fig. 5.17 Variation of TM_{11} and TM_{21} mode frequencies with the distance between the centres of the arcs for different ϵ_r and h ($r_1 = 0.04\text{m}$, $r_2 = 0.06\text{m}$)

----- experimental ——— theoretical

o : $\epsilon_r=2.2$, $h = 0.08\text{cm}$ Δ : $\epsilon_r=10.2$, $h = 0.066\text{cm}$ \square : $\epsilon_r=4.28$, $h = 0.16\text{cm}$

i : f_{11} ii : f_{21}

5.8 PATCH AREA CALCULATION OF CRESCENT-SHAPED MICROSTRIP ANTENNA

From Figure 5.18,

Two equations can be written as follows:

$$(d_2)^2 = (r_1)^2 - (d_1)^2 \quad (5.46)$$

$$(d_2)^2 = (r_2)^2 - (d + d_1)^2 \quad (5.47)$$

Equating (5.46) and (5.47)

We get

$$d_1 = (r_2^2 - r_1^2 - d^2) / 2d \quad (5.48)$$

From (5.46),

$$d_2 = \sqrt{r_1^2 - d_1^2} \quad (5.49)$$

$$\theta_1 = \sin^{-1} (d_2 / r_1) \quad (5.50)$$

$$\theta_2 = \sin^{-1} (d_2 / r_2) \quad (5.51)$$

$$\text{removed area } a_2 = r_2^2 \theta_2 - (d + d_1) d_2$$

$$\text{Patch area} = r_1^2 \theta_1 - a_2 - (d_1 d_2) \quad (5.52)$$

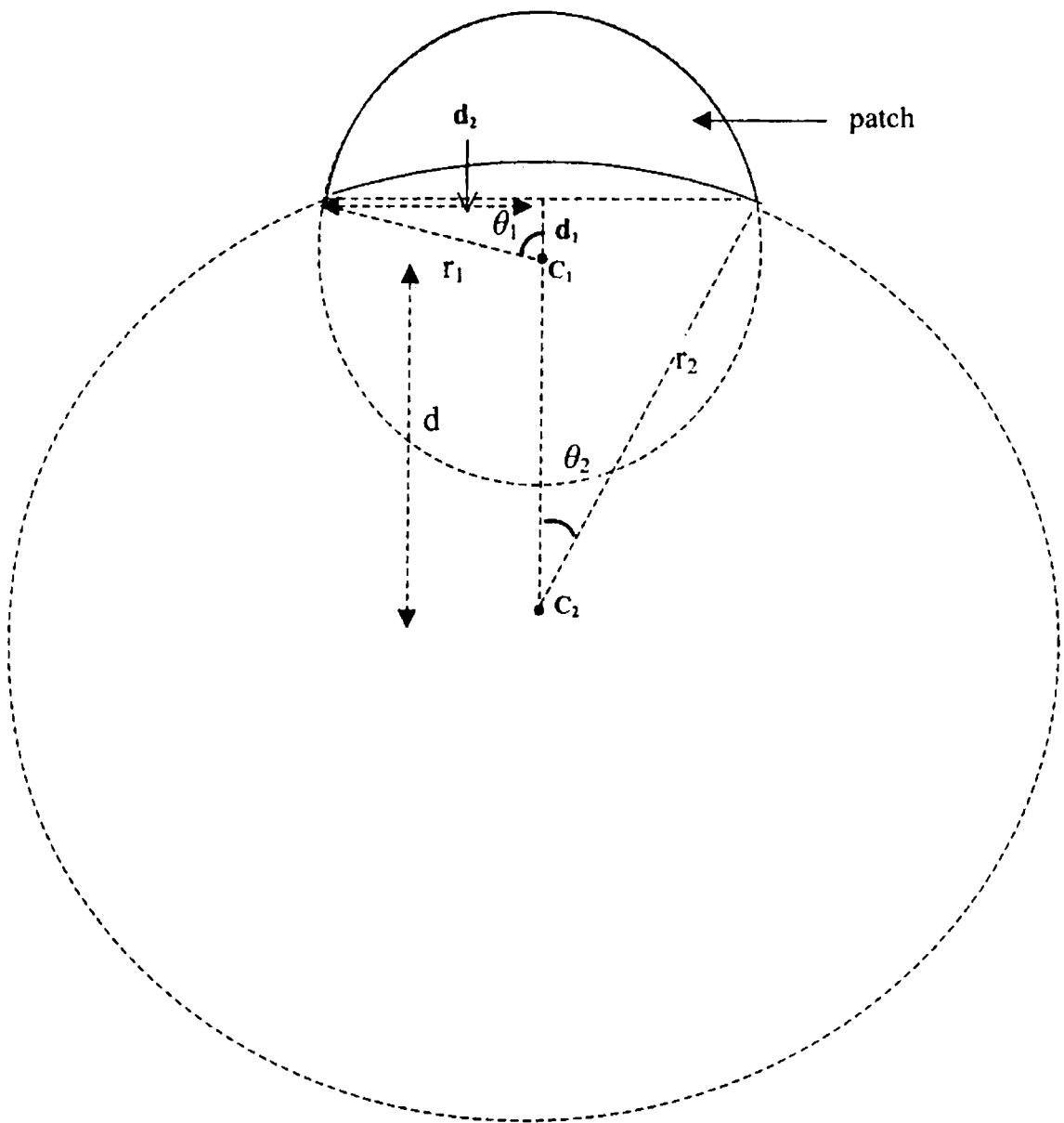


Fig. 5.18 Geometry for calculating the area of the crescent shaped patch

5.9 PATCH AREA CALCULATION OF CIRCULAR SIDED PATCH (with two concave sides)

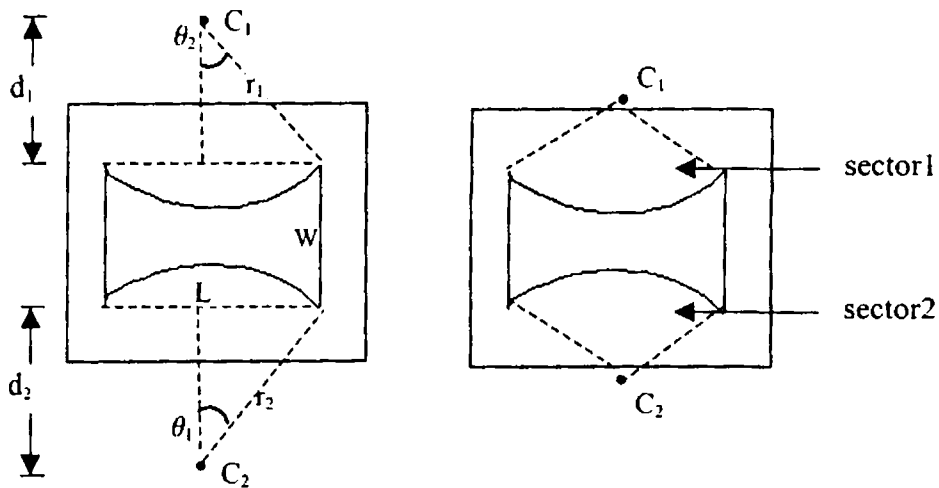


Fig. 5.19 Geometry of the structure

$$d_1 = \sqrt{r_1^2 - \left(\frac{L}{2}\right)^2} \quad (5.53)$$

$$d_2 = \sqrt{r_2^2 - \left(\frac{L}{2}\right)^2} \quad (5.54)$$

where d_1 and d_2 are the distance between the centres C_1 and C_2 to the corresponding chords, respectively.

$$\theta_1 = \sin^{-1} (L/2r_1)$$

$$\theta_2 = \sin^{-1} (L/2r_2)$$

$$\text{Area of first sector, } A_{\text{sec}_1} = r_1^2 \theta_1$$

$$\text{Area of second sector, } A_{\text{sec}_2} = r_2^2 \theta_2$$

$$\text{Area of reduction due to the upper curve } a_1 = A_{\text{sec}_1} - L d_1 / 2$$

Area of reduction due to the lower curve $a_2 = A \sec_2 - L d_2 / 2$

$$\text{Patch area, } A = L * W - a_1 - a_2 \quad (5.55)$$

5.10 CONCLUDING REMARKS

The identification of resonant modes of the compact patches discussed in this thesis work was done by calculating the magnetic current distribution on the surface of the patches using IE3D simulation software. Resonant frequency calculation of two compact microstrip patches (the circular sided microstrip patch and the crescent-shaped patch) are carried out in this chapter. The former geometry is more similar to the rectangular patch and its frequency calculation was done by modifying the equations of a standard rectangular patch, whereas the empirical equations for the crescent-shaped patch were derived by modifying the equations of a standard circular disk. These simple relationships predict the resonant frequencies accurately and it is a fast method for calculating the frequencies.

CONCLUSIONS

This chapter summarizes the inferences drawn from the experimental and theoretical investigations done on different compact microstrip patch geometries. Some possible applications of the presented patches and suggestions for further work in this field are also included.

6.1 INTRODUCTION

Microstrip antennas are being used for aerospace applications and in small portable wireless communication equipment, because of their compactness, light-weight, low profile, and relative ease of fabrication. The small size is an important requirement for portable applications. It is well known that the smaller the antenna size, the lower the antenna efficiency. In this thesis work, main aim was to develop a more and more reduced sized microstrip patch antenna without degrading its radiation characteristics like bandwidth, gain and efficiency. During the period of work, three different types of compact circular sided microstrip patches are developed and analysed experimentally, which have a significant size reduction compared to standard circular disk antenna. The compactness is achieved without much deterioration of its properties like gain, bandwidth and efficiency. In addition to this, interesting results of dual band operation, circular polarization and dual port operation with excellent isolation are also observed for some typical designs of these patches. These make the patches more suitable for satellite and mobile communication antennas.

6.2 INFERENCES FROM EXPERIMENTAL INVESTIGATIONS

The experimental investigations were initiated on the drum-shaped microstrip patches which are more compact than the rectangular patches. Since the circular geometry is more compact than the straight edged patches, the research work is concentrated on circular sided geometries. Here, different types of circular sided microstrip patch geometries which are expected to be compact due to their particular geometrical shapes, are analysed in detail using an electromagnetic simulation software (IE3D). The variation of the dominant mode frequencies of each geometry are studied for different combinations of its parameters. Some

typical patches with attractive characteristics of each geometry are fabricated and experimentally investigated.

Electromagnetic feeding (proximity-coupled feed) has many advantages over direct microstrip line feeding: lower level of spurious radiation, wider bandwidth and greater flexibility in impedance matching especially in a microstrip array environment. This type of feeding is used throughout of this work due to above mentioned reasons.

The circular sided microstrip patch (with two concave sides) has a good size reduction compared to the circular disk, as indicated in the tables and graphs in chapter 4. In addition to its compactness, the patch shows dual band operation and the experimental results on this aspect are also discussed.

Dual frequency operation is obtained by a simple technique of having one dimension of the element resonant at one frequency and the other at a second frequency. Proper matching at both frequencies is obtained by adjusting the position of the microstrip feedline. The ratio of the two operating frequencies is mainly controlled by the aspect ratio of the patches.

The length L and width W of the patch affects the TM_{10} and TM_{01} frequencies as in the case of rectangular microstrip antenna. Here, the resonant frequencies can also be controlled by changing the radii of curvature. Impedance bandwidth for the dual frequencies is of the order of 1-2% for VSWR ratio varying in between 1 and 2. The radiation properties of the patch are also similar to standard patches. Some of the patches are showing a slight enhancement in gain compared to the circular disk patches designed for the same frequency. Moreover, by suitably modifying the aspect ratio of the patch, a circularly polarized radiator is resulted. This antenna has a 3dB axial ratio bandwidth of 28MHz (1.5%). Measured radiation patterns of the antenna are shown in Chapter 4. The copolar

and crosspolar radiation patterns are almost identical in the entire radiating angular region.

The results of the experimental study on the circular sided patch (with one concave and other convex side) show that the characteristic behavior of the patch is very similar to that of the previously mentioned patch as shown in the experimental results (chapter 4). This compact patch can also provide dual band operation and circular polarization by suitable modification of the design. This patch has also considerable size reduction compared to circular disk microstrip antenna with a slight reduction in gain.

The microstrip patch which is found to be giving maximum size reduction is the crescent-shaped patch. This patch has an area reduction of ~90% for some particular designs compared to standard circular disk microstrip antenna. The characteristics of this patch is more similar to circular disk microstrip patch. The two dominant modes of excitation are TM_{11} and TM_{21} .

Geometry of the patch is a half moon shaped one and hence the name 'crescent- shaped' patch. The structure incorporates two circular arcs of different radii of curvature and displaced by a distance d between their centres. The variation of both TM_{11} and TM_{21} mode frequencies are studied in detail by changing the parameters r_1 , r_2 and d of the patch. The results tabulated in the experimental results show that as the distance between the centres 'd' increases, the frequencies f_{11} and f_{21} are decreased, since both the frequencies are dependent on this parameter. When the distance d is very large ($d > 4\text{cm}$), the frequencies mainly depend upon the radius of curvature of the outer curve whereas the distance d is small ($d < 4\text{cm}$), frequencies depend upon both r_1 and r_2 .

Design of the crescent-shaped microstrip antenna for dual frequency operation excited with dual ports is also presented. As shown in Fig. 4.50, antenna

offers an isolation ~ 30 dB between the ports in the operating frequency range. Good cross polarization levels are also observed for this particular design.

Finally the radiation properties of different compact microstrip patch geometries are compared using IE3D software and the results are tabulated.

6.3 INFERENCES FROM THEORETICAL INTERPRETATIONS

The identification of dominant modes of different compact microstrip patches developed during this thesis work is done by calculating the magnetic current distribution on the surface of the patches using IE3D simulation software.

Equations for calculating resonant frequency of two compact microstrip patches (the circular sided microstrip patch with one concave and other convex side and the crescent-shaped microstrip patch) are developed and presented in chapter 5. The former geometry is similar to the rectangular patch and its frequency calculation was done by modifying the equations of a standard rectangular patch, whereas the empirical equations for the crescent-shaped patch were derived by modifying the equations for a standard circular disk antenna.

These relationships predict the resonant frequencies accurately and they offer a simple and fast method for calculating the frequencies of the antenna.

The design of the microstrip feedline used in this thesis work for the electromagnetic coupling is also done for 50Ω characteristic impedance.

6.4 SOME POSSIBLE APPLICATIONS OF THE PRESENT WORK

Recently there is great attraction in miniaturizing microstrip antennas for their applications in mobile communications and monolithic microwave integrated circuits (MMIC). The integration of wireless services necessitates the development of antennas with low profiles, which have to fit in an increasingly reduced space.

The practical applications of microstrip antennas for mobile systems are in portable or pocket-size equipment and in vehicles. Antennas for VHF/UHF hand-held portable equipment, such as pagers, portable telephones and transceivers, must naturally be small in size, light in weight and compact in structure. There is a growing tendency for portable equipment to be made smaller and smaller as the demand for personal communication rapidly increases, and the development of hand-held or hand-portable units has become urgent.

Dual frequency dual polarized microstrip antennas have an important role in satellite communication applications for the transmitting and receiving operations.

Since circularly polarised antennas do not need polarisation tracking they will have an important role in Global Positioning Systems (GPS) in addition to its applications in mobile satellite communication and direct broadcasting satellite systems.

Crosstalk is a severe problem in the dual port operation in which simultaneous transmit and receive operations are to be carried out. A good isolation between the ports eliminates the crosstalk and thus avoids the interference of communication channels.

6.5 SUGGESTIONS FOR FURTHER WORK IN THE FIELD

Antennas suitable for integration with monolithic microwave integrated circuits (MMICs) and optoelectronic integrated circuits (OEICs) have found numerous applications, such as fibre-based antenna remoting and phased arrays. The integrated antennas generate compact planar structures. For these integrated circuits, the antenna should be fabricated on a high dielectric constant material. Since the microstrip antennas developed here are very compact, the use of these patches for the integrated circuits can be explored, by designing and fabricating the antenna on high dielectric constant materials.

The main disadvantage of microstrip antennas is its inherently narrow bandwidth. Construction of multilayer antennas, by stacking three or four microstrip patches of above mentioned compact geometrical shapes will result in large bandwidth which cannot be obtained using a single layer.

Experimental study on the effect of temperature on the properties of different microstrip patch antennas will help to develop antennas for communication in space vehicles.

The frequency reuse is an important concept in the satellite communication applications. By using two perpendicular microstrip feedlines (electromagnetic coupling), the single circularly polarised band obtained here may be used to extract left hand circularly polarized frequency at one port and right hand polarized frequency in the other port for the same frequency band.

APPENDIX A

DRUM SHAPED COMPACT MICROSTRIP ANTENNA FOR DUAL FREQUENCY OPERATION AND CIRCULAR POLARIZATION

Results of experimental studies on a compact dual frequency microstrip antenna are presented. This antenna configuration provides an area reduction ~40% compared to a standard rectangular antenna operating at the same frequency without much degradation of gain. The antenna structure is reconFig. d to merge the dual frequencies to achieve circular polarization. It has a 3dB axial ratio bandwidth of ~1%.

A.1 INTRODUCTION

With the increase of applications in communications, multi frequency planar antennas have become highly desirable. Circularly polarized microstrip antennas are very useful in satellite communication applications due to its flexibility in orientation as a transmitter or a receiver. A drum shaped microstrip antenna for dual frequency dual polarization operation is presented here. By varying the central width of the antenna the ratio of the two resonant frequencies changes and dual frequency drum shaped patches of desired frequency ratio can be constructed easily. Here the compactness is achieved due to its geometry. By the appropriate selection of the central width of the drum shaped antenna, circularly polarized radiation is obtained. Since the CP is achieved only by the adjustment of a single parameter, its construction is very simple.

A.2 DUAL FREQUENCY MICROSTRIP ANTENNA

Fig. A.1 shows the geometry of the compact drum shaped antenna for dual frequency operation. The antenna structure consists of a drum shaped patch etched on a substrate of thickness 'h' and dielectric constant ϵ_r . 'L' denotes length, 'W' is the width and 'W_c' is the central width of the antenna. The antenna is found to resonate with orthogonal polarization when excited using a coaxial feed. The ratio of these lower mode frequencies can be trimmed by the W_c/W ratio.

In a typical design, a drum shaped antenna with length L=3.4cm, width W=5.5cm, and central width W_c= 3.5cm is fabricated on a substrate of $\epsilon_r=4.28$ and h=0.16cm. By properly adjusting the feed point position $f_p(x_0=1.2\text{cm}, y_0=0.9\text{cm})$, both the resonant frequencies can be excited with good matching. This particular antenna is found to resonate with frequencies 1.593GHz and 1.797 GHz.

Fig. A.2 shows the variation of return loss with frequency. The frequency ratio is found to be 1.1278. The 2:1 VSWR impedance bandwidths of the antenna are found to be 1.88% for the 1.593GHz band and 1.78% for the 1.797 GHz band. E-plane and H-plane copolar and crosspolar patterns at the central frequencies of the two bands are shown in Fig. A.3. The gain is found to be 1.54 dB less than the standard rectangular patch. The area reduction of 40.12% compared to standard rectangular microstrip patch is obtained for this structure. Fig. A.4 shows the variation of two resonant frequencies with W_c/W ratio. It is seen that when the ratio is 0.5, the frequency ratio is minimum.

A.3 CIRCULARLY POLARISED MICROSTRIP ANTENNA

Fig. A.5 shows the proposed compact drum shaped antenna using microstrip feed for CP radiation. By choosing a suitable dimension for the central width W_c , two orthogonal resonant modes for the CP can be excited. The antenna is excited by electromagnetic coupling using a 50 ohm microstrip feed line as shown.

A drum shaped antenna of length $L=4.8\text{cm}$, width $W=5.4\text{cm}$, is fabricated on a substrate of $\epsilon_r=4.28$ and $h=0.16\text{cm}$. A microstrip line of length $L_p=5.8\text{cm}$ and $W_p=0.3\text{cm}$ on a substrate of same thickness and permittivity is kept below the antenna to provide the electromagnetic coupling. It is found that, for a central width $W_c=2.4\text{cm}$, two orthogonal resonant modes merge to produce circular polarization. Fig. A.6 shows the measured return loss against frequency. The 3dB axial ratio bandwidth is 17MHz, which is $\sim 1\%$ considering the centre frequency at 1.68 GHz. The measured axial ratio versus frequency is presented in Fig. A.7. The E-Plane and H-Plane patterns at the centre frequency are shown in Fig. A.8.

A.4 CONCLUSIONS

A dual frequency compact microstrip antenna configuration with a coaxial feed is presented. This simple design gives a reduction in patch area with a small reduction in gain compared to the standard rectangular microstrip antenna. The trimming of a single parameter (central width) of the patch geometry results in a CP antenna also.

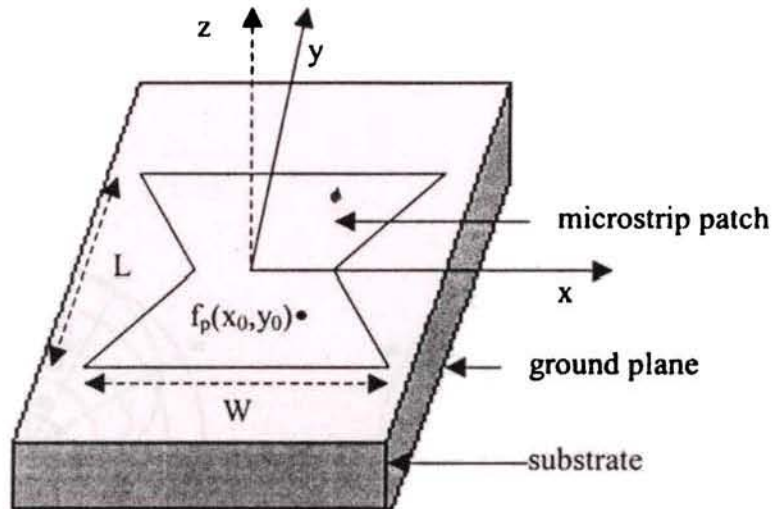


Fig. A.1 Geometry of the dual frequency microstrip antenna

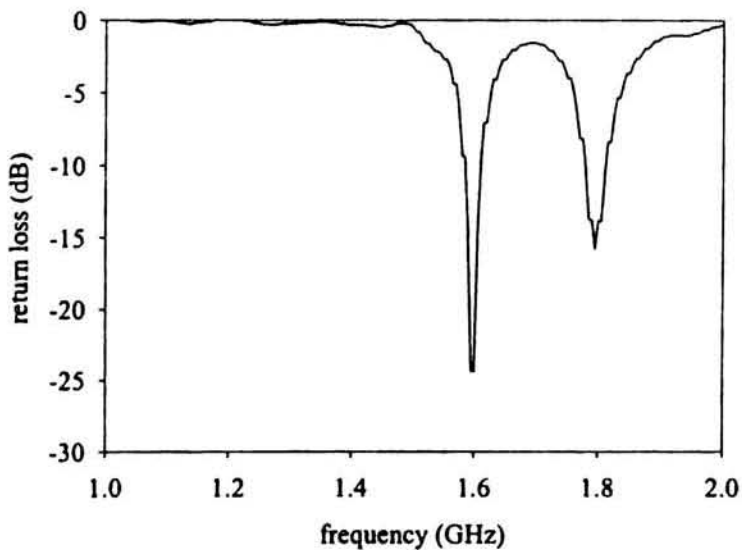


Fig. A.2 Variation of return loss with frequency

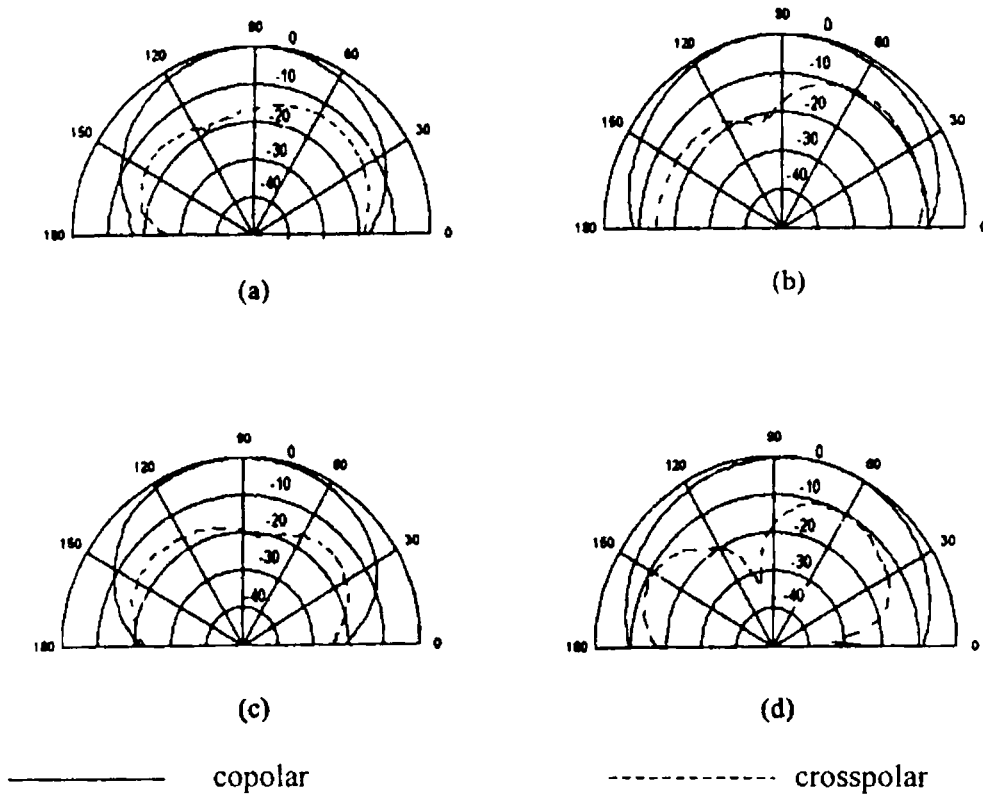


Fig. A.3 Radiation pattern of the antenna for the two resonant frequencies

(a) H-Plane (b) E-Plane patterns for 1.593 GHz

(c) H-Plane (d) E-Plane patterns for 1.797 GHz

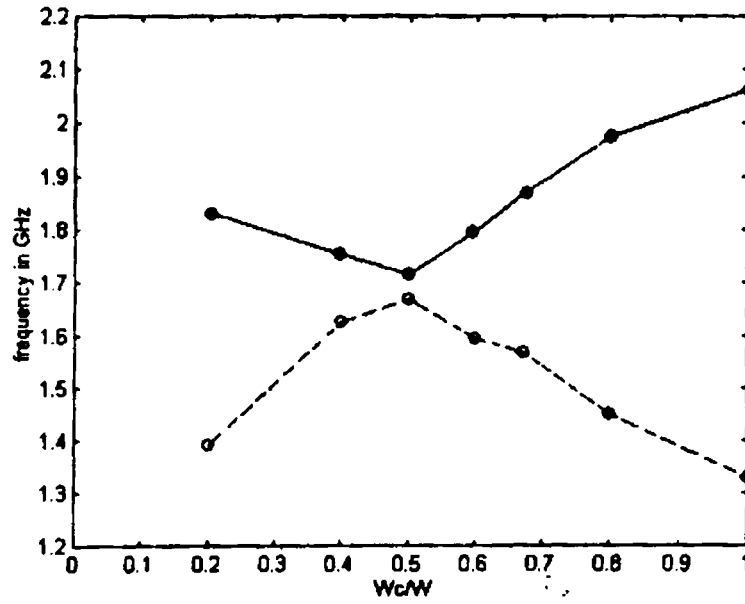


Fig. A.4 Variation of first and second resonant frequencies with central width

---○--- First frequency —●— Second frequency

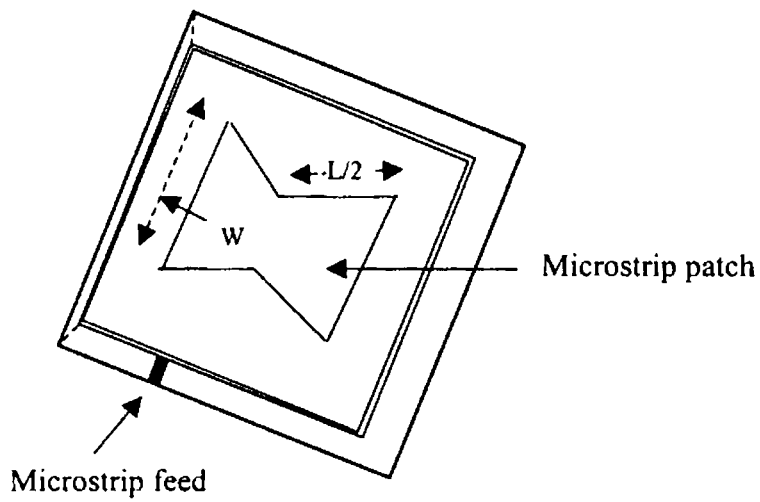


Fig. A.5 Geometry of the proposed circularly polarized compact microstrip antenna

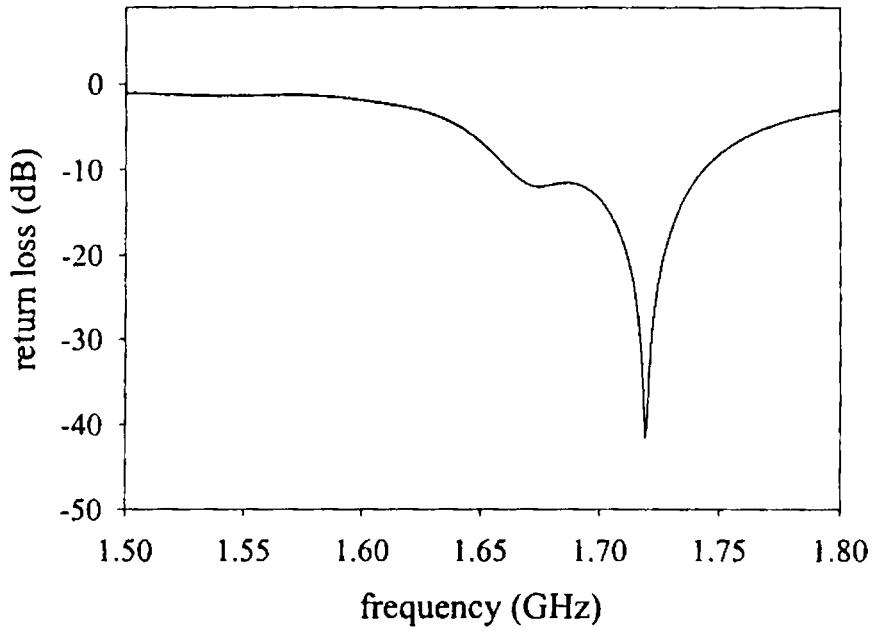


Fig. A.6 Variation of return loss with frequency for circular polarisation

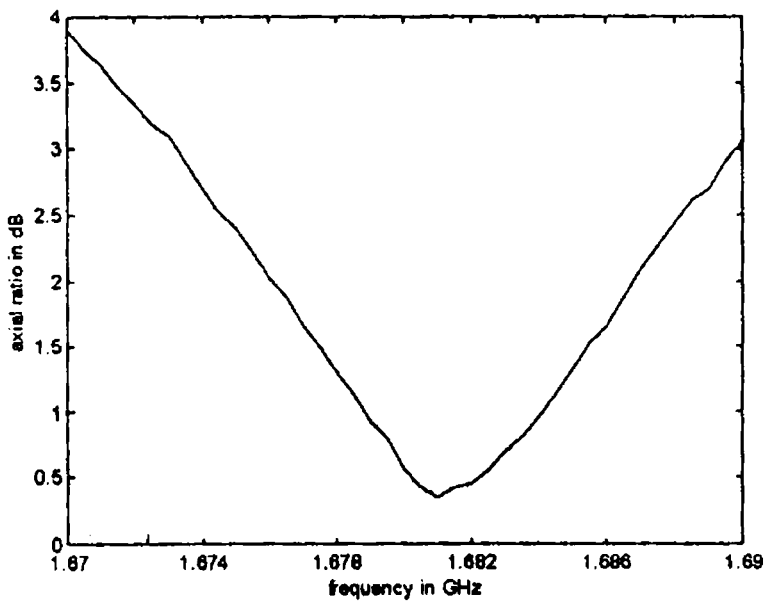


Fig. A.7 Measured axial ratio against frequency

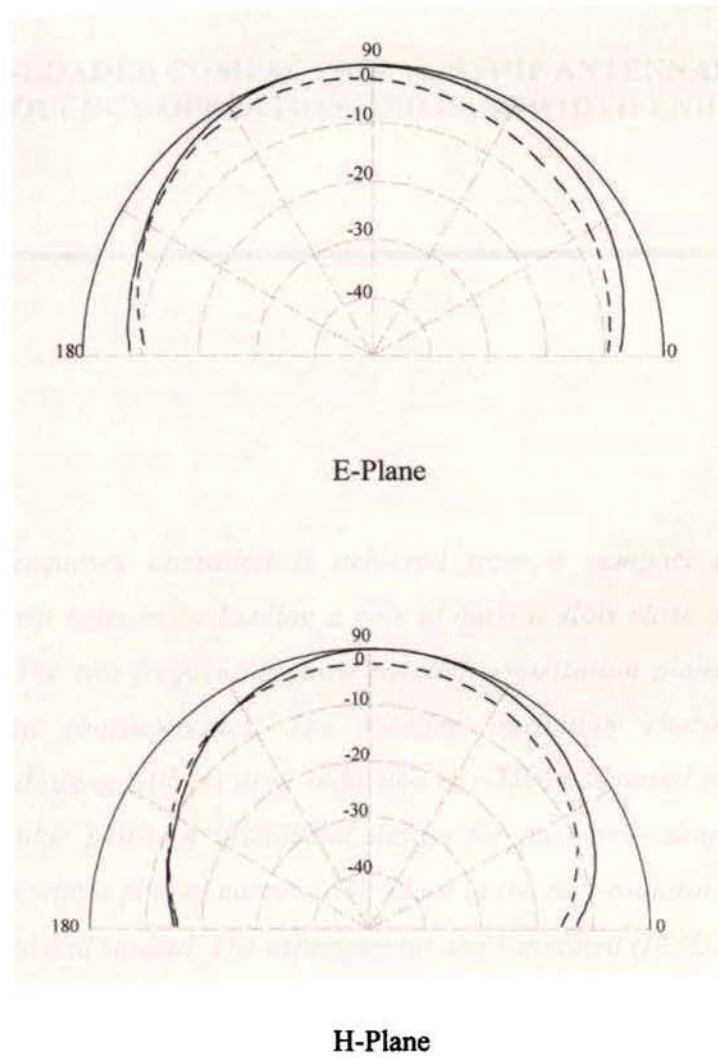


Fig. A.8 Radiation pattern of the antenna at the centre frequency 1.68GHz of the CP band

———— copolar

----- crosspolar

APPENDIX B

SLOT-LOADED COMPACT MICROSTRIP ANTENNAS FOR DUAL FREQUENCY OPERATION AND BANDWIDTH ENHANCEMENT

Dual frequency operation is achieved from a compact arrow shaped microstrip antenna by loading a pair of narrow slots close to its radiating edges. The two frequencies have parallel polarisation planes and similar radiation characteristics. The excellent radiation characteristics are achieved along with an area reduction of ~75% compared to the standard rectangular patch. A broadband design for an arrow shaped microstrip antenna with a pair of narrow slots close to the non-radiating edges is also proposed and studied. The experimental and simulated (IE3D) results shows that antenna bandwidth is ~3.5 times that of the conventional rectangular patch with an added advantage of reduced antenna size.

B.1 INTRODUCTION

A dual frequency microstrip antenna design having same polarisation planes using an arrow shaped patch in which a pair of narrow slots are embedded close to the radiating edges is proposed here. This antenna has a greater area reduction and a smaller frequency ratio compared to bow-tie antenna. In the proposed design a lower frequency ratio range is achieved by the excitation of the two adjacent resonant frequencies of TM_{10} and $TM_{\delta 0}$ modes ($1 < \delta < 2$). The ratio between the two operating frequencies can be tuned in the range (1.14-1.24), which is much smaller than that of similar designs. This makes the antenna more suitable for dual frequency applications where lower frequency ratio is required. Experimental results of the dual frequency characteristics are presented and analysed.

A broadband design of the antenna by embedding slots close to the non-radiating edges is also proposed. Here the broadband operation is achieved by the co-existence of two adjacent resonant frequencies of the TM_{10} and $TM_{\delta 0}$ modes ($1 < \delta < 2$). The proposed antenna strikes attention due to its greater size reduction compared to other wideband slot loaded patches. Experimental and simulated (IE3D) results of this broadband antenna are presented and discussed.

B.2. DUAL FREQUENCY MICROSTRIP ANTENNA WITH SAME POLARISATION PLANES

The proposed configuration of a dual frequency arrow shaped patch antenna is shown in Fig. B.1. L denotes length, W the width, W_{cd} the height of the intruding triangle, and W_{cp} the height of the protruding triangle. The structure is etched on a substrate having a thickness h and relative permittivity ϵ_r . A pair of narrow slots

having a dimensions of $(l_s \times w_s)$ are embedded in the patch parallel to the radiating edges at a distance 's' from the edges. The antenna is excited by electromagnetic coupling using a 50Ω microstrip feedline of length L_p and width W_p .

Typical design of the proposed antenna is implemented and investigated. It has dimensions $L=0.06\text{m}$, $W=0.03\text{ m}$, $W_{cp}=0.01\text{ m}$ and $W_{cd}=0.02\text{m}$ and is fabricated on a substrate of thickness $h=0.0016\text{m}$ and dielectric constant $\epsilon_r=4.28$. Slots having dimensions $l_s=0.026\text{m}$, and $w_s=0.002\text{m}$ are placed at a distance $s=0.003\text{m}$ from the radiating edges. A good impedance matching of the two operating frequencies can be obtained by using a 50Ω microstrip feed line of length $L_p=0.07\text{m}$ and width $W_p=0.003\text{m}$ etched on the substrate of same thickness and permittivity and kept below the antenna to provide electromagnetic coupling.

Fig. B.2 shows the measured return loss against frequency for different intruding triangle heights (W_{cd}). It is found that the frequency ratio is changing with W_{cd} of the arrow shaped patch. Variation of dual frequencies and the frequency ratio with W_{cd} is presented in Table B.1.

The radiation characteristics for the two excited frequencies are also studied. The H and E plane radiation patterns of the antenna for the two frequencies at 0.987 GHz and 1.13 GHz are shown in Fig. B.3 and Fig.B.4. The two modes have same polarisation planes and similar radiation patterns. The performance of the antenna is compared with a standard rectangular patch operating in the same frequency band. It is found that the new configuration offers a size reduction of $\sim 75\%$ with a reduction in gain of only 2 dB.

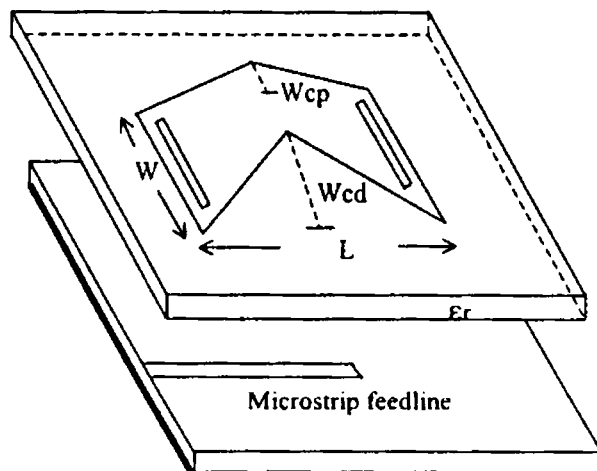


Fig. B.1 Geometry of the compact microstrip antenna with slots on its radiating edges

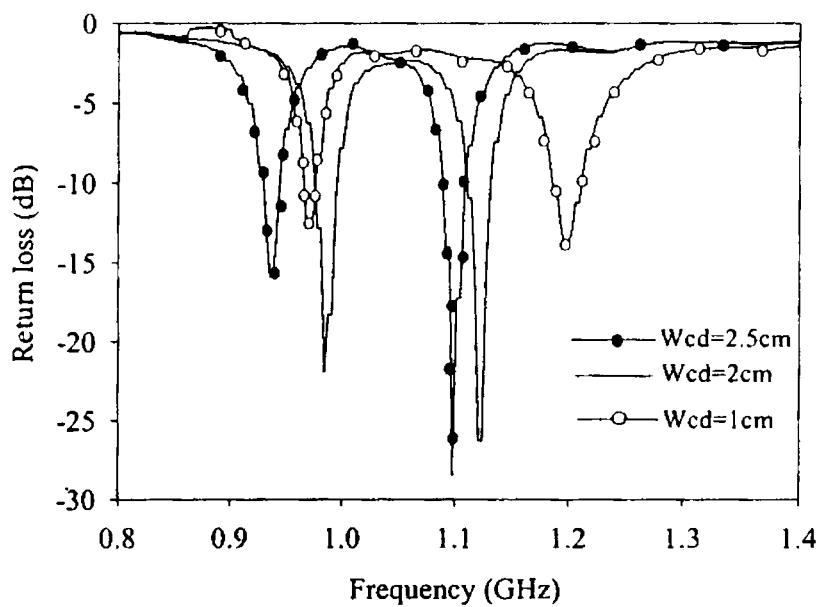
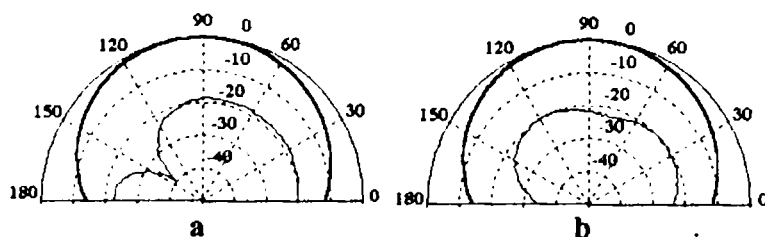


Fig. B.2 Measured return loss against frequency for different W_{cd}

Table B.1. Variation of dual frequency with W_{cd} ($W_{cp}=0.01m$)

W_{cd} (m)	Frequency f_1 (GHz)	Frequency f_2 (GHz)	f_1/f_2
0.010	0.969	1.197	1.24
0.015	0.974	1.197	1.23
0.020	0.987	1.130	1.14
0.025	0.932	1.093	1.17

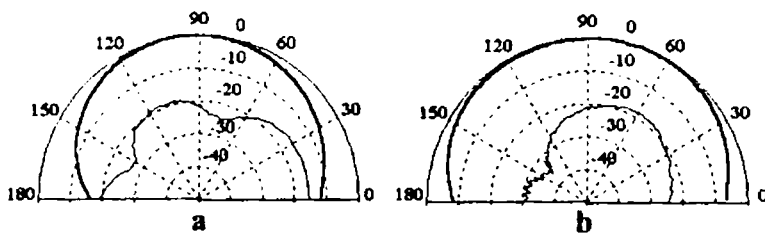
**Fig. B.3** Radiation patterns of the antenna at frequency 0.987GHz

a H- Plane

b E- Plane

— copolar

- - - crosspolar

**Fig. B. 4** Radiation patterns of the antenna at frequency 1.13 GHz

a H- Plane

b E- Plane

— copolar

- - - crosspolar

B.3. BROADBAND COMPACT MICROSTRIP ANTENNA

The configuration of a dual frequency arrow shaped patch antenna is shown in Fig B.5. L denotes length, W the width, W_{cd} the height of the intruding triangle, and W_{cp} the height of the protruding triangle. The structure is etched on a substrate having thickness ' h ' and relative permittivity ' ϵ_r '. A pair of narrow slots having width w_s are embedded in the patch parallel to the nonradiating edges at a distance ' s ' from the edges. By choosing suitable values for W_{cd} and W_{cp} two frequencies of different frequency ratio can be obtained. For a particular design these two operating frequencies merge together, and significantly enhances its bandwidth. The antenna is excited by electromagnetic coupling.

The proposed antenna configuration is simulated using IE3D software and experimentally investigated. A typical design has dimensions $L=0.06\text{m}$, $W=0.03\text{m}$, $W_{cp}=0.01\text{m}$ and $W_{cd}=0.02\text{m}$ fabricated on a substrate of thickness $h=0.0016\text{m}$ and dielectric constant $\epsilon_r=4.28$. Slots having width $w_s=0.002\text{m}$ are placed at a distance $s=0.003\text{m}$ from the non-radiating edges. A good impedance matching of the two operating frequencies can be obtained by using a 50 ohm microstrip feedline etched on the substrate of same thickness and permittivity and kept below the antenna to provide electromagnetic coupling.

By varying the height of the intruding triangle (W_{cd}) of the arrow shaped antenna, frequency ratio between two resonant frequencies of same polarization can be varied. The simulated frequency response of the arrow shaped patches with different W_{cd} is shown in fig. B.6. For an optimum value of W_{cd} these two frequencies merge together to produce large bandwidth. Results show that for $W_{cd}=0.02\text{m}$, the antenna offers a 2:1 VSWR bandwidth of 62 MHz ($\sim 6\%$).

The optimum antenna is fabricated and the radiation characteristics in the operating band are studied. Fig. B.7 shows typical radiation patterns at start, stop and centre frequencies of the operating band. The antenna offers similar radiation patterns and identical polarisation in the entire band. Also, a good cross polar discrimination better than 20 dB is obtained. For a comparison, a rectangular patch antenna operating at the same frequency is constructed and investigated. From the observations it is inferred that the arrow shaped slot antenna is giving a bandwidth of 3.5 times that of the rectangular patch with an area reduction of ~75%. The above performance is obtained with a reduction in gain of 2dB.

B.4. CONCLUSIONS

An arrow shaped microstrip antenna with slots embedded on its radiating edges having dual band operation has been implemented. The two operating frequencies of the proposed design have same polarisation plane and similar radiation characteristics. The present design has an area reduction of ~75% with a reduction in gain of 2dB compared to standard rectangular patch. In this design a lower frequency ratio range is achieved by the excitation of two nearby frequencies, which makes this design more attractive over the other slot- loaded patches.

The experimental and simulated (IE3D) results of an arrow shaped microstrip patch antenna with slots on its non-radiating edges for broadband operation is also developed. The proposed design has same polarisation plane and similar radiation characteristics throughout the operating band. The impedance bandwidth is enhanced to ~3.5 times that of a conventional rectangular microstrip antenna with a very large area reduction.

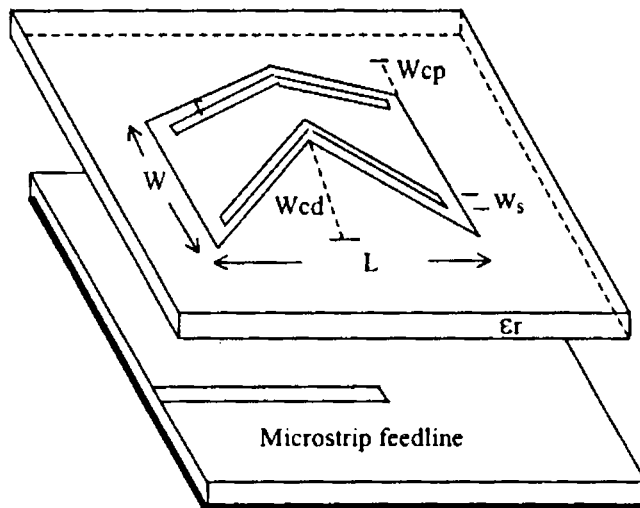


Fig. B.5 Geometry of the slot loaded microstrip antenna for broadband operation

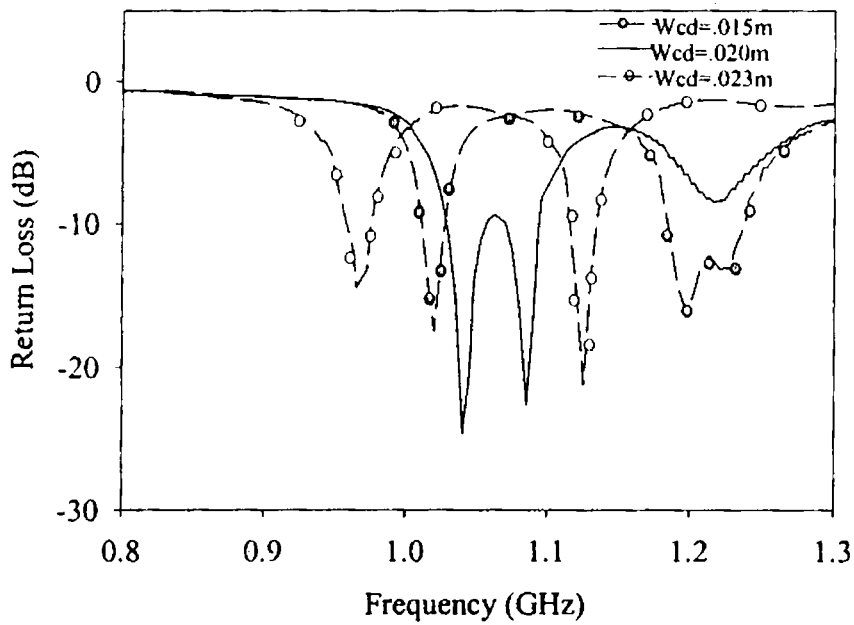


Fig. B.6 Variation of return loss with frequency for different W_{cd} ($L = .06\text{m}$, $W = .03\text{m}$, $W_{cp} = .01\text{m}$)

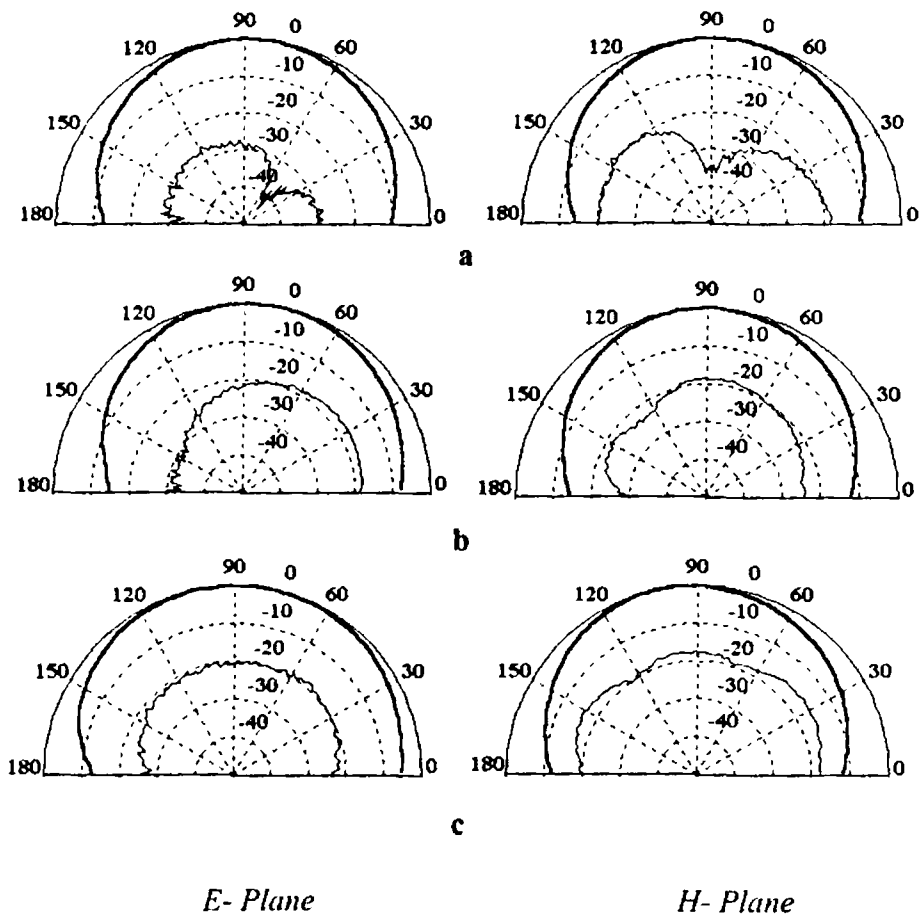


Fig. B.7 Radiation patterns for start, centre and stop frequencies in the operating band.

(a) 1 GHz (b) 1.06 GHz (c) 1.1 GHz

— copolar — crosspolar

APPENDIX C

COMPACT DUAL BAND MICROSTRIP ANTENNA WITH LINEAR AND CIRCULAR POLARISED OPERATION

A compact dual band dual polarised arrow shaped microstrip antenna is presented in this appendix. This antenna resonates at two frequencies with different polarisations, one linear and the other circular. This antenna also provides an area reduction of 70% compared to a standard rectangular patch antenna.

C.1 INTRODUCTION

In the mobile communication systems circularly polarised antennas find application due to flexibility in the orientation angle of transmitter and receiver, as they do not need polarisation tracking. Multiband, multimode handsets or data transmissions capable of communicating with terrestrial and satellite networks find wide application in the fast developing world of mobile communications. A dual band, dual polarised antenna capable of receiving both linearly and circularly polarised waves can be used for this purpose. Relatively very few designs are available in the open literature for achieving the above requirement. A compact drum shaped antenna with similar radiation characteristics of a rectangular patch antenna is available in literature. Here, a new compact microstrip antenna having greater area reduction compared to the antennas proposed above is presented. This arrow shaped antenna is capable of operating with circular polarisation at one frequency and linear polarisation at another frequency with a single feed. By trimming a single antenna parameter this antenna can be made to operate at two orthogonally polarised frequencies or at a single frequency band with circular polarisation.

C.2 EXPERIMENTAL RESULTS AND DISCUSSION

Fig. C.1 shows the geometry of the proposed microstrip antenna. This structure consists of an arrow shaped patch etched on a substrate of thickness 'h' and dielectric constant ϵ_r . L denotes length, W the width, Wcd is the width of the intruding triangle and Wcp is that of the protruding triangle. Antenna is excited by an electromagnetic coupling using a microstrip feedline of length L_p at F_p .

Typical design of the antenna is implemented and investigated. It has dimensions $L=0.06\text{m}$, $W=0.04\text{m}$, $W_{cp}=0.01\text{m}$, $W_{cd}=0.04\text{m}$ and is fabricated on a

substrate of $\epsilon_r=4.28$ and $h=1.6$ mm. A good impedance matching of the two operating frequencies can be obtained by using a microstrip feedline of length $L_p=0.07$ m and width $W_p=0.003$ m etched on a substrate of same thickness and permittivity and kept below the antenna to provide electromagnetic coupling.

Fig C.2 shows the measured return loss against frequency of the antenna. The antenna is found to be resonating at two frequencies 1.0336 GHz and 1.394 GHz. S_{21} measurement with a rotating linearly polarised antenna showed that the radiation at 1.0336 GHz is circularly polarised and that at 1.394 GHz is linearly polarised. Fig C.3 and Fig.C.4 show the E-Plane and H-Plane radiation patterns at first and second resonant frequencies respectively. The variation of axial ratio with frequency is studied. The 3dB axial ratio bandwidth of the antenna is nearly 1%.

The resonant frequencies and the polarisation can be changed by varying the values of W_{cd} and W_{cp} . Keeping W_{cp} a constant and varying W_{cd} , two orthogonally polarised frequencies with different frequency ratio is achieved. For a particular value of W_{cd} , linearly polarised and circularly polarised bands are simultaneously obtained. Hence linear or circular polarisation can be easily achieved by simply trimming the width W_{cd} . From the experimental observations it is found that these properties are achieved with a size reduction of $\sim 70\%$ compared to conventional rectangular patch antenna.

C.3 CONCLUSIONS

This novel antenna is capable of satisfying the requirements of a data communicator for specific terrestrial and satellite mobile systems. This antenna can also be reconfigured to generate two orthogonally polarised resonant frequencies or a single circularly polarised radiation. Moreover, this antenna has a size reduction of $\sim 70\%$ for the dual polarised dual frequency operation compared to a standard rectangular patch.

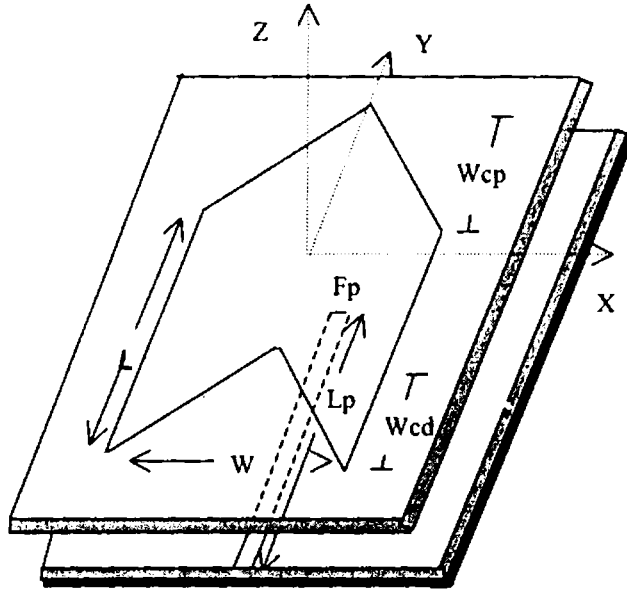


Fig. C.1 Geometry of the compact microstrip antenna for dual band operation

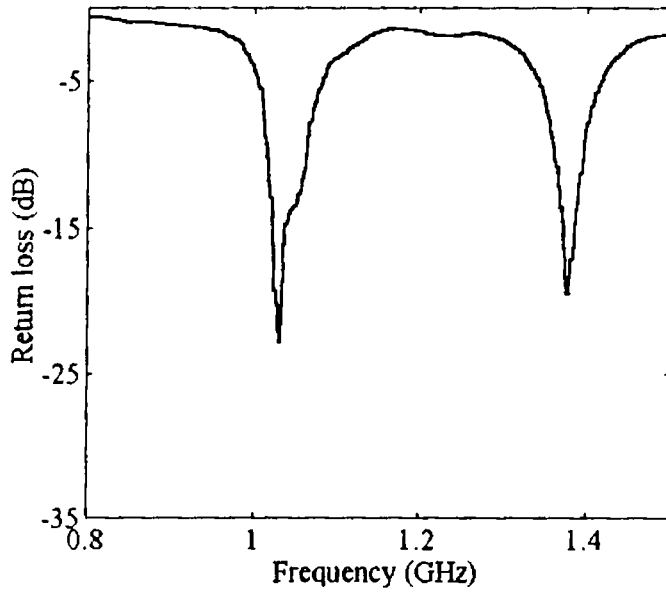


Fig C.2. Variation of return loss with frequency

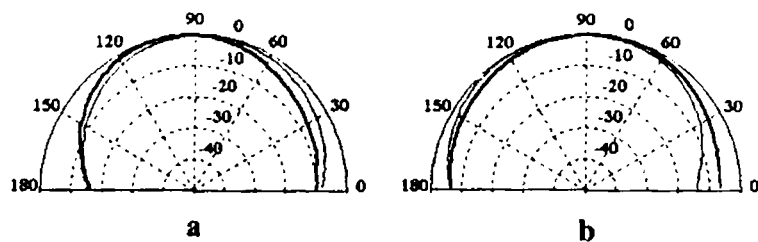


Fig. C.3 Radiation patterns of the circularly polarised band (1.0336 GHz)

a H- Plane patterns

b E- Plane patterns

—— copolar

----- crosspolar

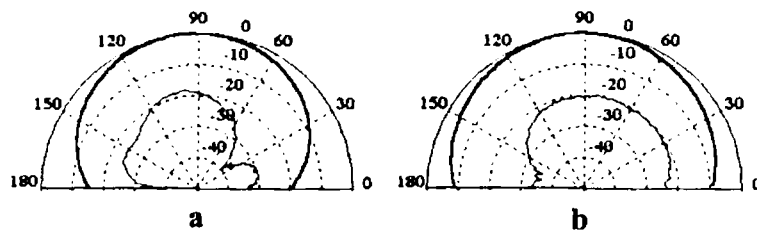


Fig. C. 4 Radiation patterns of the linearly polarised band (1.394 GHz)

a H- Plane patterns

b E- Plane patterns

—— copolar

----- crosspolar

REFERENCES

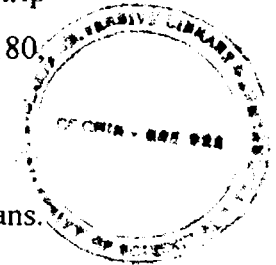
BOOKS

1. J. Bahl and P. Bhartia, "Microstrip antennas", Artech House Dedham, MA, 1980.
2. J. R. James, P.S. Hall and C. Wood, "Microstrip antenna – theory and design", London, UK, Peter Peregrinus Ltd., IEE, 1981.
3. C. A. Balanis, "Antenna theory: analysis and design", Harper and Row, Publishers, New York, 1982.
4. L. V. Blake, "Antennas", Artech House Dedham, MA, 1984.
5. Benjamin Rulf and Gregory A. Robertshaw, "Understanding antennas for radar, communications and Avionics", Van Nostrand Reinhold Company Inc., New York, 1987
6. J. D. Kraus, "Antennas", McGraw-Hill, New York, 1988.
7. J. R. James and P. S. Hall, "Handbook of microstrip antennas", Peter Peregrinus Ltd., IEE Engineers IV series, 1989.
8. F. Gardiol, "Microstrip Circuits", John Wiley & Sons, Inc., New York, 1994.

9. K. C. Gupta and M. D. Abouzahra, "Analysis and design of planar microwave components", IEEE, Inc., New York, 1994
10. IE3D User's manual, Release 7, Zealand Software, Inc. December 1999

JOURNALS/ SYMPOSIUM PAPERS

11. G. A. Deshamps, "Microstrip Microwave Antennas", presented at 3rd USAF Symposium on Antennas, 1953.
12. H. Gulston and G. Bassinot, "Flat aerial for ultra high frequencies", French Patent No. 703113, 1955
13. L. Lewin, "Radiation from Discontinuities in Striplines", Proc.IEE, vol. 107, pp 163-170, 1960.
14. E. V. Byron, "A New Flush Mounted Antenna Element for Phased Array application", Proc. Phased Array Antenna Symp., pp. 187-192, 1970.
15. R. E. Munson, "Conformal Microstrip Antennas and Microstrip Phased Arrays" IEEE Trans. Antennas Propagation, vol. AP-22, pp. 74-77, 1974.
16. J. Q. Howell, "Microstrip Antennas", IEEE Trans. Antennas Propagation, vol. AP-23, pp. 90-93, 1975.
17. G. G. Sanford, "Conformal Microstrip Phased Array for Aircraft Tests with ATS-6", Proc. Nat. Electronic Conf., vol. 29, pp. 252-257, 1974.



18. H. D. Weinschel, "Cylindrical array of circularly polarized microstrip antennas", IEEE Antennas Propagat. Soc. Int. Symp., pp. 177-180, 1975.
19. G. Derneryd, "Linearly Polarized Microstrip Antennas", IEEE Trans. Antennas Propagation, vol. AP-24, pp. 846-851, 1976.
20. G. Derneryd, "Linear Microstrip Array Antenna", Chalmers Univ. Technol., Goteborg, Sweden, Tech. Report, TR 7505, 1975.
21. J. R. James and C. J. Wilson, "Microstrip antennas and arrays Part-I: Fundamental action and limitations", IEE Proc. Microwaves Opt. and Antennas, vol.1, pp. 165-174, 1977.
22. P. K. Agarwal and M. C. Bailey, "An Analysis Technique for Microstrip Antennas", IEEE Trans. Antennas Propogat., vol. AP-25, pp. 756-759, 1977.
23. Y. T. Lo, D. Solomon and W. F. Richards, "Theory and Experiments on Microstrip Antennas", IEEE AP-S Symposium (Japan), pp. 53-55, 1978.
24. W. F. Richards, Y. T. Lo and D. D. Harrison, "Improved Theory for Microstrip Antennas", IEE Electron. Lett., vol. 15, pp. 42-44, 1979.
25. Y. T. Lo, D. Solomon and W. F. Richards, "Theory and Experiments on Microstrip Antennas", IEEE Trans. Antennas Propagat., vol. AP-27, pp.137-145, 1979.

26. K. R. Carver, "A Modal Expansion Theory for the Microstrip antenna", Dig. Int. Symp. Antennas Propog., Seattle, WA, pp. 101-104, 1979.
27. K. R. Carver and E. L. Coffey, "Theoretical Investigation of the Microstrip Antenna", Tech. Rept. PT 00929, Physical Science Lab., New Mexico State Univ., Las Cruces, 1979.
28. E. L. Coffey and T. H. Lehman, "A New Analysis Technique for Calculating Self and Mutual Impedance of Microstrip Antennas", Proc. Workshop on Printed Circuit Antennas, New Mexico State Univ., pp.31/1-21, 1979.
29. E. O. Hammerstad, "Equations for Microstrip Circuit Design", Proc. 5th European Microwave Conf., Hamburg, pp. 268-272, 1975.
30. N. G. Alexopoulos and I. E. Rana, " Mutual Impedance Computation Between Printed Dipoles", IEEE Trans. Antennas Propog., vol. AP-29, pp. 106-111, 1981.
31. E. L. Newman, "Strip antennas in a dielectric slab", IEEE Trans. Antennas Propog., vol. AP-26, pp. 647-653, 1978.
32. E. L. Newman and D. M. Pozar, "Electromagnetic modeling of composite wire and surface geometries", IEEE Trans. Antennas Propog., vol. AP-26, pp. 784-787, 1978.
33. P. Hammer, D. Van Bouchante, D. Verschraevan and A. Van de Capelle, "A model for calculating the radiation field of microstrip antennas", IEEE Trans. Antennas Propog., vol. AP-27, pp. 267-270, 1979.

34. C. M. Butler, "Analysis of a coax-fed circular microstrip antenna", Proc. Workshop Printed Circuit Antenna Tech., New Mexico State University., Las Cruces, pp.13/1-17, 1979.
35. C. M. Butler and E. K. Yung, "Analysis of a terminated parallel plate waveguide with a slot in its upper plate", Ann. Telecommun., vol. 34, No.9, 1979.
36. E. L. Newman, "Strip antennas in a dielectric slab", IEEE Trans., Antennas Propagat., Vol. AP-26, pp.647-653, 1978.
37. E. L. Newman and D. M. Pozar, "Electromagnetic modeling of composite wire and surface geometries", IEEE Trans. Antennas Propagat., Vol. AP-26, pp.784-787, 1978.
38. J. H. Richmond, "A wire grid model for scattering by conducting bodies", IEEE Trans. Antennas Propagat., Vol. AP-14, pp.782-786, 1966.
39. K. R. Carver and E. L. Coffey, "Theoretical investigation of the microstrip antenna", Physical and Science Lab., New Mexico State Univ., Las Cruces, Tech. Report PT 00929, 1979. .
40. K. R. Carver, "Practical analytical techniques for the microstrip antenna", Proc. Workshop on Printed Circuit Antenna Tech., New Mexico State Univ., Las Cruces, pp.7/1-20, 1979.
41. G. Derneryd, "Analysis of the microstrip disc antenna element", IEEE Trans. Antennas Propagat., Vol. AP-27, pp.660-664, 1979.

42. C. Wood, "Curved microstrip lines as compact wideband circularly polarized antennas, *IEE Journal of Microwaves, Optics and Acoustics*, vol.3, pp.5-13, 1979.
43. J. W. Mink, "Circular ring microstrip antenna elements", *IEEE Antennas Propogat. Soc. Int. Symp.*, Quebec City, Canada, June 1980.
44. E. H. Newman and P. Tulyathan, "Analysis of microstrip antennas using moment methods", *ibid.*, pp.47-53, 1981.
45. W. C. Chew and J. A. Kong, "Analysis of a circular microstrip disc antenna with a thick dielectric substrate", *ibid.*, pp.68-76, 1981.
46. K. Araki and T. Itoh, "Hankel Transform domain analysis of open circular microstrip radiating structures", *ibid.*, pp.84-89, 1981.
47. E. F. Kuester, R.T. Johak, and D.C. Chang, "The Thin Substrate Approximation for Reflection from the End of the Slab Loaded Parallel Plate Wave Guide with Application to Microstrip patch", *IEEE Trans. Antennas Propagat.*, vol. AP-30, pp. 910-917, 1982.
48. K. Ito and N. Goto, "Dual frequency circularly polarized printed circuit antennas composed of strips and slots", *IEE Proc.*, Pt.H, Vol.130, pp.170-174, 1983.
49. K. Ito, "Circularly polarized printed antenna with wide axial ratio bandwidth using strip dipoles and slots", *IEE Proc.*, Pt.H, Vol.130, pp.397-401, 1983.
50. N. Das and J. S. Chatterjee, "Conically depressed microstrip patch antenna", *IEE Proc. Pt. H.*, vol.130, pp. 193-196, 1983.

51. D. L. Sengupta, "Approximate expression for the resonant frequency of a rectangular patch antenna", *Electron. Lett.*, vol.19, pp.834-835, 1983.
52. E. Lier and K. R. Jakobsen, "Rectangular microstrip patch antennas with infinite and finite ground plane dimensions," *IEEE Trans. Antennas Propagat.*, vol.AP-31, pp.978-984, Nov.1983.
53. H. Pues and Van De Capelle, "Accurate transmission-line model for the rectangular microstrip antenna", *IEE Proc.*, vol.131, pt.H., pp334-340, 1984.
54. V. Palanisamy and R. Garg, "Rectangular ring and H-shaped microstrip antennas-alternatives to rectangular patch antenna, " *Electron. Lett.*, vol.21, no.19, pp.874-876, 1985.
55. E. Penard and J. P. Daniel, "Open and hybrid microstrip antennas", *IEE Proc.*, Part II, vol.131, pp.38-44, 1984.
56. Das, S. K. Das and S. P. Mathur, "Radiation characteristics of higher order modes in microstrip ring antenna", *IEE Proc.*, Pt.II, vol.131, pp.102-106, 1984.
57. W. F. Richards, J. D. Ou and S. A. Long, "A theoretical and experimental investigation of annular sector and circular sector microstrip antennas", *IEEE Trans. Antennas Propagat.*, vol. AP-32, pp.864-867, 1984.
58. P. S. Bhatnagar, J. P. Daniel, K. Mahdjoubi and C. Terret, "Experimental study on stacked triangular microstrip antennas", *Electrn. Lett.*, vol.22, pp.864-865, 1985.

59. B. F. Wang and Y. T. Lo, "Microstrip antennas for dual frequency operation", *ibid.*, vol.132, pp.938-943, 1985.
60. K. Mahdjoubi, J. P. Daniel and C. Terret, "Dual frequency disc antennas studied by cavity method", *Electron. Lett.*, vol.22, pp.125-126, 1986.
61. C. K. Aanandan and K. G. Nair, "Compact broadband microstrip antenna", *Electron. Lett.*, vol.22, no.20, pp.1064-1065, 1986.
62. Benalla and K. C. Gupta, "Transmission-line model for two-port rectangular microstrip patches with ports at the nonradiating edges", *Electron. Lett. Vol.23*, pp.882-884, 1987.
63. D. M. Pozar and B. Kaufman, "Increasing the bandwidth of a microstrip antenna through proximity coupling", *Electron. Lett.*, vol.23, pp.368-369, Apr.1987.
64. J. L. Drewniak and Mayes, "ANSERLIN: a broadband, low-profile circularly polarized antenna", *IEEE Trans. Antennas Propagat.*, vol. AP-37, pp.281-288, Mar.1989.
65. A. Kishk, "Analysis of spherical annular microstrip antennas", *IEEE Trans. Antennas Propagat. Vol. AP-41*, pp.338-343, Mar. 1993.
66. T. Kashiwa, T. Onishi and I. Fukai, "Analysis of microstrip antennas on a curved surface using the conformal grids FDTD method", *IEEE Trans. Antennas Propagat.*, vol. AP-42, pp.423-427, Mar. 1994.

67. S. A. Bokhari, J.F. Zucher, J. R. Mosig and F. E. Gardiol, "Near fields of microstrip antennas", IEEE Trans. Antennas Propagat., vol. AP-43, pp.188-197, Feb.1995.
68. H. Iwasaki, "A circularly polarized rectangular microstrip antenna using single-fed proximity couple method", IEEE Trans. Antennas Propagat., vol.AP-43, pp.895-896, Aug.1995.
69. C. F. Wang, F. Ling and J.M. Jin, "A fast full-wave analysis of scattering and radiation from large finite arrays of microstrip antennas", IEEE Trans. Antennas Propagat., vol. AP-46, no.10, pp. 1467-1474, Oct. 1998.
70. J. -Y. Sze and K. -L. Wong, "Slotted rectangular microstrip antenna for bandwidth enhancement", IEEE Trans. Antennas Propagat., vol. 48, no.8, pp. 1149-1152, Aug. 2000.
71. Yen-Liang Kuo and Kin-Lu Wong, "A planar inverted-L patch antenna for 2.4/5.2 GHz dual-band operation", Microwave and Opt. Technol. Lett., vol.31, no.5, pp.394-396, December 2001.
72. H. Y. Lo and K. W. Leung , "Excitation of low-profile equilateral-triangular dielectric resonator antenna using a conducting conformal strip", Microwave and Opt. Technol. Lett., vol.29, no.5, pp.317-319, June 2001.
73. V. Palanisamy and R. Garg, "Rectangular ring and H-shaped microstrip antennas- alternatives to rectangular patch antenna", IEE Electron. Lett., vol. 21, No. 19, pp. 874-876, 1985.

74. C. K. Aanandan and K. G. Nair, "Compact broadband microstrip antenna", *Electron. Lett.*, vol.22, no.20, pp.1064-1065, 1986.
75. G. Kossiavas, A. Papiernik, J. P. Boisset, and M. Sauvan, "The C-Patch: A Small Microstrip Element", *IEE Electron. Lett.*, vol. 25, No. 4, pp. 253-254, 1989.
76. E. K. N. Yung, W. W. S. Lee and K. M. Luk, "A Dielectric Resonator on a microstrip antenna", *IEEE Antennas Propogat. Int. Symp. Michigan*, pp. 1504-1507, June 1993.
77. Supriyo Dey, C. K. Aanandan, P. Mohanan, and K. G. Nair, "A New Compact Circular Patch antenna", *IEEE Antennas Propogat. Soc. Int. Symp., Washington*, pp. 822-825, June 1994.
78. M. Sanad , "Effect of the shorting posts on short circuit microstrip antennas", *IEEE Antennas Propogat. Soc. Int. Symp., Washington*, pp.794-797, June 1994.
79. Y. Zhang, T. K. Lo, and Y. Hwang, "A dielectric-loaded miniature antenna for microcellular and personal communications", *IEEE Antennas Propogat. Soc. Int. Symp., California*, pp.1152-1155, June 1995.
80. S. Dey, S. Chebolu, R. Mittra, I. Park, T. Kobayashi and M. Itoh, "A Compact Microstrip Antenna for CP", *IEEE Antennas Propogat. Soc. Int. Symp., California*, pp. 982-985, June 1995.
81. M. G. Douglas and R. H. Johnston, "A Compact two way Diversity Microstrip U-Patch Antenna", *IEEE Antennas Propogat. Soc. Int. Symp., California*, pp. 978-981, June 1995.

82. Jacob George, P. Mohanan and K. G. Nair, "A Broadband Low Profile Microstrip Circular patch Antenna", IEEE Antennas Propogat. Soc. Int. Symp., California, pp. 700-703, June 1995.
83. R. Waterhouse, "Small Microstrip Patch antenna", IEE Electron. Lett., vol. 31, No. 8, pp.604-605, 1995.
84. M. Deepukumar, J. George, C. K. Aanandan, P. Mohanan and K. G. Nair, "Broadband Dual Frequency Microstrip Antenna ",IEE Electron. Lett., vol. 32, No. 17, pp. 1531-1532, August 1996.
85. J. George, M. Deepukumar, C. K. Aanandan, P. Mohanan and K. G. Nair, "New compact microstrip antenna", IEE Electron. Lett., vol. 32, No. 6, pp. 508-509, March 1996.
86. D. Sanchez-Hernandez, G. Passiopoulos, M. Ferrando, E.de los Reyes and I. D. Robertson, "Dual-Band Circularly Polarized Antenna with a Single Feed", IEE Electron. Lett., vol.32, No. 25, pp.2296-2298, December 1996.
87. Z. D. Liu and P. S. Hall, "Dual-band Antenna for Hand Held Portable Telephones", IEE Electron. Lett., vol.32, No. 7, pp.609-610, March 1996.
88. K. L. Wong and S. C. Pan, "Compact Triangular Microstrip Antenna". IEE Electron. Lett., vol.33, No.6, pp. 433-434, 1997.
89. M. Sanad, "A Compact Dual-Broadband Microstrip Antenna having both Stacked and planar Parasitic Elements", IEEE Antennas Propogat. Soc. Int. Symp., Maryland, pp.6-9, July 1996.

90. K. L. Wong and Y. F. Lin, "Small Broadband Rectangular Microstrip Antenna with Chip-Resistor Loading", *Electron. Lett.*, vol.33, No. 19, pp. 1593-1594, Sept. 1997.
91. Park and R. Mittra, "Aperture-coupled quarter-wave microstrip antenna", *IEEE Antennas Propagat. Soc. Int. Symp.*, Maryland, pp.14-17, July 1996.
92. Kin-Lu Wong and Jian-Yi Wu, "Single-feed small circularly polarized square microstrip antenna", *Electron. Lett.*, vol.33, No. 22, pp. 1833-1834, Oct. 1997.
93. S. Dey and R. Mittra, "Compact microstrip patch antenna", *Microwave and Opt. Technol. Lett.*, vol.13, no.1, pp.12-14, September 1996.
94. C. L. Tang, H. T. Chen and K. L. Wong, "Small Circular Microstrip Antenna with Dual Frequency Operation", *Electron. Lett.*, vol.33, No. 13, pp. 1112-1113, 1997.
95. Shan-Cheng Pan and Kin-Lu Wong, "Dual-frequency triangular microstrip antenna with a shorting pin", *IEEE Trans. Antennas Propagat.*, vol.45, no.12, pp. 1889-1891, December 1997.
96. T. K. Lo, C. O. Ho, Y. Hwang, E. K. W. Lam, and B. Lee, "Miniature aperture-coupled microstrip antenna of very high permittivity", *Electron. Lett.*, vol.33, no.1, pp.9-10, 1997.
97. R. B. Waterhouse, "Small printed antennas with low cross-polarised fields", *Electron. Lett.*, vol.33, no.15, pp.1280-1281, July 1997.

98. K. L. Wong and K. P. Yang, "Small dual frequency microstrip antenna with cross slot" *Electron. Lett.*, vol.33, No.23, pp 1916-1917, 1997.
99. Kin-Lu Wong and Wen-Shan Chen, "Compact microstrip antenna with dual frequency operation", *Electron. Lett.*, vol.33, No.8, pp 646-647, April 1997.
100. Kin-Lu Wong and Jian-Yi Wu, "Bandwidth Enhancement of Circularly Polarised Microstrip Antenna Using Chip Resistor Loading", *IEE Electron. Lett.*, vol. 33, No. 21, pp. 1749-1750, October 1997.
101. Kin-Lu Wong and Yi-Fang Lin, "Circularly Polarized Microstrip Antenna with a Tuning Stub", *IEE Electron. Lett.*, vol.34, No. 9, pp.831-832, April 1998.
102. Jui-Han Lu, Hung-Chin Yu and Kin-Lu Wong, "Compact Circular Polarization design for Equilateral-Triangular Microstrip Antenna with Spur Lines", *IEE Electron. Lett.*, vol.34, No. 21, pp.1989-1990, October 1998.
103. H. T. Chen, "Experimental results of compact microstrip antennas", *IEEE Antennas Propagat. Soc. Int. Symp.*, pp.932-935, July 1997.
104. K. L. Wong and K. P. Yang, "Modified planar inverted F antenna", *Electron. Lett.*, vol.34, no.1, pp.7-8, 1998.
105. Chih- Yu Huang, Jian-Yi Wu, Cheng-Fu Yang and Kin Lu Wong, "Gain-Enhanced Compact Broadband Microstrip Antenna", *IEE Electron. Lett.*, vol. 34, No. 2, pp. 138-139, January 1998.

106. S. Vaello and D. S. Hernandez, "Printed Antennas for dual-band GSM/DCS 1800 Mobile Handsets", *IEE Electron. Lett.*, vol. 34, No. 2, pp. 140-141, January 1998.
107. L. Zaid, G. Kossiavas, J. Y. Dauvignac and A. Papiernik, "Very Compact Double C-Patch Antenna", *IEE Electron. Lett.*, vol.34, No. 10, pp.933-934, May 1998.
108. Kin-Lu Wong and Ming-Huang Chen, "Small Slot-Coupled Circularly-Polarized Microstrip Antenna with modified Cross-Slot and Bent Tuning-Stub", *IEE Electron. Lett.*, vol.34, No. 16, pp.1542-1543, August 1998.
109. Jui-Han Lu, Hung-Chin Yu and Kin-Lu Wong, "Compact Circular Polarization design for Equilateral-Triangular Microstrip Antenna with Spur Lines", *IEE Electron. Lett.*, vol.34, No. 21, pp.1989-1990, October 1998.
110. Kin-Lu Wong and Wen-Shan Chen, "Slot-Loaded Bow-Tie Microstrip Antenna for Dual-Frequency Operation", *IEE Electron. Lett.*, vol.34, No. 18, pp.1713-1714, September 1998.
111. J. George, K. Vasudevan, P. Mohanan and K. G. Nair, "Dual Frequency Miniature Microstrip Antenna", *IEE Electron. Lett.*, vol.34, No. 12, pp.1168-1170, June 1998.
112. Gui-Bin Hsieh, Ming-Huang Chen and Kin-Lu Wong, "Single-feed dual-band circularly polarized microstrip antenna", *IEE Electron. Lett.*, vol.34, No. 12, pp.1170-1171, June 1998

113. Kin-Lu Wong and Jia-Yi Sze, "Dual-Frequency Slotted Rectangular Microstrip Antenna", IEE Electron. Lett., vol.34, No. 14, pp.1368-1370, July 1998.
114. Y. X. Guo, K. M. Luk, K.F. Lee and Y.L. Chow, "Double U-Slot Rectangular Patch Antenna", IEE Electron. Lett., vol. 34, No. 19, pp. 1805-1806, September 1998.
115. Kin-Lu Wong and Jen-Yea Jan, "Broadband Circular Microstrip antenna with Embedded Reactive Loading", IEE Electron. Lett., vol. 34, No. 19, pp. 1804-1805, September 1998.
116. N. Chiba, T. Amano and H. Iwasaki, "Dual-Frequency Planar Antenna for Handsets", IEE Electron. Lett., vol.34, No. 25, pp. 2362-2363, December 1998.
117. Yeunjeong Kim, Wansuk Yun and Youngjoong Yoon, "Dual-Frequency and Dual Polarisation Wideband Microstrip Antenna", IEE Electron. Lett., vol. 35, No. 17, pp. 1399-1400, August 1999.
118. Jui-Han Lu, "Single-Feed Dual-Frequency Rectangular Microstrip Antenna with pair of Step-Slots", IEE Electron. Lett., vol.35, No. 5, pp.354-355, March 1999.
119. R. B. Waterhouse, "Broadband Stacked Shorted Patch", IEE Electron. Lett., vol. 35, No. 2, pp. 98-99, January 1999.
120. E. Lee, P. S. Hall and P. Gardiner, "Compact Dual-Band Dual-Polarisation Microstrip Patch Antenna", IEE Electron. Lett., vol.35, No. 13, pp.1034-1036, June 1999.

121. R. Chair, K. M. Luk and K.F. Lee, "Small Dual Patch Antenna", IEE Electron. Lett., vol.35, No. 10, pp.762-764, May 1999.
122. Manju Paulson, Sona O Kundukulam, C.K. Aanandan, P. Mohanan and K. Vasudevan, "Circularly Polarised compact microstrip antenna", Microwave and Opt. Technol. Lett., vol.26, no.5, pp. 308-309, September 2000.
123. Sona O Kundukulam, Manju Paulson, C.K. Aanandan, P. Mohanan and K. Vasudevan, "Dual-band dual-polarised compact microstrip antenna", Microwave and Opt. Technol. Lett., vol.25, no.5, pp. 328-330, June 2000.
124. Manju Paulson, Sona O Kundukulam, C.K. Aanandan and P. Mohanan, "A new compact dual-band dual-polarised microstrip antenna", Microwave and Opt. Technol. Lett., vol.29, no.5, pp. 315-317, June 2001.
125. Sona O Kundukulam, Manju Paulson, C.K. Aanandan and P. Mohanan, "Slot-loaded compact microstrip antenna for dual-frequency operation", Microwave and Opt. Technol. Lett., vol.31, no.5, pp. 379-381, December 2001.
126. K. Shackelford, S. Y. Leong and K. F. Lee, "Small-size probe-fed notched patch antenna with a shorting post", Microwave and Opt. Technol. Lett., vol.31, no.5, pp. 377-379, December 2001.
127. Y. X. Guo, K. M. Luk and K. F. Lee, "Small broadband semicircular patch antenna with an L-probe feeding", Microwave and Opt. Technol. Lett., vol.29, no.5, pp. 289-290, June 2001.

128. M. V. Schneider, "Microstrip Lines for Microwave Integrated Circuits",
Bell System Technical Journal, vol.48, No.5, pp.1421-1444, May-June
1969.

129. E. O. Hammerstad, "Equations for Microstrip Circuit Design",
Proceedings of the 5th European Microwave Conference, Hamburg,
September 1975.

INDEX

Anechoic chamber	50
Antenna Efficiency	22,28
Antenna parameters	29
Antennas	1
Aperture coupling	7
Area reduction	68,83
Axial ratio	52, 87
Circular microstrip antenna	23,28,108
Circular polarization	22,31,38, 39,40
Circular sided Antenna	22,34,55,113,140
Coaxial feed	7
Compact micro strip antenna	28,38,180
	143,144,164
Concave side	63
Convex side	90
Crescent shaped antenna	108
Dipole	1
Drum shaped antenna	62
Dual band	32,33,94,195
Dual ports	120
Electromagnetic coupling	7,45,64,108,185
IE3D simulation software	53,128
Microstrip	1
Moon shaped	119
Network analyzer	49,50
Optimum Design	28,63
Orthogonal polarization	34
Printed circuit	2
Radiation pattern	66,121
Rectangular microstrip antenna	23,29,36,41
Resonant modes	65,96
TM ₁₀	65,68,91,128
TM ₀₁	65,68,91,128
TM ₁₁	108,110,128,163
TM ₂₁	108,110,128,163

LIST OF PUBLICATIONS OF THE AUTHOR

INTERNATIONAL JOURNALS

1. M. Paulson, S.O. Kundukulam, C. K. Aanandan and P. Mohanan, **IEE Electronics Letters**, "Resonance frequencies of compact microstrip antenna", Vol. 37, No. 19, September 2001, pp 1151- 1153.
2. S.O. Kundukulam, M. Paulson, C. K. Aanandan, P. Mohanan, and K. Vasudevan, **Microwave and Optical Technology Letters**, "Dual band dual polarized compact microstrip antenna", Vol. 25, No. 5, June 5 2000, pp 328-330
3. M. Paulson, S.O. Kundukulam, C. K. Aanandan, P. Mohanan, and K. Vasudevan, **Microwave and Optical Technology Letters**, "Circularly Polarized compact microstrip antenna", Vol. 26, No. 5, September 5 2000, pp 308-309
4. M. Paulson, S.O. Kundukulam, C. K. Aanandan and P. Mohanan, **Microwave and Optical Technology Letters**, "A new compact dual-band dual-polarized microstrip antenna", Vol. 29, No. 5, June 5 2001, pp 315-317
5. S.O. Kundukulam, M. Paulson, C. K. Aanandan and P. Mohanan, **Microwave and Optical Technology Letters**, "Slot loaded compact microstrip antenna for dual frequency operation", Vol. 31, No. 5, December 5 2001, pp 379-381
6. M. Paulson, S.O. Kundukulam, C. K. Aanandan and P. Mohanan, **Microwave and Optical Technology Letters**, "Analysis and design of a dual port compact microstrip antenna", Vol. 32, No. 2, January 20 2002, 125-127
7. Sona O Kundukulam, Manju Paulson, C.K. Aanandan and P. Mohanan, **International Journal of RF and Microwave Computer Aided Engineering**, "Analytical Equations for Compact Dual Frequency Microstrip Antenna" (Accepted for Publication)
8. Sona O Kundukulam, Manju Paulson, C.K. Aanandan and P. Mohanan, **Microwave and Optical Technology Letters**, "Compact Circular Sided Microstrip Antenna for Circular Polarisation", (Accepted for Publication)

INTERNATIONAL SYMPOSIA

1. Manju Paulson, Sona O Kundukulam, C. K. Aanandan and P. Mohanan, **IEEE APS Symposia 2002**, "Compact Arrow Shaped Antenna with Embedded Rectangular Slot for Dual Frequency Dual Polarisation Operation", June 16th to 21st at Texas, (Accepted)

2. Sona O Kundukulam, Manju Paulson, C. K. Aanandan, P. Mohanan and K. Vasudevan, **IEEE AP Symposia 2002**, "A Circular sided compact microstrip antenna", June 16th to 21st at Texas (Accepted)

NATIONAL SEMINARS/SYMPOSIUMS

1. Manju Paulson, Sona O Kundukulam, C. K. Aanandan and P. Mohanan, "New Compact microstrip antenna for dual frequency operation" **Proceedings on National Symposium on Antennas and Propagation (APSYM-2000)**, 6-8 December, Cochin, pp.94-97, 2000.
2. Sona O Kundukulam, Manju Paulson, C. K. Aanandan and P. Mohanan, "Dual frequency dual polarized crescent-shaped microstrip antenna" **Proceedings on National Symposium on Antennas and Propagation(APSYM-2000)**, 6-8 December, Cochin, pp.90-93, 2000.
3. Sona O Kundukulam, Manju Paulson, C. K. Aanandan and P. Mohanan, "Dual port dual polarized microstrip antenna" Nov 2-4, **Microwave-2001 Symposium proceedings**, Jaipur, pp 11-13
4. Manju Paulson, Sona O Kundukulam, C. K. Aanandan and P. Mohanan, "Arrow-Shaped Microstrip Antenna for Broadband Operation" **Proceedings on National Conference on Communication (NCC 2002)**, 25-27 January, Indian Institute of Technology, Bombay, pp 210- 213
5. Manju Paulson, Sona O Kundukulam, C. K. Aanandan and P. Mohanan, *Compact Dual band Microstrip Antenna with slots on its radiating edges* **Proceedings on Microwave Measurement Techniques and Applications (MMTA 2002)**, 4-6 February, Jawaharlal Nehru University, Delhi, 2002.
6. Sona O Kundukulam, Manju Paulson, C. K. Aanandan and P. Mohanan, "Design and Analysis of Circular sided Microstrip Antenna" **Proceedings on Microwave Measurement Techniques and Applications (MMTA 2002)**, 4-6 February, Jawaharlal Nehru University, Delhi, 2002.

RESUME OF THE AUTHOR

SONA O. KUNDUKULAM

Permanent Address

(W/o) Litto Palathingal,
Near Popular Candles,
P.O. Edappally,
Cochin 682 024
Kerala, India
Phone: 91 484 577257
Email: sonalitto@yahoo.com .

Present Address

Senior Research Fellow
Department of Electronics
Cochin University of Science and Technology
Cochin 682 022
Kerala, India
Phone: 91 484 576418

Objective

To involve in Research and development activities in the field of microstrip antennas, microwave propagation, microwave devices etc.

EDUCATION

- a) **Ph. D in Microwave Electronics** Thesis submitted in June 2002
- b) **Master of Science in Electronics**
Cochin University of Science and Technology,
Kerala, India (May 1998)
- c) **Bachelor of Science in Physics**
Calicut University, Kerala, India (June 1995)

COMPUTER PROFICIENCY

Programming Languages Basic, Visual C++, C++, C, LISP, Matlab, Mathematica

Simulation Softwares IE3D, FIDELITY.

AWARDS OBTAINED

Participated in the **Young Collaborator Programme** of The International Centre for Theoretical Physics (ICTP), Italy for two months during February, March 2002.

Council of Scientific and Industrial Research, Government of India awarded direct **Senior Research Fellowship** in May 2001.



G8521